CONTROL OF CRACKING IN CONCRETE BY STEEL REINFORCEMENT

An examination of some of the mechanisms involved

A thesis submitted in partial fulfilment of the requirements for the degree of Master of Science in Engineering at the University of Cape Town.

Derek Leslie Skeeles Wilson

April 1986.

DECLARATION BY CANDIDATE

I, Derek Leslie Skeeles Wilson, hereby declare that this thesis is my own work and that it has not been submitted for a degree at another university.

Signed by candidate

D.L.S. Wilson

April 1986.

TO JUDY

SYNOPSIS

The techniques tried up till now to model the problem of cracking in reinforced concrete have been largely empirical. Many relationships have been identified between certain parameters and the occurrence and size of cracks. This thesis reviews these, reports on the current state of knowledge, and discusses some of the theories proposed.

Because of the great variation and complexity of the materials and stress interactions involved, the problem has to date defied completely objective theoretical modelling. The finite element method provides a powerful new modelling tool for theoretical simulation of complex real problems. Recent developments on constitutive models for concrete make this method extremely attractive for use in this case.

This thesis attempts to make use of these tools by carrying out some analyses of the cracking of reinforced concrete prisms stressed in tension. The method is found to be a viable way of examining mechanisms and effects which are not ordinarily visible in laboratory experiments. These mechanisms are discussed in the light of the experimental findings recorded in the literature.

The F.E. models showed that three distinct modes of cracking occur. All occurred at questionably low load levels. The major source of bond between bar and concrete was shown to be a strut and hoop tension effect after very early internal cracking has destroyed the ability of the concrete to carry load by shear. The distribution of longitudinal stress near primary cracks is discussed and an explanation is proposed for surface compressive stresses found in tension members.

Finally, a proposal is made for a new method of describing cracking in reinforced concrete by correlation of the load-strain behaviour of reinforced concrete members. A series of future experimental work is suggested to explore the possibilities of the proposed method.

oooOOOooo

ACKNOWLEDGEMENTS

I would like to express my sincere gratitude to the following:

My supervisor, Mr. R.D. Kratz, for his interest and advice during my period of post-graduate study.

All the staff of the Department of Civil Engineering for their help and friendship during this period.

The Council for Scientific and Industrial Research for their financial assistance.

The Concrete Society of Southern Africa for their financial assistance.

Mrs. Julie Gris for typing the manuscript.

My parents, for their patience, support and assistence.

Especially, I would like to thank my wife, Judy, for her patience and support, and for working beyond the call of duty on assembling the final document.

CONTENTS

GLOSSARY OF TERMS USED

a = displacement

a_{cr} = distance from surface of nearest bar to the point being considered

A = area

A = average area of concrete surrounding reinforcing bars

A_c = area of concrete

$A_{c,ef}$ = effective area of concrete

A_{st} = area of steel in tension

c = (subscript) - concrete

c = cover to reinforcement

c_e = effective cover to reinforcement

E = modulus of elasticity

f_{ct} = tensile stress of concrete (sometimes used as tensile strength)

f_{ct}^u = tensile strength of concrete (sometimes f_{ct} or f_t are used)

f_s = tensile stress in steel

f_y = yield strength of steel

h = overall depth of a member

h_{cr} = height of crack

h_o = initial crack height

k, K = constant

K = stiffness

K' = stiffness with respect to strain

l, ℓ = length

ℓ_o = length of lost bond

n = number (eg. of bars)

P = force

r = radius or name of axis in radial direction

s = (subscript) - steel

S = actual spacing between two primary cracks

S_o = minimum spacing between cracks

S_m = average spacing between cracks

w_m = average surface crack width

w_{max} = maximum probable surface crack width

x = neutral axis depth

ε = strain (at a particular depth in a beam)

ε_{cm} = average residual strain in concrete between cracks

ε_{m} = average strain in cracked member

π = 3,14285

$\rho = \frac{A_{st}}{A_c}$

$\rho_{ef} = \frac{A_{st}}{A_{c,ef}}$

$\sigma_{s,r}$ = stress in steel at cracking of concrete

σ_{sm} = average stress in steel reinforcing

σ_{o} = stress applied to reinforcing bar at a crack

τ_{m} = average bond stress

τ_{ult} = ultimate bond strength

ϕ = bar diameter

NOTE: In accordance with the South African standard, the decimal comma has been used to signify decimals when used within the text. However computers as well as other authors referenced, make use of the decimal point. Decimal points will therefore be found in computer produced graphs and tables, and in figures referenced from other works.

CHAPTER 1

INTRODUCTION

1.1 THE INITIAL MOTIVATION BEHIND THE RESEARCH TOPIC

The initial motivation behind the research topic was the fact that cracks had been found in two local reinforced concrete reservoirs which had been severe enough to cause leaking. The cracking was thought to have been caused by early thermal shrinkage of the concrete. The reservoirs, however, had been designed in accordance with the relatively new code of practice for liquid retaining structures BS 5337 (1976) which has specific clauses to prevent just this type of cracking.

The original idea was that this thesis should consist of a largely experimental study of cracking in concrete due to early age effects. The findings would be related to the literature and the provisions of the codes in this regard, particularly those of BS 5337 on liquid retaining structures. As far as possible the investigation was to have concentrated on the seeking out of areas of inapplicability of the existing theories which could result in instabilities in the consistency of predictions of crack widths made using these theories.

Preliminary examination of the literature showed that there <u>are</u> areas where the theory on which the anti-cracking clauses are based is doubtful. With regard to water retaining structures, there are also areas where the code is open to misinterpretation or, indeed, might actually be misleading.

Investigation of the general theory of cracking as reported in the literature showed that almost every aspect of cracking, when this is caused by interaction between steel and concrete, is poorly understood. It began to appear to the writer that all of the theories expounded in the literature might be seriously flawed. At least, there are certain fundamental assumptions which appeared to the writer to be in error. How then can a theory built upon these suppositions be valid?

Whilst not the only manner of controlling cracking in concrete, the addition of reinforcement for this purpose is by far the commonest. Yet it is the lack of understanding of the interaction of stresses between reinforcing bars and concrete that seems to lie at the heart of the problem.

It was thus decided to examine the validity of some of the fundamental assumptions by examining this interaction. Since the measurement of internal stresses and strains in real models is fraught with difficulty it was proposed, and agreed between the writer and his supervisor, that an attempt should be made to model the problem mathematically, using the finite element method and the best constitutive model (or models) of concrete currently available at the University of Cape Town.

1.2 GENERAL STATEMENT OF THE PROBLEM

1.2.1 The ill-defined nature of concrete

When concrete hardens and subsequently gains strength over a period of many months and, indeed, years, it is not the inert substance it appears to be superficially.

The initial set of concrete is really only the beginning of the process during which it gains strength. Throughout this process, which continues almost indefinitely, almost every property of concrete is in a state of flux. There are ongoing chemical reactions which are continuously changing the crystal structure of the concrete. There are internal consequences of external events, such as changes in the environment (e.g. temperature and humidity) and changes in load applied to the concrete.

There are the consequences of the chemical reactions occurring internally. Heat is given off into the concrete mass, and then lost to the environment. Some of the products of the chemical reactions have different volumes to those of their constituents. If the concrete dries out, it shrinks. Thus there are several different internal causes of straining occurring in the concrete plus the obvious external one of that due to an applied load.

But even if we know all of these effects this does not yet mean we can calculate stresses, strains and displacements exactly, for one of the changing properties of concrete is its modulus of elasticity. Then there are also the properties that give rise to inelastic strains. Yield stresses alter with age, as do the criteria for the occurrence of fracturing. All strains and stresses are affected by creep, which is itself a varying phenomenon.

1.2.2 The composite nature of concrete

Even when all of the above is considered we still need to consider the heterogeneous nature of concrete and the fact that its components have different properties from each other.

From the point of view of cracking the most important properties of the components are their characteristics of expansion and contraction under various states of stress, temperature, or moisture content.

It is here that the problem of cracking in concrete really starts. Before one has even begun to apply any external loading, there are internal effects which come into play, such as differential drying shrinkage, thermal shrinkage, and creep, which cause micro-cracking to occur.

1.2.3. Concrete as a structural material

Despite our knowledge of the composite, unhomogenous nature of concrete, when we use it as a structural material we usually treat it as being homogeneous and isotropic. We do however acknowledge one of its major weaknesses, that of its lack of tensile strength, and accordingly we add steel reinforcing to compensate for this. The point of relevance to this investigation of cracking is that, in order to utilise the greater tensile strength of the steel, we must allow the concrete to crack and thus shed its tensile stresses onto the reinforcing.

1.2.4 Types of loads imposed on concrete

There are two broad categories of loading, which may be identified:-

(i) Category one includes tensile, bending, shear and torsional loads that might be externally applied to concrete.

(2) The second category encompasses all the internally applied loads caused by various forms of restraint to differential movement.

1.2.4.1 Externally applied loads

Although the original brief in this thesis was to examine cracking due to early age phenomena, most of the existing formulae have been derived from experimental data on externally loaded specimens. For that reason they must be considered. They are too, the simplest cases to analyse in greater detail.

The quantification of the loading that will be applied to structures during their lifetimes is the subject of considerable debate, nevertheless it is possible in most cases to achieve a fair degree of accuracy in this regard. Where doubt exists, because the consequences of under-design are often severe, engineers usually do not think twice about adopting a very conservative estimate, (i.e. applying a very large factor of safety.)

1.2.4.2 Internally applied loads

When, however, the loading is applied internally it is as a result of various forms of restraint coming into play to prevent free movement due to internally occurring thermal and drying shrinkage strains. This is often not perceived as being of particularly great importance. Indeed, this type of loading is unlikely to cause a structure to collapse catastrophically. It can and does, however, have a great effect on the serviceability of structures when factors such as cracking and durability are considered.

There are two main categories of internally applied loads. These are due to:

a) externally applied restraints

and b) internally applied restraints

Examples of the first type are walls cast on unyielding foundations or cast as infill panels between other already hardened panels. There are several causes of the second type of restraint including:-

(i) Differential drying and thermal shrinkage due to differing properties of paste and aggregate.

(ii) Differential drying shrinkage due to moisture gradients existing across a concrete section.

(iii) Differential thermal shrinkage (or expansion) due to temperature gradients existing across a section.

(iv) Differential drying and thermal shrinkage occurring between the concrete composite and the reinforcing bars.

Although the various strains that occur during the early life of concrete are fairly easy to quantify within tolerable limits, this only represents half of the problem. The remaining half lies with the quantification of the properties of the material - concrete - which are known to be changing rapidly at these early ages.

1.2.5 Summary

Thus, we have a picture of a situation where it is extraordinarily difficult both to quantify the causes and to calculate the results. We might ask ourselves, "why bother?" Concrete has proved itself over very many years as an extremely reliable building material. Certainly it has cracked, but we have rules and safety factors which, if applied properly, mostly prevent this.

The answer to the question lies in the fact that we can only keep cracking down to acceptable limits most of the time. When we do get wider cracks these are not only unsightly, but they cause corrosion in the steel, and, in water retaining structures we get leaks. A huge amount of money is wasted every year because of corrosion of reinforcement causing spalling of concrete and the structures, as a result, eventually becoming unfit for use.

Many authors have observed that the problem of cracking in concrete has become worse in recent years and it is thought that one of the main causes to have exacerbated it has been the continuing rises in the permissible steel stress used in design.

Beeby (1970), had the following to say about this phenomenon:

"Since crack widths are proportional to steel stresses, it may be seen that a beam designed to carry a particular load in 1969 is likely to have cracks which are 1.64 times as big as those in a similar beam designed in 1945. Similarly, a beam designed according to the new British Draft Code of Practice for Structural use of Concrete could have cracks 1.3 times as wide as those in a beam designed to the present CP114 and 2.15 times as large as those in the beam designed in 1945."

More recently, we have seen the introduction of a new code of practice for liquid retaining structures, BS 5337. This code has similarly led to increased stresses being permitted in reinforcing steel. Whilst these are lower than those allowed under the general codes the consequences of cracks in water retaining structures become very much worse, as not only do leaks start to occur, but the presence of the liquid, usually water, will mostly increase the rate of corrosion in the reinforcing steel.

1.3 AIMS OF THE THESIS

This thesis will attempt to explore some of the mysteries surrounding cracking in concrete which, in many instances, appears to be a totally random phenomenon.

Initially, a survey will be made of the state of current knowledge and theories of the problem. This can be broken down into two broad groupings of theories, both of which are based on quite substantial stores of experimental observations.

(i) Theories on the "macro" behaviour of concrete and reinforced concrete.

(ii) Theories on the "micro" behaviour of concrete.

A distinction is made between these two groupings because, very often there is little or no overlap between the work carried out in the two fields.

Although one does not generally want to criticize others and their work, the writer feels that there is some justification to be critical in the case of much of the "macro" theory of cracking as presented in the literature.

The experimental results of "macro" behaviour have certainly shown that relationships appear to exist which relate various parameters such as cover, bar diameter, reinforcement ratios, etc., to crack widths and spacings. Often, however, the authors of papers presenting these results have made use of a rather simplistic theory of cracking (based on bond strength for example). This is not to say that all of the theories are necessarily wrong but, more likely, that they only represent a small fraction of the whole picture. Then, at great length, rambling "theories" are constructed based on these rather shaky foundations.

The writer has spent a great deal of time trying to unravel some of these theories to find that there is often no theory at all but rather, just a relationship between a visible parameter and an effect, which for all we know may be fortuitous. Certainly none of the theories presented appears to prove conclusively, in any rigorous manner that the relationships have a real foundation in cause and effect. In the writer's opinion some of these cracking theories would be better described as rules of thumb. For the most part they work, and therefore are a very useful tool to practising engineers, but it is only by recognizing them as the rules of thumb that they are that their limitations will be appreciated.

The "micro" theorists have accepted the daunting task of trying to describe mathematically the elastic and inelastic response of concrete. At present, there appears to be little overlap between these two fields, and it is here that the writer hopes to make a small contribution.

The thesis will summarise some of the existing cracking theory for hardened concrete in Chapter 2. In Chapter 3 the writer will comment on some of the problems inherent in trying to predict cracking due to early age effects in immature concrete. In the Addendum the writer will deal more fully with the argument that to construct theories on the basis of empirically determined relationships that have not been rigorously proved is, at best, dangerous. In the balance of the thesis, by using some of the tools developed by the "micro" analysts, an attempt is made to model some simple cases of cracking and examine the validity of some of the parameters and theories proposed by the "macro" analysts. Obviously, any exercise in attempting to model a real problem will also provide a significant test of the validity of the mathematical model employed and the "micro" theory on which this was based.

CHAPTER 2

A HISTORY OF THE DEVELOPMENT OF CRACK WIDTH FORMULAE

2.1 GENERAL

In the everyday practice of Civil and Structural Engineering, time does not permit that a complicated cracking analysis be carried out every time a piece of reinforced concrete is specified or designed. As has been outlined in Chapter one however, we do expect that the concrete will crack. We do therefore need to be able to predict the extent of this cracking. Thus we need simple formulae that will enable us to make these predictions with an acceptable degree of accuracy.

It is essential too that the formulae are given in terms of parameters whose values are readily available to us, otherwise they become too difficult to apply. This, however, could be a bit of a contradiction in that the parameters required depend on what is being described and are not readily specified by the analyst.

When carrying out experimental work, relationships are often observed between various parameters and the result being modelled. This kind of observation is not usually a completely fortuitous happening, since the very fact that the investigator is looking at a particular variable, and quantifying it, implies that it has assumed some importance in his mind. Indeed, the usual situation is that, before the experiments are begun, the investigator selects various parameters which he will measure and then try to relate to the subject of the investigation.

Since cracking in reinforced concrete is such a complex phenomenon, modelling of it has to date largely been confined to empirical modelling of the type described above. Theories have been derived in an effort to explain the experimental data. The major developments of these theories are presented here, along with the simplifying assumptions upon which they depend.

2.2 GENERAL ASSUMPTIONS FOR ALL CRACK WIDTH PREDICTION THEORIES FOR EXTERNALLY LOADED HARDENED CONCRETE

All of the formulae surveyed have two basic premises:

(1) It is assumed that, for any "adequately" reinforced concrete member, a stabilised pattern of cracks will form, beyond which no further cracking will occur.

(2) It is assumed that, given the stabilised crack pattern assumed in (1) above, the widths of the cracks are roughly proportional to the average strain in the member.

2.2.1. The proportionality of crack width to crack spacing

Assuming for the moment that premise (1) is valid, we can first examine the validity of premise number (2)

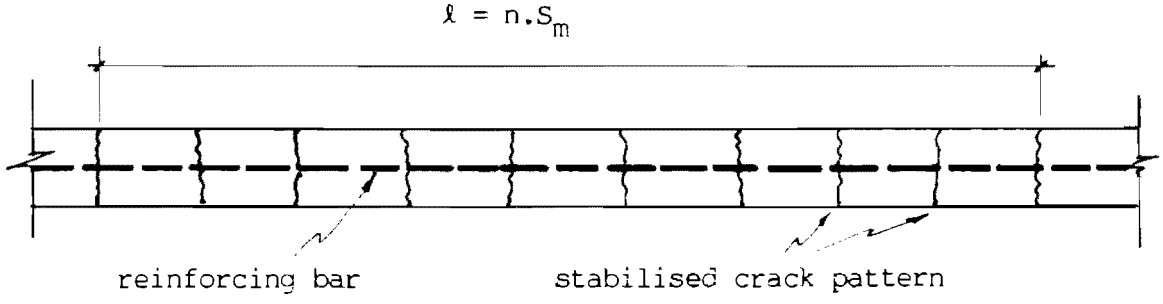

Figure 2.2: Singly reinforced concrete member with stabilised crack pattern.

Figure 2.2 represents an unstrained section of length l of a singly reinforced concrete member with cracks at a stabilised average spacing, S_m, apart. If this member now has a tensile force, P, applied to each end it may be expected to deform as shown in figure 2.3

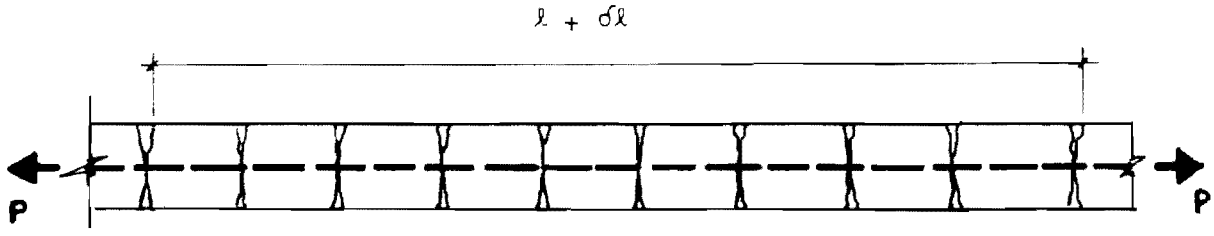

Figure 2.3: Deformation of singly reinforced concrete member.

Using the centres of two arbitrarily chosen cracks as reference points we can now define the average strain, ε_m, in the cracked member as:

$$\varepsilon_m = \frac{\delta\ell}{\ell} \qquad \ldots (2.1)$$

Assuming the residual average strain in the uncracked concrete at the surface to be ε_{cm} it is now possible to write a formula for the average surface crack width, w_m.

$$w_m = S_m(\varepsilon_m - \varepsilon_{cm}) \qquad \ldots (2.2)$$

This concrete strain is normally ignored and the average crack width is written as:-

$$w_m = S_m\varepsilon_m \qquad \ldots (2.3)$$

Thus, providing we can assume that the residual concrete strain is small, premise number (2) is shown to be valid (to a first order of approximation).

2.3. PREDICTION OF CRACK SPACING - CLASSICAL THEORIES FOR HARDENED CONCRETE

Equations 2.2 and 2.3 indicate that if we are to be able to calculate the width of cracks to any degree of accuracy we must know the spacing of the cracks to as least that same degree of accuracy.

This brings us back to the consideration of the first of the assumptions enumerated at the beginning of this section. This supposition of the existence of a stabilised crack pattern is of crucial importance to the ability to predict crack widths. More important however is that we should have the ability to predict the size, and expected distribution of sizes of crack spacings.

2.3.1. Basic assumptions of classical theories.

All classical theories start with certain basic assumptions with regard to the maximum and minimum crack spacings possible in a fully developed crack pattern.

1) Assuming the first crack has just formed. The stress in the concrete on the surface of the member immediately adjacent to the crack must be zero.

2) It is assumed that with increasing distance from the crack the surface stress will increase.

3) It is assumed that at some distance, S_o, the stress distribution in the member remains unaffected by the crack. (i.e. the crack affects the stresses only within a distance $\pm S_o$ from the crack.)

4) Since the crack has reduced the concrete surface stress to below the tensile strength of concrete within $\pm S_o$ of the crack, the next crack must form outside of this region. The minimum distance between cracks is thus S_o.

5) If two cracks form at a distance apart greater than $2S_o$, there will be an area between the cracks where the stress is not affected by either of the cracks and so another crack can form. Thus the maximum crack spacing is $2S_o$.

6) If, however, the cracks had formed at a distance of less than $2S_o$ apart, the stress would have been reduced to below the cracking stress for the whole distance between the cracks and therefore no further cracks will form. Thus, when all cracks have formed the final crack pattern will consist of cracks having a distribution of spacings within the range.
$S_o \leq S \leq 2S_o$

The above argument is most simply illustrated by figure 2.4 below:

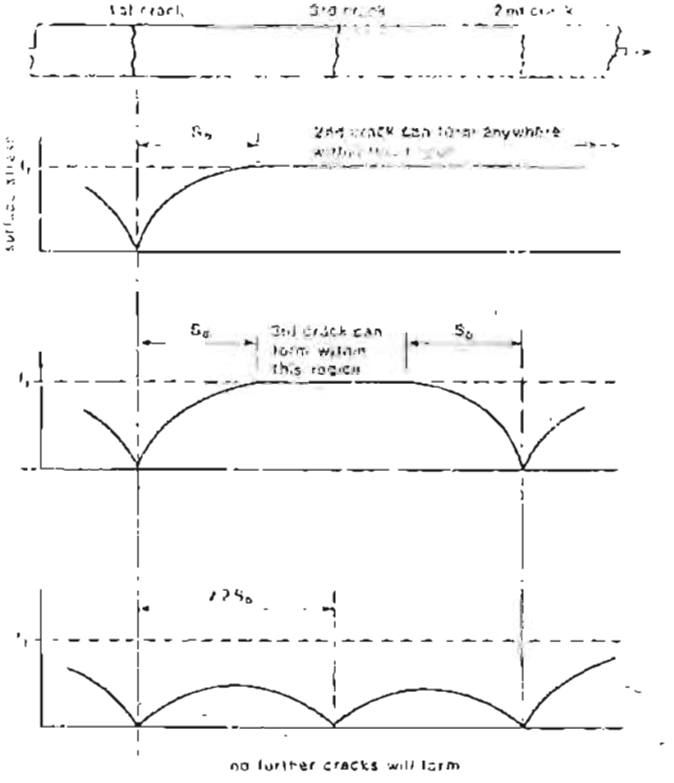

Figure 2.4: Conditions on the surface of an axially reinforced member during the development of cracking (after Beeby (1979)).

The mean final crack spacing is commonly assumed to be $1{,}5\ S_o$, although several investigators have found reasons to expect a bias towards either the minimum or maximum spacing. Regardless of what exact value the mean spacing has, the whole theory is meaningless if we cannot predict the base value S_o satisfactorily.

The real problem facing the analyst therefore, is the development of a theory to satisfactorily predict S_o.

2.3.2 Bond strength, or bond slip, theory

All of the early formulae relate the minimum crack spacing to the strength of the bond between the reinforcement and the surrounding concrete.

The following assumptions are made:

(i) When the bond stress reaches the ultimate value τ_{ult}, slipping occurs on the steel/concrete interface.

(ii) Plane sections remain plane, thus the stress in the concrete of an axially stressed member is uniform.

(iii) As a result of assumption (ii) above it is evident that if a surface crack of width w is to form this must be associated with an equal amount of bond slippage.

(iv) Since bond failure is assumed to have occurred at each crack, the distribution of bond stress along the bar between cracks can be taken as a function of the ulimate bond strength.

Using these assumptions it can then be said that the force, F , transmitted from the steel into the concrete within a distance, S_o, from a crack is given by:

$$F = \int_o^{S_o} f(\tau_{ult}).2n\pi\phi dx \qquad \ldots (2.4)$$

where n = number of bars

ϕ = diameter of bars

Substituting

$$k.\tau_{ult}.S_o = f(\tau_{ult})dx$$

where k is a constant dependent on the shape of plot of bond stress and distance

we get: $F = k\tau_{ult}.S_o.2n\pi\phi$ ... (2.5)

But is has also been assumed previously that at distance S_o the stress in the concrete will once again reach its ultimate tensile strength, f_t. Therefore, in the concrete at this point,

$$F = f_t.A_c \quad \ldots (2.6)$$

where A_c = the area of the concrete.

Equating equations (2.5) and (2.6)

$$f_tA_c = k\tau_{ult}.S_o.2n\pi\phi \quad \ldots (2.7)$$

rearranging:

$$S_o = \frac{f_t.A_c}{k\tau_{ult}.2n\pi o\phi} \quad \ldots (2.8)$$

Let

$$\rho = \frac{A_{st}}{A_c} = \frac{n\phi^2\pi}{4A_c}$$

Now, multiplying the right hand side of equation (2.6) by

$$\frac{\rho}{\rho} = \frac{n\pi\phi^2}{4A_c\rho}$$

we get:

$$S_o = \frac{1}{8k} \cdot \frac{\phi}{\rho} \cdot \frac{f_t}{\tau_{ult}} \quad \ldots (2.9)$$

and letting

$$\frac{1}{8k} = k_1$$

$$S_o = k_1 \frac{\phi}{\rho} \cdot \frac{f_t}{\tau_{ult}} \qquad \ldots (2.10)$$

It has been found experimentally that τ_{ult} is directly proportional to f_t for a particular bar type. Substituting into equation (2.3) gives

$$w_m = K \frac{\phi}{\rho} \varepsilon \qquad \ldots (2.11)$$

The constant K can be directly determined experimentally and therefore it is held that the assumptions concerning the relationships between the minimum, maximum, and average crack spacings, as well as the shape of the bond stress distribution, become irrelevant.

2.3.3 Theories of Hognestad, Mattock & Kaar

One of the early researchers into the crack control characteristics of high strength, deformed reinforcing bars was Hognestad (1962) who, in particular, researched crack widths in flexural members.

Hognestad started with the basic bond slip theory outlined in section 2.4, but raised several points that are questionable about this theory.

(i) He questions whether the assumptions that the concrete stresses are uniform a distance S_o away from a crack is valid. His own experimental results confirm that in fact the assumption is not valid.

(ii) He points out that if equations 2.10 or 2.11 are applied to flexural members, additional assumptions must be introduced, most notably the concept of effective concrete area. This needs to be defined for the formula to have any value.

(iii) He points out that European test data had shown that the inverse proportionality to ρ was over emphasized,

and cites the then CEB formula of:

$$w_{max} = (4.5 + \frac{0.40}{\rho_{ef}}) \phi \frac{f_s}{k} \quad \ldots (2.12)$$

(iv) He found that crack width was strongly influenced by cover, less so by reinforcement ratio (especially with deformed bars) and was essentially independent of concrete compressive strength and beam depth.

(v) He found that crack width was not directly proportional to crack spacing. (The writer does not consider Hognestad's findings in this regard to be too significant - further discussion is made on this point in the summing up of evidence for and against various parameters).

Kaar & Mattock (1963), continuing the work of Hognestad (1961) investigated the effect of distribution of reinforcement in beams and found that for a given steel stress the crack widths tended to be greater in members having widely spaced bars than in those with more closely spaced reinforcing. More specifically they found that the crack widths and spacings at the level of the steel appeared to be related to the average area of concrete surrounding each bar in the member concerned.

This area of concrete, A, is defined as follows:

$$A = \frac{A_{c,ef}}{n} \quad \ldots (2.13)$$

where: $A_{c,ef}$ = the area of concrete surrounding the bars and having the same centroid as the bars

n = the number of bars.

Kaar and Mattock's test results are plotted in figures 2.5(a) and (b)

As a result of their tests showing a relationship between crack spacing and the area of concrete around each bar, Kaar and Mattock decided to review the other data at their disposal and produced the plot shown in figure 2.6.

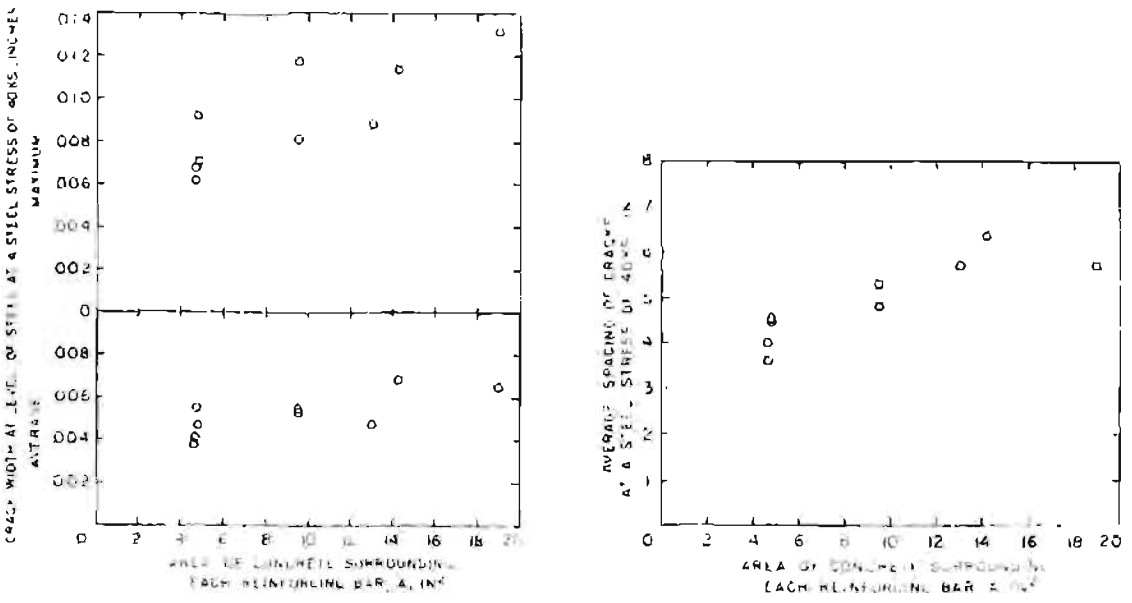

(a) (b)

Figure 2.5: (a) Variation of crack width and (b) variation of crack spacing with area of concrete surrounding each reinforcing bar at a steel stress of 40 ksi (275 N/mm^2) - After Kaar & Mattock (1963)

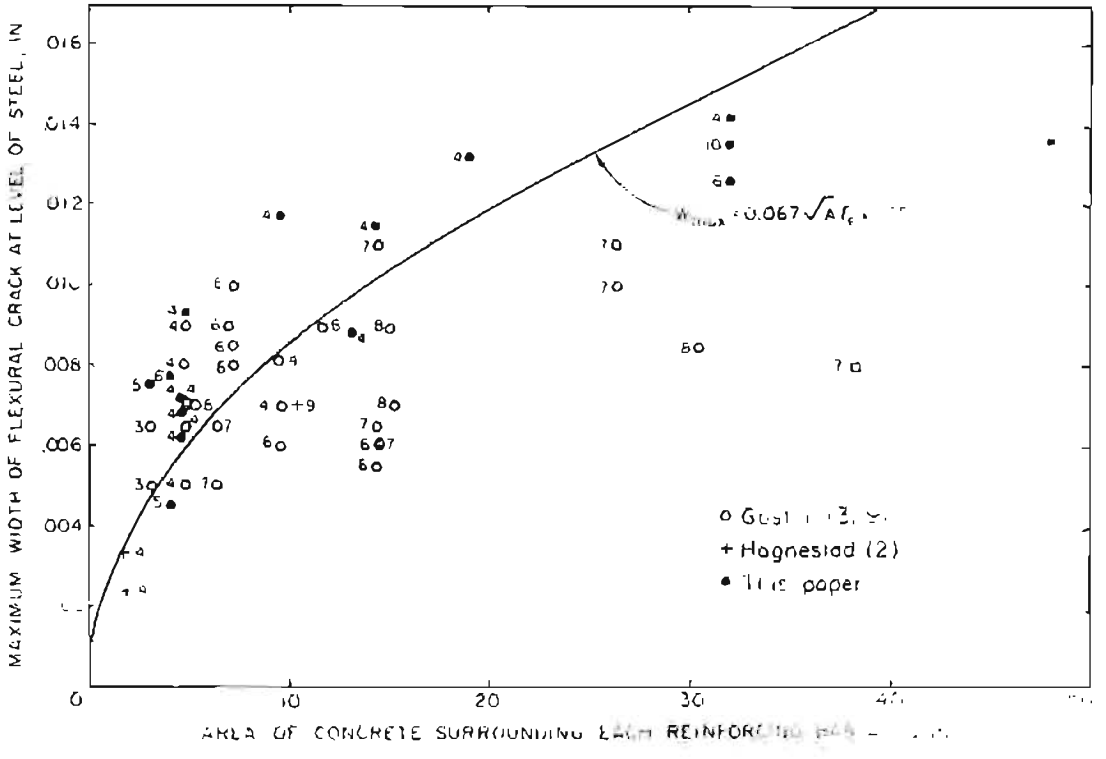

Figure 2.6: Relationship of maximum width of flexural crack and the area of concrete at a steel stress of 40 ksi (275 N/mm^2) - After Kaar and Mattock (1963)

As may be seen in figure 2.6 Kaar and Mattock have superimposed a plot of the following equation for crack width in terms of the square root of the area of concrete around each reinforcing bar:

$$w_{max} = 0.067 \sqrt{A}\, f_s * 10^{-6} \quad \text{(inches)} \quad \ldots (2.14)$$

Kaar & Mattock considered the completely different variables in the formula compared with the then CEB formula (eq. 2.12) and say the one may be "derived" from the other as described below:

Taking the empirically corrected equation 2.12 and writing it in the form of equation 2.11 which was derived on the basis of bond slip theory one gets:

$$w_{max} = \frac{\phi}{\left(\frac{\rho_{ef}}{4.5\rho_{ef} + 0.40}\right)} \cdot \frac{f_s}{k} \quad \ldots (2.12a)$$

(where K now includes Young's modulus, E_s)

They then show that, within a certain range, an alternative function in ρ_{ef} could have been selected empirically by plotting two functions over the range of $0{,}02 < \rho_{ef} < 0{,}20$. They observe that such a function is $0.357\sqrt{\rho_{ef}}$ and demonstrate the approximate equivalence by plotting the two on the same set of axes (see figure 2.7)

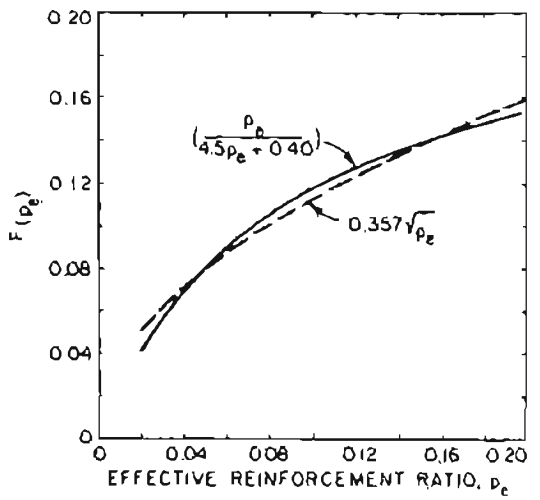

Figure 2.7: Equivalence of functions in ρ_{ef} - Kaar and Mattock (1963)

Substituting this alternative function into equation 2.12a, one gets:

$$w_{max} = \frac{\phi}{0.357\sqrt{\rho_{ef}}} \frac{f_s}{k} \qquad \ldots (2.15)$$

Now taking $\rho_{ef} = \left(\frac{\pi\phi^2}{4}\right)/A$

this implies $\sqrt{\rho_{ef}} = \sqrt{\frac{\pi}{4}} \frac{\phi}{A}$

substituting into equation 2.13 one gets:

$$w_{max} = \left[\frac{A}{0.357\sqrt{\frac{\pi}{4}}}\right]\frac{f_s}{k}$$

and substituting the value of 47 500 000 psi for K gives

$$w_{max} = 0.067\sqrt{A}\, f_s * 10^{-6} \qquad \text{(inches)}$$

Which is the same as equation 2.14.

Thus, although Kaar & Mattock found crack width to be related to a completely different variable to those of the bond stress theory, empirically at least, their results are not in contradiction to those that gave rise to the other equation. Kaar and Mattock imply that this adds weight to their selection of area of concrete around each bar as the most important parameter in the determination of crack sizes and spaces. Subsequent to deriving equation 2.14 however they found that they could achieve an even better fit to their data by using an equation in $\sqrt[4]{A}$, i.e.

$$w_{max} = 0.115\sqrt[4]{A}\, f_s * 10^{-6} \qquad \ldots (2.16)$$

2.3.4. Theories of Broms (1965)

Broms (1964, 1965 (a), (b), (c)), and Broms and Lutz (1965) showed in a series of papers that cracks start at the reinforcing and extend outwards to the surface of the member. On the basis of calculated and measured stress distributions (the analyses are described in chapter

4), Broms (1965 (c)) advanced the hypothesis that the lengths of cracks initiated close to the reinforcement will be governed by the circles inscribed between two cracks. This hypothesis is described in figure 2.8.

This hypothesis leads in turn to the prediction that the minimum crack spacing, S_o, is equal to distance from the point considered to the nearest bar; i.e. normally the cover to a bar. With the maximum crack spacing having a value of $2S_o$, according to the argument put forward in section 2.2.1, the average crack spacing may reasonably be expected to approximate $1\frac{1}{2}$ times this value. Broms's experimental observations, however, showed that the real average crack spacing in a stabilised pattern was equal to twice the cover, c,(i.e. exceeding the predicted value by 30%). Substituting the observed value of S_m into equation 2.3 Broms obtained the equation for predicting width:

$$w_m = 2c\varepsilon_m \qquad \ldots (2.17)$$

where the symbols have the meaning previously ascribed to them.

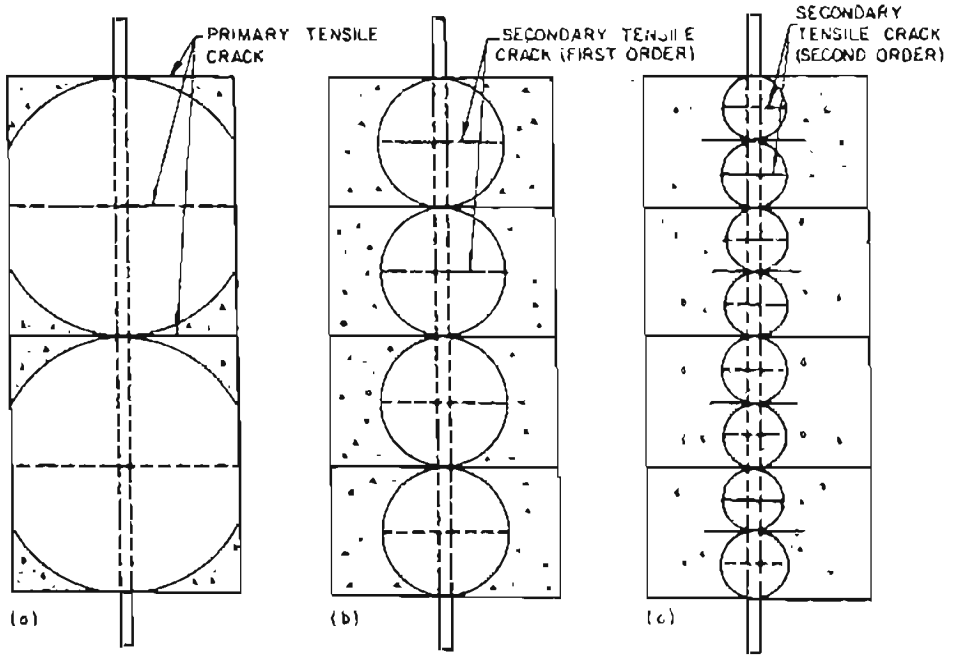

Figure 2.8: Mechanisms of tension cracking in singly reinforced member according to Brom's hypothesis.

Broms reiterates the original assumption that the crack patterrn has to have stabilised before equation 2.3 and thus 2.17 apply. He found that this only happened at average steel stresses above 20 000 to 30 000 psi (140 to 210 MPa).

Broms proposed that flexural members could be treated in the same way as tension members if the tension reinforcement plus its surrounding concrete were treated in isolation from the rest of the member. (Of course this would only predict cracks in the immediate vicinity of the reinforcement, whereas these could go right up to the neutral axis.)

Besides contrasting to existing theories in that he found that the crack width depended primarily on cover (or distance to the reinforcement), further findings of Broms were that his results showed that the crack size was <u>independent</u> of (i) the percentage and size of reinforcement, and (ii) the tensile and compressive strength of the concrete.

Broms and Lutz (1965) extended the scope of experimental results to include members with more than one reinforcing bar to establish the relationship between cracking and the parameters of reinforcement layout, bar surface area (i.e. more small bars rather then one large one) and further to check whether reinforcement ratio had any effect.

Their findings were that the proportionality to cover remained in the multi-bar systems with the proviso that the value for cover, c, be changed to an effective value, c_e, in equation 2.17

$$w_m = 2c_e \varepsilon_m \qquad \ldots (2.17a)$$

Their investigation therefore confirmed the lack of effect of other parameters such as amount of steel, number of bars, etc., on cracking. A further observation was that the widths of the largest cracks were found to be considerably larger than those of the average cracks, at about twice the average crack size.

An interesting point raised in discussion of the paper by Broms and Lutz is that cover is closely related to area of concrete (i.e. $c_e = k\sqrt{A}$). Thus, there is little to choose between these two

parameters for most situations where the reinforcement is evenly distributed. Broms & Lutz, however believe that cover (or rather effective cover) is a better variable to use when the bars have varying distributions.

2.3.5 "No Slip" Theory

Beeby (1979) cites a different, "theoretical" justification of the choice of cover as a variable in cracking equations which are derived from assumptions that are exactly opposite to those made for the bond slip approach.

This time it is assumed that no bond slip takes place and that plane sections do not remain plane. These assumptions were prompted by the advent of deformed bars and the work of Goto (1971) who demonstrated that for deformed bars the bond failure takes the form of internal cracking (see figure 2.9)

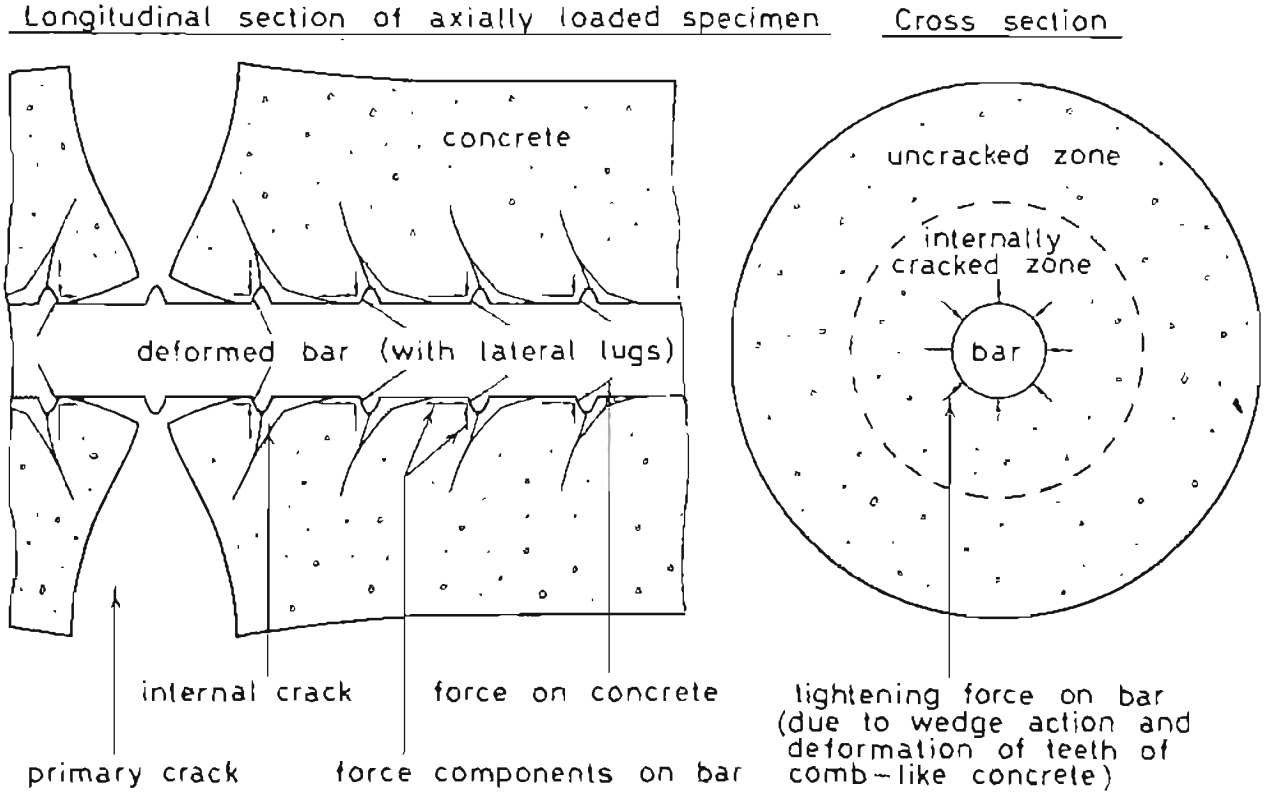

Figure 2.9: Deformation of concrete around reinforcing steel after formation of internal cracks (schematic diagram; after Goto (1971)).

With this type of failure one clearly cannot use the bond strength as a parameter anymore and therefore in equations (2.10) and (2.11) one needs to find a replacement for the $\frac{\phi}{\rho}$ factor. This has been done by application of the intuitive 45° rule (see figure 2.10) which using the pre-Broms assumption of uniform distribution of stress, predicts that the minimum crack spacing, S_o, is equal to the cover, c, to the reinforcement. (This is despite Broms's work which showed that the 45° rule does not apply in this case).

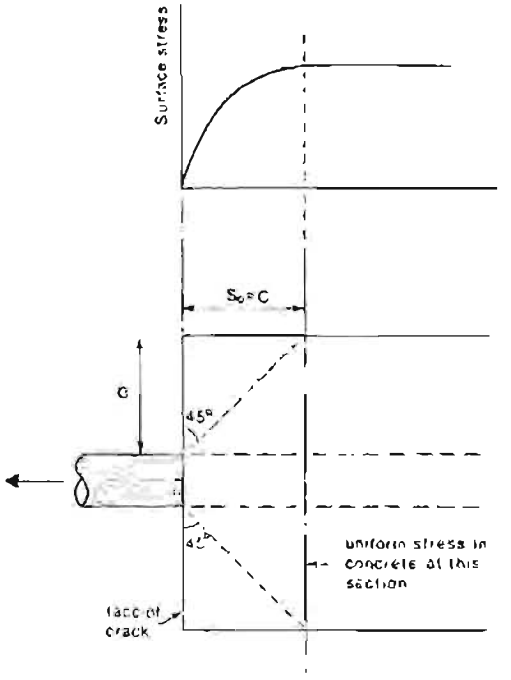

Figure 2.10: No-slip mechanism of cracking: relationship between c and S_o - after Beeby (1979).

Now we can write the equation for the crack width as:

$$w_m = kc\varepsilon_m \qquad \ldots (2.17b)$$

Which may be compared to Broms's equation 2.17.

2.3.6 Theory of Base et al (1966)

An alternative theory explaining the proportionality of crack width to cover is that postulated by Base et al (1966) who proposed that it exists because cracks taper from a certain width on the concrete surface to approximately zero width at the steel-concrete interface.

Postulating that "the crack width is essentially a function of the elastic strain of the concrete", Base et al have carried out a two dimensional elastic analysis of the zone between two cracks of a singly reinforced tension member (see figure 2.11). This analysis is very similar to that carried out by Broms which is discussed in more depth in chapter 4.

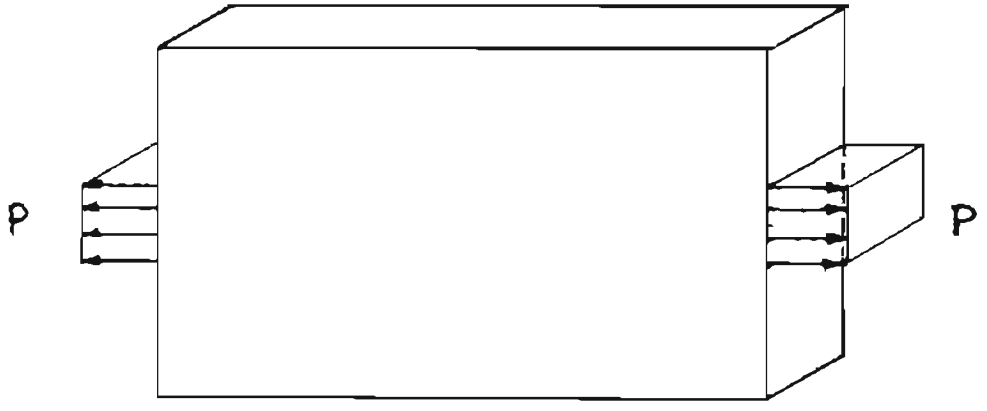

Figure 2.11: Mechanisms of cracking - 2D elastic model used by Base et al (1966).

From this analysis they conclude that:-

(i) An almost direct proportionality between crack spacing and cover is predicted.

(ii) Proportionality is predicted between crack width and cover.

It should be borne in mind that this is a very crude analysis, assuming as it did that the concrete is linear elastic with, apparently no limit being put on the amount of tension it can carry. Subsequent work by Goto (1971) indicated that secondary cracking associated with any primary crack forms shortly after the formation of the primary crack.

Base et al acknowledge that there will be "micro-cracking" near the steel concrete interface, particularly on either side of a primary

crack.

They acknowledge too, that the sum of the widths of the micro cracks will approximately equal the sum of the widths of the primary cracks at the surface of the beam. Then, however, they escape giving further attention to this phenomenon by implying that it only occurs at steel stresses outside of the range used in current practice.

In this regard it is worth noting Goto's estimate of steel stresses of about 100 N/mm^2 for the commencement of this secondary cracking. This is well within the range of normal working stresses of steel reinforcing.

Examination of figure 2.9 from Goto (1971) indicates that it might be reasonable to expect cover and crack width to remain approximately proportional to each other even after secondary cracking has commenced, provided the individual crack widths taper in an approximately linear way.

In addition to predicting proportionality between cover and crack width based on their elastic analysis, Base et al found the same result experimentally and proposed the following empirical formula for members in flexure

$$w_{max} = kc \frac{f_s}{E_s} \left(\frac{d - d_n}{d_1 - d_n} \right) \qquad \ldots (2.18)$$

where c = distance from point of measurement to surface of nearest reinforcing bar.

d = distance from compression face to point of measurement of the crack.

d_1 = distance from the compression face of the section to the centroid of the main tension reinforcement.

d_n = the distance of the neutral axis from the compression face of the beam.

f_s = mean stress in the reinforcement.

E_s = modulus of elasticity of the reinforcement.

k = a constant of value 3.3 for deformed bars and 4.0 for round bars.

The expression $\frac{f_s}{E_s}\left(\frac{d - d_n}{d_1 - d_n}\right)$ simply defines the strain, ε , at any depth in a beam in terms of the strain in the reinforcement, f_s/E_s. Hence we may write:

$$w_{max} = k\, c\, \varepsilon \qquad \ldots(2.19)$$

which has the same form as equation 2.17 except here the constant k will be increased as a result of the inclusion of a statistical factor which relates the average crack width to the maximum likely crack width (with some reasonably low statistical chance of being exceeded).

The above formula was developed from the results of tests on beams and is therefore really only applicable to beams. Having reduced the formula to the form shown in equation 2.14 however, it seems reasonable that, now that the beam related terms have disappeared, the formula should be applicable to tension members. This is in line with the proposal of Broms that the reinforcing bar and its surrounding concrete can be treated as a tension member separately from the member to which it is attached.

2.3.7 Empirical formulae developed by Beeby

Beeby (1970) continued the empirical work of Base et al (1966) by investigating the effect of the remoteness of the nearest reinforcing bar on the widths of cracks. To this end he conducted tests on slabs subjected to flexural stresses.

He came to the conclusion that in a flexural member there were two modes of cracking and that the crack pattern obtained was the result of an interaction between the two, in a further paper, Beeby (1971) defines these as follows:

"(1) At points on the surface of a member distant from a reinforcing bar, crack spacings and crack widths approach a value which is directly proportional to the height of the cracks immediately after first cracking."

"(2) At points on the surface of a member perpendicularly away from a longitudinal bar, crack spacings and crack widths will dominantly be proportional to the cover, c."

The first mode above is easily explained if one considers the behaviour of a completely unreinforced member loaded in flexure and axial compression. If the compressive forces are still within the elastic range one would expect cracking and stress distributions as shown in figure 2.12

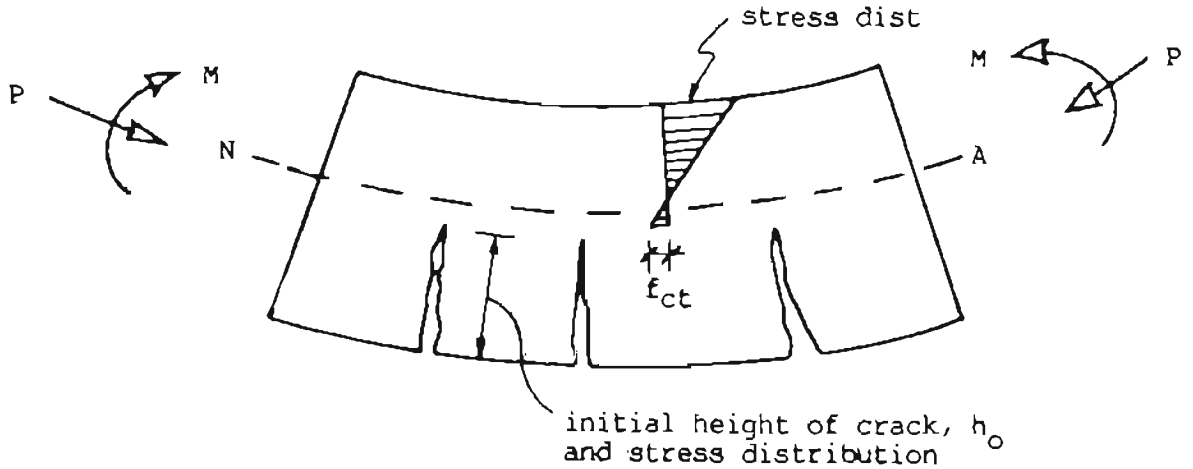

Figure 2.12: Cracking and stress distribution in an unreinforced member subject to flexure.

If there were no applied compressive forces at the ends of the member in figure 2.12, one would expect the member to rupture right through; but by applying the compressive force we immediately have a controlled crack situation. In the normal reinforced concrete situation, in pure flexure situations, the reinforcing may be thought of as providing the missing compressive force needed to provide the stable crack pattern. Since there is likely to be little residual stress in the teeth (figure 2.12) between cracks, the widths of the cracks at any point should be proportional to the distance from the crack tip.

The second mode of cracking is exactly that which was identified by Broms for cracks in close proximity to reinforcing bars. Beeby however has now tried to include some empirical modification functions to allow for internal failure which occurs close to the bar.

Beeby explains the manner of interaction of the two modes with the

idealized diagram in figure 2.13(a) and the way the smaller cracks tend to run into the larger (flexural) cracks in figure 2.13 (b)

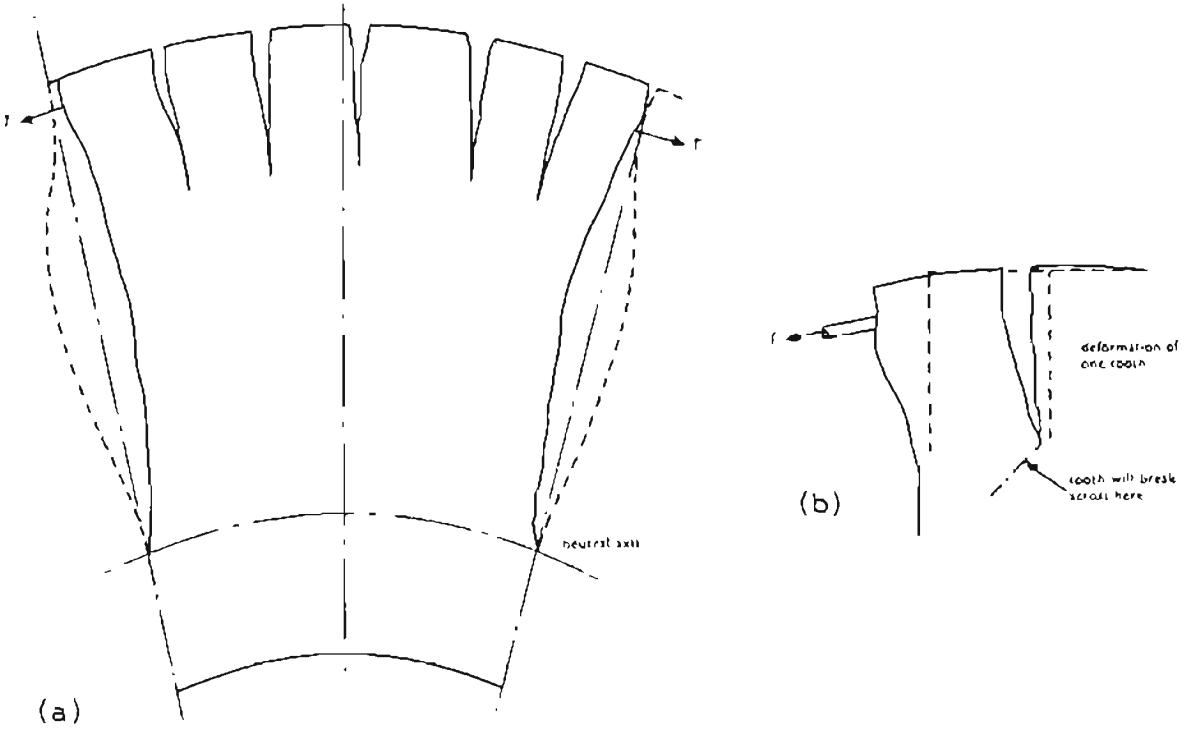

Figure 2.13: Idealized depiction of interaction of two modes of cracking in flexural members - after Beeby (1971)

Although his equations were developed for flexural members, Beeby (1972) investigated their applicability to members subjected to pure tension. He found that these could be treated as limiting cases of flexural members where the initial crack height, h_o , is equal to infinity. Including some further empirical modifications of a minor nature, the final form of Beeby's equations is as given below (taken from Beeby (1971))

$$(w/\varepsilon)_{lim} = k_1 h_o \qquad \ldots (2.20)$$

$$(w/\varepsilon)_o = k_1 c + k_2 \frac{c_2}{2} \sqrt{\frac{c_1}{c_2}} \frac{c}{\beta} e^{-4c/h_o} \qquad \ldots (2.21)$$

$$(w/\varepsilon) = \frac{a_{cr} (w/\varepsilon)_{lim} (w/\varepsilon)_o}{c(w/\varepsilon)_{lim} + (c - a_{cr}) (w/\varepsilon)_o} \qquad \ldots (2.22)$$

$$\iota = w/c + \frac{0.05}{\varepsilon} e^{-0.0135 a_{cr}} \qquad \ldots (2.23)$$

where

w = crack width

ε = surface strain at point considered

$(w/\varepsilon)_o$ = crack width divided by strain where $a_{cr} = c$

$(w/\varepsilon)_{lim}$ = crack width divided by strain where $a_{cr} = \infty$

h_o = initial height of cracks

c = minimum cover

a_{cr} = distance from point considered to the surface of the nearest longitudinal bar

$\emptyset$ = diameter of reinforcing bar

c_1, c_2 = maximum and minimum average covers in the equivalent prism of concrete surrounding the bar as defined in reference (3)

l = average crack spacing

e = base of the natural logarithm

k_1, k_2 = coefficients, the values of which depend on the required probability of the resulting calculated width being exceeded. Values are given in Table 1.

As may be seen, these equations are already fairly cumbersome formulae. For example, Beeby gives the following formulae for calculating the initial crack height of T-beams with one layer of reinforcement.

(The assumptions and notation are as shown in figure 2.14)

$$\beta_n = \frac{x}{d} = \frac{2\alpha_e \rho + \beta_r \beta_c^2 + (1 - \beta_r)\beta_s^2}{2(\alpha_e \rho + \beta_r \beta_c + (1 - \beta_r)\beta_s)} \qquad (2.24)$$

$$\frac{M}{b d^2 f_{ct}} = \frac{\beta_r \beta_n^2 (3 - \beta_n) - \beta_r (3 - 2\beta_c - \beta_n)(\beta_c - \beta_n)^2 - (3 - \beta_n + \beta_s)(\beta_n - \beta_s)^2 (1 - \beta_r)}{6 \beta_n} \qquad (2.25)$$

where

β_n = ratio of neutral axis depth to effective depth (x/d)

β_r = ratio of rib width to flange width

β_s = ratio of flange depth to effective depth

β_c = ratio of distance to root of crack from compression face to effective depth

α_e = modular ratio

ρ = A_s/bd (reinforcement ratio)

b = flange breadth

d = effective depth

f_{ct} = tensile strength of concrete

M = moment

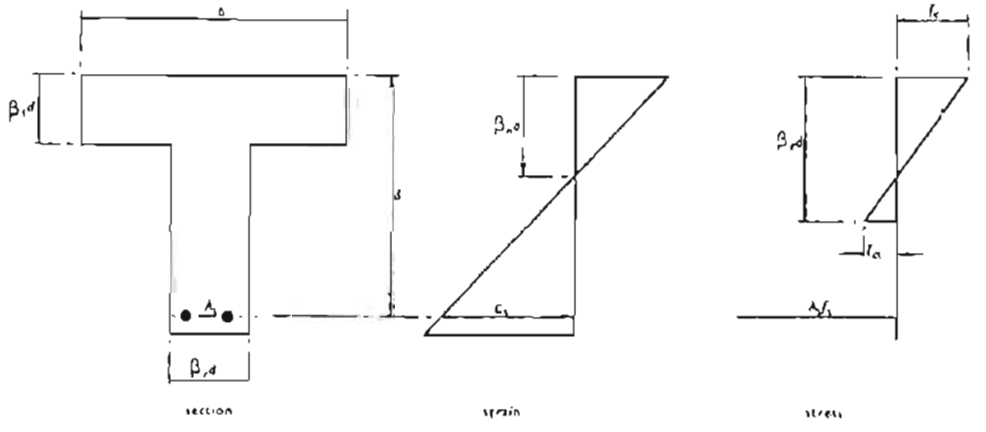

Figure 2.14: Assumptions and notation for calculations crack height - after Beeby (1971).

As shown in figure 2.15 there are two roots to the equation. The initial cracking moment may be calculated by substituting a value of zero for crack height. Then the height to which the crack would jump may be found by iteration.

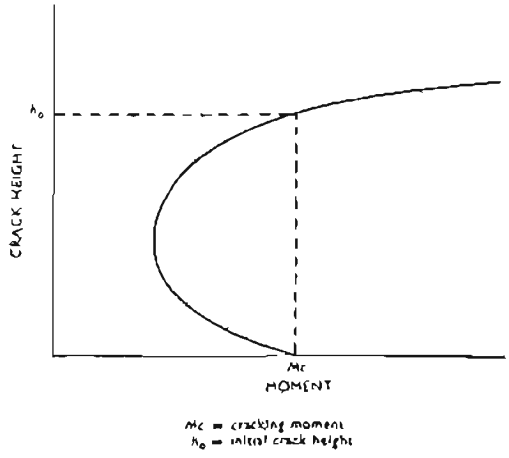

Figure 2.15: Relationship between crack height and moment - after Beeby (1971)

Beeby (1979) uses the concepts of the bond-slip approach (section 2.3.2) and the no-slip approach (section 2.3.5) to derive equation 2.26.

Acknowledging that, with deformed bars "bond" failure takes the form of internal cracking of the type identified by Goto, Beeby states that the minimum crack spacing is determined by cover and then modified towards the average (and then maximum crack spacings) by the addition of a term showing the average influence of internal failure. This justifies the inclusion of both theories into one formula. Therefore:

$$S_m = k_1 c + k_2 \frac{\phi}{\rho} \qquad \ldots (2.26)$$

$$w_m = (k_1 c + k_2 \frac{\phi}{\rho}) \varepsilon_m \qquad \ldots (2.26a)$$

Next, he extends his theory to include flexural members by considering the initial crack pattern that would occur in an unreinforced flexural member (as has been previously described). Applying the 45° rule and the general principle of section 2.3.1 he argues that:

$$h_{cr} \leqslant S \leqslant 2h_{cr} \qquad \ldots (2.27)$$

and therefore $S_m = k_3 h_{cr}$ ... (2.28)

$$w_m = k_3 h_{cr} \varepsilon_m \quad \text{... (2.28a)}$$

where h_{cr} = crack height

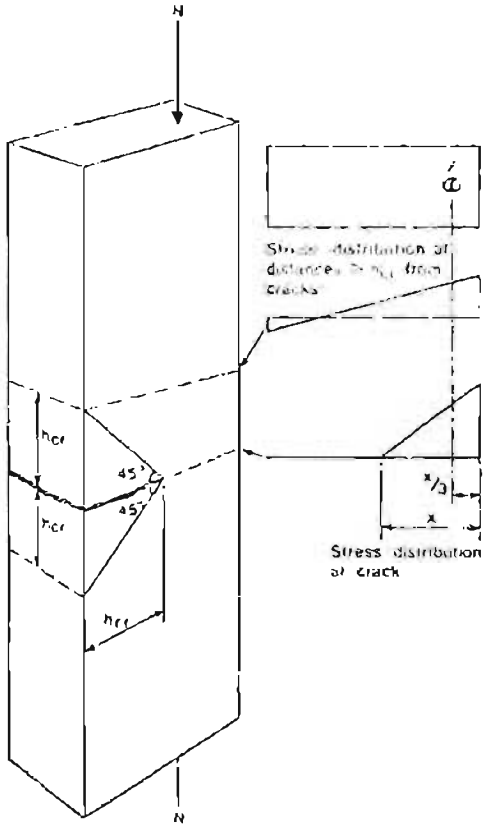

Figure 2.16: Cracking in an unreinforced member - after Beeby (1979).

Assuming that, since the derivation of the first term in eq. 2.26 was the same as that of eq. 2.28, Beeby assumes that $K_1 = K_3$. Now, considering the limiting case where $h_{cr} = c$, because the cracks do not penetrate past the reinforcement the bond characteristics become irrelevant. Therefore, for their situation equations 2.22 and 2.28 may be equated.

$$S = k_1 c + k_2 \frac{\phi}{\rho} = k_1 h_{cr} \quad \text{... (2.29)}$$

Using some logic which, in the writer's opinion, is rather dubious, Beeby now extends equation 2.26 to include flexural cases by including a factor which is a function of (c/h_{cr}):

$$S = k_1 + k_2' f\left(\frac{c}{h_{cr}}\right) \quad \text{... (2.30)}$$

Postulating now that, for flexural members the crack size will be governed by eq. 2.30 near a bar, but approach that defined by eq. 2.28 asymptotically when well away from the nearest bar. Thus he proposes the hyperbolic equation:

$$w = S\varepsilon_m = \frac{a_{cr} w_o w_{lim} \varepsilon_m}{c\, w_{lim} + (a_{cr} - c)\, w_o} \qquad \ldots (2.31)$$

where: a_{cr} = distance from surface of nearest bar to the point being considered

w = crack width at the point considered.

w_o = crack width over a bar given by eq. 2.26a

w_{lim} = crack width controlled by crack (eq. 2.28a)

c = cover

Beeby notes several areas where this theory cannot be applied directly and where he believes further development is required.

(i) For pure tension in walls and slabs, Beeby points out that w_{lim} becomes infinite and that equation 2.31 reduces to:

$$w = \left(\frac{a_{cr}}{c}\right) w_o \varepsilon_m \qquad \ldots (2.32)$$

(ii) The theory does not directly cover cracking in situations where the principal (applied) tension is not parallel to the bars.

(iii) Transverse bars can influence cracking to the extent that their presence can completely override other factors.

(iv) In some circumstances the disregarding of the residual surface strain in equation 2.2 may lead to error.

(v) Different types of bars need their own empirically determined coefficients.

(vi) Prestressed and partially prestressed concrete are not adequately included by the theory.

(vii) Finally, Beeby acknowledges that others, notably Hughes (1970), have come to rather different conclusions when examining cracking due to early thermal movements.

2.3.8 Observations of Leonhardt (1977)

Leonhardt (1977), sums up the theory which appears to be that which has been adopted by the CEB-FIP for their anti-cracking clauses. The theory is based largely on the assumptions of the minimum length of bond required to transfer sufficient stress to cause cracking.

He has taken note of Goto's (1971) observations regarding internal cracks and postulates that these result in length of lost bond, ℓ_o, which he estimates (for ribbed bars) to be:

$$\ell_o = \frac{\sigma_{s,r}}{45}\phi \qquad \ldots(2.33)$$

where $\sigma_{s,r}$ = stress in steel at cracking of concrete in N/mm^2

ϕ = diameter of bars

He proposes an equation that is basically of the bond slip type but is empirically modified to take account of other effects such as cover, bar spacing and the stress distribution in the particular member.

Leonhardt concentrates his thinking on the various factors that influence the jump in stress in the reinforcement at a crack, and in turn, what influence the size of this jump in stress must have on the function governing factors such as the length of lost bond, bond transfer length, initial crack width, etc. Discussing the latter he comments:

> "The testing procedures, like the different pull out tests, which we (have) use(d) so far for measuring this function, have no similitude to the proceedings which actually happen at cracking in structures and can, therefore, not give a correct basis for crack width theories. New methods of testing, imitating this sudden jump in steel stress must be developed for getting the correct physical data."

2.4 CODES OF PRACTICE

2.4.1 British Codes

The following codes of practice all have the same treatment of cracking due to imposed loads on reinforced concrete, with minor variations which will be discussed: CP 110: 1972 (1977), BS 8110:1985, BS 5337:1976 (1982).

The derivation of the formulae used in these codes is given by Beeby (1979). Starting with the equations previously developed by himself Beeby states that these needed simplification before inclusion in the code of practice. Assuming proportionality between crack height and (h-x), and including a coefficient which gave a 20% chance that the maximum crack might be exceeded, equation 2.28a simplifies to

$$w_{lim} = 1.5(h-x)\,\varepsilon_m \qquad \ldots(2.34)$$

Equation 2.26a was more drastically simplified on the basis that the critical crack width does not commonly occur near a bar and that therefore this portion of the prediction formula can be crude. According to Beeby, the influence of cover is far greater than that of ϕ/ρ, hence the term in the latter variable is neglected, giving:

$$w_o = 3c\varepsilon_m \qquad \ldots(2.35)$$

Substituting into equation 2.31 and rearranging we get:

$$\text{Design crack width} = \frac{3a_{cr}\,\varepsilon_m}{1 + 2\dfrac{(a_{cr} - c)}{(h - x)}} \qquad \ldots(2.36)$$

which is the equation given in the codes, except that BS5337 uses a slightly different set of coefficients to allow for a lower (5%) chance of the design crack width being exceeded.

In all cases the codes recommend that the average strain be calculated with allowance for the residual "tension stiffening" which is provided by the cracked concrete around the bars. This concept is discussed in more depth later on.

2.4.2 European Code (CEB-FIP Model Code (1978))

The CEB-FIP have included a formula into their code which is still closely based on the "bond-slip" theory, with extensive empirical modifications to allow for the observed influences of other parameters. In the 1978 model code the formula is:-

$$w_{max} = 1,7 S_m \varepsilon_m = 1.7[2(c + \frac{S}{10}) + k_1 k_2 \frac{\Phi}{\rho_{ef}}].\varepsilon_m \quad ...(2.37)$$

where k_1 and k_2 are constants to allow for type of bar and distribution of stress, and the rest of the symbols are as already defined.

This formula has been retained unchanged in the FIP (1982) draft recommendations on practical design.

2.4.3 American Code

The American Code ACI-318 (1983) mentions reinforcement for prevention of shrinkage and temperature cracking but does not seem to deal directly with calculation of crack sizes due to imposed loads.

2.5 Summary of empirically derived theories of cracking.

The writer, in summing up impressions gained from this survey of formulae for the prediction of crack widths, feels that the most important point to be made is that all of the formulae should be treated with caution. They have been based on experimental data and as such, have an origin in fact. Theories have been advanced in an attempt to explain some of the observed relationships but none of these has been proved rigorously without the inclusion of many severely limiting assumptions.

The writer believes care should be taken that too much weight is not placed on these theories. This review has shown how a great many different relationships can be derived that predict cracking with reasonable accuracy and consistency. Many of these use completely different parameters and have quite different forms from each other.

Some investigators have tried to show that certain parameters are equivalent to each other, for example Kaar & Mattock's "derivation" of their equation, using area as the major parameter, from the more traditional type of equation based on bond stress.

The writer would like to stress that the equivalence of these two relationships was never absolute but rather based on the approximate equivalence of two completely different functions over a fairly small range.

Another way of looking at the problem is to consider whether or not relationships are "objective" as opposed to "subjective". In other words, do they give correct answers regardless of the conditions they are applied in. This has not been shown to be the case for any of the cracking formulae developed to date. Leonhardt (1977) has drawn attention to this fact, and has suggested that new methods need to be developed for obtaining correct physical data in order to have a correct basis for crack width theories.

CHAPTER 3

PREDICTION OF CRACKING DUE TO EARLY AGE EFFECTS

3.1 GENERAL

In considering cracking due to early age effects, we will consider cracking due to internally applied stresses and strains in the concrete. As was described in Chapter 1, when concrete shrinks this only results in stresses if the shrinkage is restrained in some way. Two major groups were identified: those restrained internally and those restrained externally. The derivation of the cracking formulae for externally loaded members has been discussed in the previous chapter. In the following section, some of the differences between these and the two groups of internally loaded members will be discussed.

There are three main causes of deformation in concrete which are more or less specific to the early portion of its life. These are:

(i) Early thermal expansion and contraction
(ii) Drying shrinkage
(iii) Creep

3.1.1 Early Thermal Effects

Concrete gains strength by the hydration of cement with water. This process is an exothermic one involving the release of a considerable amount of energy, known as the heat of hydration. As this heat is not usually dissipated fast enough to the surrounds, especially in large structures, the temperature in the hardening concrete rises, and corresponding thermal expansions occur in all of its components. As the heat does eventually dissipate, the various components contract again to their original size. Since, at the beginning of this cycle the concrete was fully plastic, whilst at the end it is an elastic, brittle material, any restraints imposed during the heating and cooling cycle will have a lasting effect caused essentially by the non-recoverability of the initial plastic deformation that occurs as

the concrete heats up.

Thus there are three factors which can be readily identified as being crucial to the ability to quantify the rise of cracking due to early thermal shrinkage.

(i) The amount of the thermal deformation which is plastic,
(ii) The temperature rise (and subsequent fall)
and (iii) The amount of restraint present.

Point (i) is usually easily dismissed by making the greatly simplifying (and conservative) assumption that the concrete becomes instantaneously elastic at its peak temperature and that at this temperature it is therefore unstressed. Thus all of the cooling cycle has the potential to give rise to tensile stress depending on the degree of restraint and the amount of subsequent creep which takes place.

The amount of the temperature rise is not an easy quantity to predict. There has, however, been considerable experimentation done on this subject and some of these results, as well as ideas of the writer, are discussed in section 3.5.

This leaves us to consider the various forms of restraint and their effects. These were briefly identified in Chapter 1 but are considered now in a slightly more quantified way.

3.1.2. Drying shrinkage

Besides early thermal expansion and contraction due to heat of hydration, concrete is usually subjected to volume changes due to drying shrinkage in the early stages of its life. This gives rise to restrained strains in the concrete that are very similar to those of the thermal shrinkage and unless specifically stated otherwise, the logic applied to analysing for thermal shrinkage applies to drying shrinkage too.

The only differences are as follows:

(i) Drying shrinkage can occur over a longer period of time than thermal shrinkage.

(ii) When the restraint is internal (i.e. due to reinforcement etc.) the relative amounts of straining in the various components will be different to those of thermal shrinkage.

Quantification of the amount of drying shrinkage likely to occur in concrete has been the subject of a considerable body of research. This and the theories explaining the mechanisms and occurence of drying shrinkage are beyond the scope of this thesis and are not therefore dealt with here. It should be noted however that as drying (except surface drying) will normally take much longer than cooling due to heat of hydration, strains due to the latter will dominate in the determination of crack patterns at early ages.

This is confirmed by Hughes & Miller (1970) who say that "shrinkage movement in walls exposed to climatic conditions is small compared with the thermal movement." They found in their tests that shrinkage was less than 40 microstrain after one year.

3.1.3 Creep

Creep is the time dependent deformation of concrete subjected to stress. It is not therefore usually the source of any internal loading but rather, tends to alleviate stresses due to such loading (or any other loading). As with drying shrinkage, its quantification, and the mechanisms by which it occurs, are the subject of a large body of research work which lies outside of the scope of this thesis. In this thesis, its existence is noted, as is the fact that creep is proportional to the amount of applied stress, and the fact that creep occurs much more easily in younger concrete than in old. These facts are considered when developing formulae for the prediction of cracking.

It is also worth noting Hunt's (1971) statement that, "It is now widely accepted that, although creep at low levels of applied load is mainly due to a combination of viscous flow and seepage of the cement paste, at higher levels of load most of the time-dependent deformation

in concrete may be attributed to microcracking and it may be postulated that creep under load is at least partly destructive in nature."

3.2 FORMS OF RESTRAINT

3.2.1 External restraint

This type of restraint gives rise to stress distributions in reinforced concrete that are very similar to those of externally strained systems. Considering figure 3.1 (a), which shows a member fully restrained at each end, we can examine the stresses due to early thermal and drying shrinkage.

During the heating cycle, as has been said, the concrete is largely plastic and therefore deformation takes place freely. Since the reinforcement will be at the same temperature as the surrounding concrete it will expand too. Rather than go into compression because of the external restraint, in any but the shortest of members, the steel will probably buckle slightly to accommodate the increase in length. Thus at the maximumm temperature it can be assumed that there is, for all practical purposes, no stress in either steel or concrete.

On cooling, both steel and concrete will contract. As it will now be encased in hardened concrete, the steel will not simply be able to straighten out again, thus it will go into tension as will the concrete which has now hardened.

This analysis is the writer's and is in contrast to that typically found in the literature where the steel is assumed to be unstressed until the first crack occurs (e.g. Hughes (1980) p.287). Before the first crack occurs, as neither the steel nor the concrete will physically change length there will be no transfer of stress between them regardless of how much restrained strain exists in each. The potential strain in each will be proportional to its coefficient of thermal expansion and because these are fairly similar for steel and concrete the resulting distribution of stress is almost identical to that which is obtained by applying an external load to a completely unstrained system.

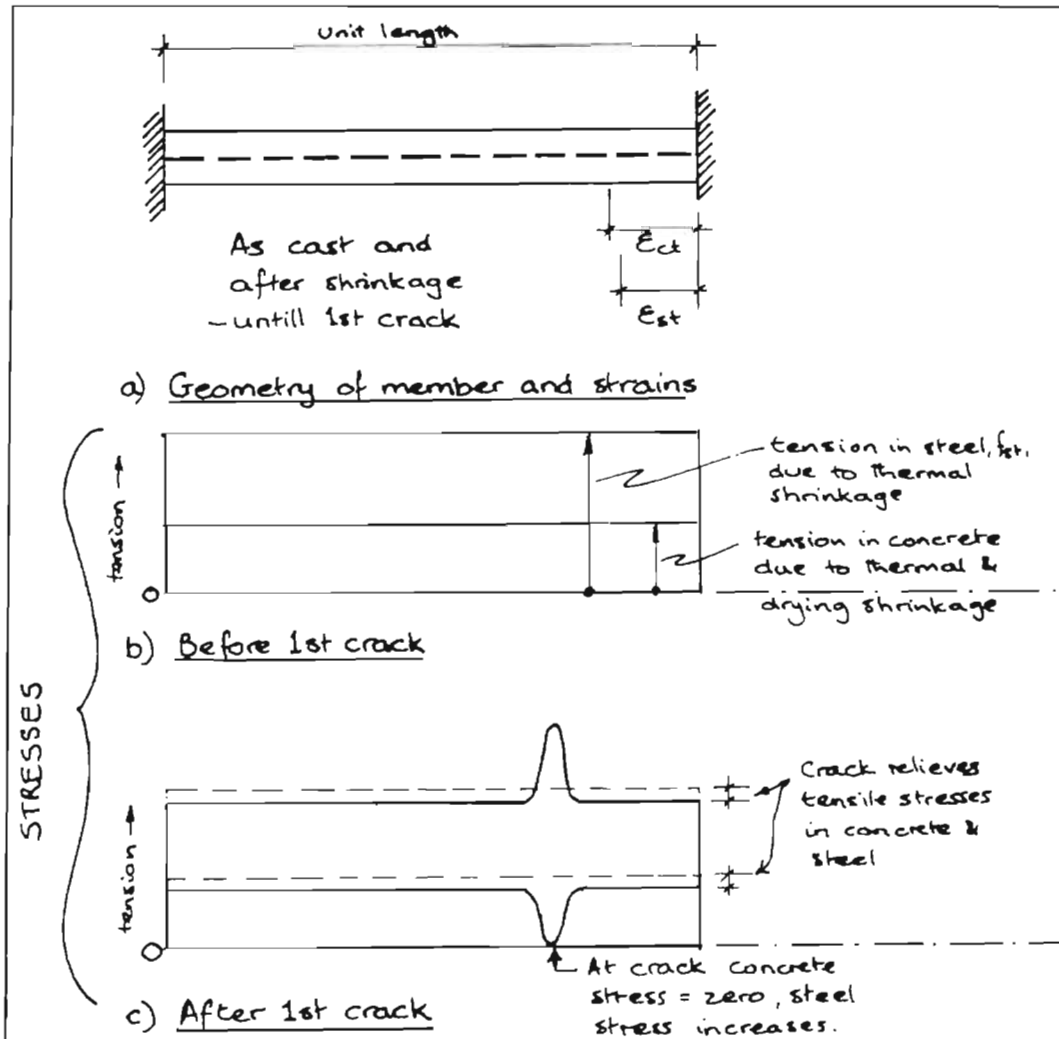

Figure 3.1: Cracking in a reinforced concrete member due to differential external restraint.

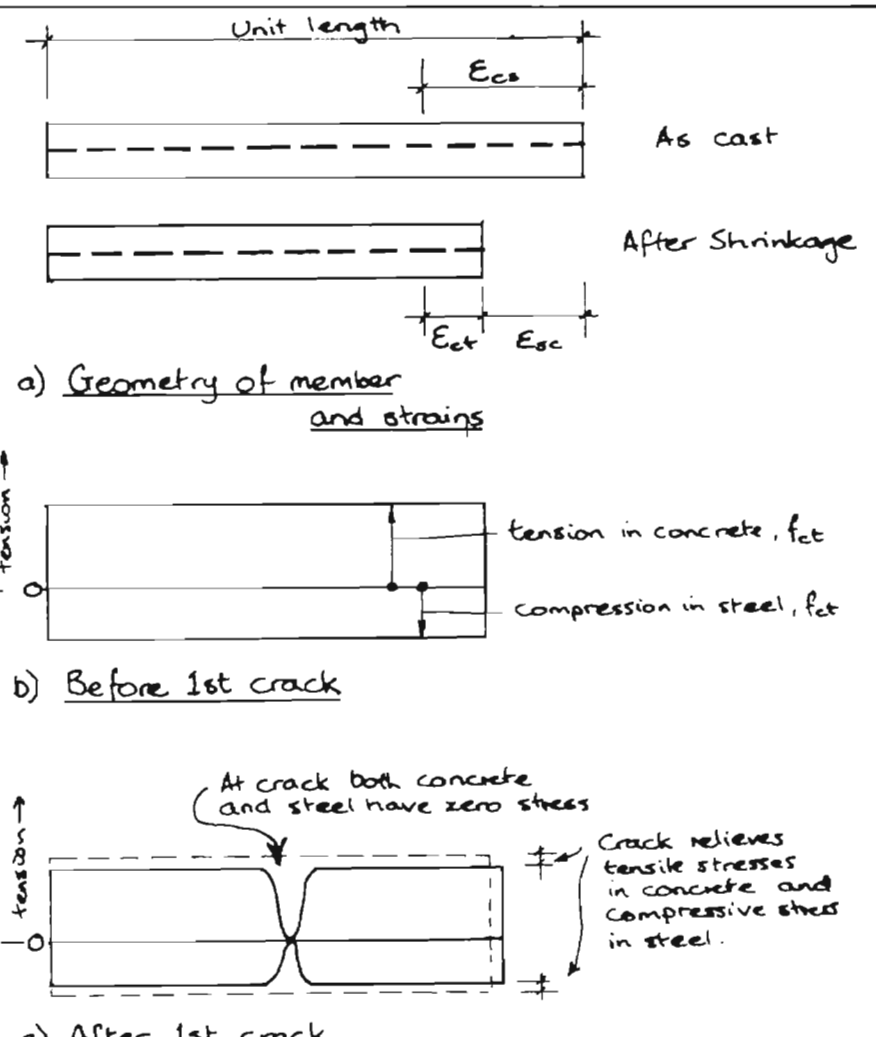

Figure 3.2: Cracking in a reinforced concrete member due to differential internal restraint.

Thus for this type of restraint the approach used for developing theories to explain and predict cracking has been exactly the same as that which was first noted for externally loaded tension members, using the bond slip theory, and the assumption of a stabilised crack pattern.

As a result, the equation for maximum crack spacing due to early age effects which is given in the code of practice for liquid retaining structures BS 5337, has exactly the same form as that derived from those principles and given in equation 2.10, i.e.

$$S_{max} = \frac{f_{ct}}{\tau_m} \cdot \frac{\phi}{2\rho} \qquad \ldots (3.1)$$

where f_{ct} = tensile strength of the concrete.
τ_m = average bond strength between concrete and steel.

As was the case for externally loaded mature concrete where Beeby (1979) reported that it has been found that the tensile strength of the concrete and the ultimate bond strength are proportional to each other for a particular bar type, BS 5337 gives values for this ratio for different types of bar.

Hughes (1980) states that it is here that the essential difference may be found between early age and mature age cracking. At early ages, he says, extensive bond creep can be assumed and the ratio of bond strength to tensile strength for the immature concrete is much lower than that for mature concrete.

The maximum width of crack is again given as

$$w_{max} = S_{max} \cdot \varepsilon \qquad \ldots (3.2)$$

Where determination of the strain, ε, will be discussed in more detail in section 3.4.

Equation 3.1 is reported by Hughes & Miller (1970) as having been developed by Evans and Hughes (1968). Further work by Hughes and Miller (1970) confirmed the earlier findings on the basis of in situ

measurements made on several full scale walls being constructed at the time. In addition Hughes and Miller reported some findings that confirm that cracking due to early age effects requires slightly different treatment to that due to external loads.

(i) They found that the "no-slip" theory does not apply to members in direct tension.

(ii) Bond slip did occur near cracks caused by shrinkage and thermal contraction.

(iii) Further to (i) and (ii) above, they found that the crack width varied only slightly with distance from the nearest bar.

The writer however has identified several problems with the measurements upon which the authors based their formula. These are discussed briefly in section 3.7.

3.2.2 Internal Restraint

This type of restraint includes any situation where there is a difference between the internal strains that would occur in any components of reinforced concrete element if those components were able to move freely. It is the restraint of these "free" strains of various components by each other that gives rise to stresses in the member and the corresponding restrained strains. There are two subgroups into which those types of restraint may be categorised.

(i) Restraint due to varying material properties

Amongst the causes of such stresses and restrained strains are, as before, thermal and drying shrinkages and, usually in a stress relieving manner, creep. The difference, as stated above, is that now it is only the differential amounts of these strains, that have any effect. In the case of differential straining between steel and concrete, this is explained by consideration of figure 3.2.

Here ε_{cs} = the free shrinkage strain in the concrete, for an unreinforced section.

ε_{ct} = the tensile strain induced in the concrete as a result of restraint provided by the reinforcement.

and ε_{sc} = the corresponding compressive strain in the reinforcement.

The manner in which internally restrained members crack and transfer stress on cracking is shown in figures 3.2 (b) and (c). These may be compared with figures 3.1 (b) and (c) which show how the externally restrained member behaves on cracking. The main difference lies in the stress in the steel. It may be seen that very much higher stresses are to be expected when the restraint is external.

(ii) Restraint due to thermal and moisture gradients

In addition to the above, as was pointed out in Chapter 1, there are internal restraints due to differential drying and thermal shrinkages between different parts of the concrete itself.

Many researchers have devoted a great deal of effort to attempting to devise methods for predicting cracking due to this type of strain. A few rules of thumb have been produced. Typically a limit of about 20°C is set as the limiting differential temperature. Figure 3.3 shows two ways in which this can come about.

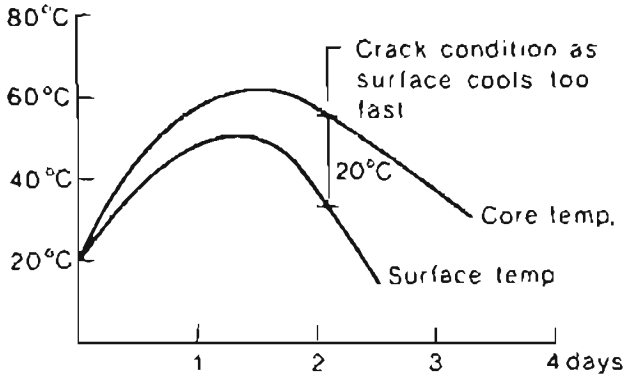

(a) External thermal cracking

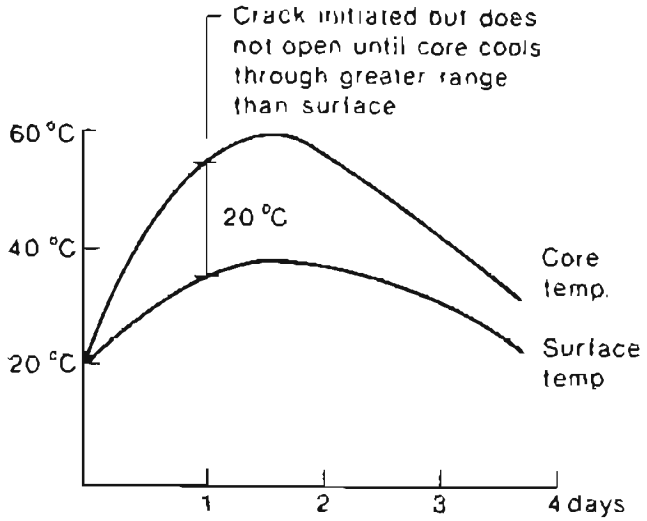

(b) Internal thermal cracking

Figure 3.3 : Cracking due to thermal gradients in concrete - after FitzGibbon (1976)

The real differences then, between predicting cracking in reinforced concrete due to early age effects and normal external loads, may be summed up as follows:

(i) In attempting to analyse for the steel - concrete interactions, allowance must be made for the fact that the elastic, and inelastic, properties of fresh concrete are vastly different from those of mature concrete. In addition these are changing rapidly at these early ages.

(ii) One needs to quantify the thermal and drying shrinkage strains that will take place at early ages.

(iii) One needs to quantify the degree of restraint of the various types previously identified, that will be present in any particular member or, part of a member. It should be borne in mind that the resulting restraints will inevitably be a combination of all of the various types mentioned.

Item (ii) above is reasonably easy to estimate with sufficient accuracy, but the other two make "exact" modelling of early age cracking an incredibly formidable task. Some data on shrinkage and thermal strains are presented in section 3.4 followed by some discussion of the problems of carrying out accurate thermal modelling of hydrating concrete.

3.3 MINIMUM STEEL

A point always made in the derivation of formulae to predict cracking due to early-age effects is that, contrary to the situation with members subjected to conventional loads due to gravity, etc., members where early-age cracking assumes importance usually only have nominal reinforcement. There is, however a certain minimum requirement for steel in order to satisfy the requirements of the theory. This minimum requirement is derived as follows.

The assumption is made that prior to the first crack forming, the concrete is in tension due to thermal and drying shrinkage, whilst the steel is unstressed. (This implies that the stresses are induced by total external restraint of the shrinkage forces, otherwise the steel would be in compression, as shown in figure 3.2. The assumption of zero stress in the steel may be compared with the writer's analysis - section 3.2.1. and figure 3.1). Uniform stress distribution is assumed in the concrete, thus the total tensile force, F, is given by:

$$F = A_c f_{ct} \qquad \ldots (3.3)$$

where A_c = Area of concrete

f_{ct} = tensile stress in concrete.

At a crack this force is assumed to be entirely transferred to the

steel. In addition, it is assumed that the formation of the crack alleviates the stress in the remainder of the concrete and, since the steel is assumed to start with zero stress, this causes the rest of the steel to go into compression. Thus the stress in the steel is given by,

$$A_s f_{st} = A_c f_{ct} - A_s f_{sc} \qquad \ldots (3.4)$$

where, A_s = Area of steel
f_{st} = tensile stress in steel (at crack)
f_{sc} = compressive stress in steel (away from crack)

substituting, $\rho = \frac{A_s}{A_c}$, and rearranging,

$$f_{ct} = \rho(f_{st} + f_{sc})$$

when the concrete and steel reach their maximum values simultaneously the critical ratio, ρ_{crit}, is reached.

$$\rho_{crit} = f^u_{ct} \Big/ (f_{yt} + f_{sc}) \qquad \ldots (3.5)$$

where f^u_{ct} = tensile strength of concrete
f_{yt} = tensile strength of steel (yield)

Neglecting the compressive force induced in the steel away from the crack,

$$\rho_{crit} = f^u_{ct} \Big/ f_{yt} \qquad \ldots (3.6)$$

which is the formula given in the code of practice for water retaining structures BS 5337.

At steel ratios less than the critical ratio, when cracks form, the steel will yield until the stresses in the remainder of the member are reduced sufficiently to restore equilibrium. Thus wide cracks will occur.

The writer suggests thatthis formula will seriously underestimate the tensile force on the steel in the case of a fully restrained section

because of the assumption that there is no tension in the steel prior to the first cracking. It is possible that the reason we have not had more cases of serious cracking occuring is that it is seldom that we get full external restraint of the nature assumed in the development of the formula. The new code for structural use of concrete, BS 8110 (1985), recognises this latter point and gives a table of restraint factors for various situations. The writer warns, however, that use of these factors in conjunction with an equation like equation 3.6 above, is liable to lead to a greater frequency of wide cracks forming.

3.4 QUANTIFICATION OF SHRINKAGE STRAINS

3.4.1 Drying shrinkage

CP 110 (1972) gives the figures of 100 microstrain (at 90% relative humidity) and 300 microstrain (at 70% relative humidity). These figures agree fairly well with those of the CEB-FIP model code (1978) which gives values of the "basic shrinkage coefficient" ranging between 100 and 380 microstrain for the same range of humidities. (for samples in water the CEB/FIP code indicates that this coefficient drops to about 80 microstrain, whilst for samples in a very dry atmosphere, (40% relative humidity) it can go as high as 620 microstrain).

These figures are all total shrinkages, i.e. from casting till time infinity. Typically, for the first year, about half of the shrinkage might be expected to occur, thus the figure found by Hughes and Miller (1970) of 40 microstrain in one year is within the correct range for a well cured concrete.

3.4.2 Early thermal movement

Experimental data reported by RILEM (1981) indicate that the coefficient of expansion of fresh concrete has values of the order of:

20 microstrain/°C	-	freshly mixed
15 microstrain/°C	-	8 to 24 hours old
12 microstrain/°C	-	1 to 6 days age.

For mature concrete they report that the coefficient of thermal expansion is dependent upon the volumetric weighted average of those of its ingredients. The thermal coefficient of expansion of aggregates is less than those for cement pastes and therefore the overall coefficient increases with the richness of the mix. Fulton (1977) confirms this but says the effect of richness of the mix is small.

Fulton (1977) gives the following table of typical values of coefficient of thermal expansion for various South African aggregates:

Table 3.1 Effect of aggregate type on coefficient of thermal expansion of concrete - after Fulton (1977).

Aggregate type	Coefficient of thermal expansion of concrete $\times 10^{-6}$/°C	Reference
Granites and rhyolites	6,8–9,5	7, 10
Sandstones	11,7	7
Quartzites	12,8	7
Limestones	6,1–9,9	7, 9, 10
Marble	4,1	9
Dolerite	9,5	7
Quartz	10,4	9
Blastfurnace slag	10,6	7
Witwatersrand quartzite	12,2	17
Granite from North of Johannesburg (Jukskei)	9,4	17
Dolomite from Olifantsfontein	8,6	17
Malmesbury hornstone from Cape Peninsula	10,9	17
Limestone (50/50 by mass Lichtenburg/ Ulco)	9,7	17
Namaqualand onyx	10,3	17
Dolerite from the Orange Fish Tunnel	7,5	17
Felsite from Witbank	9,2	17

Compared with these values we have the coefficient of thermal expansion of steel of about 10 microstrain /°C (Reynolds (1974)). Thus it is apparent that the amount of differential thermal shrinkage (between different materials) is very small compared to the total thermal shrinkage. This bears out how vital it is to know the degree of restraint applied to any member as it is this that determines the resulting stress in the concrete.

For a typical temperature rise due to heat of hydration of 30°C

(recommended by BS 5337), a typical (high) coefficient of thermal expansion of 11 microstrain/°C, and a fully externally restrained section, we would get thermal shrinkage of 330 microstrain.

This may be compared with almost no effect if there is no external restraint because of the similarity of coefficients of thermal expansion of concrete and steel. In both cases the differential stresses due to thermal gradients must be superimposed onto the other strains.

3.5 QUANTIFICATION OF TEMPERATURE RISES DUE TO HEAT OF HYDRATION

Estimation of temperature rises becomes a very difficult problem in that temperature rise is dependent on very many variables which are impossible to predict accurately at the design stage. Some of these are:

(i) The temperature at which the hydration reaction occurs. Here the initial temperature is required in addition to any subsequent rise as the rate of the reaction is dependent on the current temperature. In addition, if one is to do a proper heat flow analysis, the temperature must be known at all times throughout the sample being modelled.

(ii) The constituents of the cement being used. These affect the heat evolution characteristics of the cement.

(iii) The amount of cement in the concrete.

(iv) The thermal properties of the concrete itself, including thermal conductivity and thermal capacity (or specific heat), as well as those of any shuttering or other insulating material present.

(v) The degree of completion of the reaction. Usually the time since commencement is used to indicate this but to be strictly accurate an indiccation of the actual

percentage hydration is needed.

(vi) Finally, the rate of reaction is also influenced by the amount of self passivation of the unhydrated material from the water in the mix.

A vast amount of research has been done on the chemistry of cements, the nature of their hydration products, the manner of their formation, and the influence of various components on each other. Much is known too about the amount of heat given off by the various components of cements but the writer found that this information is usually given in isolation or seemed to be given pretty much relatively to other components. In the case of complete cement mixes, it is usually given in relation only to time and temperature, in one of two ways.

(i) Total heat given off is measured in an adiabatic calorimeter. With this method no attempt is made to monitor the rate of evolution of heat as the various other parameters listed above change.

(ii) The rate of heat given off is monitored under constant temperature using a conduction calorimeter.

3.5.1 Absolute maximum temperature rise

The first method does give information that is useful for setting an upper bound (regardless of starting temperature) to the amount of temperature rise that might be attained in any sample of setting concrete, if this were to take place under perfect insulation. This situation is approached in very thick concrete sections where, internally, the conditions are approaching an adiabatic situation. Thus the temperature of the concrete will continue to rise for as long as there is hydration of the cement taking place.

Since the amount of chemical energy stored in the unhydrated cement is finite, so too must be the potential temperature rise - even in a closed system. Since the specific heat of concrete is equal to approximately 1 kJ/kg°C and the total heat evolution of cement is equal to approximately 370 kJ/kg, we can calculate the approximate

upper limit of possible temperature rise. (We will use units of °C/100 kg of cementitious material / m^3).

If density of concrete = 2 400 kg/m^3, then to raise its temperature 1°C takes 2 400 kJ.

Since 100 kg cement will evolve 37 000 kJ of heat, the temperature rise = 37 000/24 000 = 15,4°C/100 kg cement/m^3.

This result may be compared to the value of 12°C/100 kg cement/m^3 which is given as the maximum possible temperature rise by FitzGibbon (1976). FitzGibbon's value is derived from site experience with the concreting of sections with least dimension greater than 2m. The fact that his value is less than the theoretical maximum is almost certainly explained by the fact that real concrete pours, even very large ones, do not ever achieve conditions that are perfectly adiabatic. In addition, the last part of the hydration reaction takes place over a very long period, even at very high temperatures. Thus there is plenty of time for heat loss to occur during this time, effectively limiting the maximum temperature rise to a value slightly less than the theoretical maximum.

An empirical formula for calculating temperature rise is that of Davey, reported by Fulton (1977), who cites it as perhaps the best known of similar formulae.

$$t(°C) = 0{,}0034\ Q.R.C. \qquad \ldots (3.7)$$

where Q = cement content in the mix (kg/m^3)
R = rate of lift (m/day)
C = heat of hydration of the cement at seven days (cal/g)

Examination of the validity of the parameters included above indicate some glaringly missing ones. One such is the least dimension of the pour. However since the formula is intended for mass concrete one assumes that the factor, R, is effectively the least dimension.

Another empirical approach is that given by FitzGibbon (1976) who has presented the graph shown in figure 3.4. This ties in with

FitzGibbon's empirically determined maximum rise as well as the theoretical maximum determined by the writer.

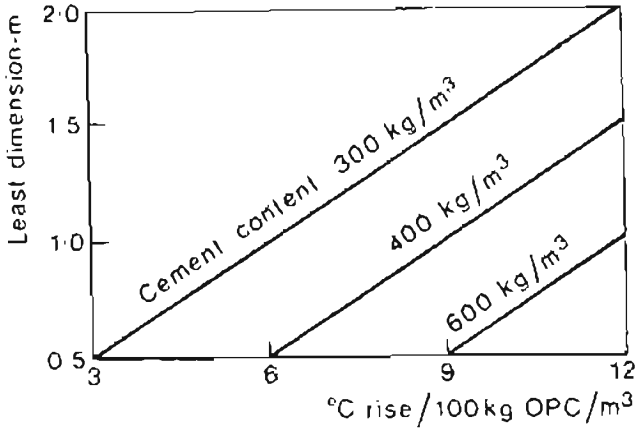

Figure 3.4 : Guide to temperature rise factor for variations in cement content and least dimension - after FitzGibbon (1976).

The writer prefers this graphical presentation as it is much less likely to be incorrectly used than, for instance, Davey's formula. In either case if there is any doubt as to the effect of missing parameters, e.g. starting or ambient temperatures, the writer suggests that it is probably safe to adjust the empirical values slightly towards the value of the maximum possible rise.

3.5.2. Modelling of temperature distributions

Simply knowing the maximum temperature rise is often not sufficient however. In most real cases we are interested in refining this, and calculating, not only how much lower than the upper bound will be our peak rise in temperature, but also, what the resulting gradients of temperature and temperature induced stresses will be.

For this purpose we need to know the rate of evolution of heat. We also need to know how this varies with temperature at various stages of completion of the hydration reaction for the particular cement that we are using. Several researchers have published "typical" curves showing the variation of the rate of evolution of heat with time under isothermal conditions for both complete cements as well as the effects of its various components. For example, the figures given in figure 3.5 are given by Verbeck. These, however, do not show the effect of changing temperature.

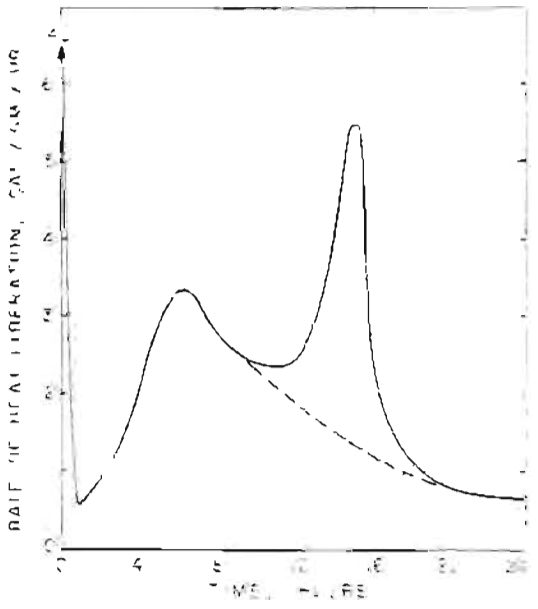

(a) Heat Liberation Pattern of a Portland Cement.

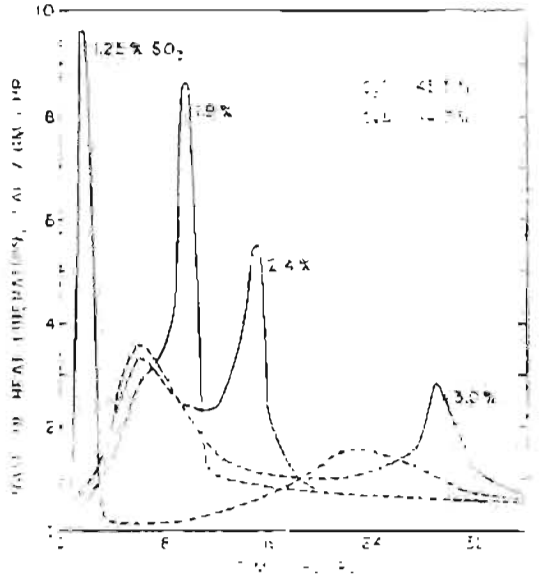

(b) Increasing the Gypsum Content Reduces and Delays the Stage 2 Hydration of the Calcium Aluminate Phase.

(c) The Primary Silicate Hydration Reactions are Retarded in the Absence of Gypsum.

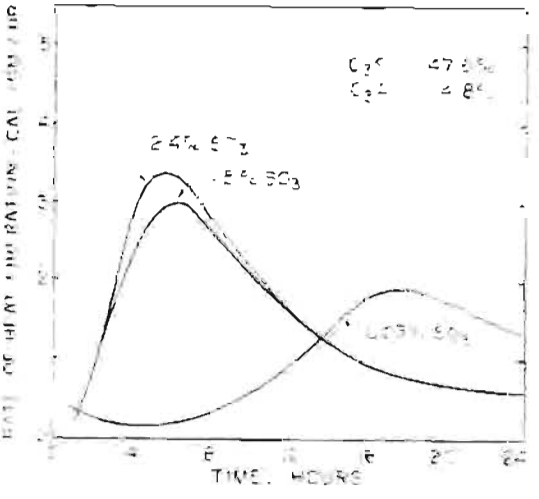

Figure 3.5 : Heat of hydration data under isothermal conditions - after Verbeck (1965)

Without going into the chemistry of cement in some detail, which is a topic outside of the scope of this thesis, discussion of the various peaks is rather meaningless. The reader is referred to Verbeck's paper as well as some excellent books such as those by Bogue (1947), Czernin (1962), and Lea (1970). The only information that the writer could find that did give some idea of how the rate of heat generation varies with both temperature and progression of the reacton is presented in figure 3.6. This was reported by Loedolff (1977) as originating from Weaver (1971).

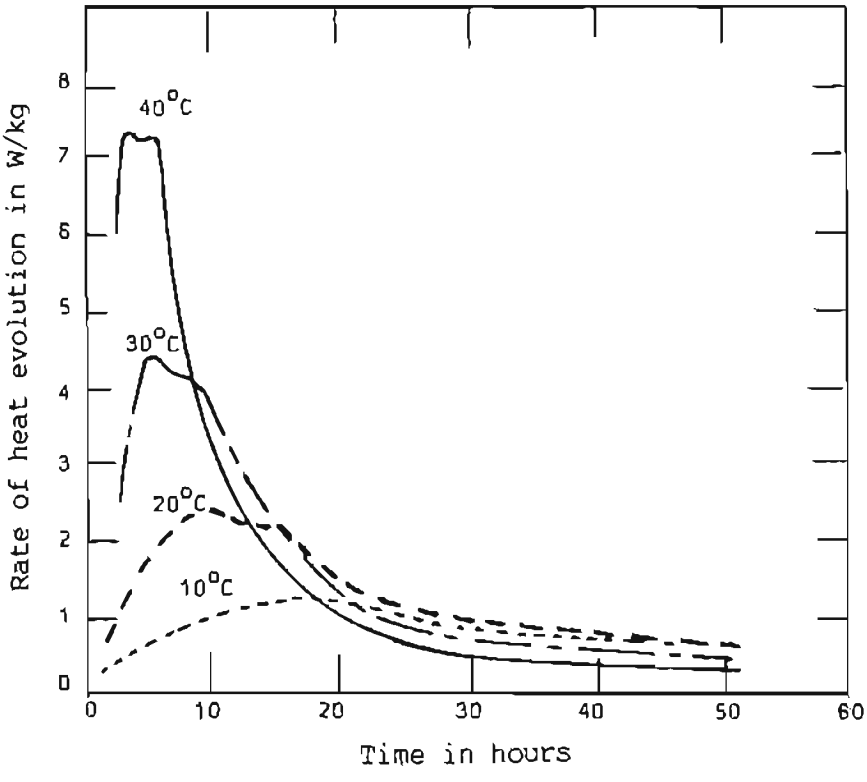

Figure 3.6: Rate of evolution of heat against time for different starting temperatures (normal Portland cement with w/c = 0,50) - after Weaver (1971), reported by Loedolff (1977).

Loedolff does not specifically say that these curves are the result of measurements made at constant temperature but for the sake of the following discussion it will be assumed that this is the case. These curves do have shapes that are similar to other "typical" curves that were found by the writer, except that the first peak (on wetting) is omitted and the next two are rather closer together than indicated by, for example, Verbeck's curve.

A problem with this type of curve is that the parameter chosen to indicate the degree of completion of the reaction is time. This is fine when all other variables remain constant but does not work when any variable (such as temperature) changes. Numerous "maturity functions" have been suggested in an attempt to define the extent of cement hydration reactions (Rilem (1981)). These have been developed to enable predictions to be made of concrete strength at any age when strength at a particular age is known. Since the strength clearly depends almost entirely on the degree to which the hydration reaction

has proceeded, it seems reasonable that the same functions should be usable for determining the latter parameter directly.

Knight (1973) and Muller (1984) have found that the product of time and temperature is a good indication of the maturity of concrete. They have used this value as a guide to the time of stripping of formwork. By considering the fact that there is a maximum total amount of energy able to be released via the hydration reaction, one can prove theoretically that the degree of hydration cannot be exactly related to the time - temperature product. However, during the time when the reaction is proceeding at its fastest pace, i.e. in the first day or two, the approximation is fairly good. Figure 3.6 could therefore have been plotted using maturity (= time x temperature) instead of time as a variable on one of the axes.

It is only from this type of curve that a suitable empirically based formula for use in more exact analysis of heat flows may be obtained. These analyses might be done, for example, by the finite element method where one needs an expression to indicate the rate of heat input at any point in the sample. From the previous discussion it is evident that this rate must be a function of at least two variables - temperature and maturity.

3.6 CODES OF PRACTICE

All modern, limit state based codes of practice include provisions to prevent shrinkage cracking to some degree. BS 5337 is the most explicit of the codes in this regard and, clearly the consequence of cracks in liquid retaining structures is most severe. CP110 (1977) takes care of these shrinkage strains by simply specifying minimum percentages of steel.

BS 5337 gives the user the option of calculating the minimum percentage of steel either on the basis of simply a minimum quantity to ensure the steel does not yield at a crack, or, for amounts of steel greater than this minimum, based on the expected distributed crack widths. (These formulae have already been discussed in sections 3.3 and 3.2 respectively).

BS 8110 (1985) is as for CP110 but also includes a provision for calculating thermal crack widths due to external restraint. Restraint factors are given for various situations and the resulting "restrained" strain used in the formula for predicting cracks due to external loads.

The CEB-FIP Model Code (1978) also has the same formula for minimum steel requirement as the "British" codes but does not otherwise have any specific way of calculating reinforcement required to distribute cracks due to early age effects. This is kept unchanged in the draft version of the FIP recommendations for practical design (FIP (1982)).

The American Code ACI 318 (1983) simply specifies minimum percentages of reinforcement which are held to be sufficient to distribute cracks due to early thermal and drying shrinkages.

None of the codes includes any explicit way of calculating for the effects of internally induced strains. Another failing of the codes, and in the writers opinion this is probably the most severe, is that they generally class reinforced members into one of the following two categories:

(i) Externally loaded, therefore well reinforced and early age effects are negligible compared to the total.

(ii) No external load, therefore only early age effects important in determing nominal steel.

There are, of course, cases which fall between these two, where both the early age effects and the subsequent applied loading have similar importance. Typical examples are circular reservoir walls cast on rigid bases (such as an earlier lift) where the restraint forces can be as high as or higher than the ring tension forces due to subsequently applied hydraulic loading. In such cases the reinforcement requirement for each loading condition must be <u>added</u> to arrive at the total reinforcement requirement. (i.e. the effect of tensions due to restraint by a lower section of wall is not the same as prestressing the wall). This is not spelt out in the codes.

3.7 SUMMARY OF THE STATE OF KNOWLEDGE OF EARLY AGE CRACKING

The existing formulae for the prediction of early age cracking have been shown to be in actuality a subset of those that have been developed for predicting cracking of externally loaded members. As such they only really take account of cracking where this is due to external restraint (which amounts to an externally applied load). The various types of internally applied restraints which have been identified, are not catered for by the formulae at all, whereas the examination of the quantity of these internally restrained strains has shown that they are not neccessarily insignificant.

Study of a typical series of experiments carried out on reinforced concrete walls by Hughes and Miller (1970) shows that, with the best will in the world, it is almost physically impossible to gather enough data to make a proper analysis of the problem. Even though Hughes and Miller measured a very comprehensive set of strains and temperatures in the walls they studied, the writer believes that these do not go anywhere near defining the walls' full behaviour. Two significant areas exist which severely limit the value of this type of experimental result.

(i) Determination of restrained strains

The actual degree of external restaint was not known or rather, it varied in both the vertical and horizontal directions over the full area of the walls. Measuring the strain in the reinforcement is of only limited value as, with 100% effective external restraint (the worst case), there will be no measurable strain in the reinforcement. This, as previously discussed, is because the strain takes the form of restrained strain and no movement takes place (or more accurately, as thermal shrinkage takes place, the external restraints counteract it exactly by strain in the opposite direction).

The writer suggests therefore that the only way that an indication may be obtained experimentally as to the effect of restrained strain is by parallel construction of a completely unrestrained section of similar properties to the

one being monitored, and which is subjected to external restraint.

Measurements of strain taken on reinforcement subjected to only internal shrinkage effects actually give an indication of the unrestrained portion of these strains, which is the exact opposite of those strains which are implied in the formulae for calculation of crack widths.

(ii) Determination of secondary strains

Into this category the writer includes those strains which come about as a result of differential thermal shrinkage, differential drying shrinkage and strains due to steel concrete interaction at cracks. Measurements such as those taken by Hughes and Miller (197) might give an indication of the relative straining of steel and concrete due to the first three, but become hopelessley inadequate when considering the last. The problem essentially is that all that has been physically measured to date has been over gauge lengths that are far too long to be specific to any one area in a situation where strains are expected to change rapidly.

As a result of these observations, especially those in (i) above, the writer finds it difficult to accept that the formulae derived have much basis in either experimental fact or correct logic. The logic only applies to half the problem and as explained in (i) above, the experimental data against which it has been checked appears to be flawed.

In addition, as was observed in section 3.3 the formula for calculating minimum steel quantities appears to the writer to be based on an incorrect assumption which could lead to significant underestimates of "nominal" steel. The codes generally fail to take account of "restrained strains" due to internally applied restraint. They also fail to point out that there are some cases where the forces acting on a structure due to restraints may be of a similar magnitude to those due to externally applied loads. Even though stresses due

to the latter might be dissipated by the action of creep, the cracks will not and the final crack size will be the result of the cumulation of these effects.

When it comes to trying to include all of the internal differential straining effects into a simple formula, the writer believes that there is no easy way forwards. Because of the very small scale on which large changes of stress occur in the vicinity of cracks and reinforcing bars and the problems associated with measuring these physically, it is not easy to gain further insight into the mechanisms of cracking under these circumstances by experimental means.

In the next chapters the proposal is made, and partially followed through, that theoretical modelling using the finite element technique might be a way of studying some of these phenomena that defy physical measurement.

CHAPTER 4

CONSIDERATION OF THEORETICAL MODELLING

4.1 JUSTIFICATION OF THE CHOICE OF COMPUTER MODELLING OVER EXPERIMENTAL MODELLING

The literature survey, reported in chapters 2 and 3 has identified many quite widely differing theories which attempt to predict crack widths based on experimental evidence. As discussed in the summary of chapter 2, there is a general lack of cohesiveness in the theory (or theories) which intimates that it would not stand up too well to rigorous analysis if this were possible. In chapter 3 it has been shown that the only theory used for early age cracking is really a subset of those developed for cracking due to external loads. The more specific problems of early age cracking have not been addressed by the theory at all.

In the addendum the writer has attempted to set down what he believes to be the underlying cause of the lack of objectivity of the empirical formulae.

It is worth considering some of the problems associated with experimental investigations of cracking.

(i) One of the major problems of lab experiments is that it is very difficult to monitor what is happening inside a test member. Thus the exact mechanism of formation of cracks and crack patterns is still unsure.

(ii) Cracks are inherently very small and difficult to measure. In the early stages of cracking when the cracks are microscopic in size, they are difficult to identify at all.

(iii) Lab tests are very time consuming. A completely new test is required each time a parameter is altered even slightly.

(iv) Each test has to be repeated several times to remove random errors from the results.

(v) It is not usually practical to vary only one parameter at a time in experimental tests.

As a result of the above considerations, and in view of the fact that an enormous amount of empirical investigation has already been done on the subject of cracking in concrete, the writer proposed analysing a series of mathematical models of reinforced concrete being subjected to cracking stresses. These would be modelled by computer using the finite element method and, as far as possible, would make use of the latest available constitutive models for concrete.

The advantages of using finite element models as opposed to laboratory models are as follows:

(i) Interference by random occurences on results is eliminated. Once specified, material properties and loading characteristics are consistent.

(ii) As a result of (i) above, one is much more readily able to isolate particular parameters for study than is the case in a laboratory.

(iii) One can "see" what is happening inside a finite element model.

(iv) Effects of small changes can be studied relatively quickly.

Disadvantages of using finite element models include the following:

(i) Although they are being improved rapidly, the available constitutive models of concrete for use in finite element packages are still far from perfect. Indeed, concrete, being an unhomogeneous material, does not lend itself to exact modelling of its properties.

(ii) Numerical instabilities can and do occur in mathematical models, especially where the events modelled are of a highly non-linear nature, as is the case with cracking of concrete.

Despite the disadvantages, it was thought that by carrying out a suitable series of finite element analyses it would be possible to gain a significant amount of information about the mechanisms involved in crack formation around reinforcing bars. It was hoped too, that as a result, it might be possible to establish the validity or otherwise of some of the relationships postulated between cracking and various parameters by the empiricists.

4.1.1 Verification of analysis results

Obviously, any results obtained from a theoretical analysis using slightly suspect analytical tools is useless unless verified in some way. The original plan was to verify the results by:

(i) Comparison with published work,
and (ii) by carrying out some selected "control" lab tests.

In the event, time has not permitted that all of the desired computer modelling be carried out, let alone full verification of the results. The results that have been obtained are compared in fairly general terms to the data available in the literature and their validity is discussed. Even based on this work a considerable amount has been learned that should be of benefit to future researchers in the field.

4.2 BRIEF HISTORY OF THE DEVELOPMENT OF CONSTITUTIVE MODELS FOR CONCRETE

The development of the finite element method has spurred a tremendous amount of research work on the development of various mathematical material models, or constitutive models. One of the materials that continues to defy accurate modelling is concrete. Great strides have however been made since the earliest days when only linear elastic analyses could be carried out.

Ever since concrete has been used as a construction material, its most obvious non-linear property, that of fracturing under fairly low tensile stress, has been well known and allowed for in design. Traditionally designers and analysts have assumed that concrete fails at some limiting tensile stress and for most purposes this assumption is adequate.

As early as 1920, the Griffith theory of fracture mechanics was postulated which predicted that a brittle material would rupture when a critical strain-energy-release rate was reached. At this point the rate of release of strain energy on fracturing would be at least equal to the rate of increase in free surface energy due to the formation of a new crack. Kaplan (1961) was the first researcher to attempt to apply this concept to concrete, concluding that the concept of a critical strain-energy-release rate was a valid condition for fracture of concrete.

Since that time researchers have tried the application of several different criteria for the modelling of the propagation of discrete cracks. Hillerborg et al (1976) cites several of these:-

(i) The stress intensity factor approach. Here the stresses near the crack tip are studied. These theoretically approach infinity near the tip according to the expression.

$$\sigma = K/\sqrt{2\pi r} \qquad \ldots (4.1)$$

where r = distance to the crack tip

K = stress intensity factor. (At $K = K_c$ the crack propagates).

Drawbacks of this method are that a very fine mesh is required at the crack tip, and also, more seriously, the method does not predict crack formation, but rather only their propagation.

(ii) The energy balance approach. This method has been briefly described above. This method too, has the

drawback that it does not predict the formation of new cracks.

(iii) The "strip-yield" model according to Dugdale. This method assumes that there is a plastic zone near the crack tip as shown in figure 4.1

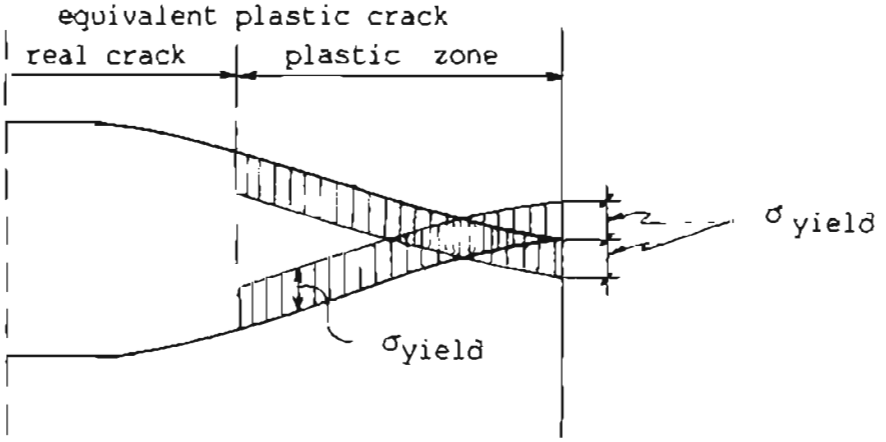

Figure 4.1 : Dugdale model for crack tip plasticity after Hillerborg et al (1976)

(iv) The cohesive force model according to Barenblatt. This is similar to the Dugdale model but the stress in the "plastic zone" of the crack is assumed to vary with the deformation.

Hillerborg et al carried out some F.E. analyses using models similar to that of Barenblatt. The basic idea of this model is shown in figure 4.2.

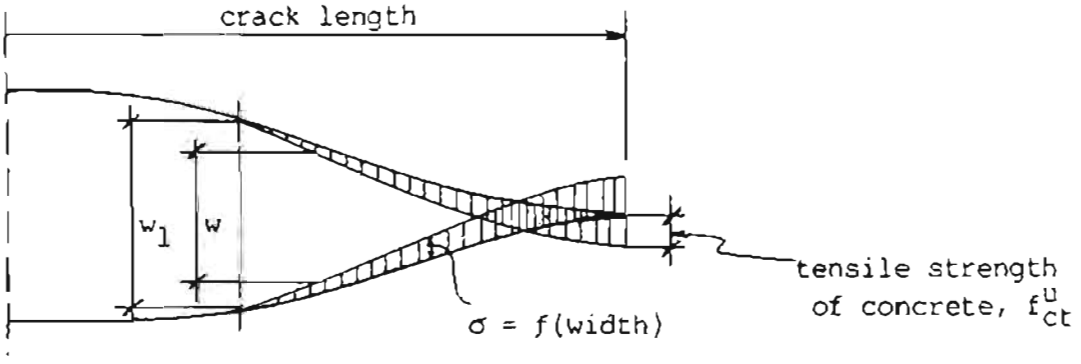

Figure 4.2 : Fracturing model after Hillerborg et al (1976)

Integrating, to obtain the amount of energy absorbed in opening the crack, the energy per unit crack area is

$$\int_0^{w_1} \sigma dw \qquad \ldots (4.2)$$

This can now be equated with the critical strain energy release rate, G_c , which would mean that the energy absorbed per newly formed crack would be the same as in the energy balance approach, indicating equivalence of those methods. In addition the assumption of gradual decline of stress with the opening of a crack is a reality. This is discussed in greater detail in section 5.1.1.3 on tension stiffening and strain softening.

In contrast to the other methods listed above, Hillerborg's method models not only the propagation of existing cracks but also the formation of new cracks. These are assumed to form when the tensile stress reaches , which is the same criterion used to determine the propagation of the cracks.

Besides the fact that concrete cracks in tension, it exhibits non-linear behaviour in other ways. Its failure in compression is essentially plastic in nature and various models have been proposed to predict this. Of greater concern to this thesis however, is the fact that, prior to cracking in tension, the behaviour of concrete is not strictly elastic.

It is generally accepted that the inelastic behaviour exhibited by concrete prior to cracking in tension is in fact the result of the formation of very many microcracks which begin to coalesce into fewer, larger cracks as the stress approaches its maximum. In addition, as has already been noted, it is now accepted that as these larger cracks form, the stress across them does not fall immediately to zero. As was shown earlier, an energy based fracture criterion seems to take care of the latter non-linearity of concrete's behaviour but provision must also be made for its non-linear behaviour prior to cracking.

Chen and Chen (1975) have produced a concrete model that is essentially a modified plasticity theory to explain the general non-linear behaviour of concrete. This model has the drawback that it

does not incorporate a very good model of the actual formation of discrete cracks, in that it does this by a simple tension cut off which causes the stress to drop immediately to zero.

Others have devised non-linear fracture mechanics models to include the non-linear behaviour of concrete. Recently, more cognizance has been taken of the progressive manner of concrete failure by microcracking, and "damage mechanics" models have been developed which use a "damage" parameter as the controlling influence for the progressive degradation of concrete's elastic properties. (e.g. Resende (1985(a))).

Besides making advances on the actual material models, researchers have had to devise ways of applying these using the finite element technique. A significant problem is how best to represent fracturing of concrete. Two techniques are used, namely:

(i) discrete cracks
(ii) smeared cracks

Bazant and Cedolin (1979) noted that modelling cracks as smeared rather than discrete, offers considerable savings in complexity in the formulation of the finite element model. The main saving is a practical one in that all that needs to be changed after cracking occurs is the element stiffness whilst with discrete cracks, one has to cope with topological changes which necessitate node renumbering. Besides this, a very important point in favour of smeared cracks is that the direction of the cracks does not have to be known in advance (discrete cracks between elements can only proceed along element boundaries.)

Modelling cracks as smeared over a finite zone of the concrete continuum also presents problems as the width of the crack front has an influence on its propagation. Bazant and Cedolin (1979, 1980) considered the objectivity of various ways of predicting cracking. They concluded that stress cannot serve as an objective propagation criterion for the propagation of an element-wide crack band. This is explained as follows: if we consider finer and finer meshes, then the

stress concentration just ahead of the element-wide crack band increases, approaching infinity as the element size tends to zero. The authors continue that "In general, failure criteria in terms of stresses (strength criteria) are objective only if they are of the plastic type, i.e. if the stress is kept constant after attainment of the failure criterion. If the stress is reduced, however, the criterion is unobjective." Bazant and Cedolin introduced an energy criterion for their crack band model which they found was objective in that they found that their results were independent of the element size chosen. They state that although the application of fracture mechanics to concrete has been doubted by experimentalists, it is definitely applicable to large structures such as reactor vessels. For smaller structures, they say, one is in a transition region from the energy criterion to the strength criterion, which applies for a certain limiting small size at the limit of continuum modelling. For a reinforced concrete composite the authors found that the fracture energy criterion changed, but this is of little concern to this investigation where only cracking in unreinforced concrete is to be considered, albeit in very close proximity to reinforcement, and as a direct result of the presence of the reinforcement.

Kostovos and Newman (1981) have investigated the fracturing of concrete under various states of triaxial stress and developed a model of the fracture processes under generalised loading conditions. This is an area where there is not yet sufficient experimental data available however and is the subject of ongoing research.

Nallathambi et al (1984) have investigated the effects of size, as well as the effects of water/cement ratio and coarse aggregate texture on the fracture toughness of concrete.

4.2.1 Size effect

It has long been known that the size of structures can have an effect on the stresses at which they fail. Indeed this was really the primary reason for the development of the fracture mechanics approach over the simple strength criterion for determining failure. Where the latter does not predict any effect due to size, the main purpose of the former is to do just this. Bazant and Kim (1984) have found that

linear elastic fracture mechanics greatly overestimates the effect of size, and have found that non-linear fracture mechanics can greatly improve this situation. Figure 4.3 shows a plot of log of failure stress against the log of the characteristic dimension for the three methods of predicting failure.

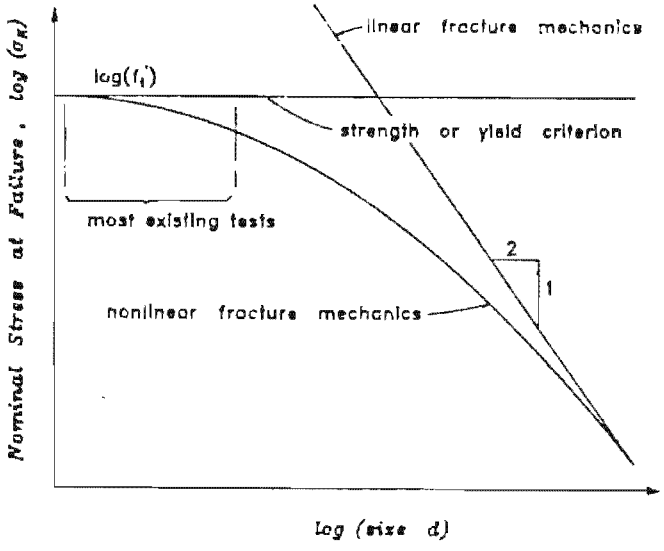

Figure 4.3: Illustration of prediction of size effect by various models - after Bazant & Kim (1984)

The authors report that Bazant has found in previous work that the structural size effect is related to the ratio of characteristic dimension to maximum aggregate size (d/d_a). This sounds plausible when one considers the strong effect on cracking which the aggregate has. Firstly, cracks tend to form on the aggregate-paste interfaces and secondly, the micro-cracking and subsequent fracturing happens in the spaces between the aggregate (for normal strength concretes). Thus, indirectly, the aggregate size determines the size and frequency of flaws in concrete which is essentially what size effect is all about.

4.3 PREVIOUS ATTEMPTS TO MODEL CRACKING AROUND REINFORCING BARS AS A CONTINUUM PROBLEM.

Prior to the development of the finite element technique, because of the complexity of analysing for the actual stress distribution in cracked and cracking concrete around reinforced bars most researchers made the kind of simplifying assumptions that allowed their theories

to be based on a simpler, single value such as the surface stress in the concrete. Having only one value of stress to worry about at any particular distance along a reinforcing bar away from a primary crack certainly was easier to visualize, not to mention portray, on paper (for example see figure 2.4).

Several researchers made attempts to model the stresses in the concrete as stress in a continuum rather than simply assuming some distribution of surface stress as portrayed in figure 2.4.

Broms (1965(a)) devised a method of injecting resin into cracked members whilst they were still under load. When they were unloaded and cut open he discovered the presence of internal cracks and also the fact that new primary cracks appeared to grow from the bar outwards to the member surface. Figure 4.4 shows a typical example of his test members.

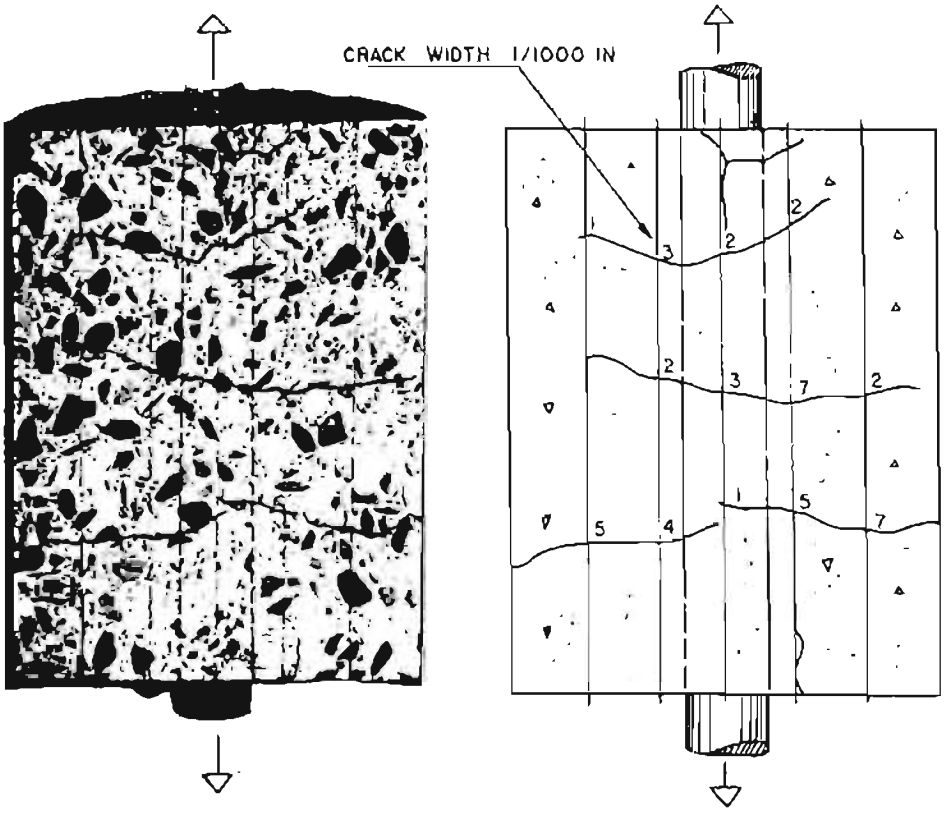

Figure 4.4 : Crack formation in singly axially reinforced cylindrical tension member - after Broms (1965(a))

In the next paper of a series Broms (1965(b)) attempted to analyse for the actual stress distribution in members with tension cracks. His analysis carried out on a model as shown in figure 4.5(c) which was

intended to represent a portion, between primary cracks, of the tension member in figure 4.5(a) cracked as shown in figure 4.5(b).

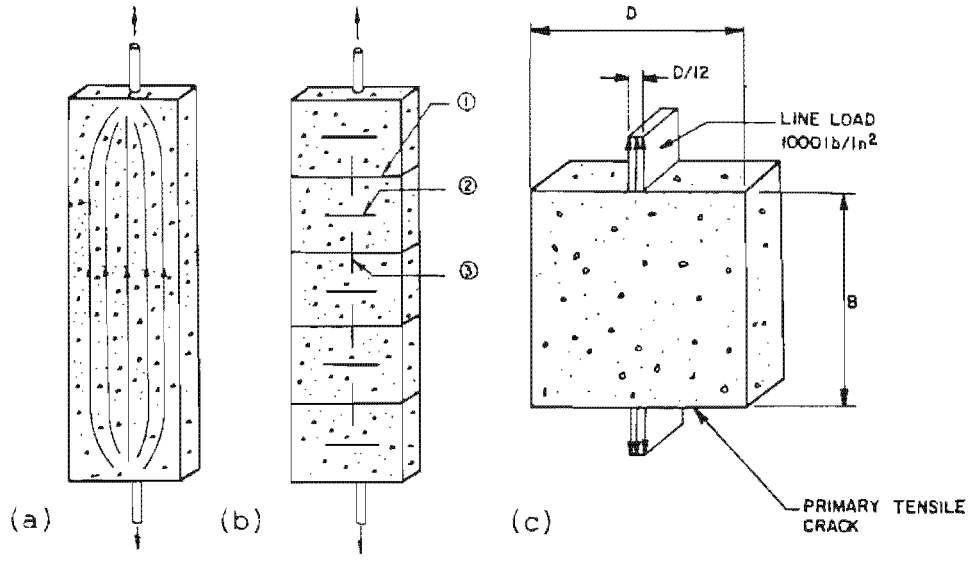

Figure 4.5: a) Uncracked tension member and c) model of concentrically loaded portion of tension member between two cracks - after Broms (1965(b))

Although an enormous step forward from the consideration of only the surface stress of the concrete, Broms's analysis was fairly crude in that:

(i) the concrete was assumed to be linear elastic.

(ii) the analysis was two dimensional (plane stress) with the load being applied as a strip load on either end of the section under analysis rather than over two circular areas of finite size (as in a 3-D or axisymmetric case).

(iii) The model represents only a section of concrete and does not include any way of representing the steel.

(iv) Broms only analysed for stresses in the directions parallel and perpendicular to the applied load. The shear stress distribution was not reported on and thus, neither were the resultant maximum or minimum principal stresses or their directions.

Some of the results that were obtained by Broms are shown in figure 4.6. They appear to confirm what he had already discovered experimentally - i.e. that cracks seem to propagate outwards and not inwards from the surface.

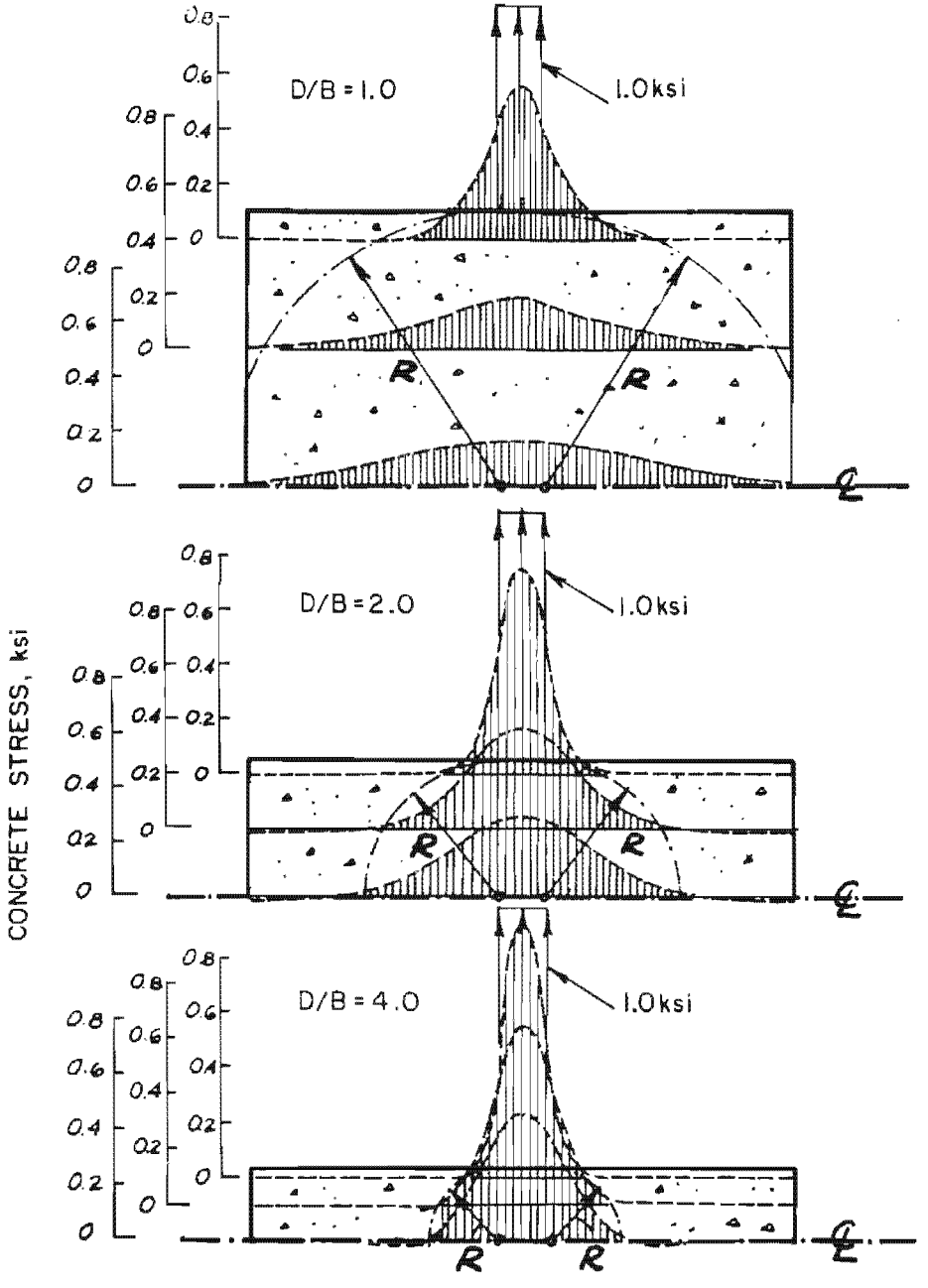

Figure 4.6: Calculated longitudinal stress distribution in concentrically loaded tension members - after Broms (1965(b))

As may be seen in figure 4.6, Broms noted that if one drew a circle at any point along the reinforcing bar, using the distance to the nearest primary crack as radius, the circle would encompass the whole area that was subjected to any significant amount of stress. This tied in

well with his observations of how far cracks would propagate in any given circumstance and led to his proposal that this distribution of stresses explained the apparent proportionality of crack widths and spacings to cover.

The potential for carrying out significantly better analyses than those attempted by Broms only really came about with the development of the finite element technique.

Amongst the earliest workers to attempt the application of the finite element technique to cracking were Ngo and Scordelis (1967) who used a linear elastic constitutive equation for the concrete. They then had to manually insert the cracks into the model as initial boundary conditions (i.e. as discontinuities between elements). The bond between the reinforcing and the concrete was modelled by inserting a "bond slip" element (also linear elastic) into the interface.

Despite the obvious shortcomings of their model, Ngo and Scordelis stated in their conclusions that "From the results it can be seen that the finite element analysis offers a complete picture of the stress distribution in the entire beam, which generally cannot easily be obtained by other analytical or experimental methods."

Lutz (1970) carried out an elastic axisymmetric finite element analysis on a short cylinder to model the conditions in concrete between two flexural cracks. He was aiming to "obtain quantitative information on and an understanding of the stresses and deformations that occur in the vicinity of reinforcing bars after transverse cracks have formed."

Lutz observed that if perfect bond was maintained after cracking in the vicinity of a crack, the stresses would have to be impossibly high. He observed that a stress concentration exists at the steel concrete interface at the ends of the cylinder, and that the radial tensile stress at these points was especially high. Accordingly he postulated that failure in this region must occur by separation between the bar and the surrrounding concrete. Assuming a length of separation he constrained the concrete to move diagonally outwards (to simulate the concrete sliding on tapered ribs). An exaggerated

drawing of the displaced shape obtained in this way is shown in figure 4.7.

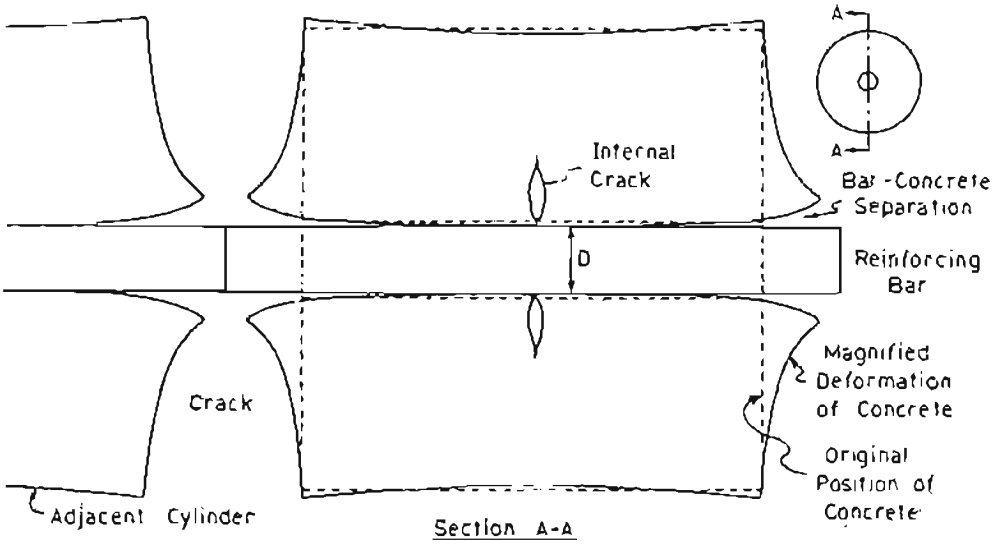

Figure 4.7: Deformation of concrete cylinder between cracks - after Lutz (1970)

In addition, Lutz noted that very high circumferential stresses occurred near the faces of the cracks, and postulated this would be where longitudinal cracking would commence. Next, Lutz introduced bond slip which, he states, made it possible to better approximate the shape of experimentally observed transverse cracks.

Lutz noted that his analysis indicated that, at the surface of the cylinder, longitudinal extension was negligible and in fact actually became compressive. This agrees well with some of the experimental findings of Broms (1985(a)) and Hognestad (1962) (see Chapter 2). In contrast the longitudinal stresses at the bar were large enough midway between primary cracks for a new crack to form here and radiate outwards. Once again, this phenomenon has been confirmed experimentally (Broms (1965(a)) and (Broms and Lutz (1965)).

Labib and Edwards (1978) carried out "non-linear" analyses of similar models to Lutz. They modelled bond slip using linkage elements governed by a non-linear stress-strain law. The concrete material model used by the authors assumed linear elasticity in both tension and compression. It appears to the writer that the fracture criterion was stress, with the tensile stress dropping immediately to zero after

cracking, although some shear capacity was maintained. A further limitation of these analyses was that they were only in two dimensions (i.e. the steel was assumed to be smeared over the full depth of member).

Labib and Edwards carried out analyses on long members to attempt to simulate the development of primary cracks and analysed short members (sections between primary cracks) to investigate secondary cracks. Typical plots of their results are given in figures 4.8 and 4.9. (Note that only a quarter of each member is showing). The member properties for their two examples are as in table accompanying the figures.

Several other researchers have carried out work on analysing the bond of steel to concrete via finite element analyses of the response of the concrete around the reinforcing bar. (For example: Somayaji & Shah (1981), Gerstle et al (1982), Jiang et al (1982), Giuriani (1982), Ingraffea et al (1984), Yankelevski (1984), and Negemier et al (1985)). This work however has not been carried out with a view to being able to predict crack spacings and crack widths, but rather with a view to being able to determine the composite response of reinforced concrete to stress.

4.4 CHOICE OF FINITE ELEMENT CODE AND CONSTITUTIVE MODEL

In the light of what has been discussed in section 4.2 it is clear that some very fine concrete models have been developed. In making a choice of which to use, however, the writer was limited by the finite element codes available for use at the University of Cape Town. These are (non-linear codes only):

(i) ABAQUS
(ii) ADINA
(iii) NOSTRUM

Of the above, both ADINA and ABAQUS are well known, commercially available finite element codes, made available for use by the University of Cape Town under academic license. Both are large scale codes capable of analysing a very wide range of problems, including various types of non-linear effects.

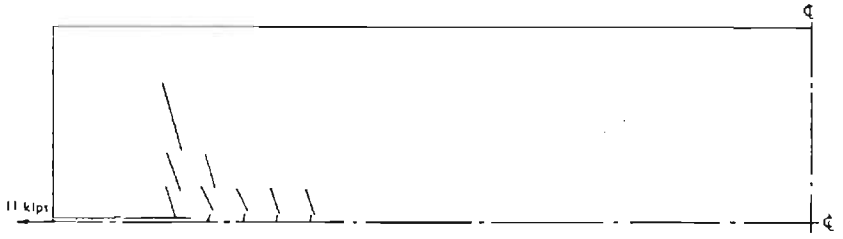

(a) Crack pattern before the formation of first primary crack; member T-RC2

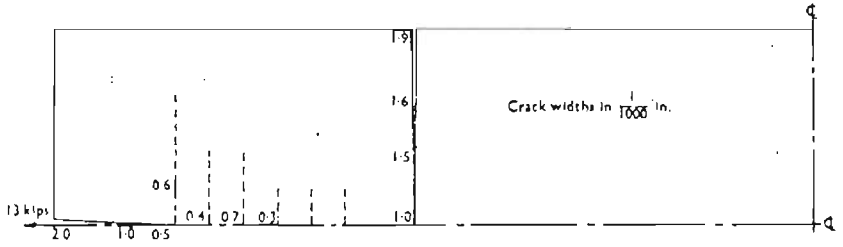

(b) Crack width after formation of first primary crack; member T-RC2

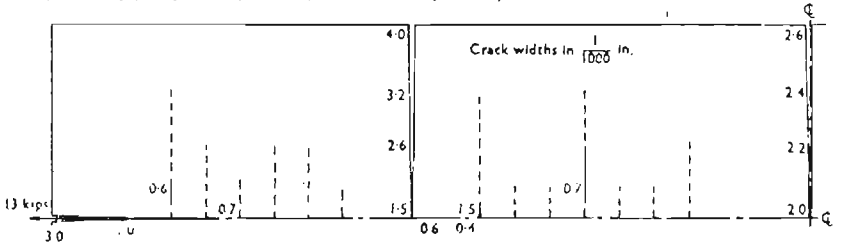

(c) Crack width after formation of second primary crack; member T-RC2

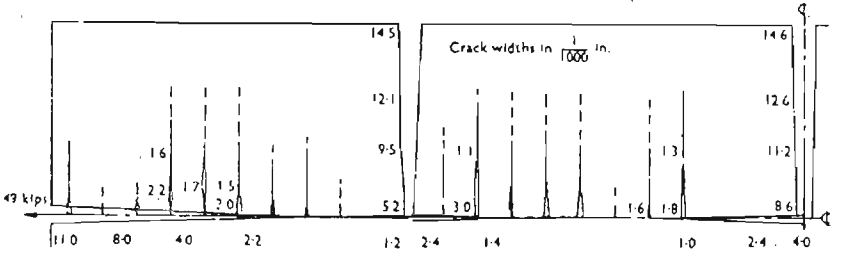

(d) Crack width at 49 kips; member T-RC2

Figure 4.8: Analysis of primary cracking in long member - after Labib & Edwards (1978).

Member	Cross-section, *in.* × *in.*	Length, *in.*	Concrete strength, f_c, *lb/sq. in.*	Modulus of rupture, *lb/sq. in.*	Modulus of elasticity, *lb/sq. in.*
T-RC2	3·50 × 8·10	32·00	3450	469	4 343 080
T-RC3	3·50 × 8·10	8·00	5140	605	5 012 980

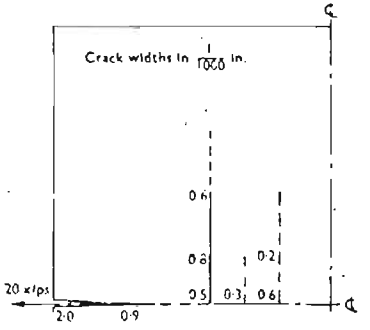

(a) Crack width at 20 kips; member T-RC3

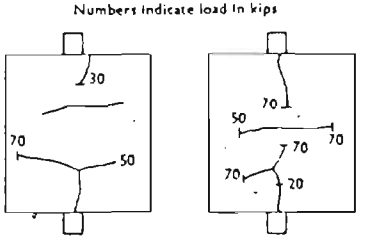

(b) Experimental crack pattern; member T-RC3

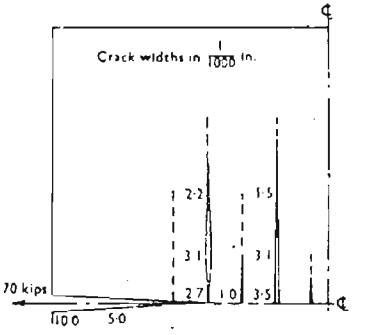

(c) Crack width at 70 kips; member T-RC3

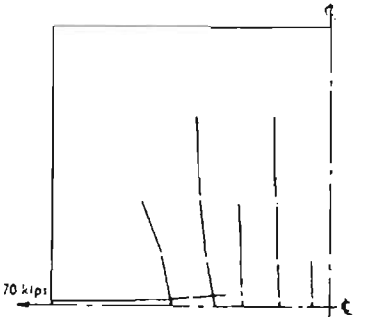

(d) Crack pattern at 70 kips; member T-RC3

Figure 4.9: Analysis of secondary cracking between primary cracks - after Labib & Edwards (1978).

ABAQUS is available from Messrs Hibbitt, Karlsson and Sorenson, Inc., 35 South Angell St., Providence, Rhode Island, 02906, USA. Its full capabilities are described by Hibbitt et al (1984).

ADINA is available from Messrs ADINA Engineering AB, Munkgatan 20 D, S-722 12 Västerås, Sweden. Its capabilities are described in full by ADINA Engineering (1984).

NOSTRUM is a non-linear finite element code under ongoing development by the Applied Mechanics Research Unit at the University of Cape Town. Its full capabilities are described by the Applied Mechanics Research Unit (1984). Details on the damage mechanics model were provided by Resende (1985b).
Initially it was thought that the selection would be made from either ABAQUS or ADINA as NOSTRUM was limited to two-dimensional and axisymmetric analyses and it was hoped that the effects of different bar layout geometries would be studied.

Of these two ABAQUS was selected as it had the better concrete model in that it allowed the user to model the descending part of the stress/strain curve after the concrete had failed in tension. ADINA, on the other hand, only allowed the user to model the failure point of concrete as a simple tension cut-off. The inclusion of the descending portion of the stress/strain curve was thought to be an important factor in the accurate modelling of concrete behaviour.

A point against using NOSTRUM was that, although it had a damage model implemented in the code which would allow the modelling of the full stress/strain curve for concrete, this was much more difficult to calibrate than the other models.

Points which weighed heavily in favour of using ABAQUS as the analysis code were that it was able to incorporate into the analysis many effects that could not be modelled by NOSTRUM. These related to the adequate portrayal of the early age effects of thermal and drying shrinkage, inclusion of pre-existing strains into the model before analysis, and the ability to incorporate user defined modelling laws into many of the cases described above.

Thus ABAQUS was chosen as the preferred package for use in the investigation. A problem however, immediately surfaced with respect to its use: the "concrete model", which was the prime reason for choosing the package, was not available on the version installed on the UCT computer at that time. Since there were plans already in existence to install a revised version with the concrete model, the writer decided that a start would be made with the analysis of some simple linear elastic cases to create familiarity with the package.

These models did give a few preliminary indications of what might be expected to occur in a non-linear analysis but were not much more helpful than that. The most important thing that showed up immediately was the degree to which stress concentrations could be expected in the concrete immediately surrounding the bar and adjacent to a primary crack. To model the stresses in this area with any reasonable degree of accuracy, it was immediately apparent that a proper non-linear model was needed for the concrete.

Before the revised version of ABAQUS arrived, a constitutive model for the Damage Mechanics modelling of concrete became available on NOSTRUM and the writer decided to utilize this code and constitutive model for modelling of some basic situations of cracking of concrete due to steel/concrete interaction. Some salient features of the "damage" model, its calibration and the use made of it are described in chapter 5. Problems were subsequently experienced with the use of this model but by then the revised version of ABAQUS was available on the UCT computer and that package was then used for the remainder of the computer models analysed for this thesis. Some salient features of the ABAQUS "concrete" model, its calibration and the use made of it are described in chapter 6.

4.5 SERIES OF COMPUTER MODELS

Although it was originally hoped to explore the effects of differing reinforcement layouts and section shapes by three-dimensional modelling, a logical first step was to attempt to analyse some two-dimensional models. These could have two forms: either plane stress or axisymmetric.

In the initial models the intention was to model some prisms of concrete with a single reinforcing bar down the centre. These would be compared to similar tests done by various authors (eg: Beeby (1972)). Although the tests reported in the literature were done on rectangular prisms it was felt that axisymmetric modelling, which meant approximating the rectangular concrete prisms by cylinders, was preferable to plane stress modelling. This latter would entail modelling of the bar as being "smeared" over the whole depth of the section. The two alternatives are compared in figure 4.10.

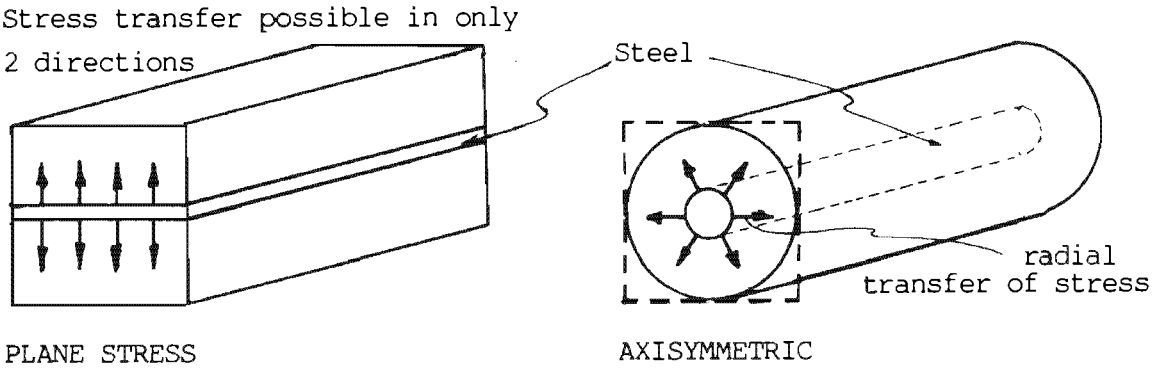

Figure 4.10: Alternative finite element models for a singly reinforced prism.

Since the transfer of stresses between bar and concrete is essentially something that happens radially, it was felt that limiting this to only two directions, as in the plane stress model, would involve a significant loss of realism in the model. The axisymmetric model also enables one to model effects such as ring tension and compression, which cannot be included in a plane stress model.

In contrast with the techniques used by others who have incorporated various bond-slip or bond-separation elements, the writer decided to try to model all of the concrete using the same constitutive model with no special linkage elements. The writer hoped that since the material model used would be better than those previously used to model the same problem the need for these special elements would disappear.

Certainly in the case of the bond separation noted by Lutz (1970), for instance, this would hopefully be taken care of in the writer's models

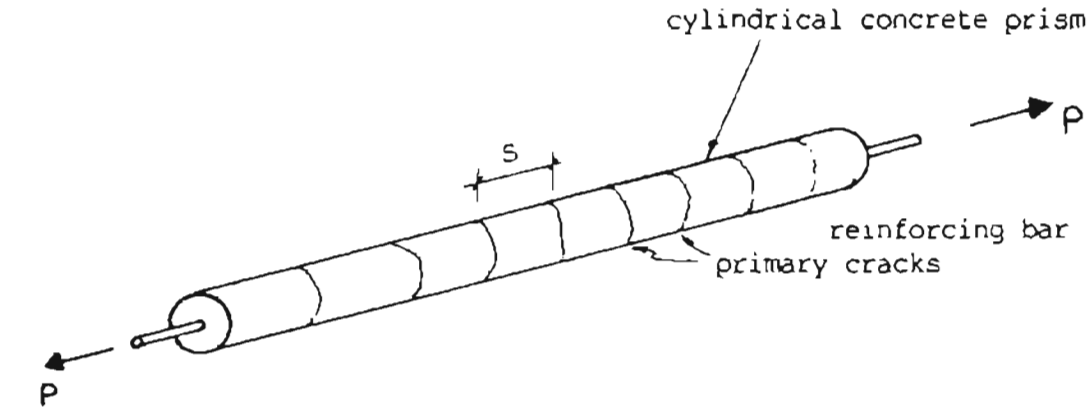

(a) Whole reinforced concrete prism

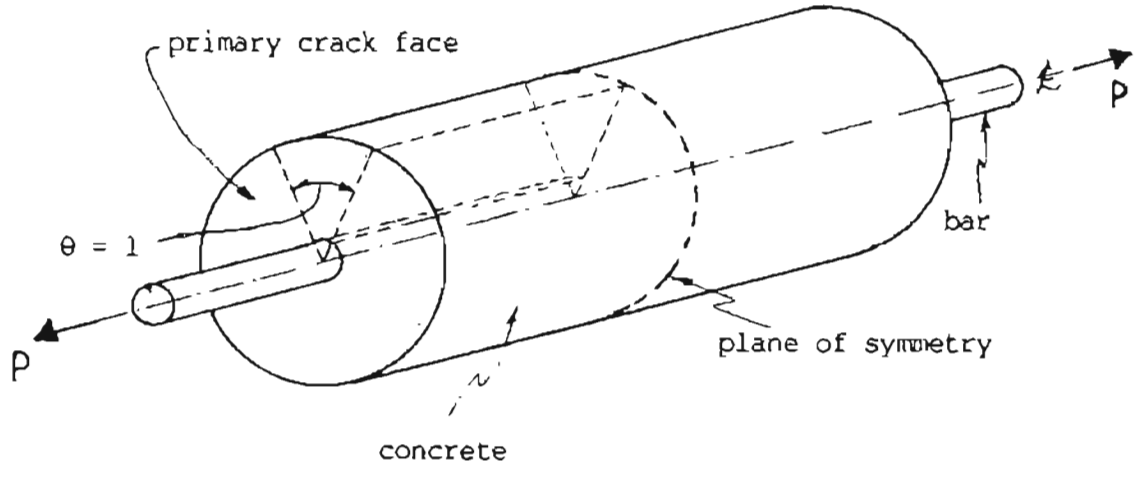

(b) Section of prism between primary cracks

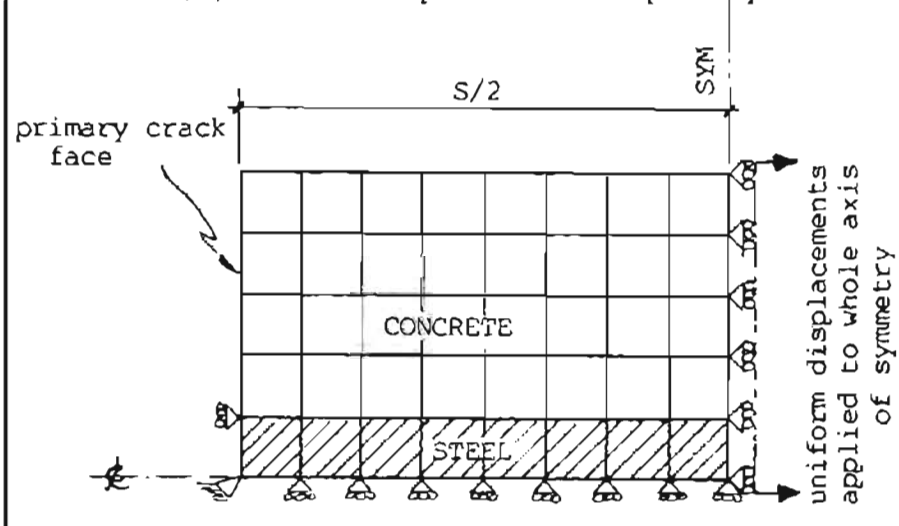

(c) Discretized finite element model

Figure 4.1: Relationship of a Finite Element model to a complete reinforced concrete prism.

in a more natural way by yielding and fracturing in the concrete around the bar. Actual differences between the bar to concrete and the concrete to concrete adhesion would not be modelled but it was thought that the inaccuracies introduced by this simplification would be minor.

In the case of bond slippage along the bar, experimental evidence has shown that for deformed bars this is usually negligible. Since this was the type of bar to be modelled the writer felt that having the concrete securely fixed to the steel at their contact surface would not be an unreasonable simplification. It has been shown experimentally that when bond failure does occur with deformed bars it occurs by localized crushing of the concrete that bears on the ribs of the reinforcement. The writer felt that observing the development of any substantial compressive forces in this area would be a sufficient check against gross errors in the analyses due to this type of failure occurring.

Figure 4.11 shows how the finite element models relate to the complete prisms. Firstly (fig. 4.11(a)) we start off with the long prism, cracked at intervals, S, apart. In the next figure (figure 4.11(b)) we isolate a section of the prism between two primary cracks. Noting the plane of symmetry in the centre between the two primary cracks and since we have symmetry about the centreline, we can limit our analysis to the slice shown dotted in figure 4.11(b). The next step is to discretize this section into finite elements and apply suitable boundary conditions (see figure 4.11(c)).

Because the subject of most interest is the behaviour of the model as the concrete progressively fails, it was decided that it was preferable to apply the load to the model by way of increasing displacements rather than increasing load. Again, since we are interested in knowing the width of the primary crack, if we apply a uniform displacement to the plane of symmetry rather than the bar at the crack end, we can obtain this directly by monitoring the displacement of the nodes along the primary crack.

All of the models analysed using either the damage mechanics or ABAQUS concrete constitutive models are of this same basic type. Different

situations were created for comparison by changing, one at a time, several of the parameters identified by previous experimental studies as being related to crack size. These were:

(i) Primary crack spacing
(ii) Cover
(iii) Bar diameter
(iv) Axial stress and strain

4.5.1 Choice of model configurations

The first model to be analysed was taken as being typical of the tension members tested by Beeby (1972) and comprised a 20 mm diameter bar encased by a concrete cylinder of overall diameter 100 mm (i.e. cover = 40 mm).

For this configuration, Beeby had found that the mean value of w/ε was equal to 76 mm

(where: w = crack width
ε = strain)

Since, according to the theory outlined in Chapter 2,

$$w = S\varepsilon ,$$

where S = the distance between cracks, this value also represents the average crack spacing S_m. Accordingly a length between primary cracks of 80 mm was chosen for the first model. Subsequent models would be derived as alterations of this one by changing cover, bar size, and distances between cracks.

The ranges of these values examined were as follows:

cover: 20 mm to 80 mm
bar size: 10 mm to 30 mm
distance between primary cracks: 80 mm to 320 mm.

The full series of analyses carried out is given in table 4.1. The labels attached to the models are in accordance with the method of labelling as defined in Appendix A.

Table 4.1: Finite element analyses carried out on singly reinforced tension members (axisymmetric).

Cover	20	40	80
S = 80	A1H		A1K
S = 120			
S = 160			
S = 240			
S = 320			

bar size = 30 mm

Cover	20	40		80
S = 80	A1C	A1B*	D1A*	A1L
S = 120			D2A	
S = 160	A3C	A3B*	D3A	A3L
S = 240			D4A	
S = 320	A5C	A5B*		

bar size = 20 mm

Cover	20	40	80
S = 80	A1E	A1F	
S = 120			
S = 160			
S = 240			
S = 320	A5E	A5F	

bar size = 10 mm

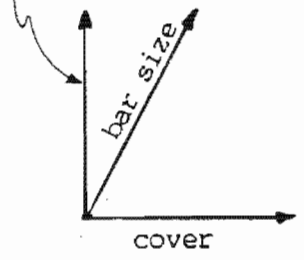

* indicates other parameters changed for these models.

CHAPTER 5

FINITE ELEMENT MODELLING CARRIED OUT USING "NOSTRUM" AND DAMAGE MECHANICS MODELLING OF CONCRETE

5.1 CALIBRATION

The damage mechanics model for concrete, implemented on the NOSTRUM finite element code, was authored by Resende (1985(a)). Detailed consideration of the model is outside of the scope of this thesis but a few salient points should be mentioned.

(i) The model includes two basic damage mechanisms to model inelasticity, namely, shear damage and hydrostatic tension damage. As the damage increases the elastic properties of the model are progressively degraded.

(ii) Under hydrostatic compression loading the model is bounded by a plasticity yield surface.

(iii) The parameter used to represent damage is a scalar quantity, i.e. if the material becomes damaged in one direction it is damaged in all directions.

Resende (1985(a)) calibrated the model to match concrete data reported by Kupfer et al (1969, 1973). The writer metricated the data supplied by Resende (1985(b)) and ran the following three tests on single element models to check on the behaviour of the constitutive model.

(i) Uniaxial compression test
(ii) Uniaxial tension test
(iii) Biaxial tension test

5.1.1 Compression response of model

Figure 5.1 shows that the uniaxial compressive strength of the concrete is 29,6 MPa which is typical of that used by other investigators. The compression response exhibits progressive softening as the strain is increased until at the peak stress the

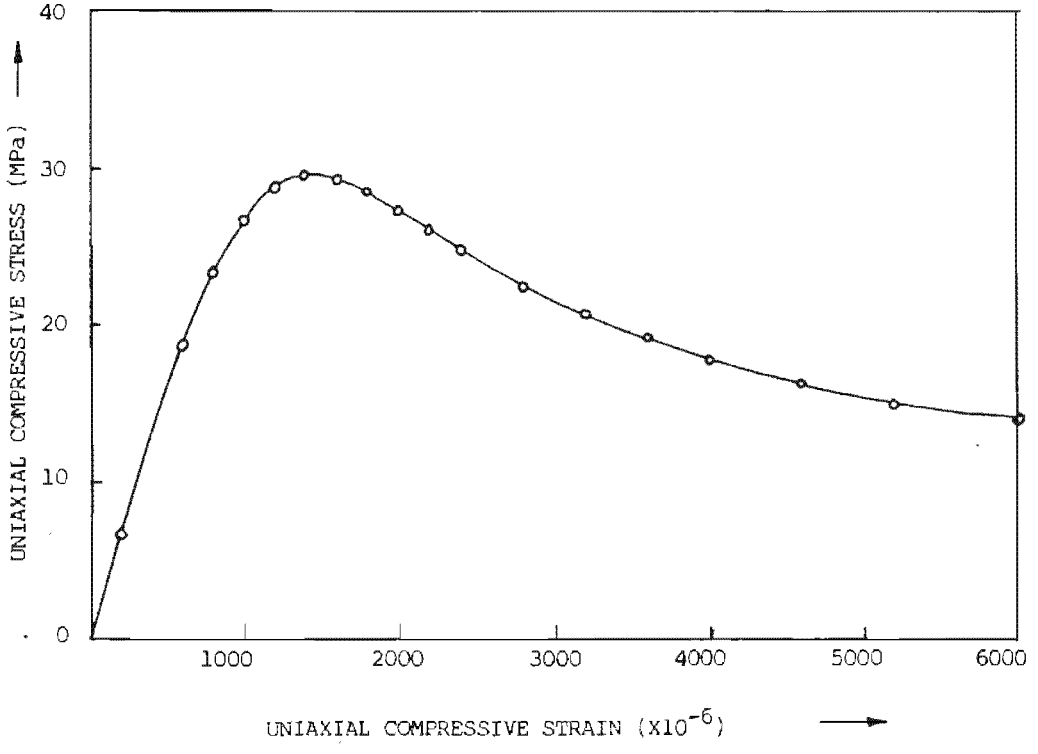

Figure 5.1: Behaviour of Damage Mechanics Model in uniaxial compression

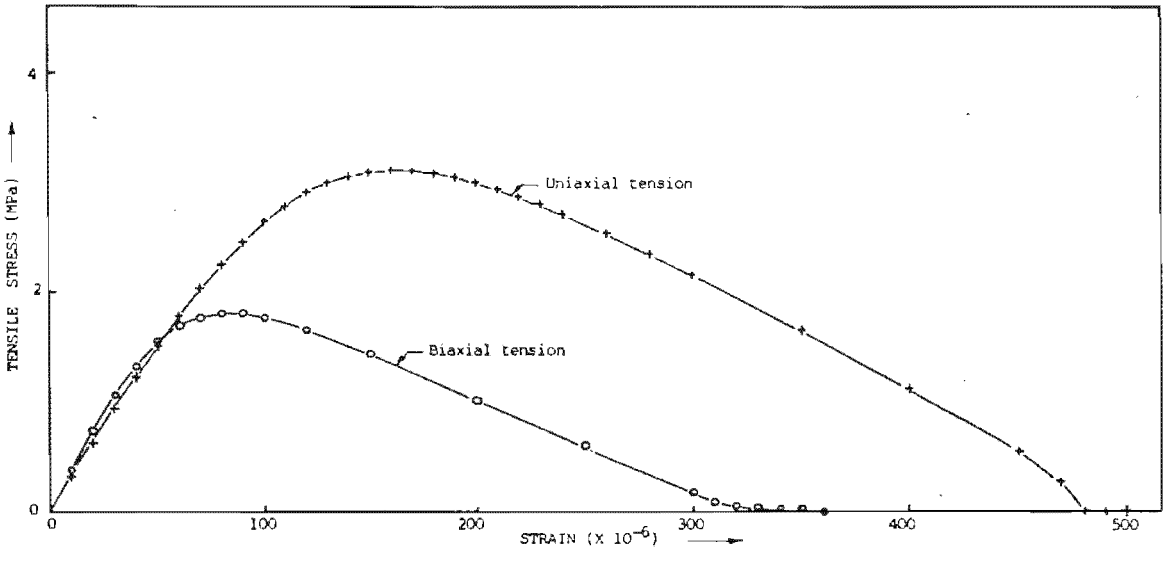

Figure 5.2: Behaviour of NOSTRUM Damage Mechanics Model in (a) uniaxial and (b) biaxial tension.

material is momentarily perfectly plastic. Thereafter, the model continues to exhibit strain softening and actively yields towards failure. The compressive stress appears to be asymptotic towards a value that is greater than zero but this is of little concern to the analyses to be carried out here which should be entirely dependant on the tensile cracking response of concrete.

5.1.2 Tensile response

Figure 5.2 shows both the uniaxial and biaxial response of the calibrated model to tensile stresses. Resende (1985(a)) has shown that the rising parts of the curves match well to the experimental data of Kupfer et al. Certainly the order of magnitude of the peak tensile stress at just over ten percent of the peak compressive strength agrees well with typical experimental findings. Raphael (1984) examined a very large number of test results and produced the graph shown in figure 5.3.

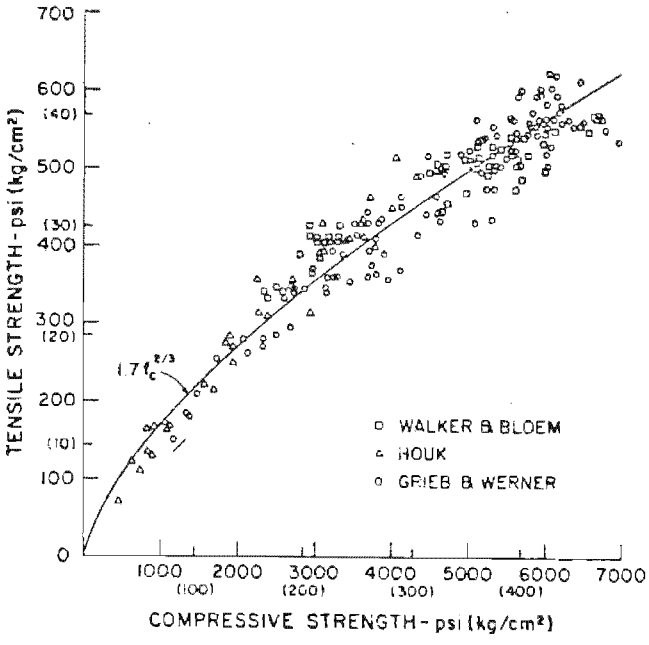

Figure 5.3: Tensile strength versus compressive strength of concrete - after Raphael (1984).

The beginning of the non-linear behaviour under tensile stress occurs at the right order of magnitude. There is experimental evidence to show that the start of "plastic" behaviour of concrete actually coincides with the commencement of micro-cracking. Kaplan (1963) used this fact when studying the formation of micro-cracking in concrete. He

determined, via the proportional limit of elasticity, that micro-cracking could start at between 30 and 80 micro-strain depending on the percentage of coarse aggregate in the mix. These results are shown in figure 5.4. Also shown in this figure are Kaplan's findings of the strains which represent 95% of the ultimate load. These vary from between 70 to 130 micro strain.

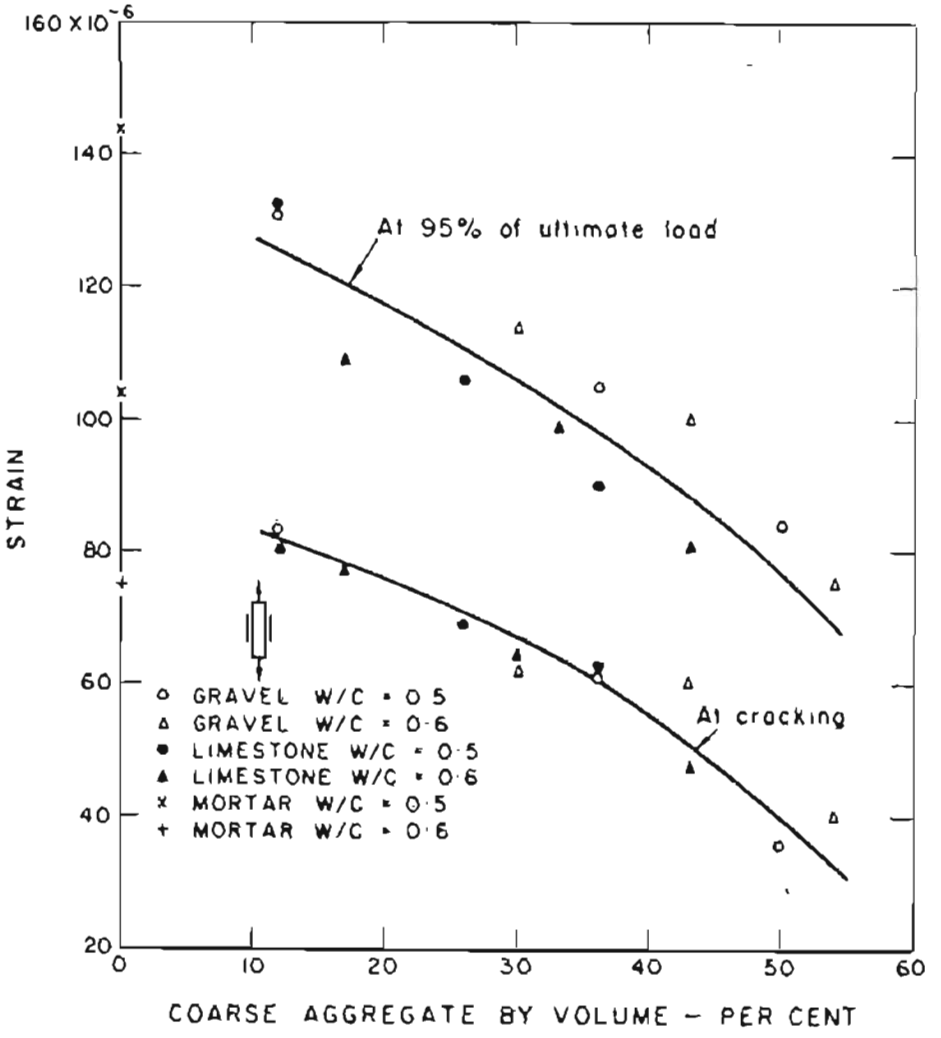

Figure 5.4: Relation between tensile strains in direct tension test, and percentage of coarse aggregate by volume – after Kaplan (1963).

Evans and Marathe 1968, using a microscope rather than the limit of proportionality between stress and strain found that micro cracking occurred at somewhat higher strains than those found by Kaplan. In fact their values of 90 to 140 micro strain for the commencement of cracking coincides almost exactly with Kaplan's 95% of load range. Although there appear to be quite considerable differences in these findings, in actual fact, in terms of the overall behaviour of the

concrete (up to the peak stress) the actual mechanism of the "plastic" deformations is not that important. For the purposes of the present study the rising part of the tensile stress-strain curve as shown in figure 5.2 is quite accurate enough. The descending portion of the stress-strain curve is another matter entirely. Initial information available to the writer was that there was no accurate data available on this subject. As a result the NOSTRUM damage mechanics model has not been calibrated to any experimental data, but rather, the slope of the descending portion of the curve is the subject of guesswork (Resende 1985(b)). Information which subsequently came to hand indicates that the calibration of the model, as used for the various analyses, is not very accurate. This information is discussed in the next sub-section, and the possible consequences of using a poorly calibrated model are discussed in chapter 7.

5.1.3 Tension stiffening and tensile strain softening

Many experimenters have measured the rising portion of the tensile stress-strain curve of concrete. Similarly the point at which the concrete will fracture has been given wide attention and several proposals exist on how to predict fracturing theoretically. There is another portion of the stress-strain response curve that has been assuming greater importance in recent years, namely the descending portion.

This portion of concrete's response is very difficult to measure because one needs an extremely stiff testing machine that will not suddenly rip the sample apart with stored energy as the latter reaches fracture point. Nevertheless there is considerable evidence that it exists. Hughes and Chapman (1966) and Evans and Marathe (1968) both tried to determine the complete stress-strain curve for concrete in direct tension. Typical curves established by Hughes & Chapman and Evans & Marathe are shown in figures 5.5 and 5.6.

Comparison of these curves shows that there is a considerable scatter of strains at which the curves peak - from approximately 50 micro-strain for Hughes & Chapman's results up to 800 microstrain for those of Evans & Marathe. There is likewise a large scatter of different descending portions of the stress-strain curves amongst these results,

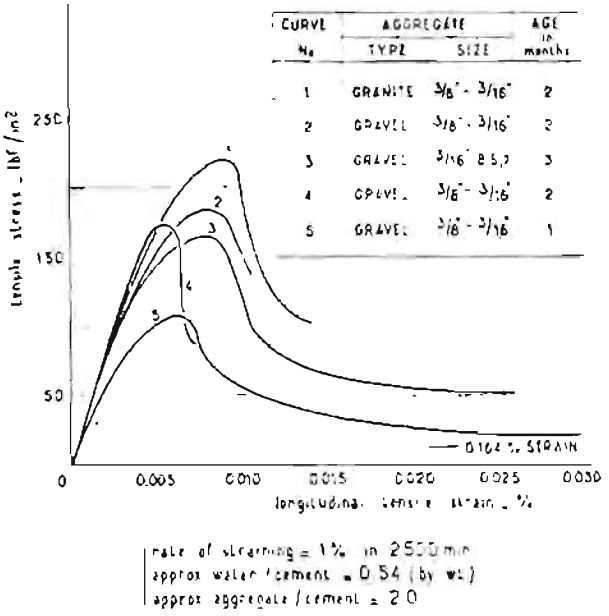

Figure 5.5: Complete stress-strain curves for concrete in direct tension - after Hughes and Chapman (1966).

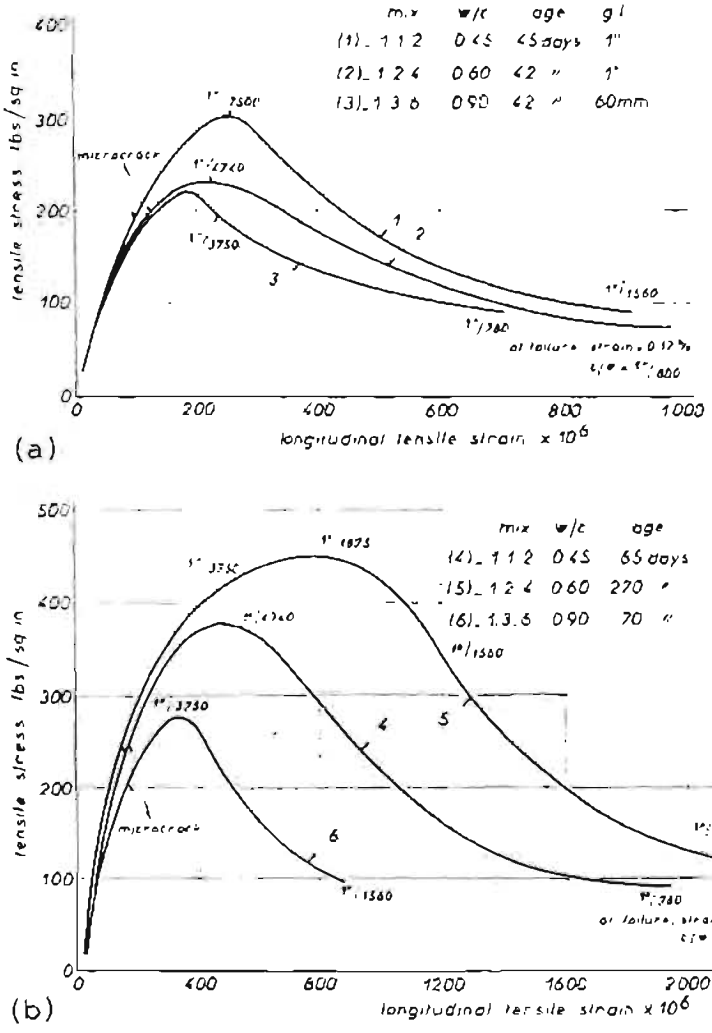

Figure 5.6: Complete stress-strain curves for concrete in direct tension - after Evans and Marathe (1968).

with failure strains ranging from about 75 microstrain (Hughes & Chapman curve no. 4) to 3 200 microstrain (Evans and Marathe curve no. 5) In all cases the stress in the concrete never reduces gradually all the way to zero but fails abruptly at some point above zero stress. The curve derived in figure 5.2 from the uniaxial tension test on a single finite element is approximately in the same range as Hughes and Chapman's results, but slopes down to zero considerably more sharply than the curves obtained by Evans & Marathe. It is, however, generally acknowledged that the last word has not yet been written on this portion of concrete's behavior and the determination of reliable data on the strain softening of concrete is the subject of ongoing research using very stiff and sophisticated testing machinery.

There is another aspect of descending portions of tensile stress-strain curves of concrete that needs to be clarified at this point. For years, it has been observed that when a beam cracks in flexure, its resulting stiffness is somewhat higher than would be expected if the concrete's tensile contribution had suddenly dropped to zero. Since the concrete could be well into the range at which it has developed discrete cracks across which load could no longer be carried in tension or shear, this effect appears to be due to the individual contributions of the remaining small sections of concrete clinging to the bar. There could still be a transfer of stress away from the bar and through the crack zone by way of cantilever and strut actions of the remaining "teeth" of concrete, such as those identified by Goto (1971) (Figure 2.5).

Accordingly a descending part of the stress-strain curve of concrete has been incorporated into constitutive models and finite element codes primarily as a way of artificially allowing for this residual retention of overall stiffness of the bar and concrete combination. Figure 5.7 shows a typical experimentally obtained stress-strain curve for a reinforced prism of concrete showing how, even after the concrete has "fully" cracked it still provides an increase in stiffness over that provided by the reinforcing bar alone. This effect has become known as "tension stiffening."

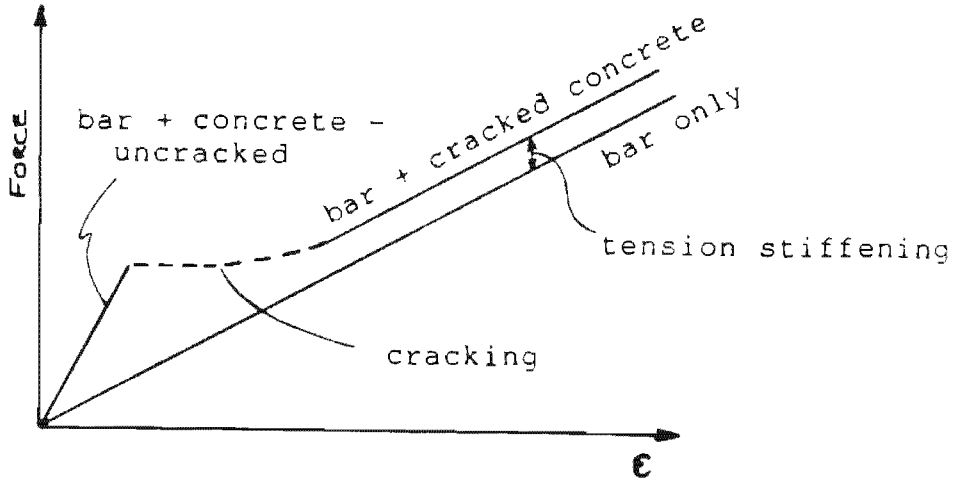

Figure 5.7: Typical stress-strain curve for a reinforced prism of concrete loaded in tension.

The writer believes it is important that this difference between strain-softening and tension stiffening be clearly understood as this has great relevance to the detailed analysis of reinforced concrete. If one is analysing, for instance, the load-displacement response of a beam the incorporation of some "tension stiffening" into the concrete material model will be sufficient to provide results that agree well with the experimental ones. If, however, one wants to match the detailed interaction of reinforcing bars and concrete the tension stiffening approach begins to lose relevance. If we could model the formation of discrete cracks properly, and we had a sufficiently fine discretization of the problem it is probable that to obtain correct overall results, the descending portion of the concrete's stress-strain curve would tend towards the strain softening value, and the tension stiffening, which is there to compensate for inadequate modelling would tend to zero.

Thus it is probable that the ideal slope of the descending portion of the concrete's tensile response should be somewhat flatter than the actual experimental values obtained from unreinforced tension specimens in order to compensate for some of the modelling deficiencies. This argument is illustrated by figure 5.8.

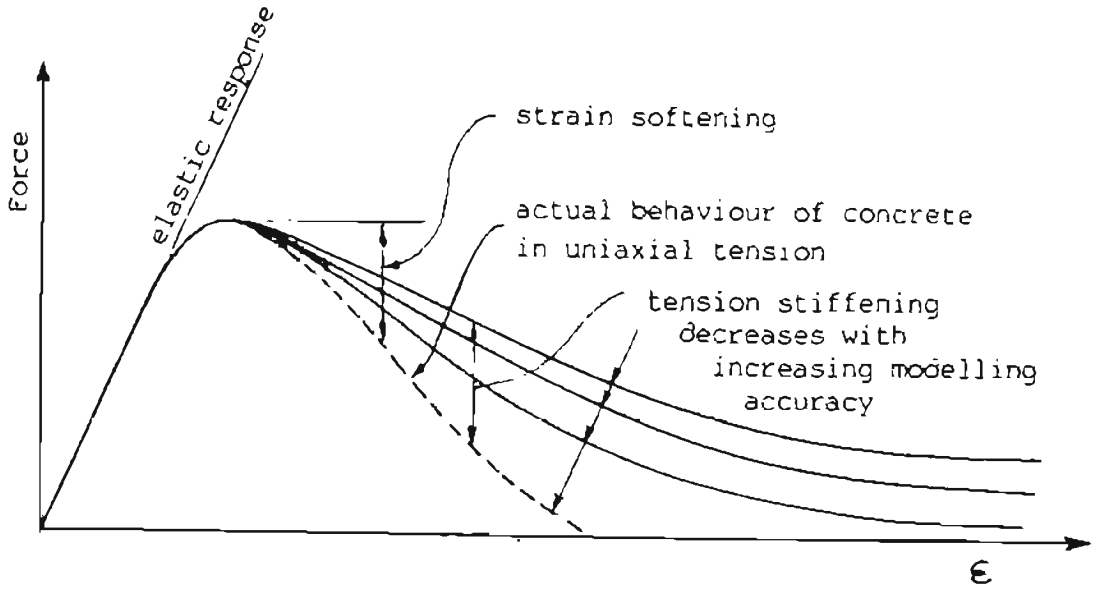

Figure 5.8: Comparison of "tension stiffening" and strain softening on concrete.

It was originally hoped that the slope of the descending portion of the curve might be varied in subsequent analyses in an attempt to approach a match to experimental results. In the time available, and in view of other technical problems, this, however, was not possible.

5.2 DISCUSSION OF ANALYSES USING NOSTRUM

5.2.1 Model D1A (distance between primary cracks = 80 mm)

The geometry and discretization of the first axisymmetric model to be analysed is shown in figure 5.9. It has been given the name D1A in accordance with the method of naming adopted by the writer and described in appendix A.

The mesh for this analysis was chosen as being fairly coarse in anticipation of extending the model to simulate the situation where there is a greater distance between cracks, although it was expected that a finer mesh might be needed to improve the accuracy of the model. Since the damage model had performed well and usually reached equilibrium within one or two iterations in the uniaxial and biaxial tests carried out for calibration, the same value of equilibrium tolerance was chosen for model D1A at 0,1%. With this tolerance,

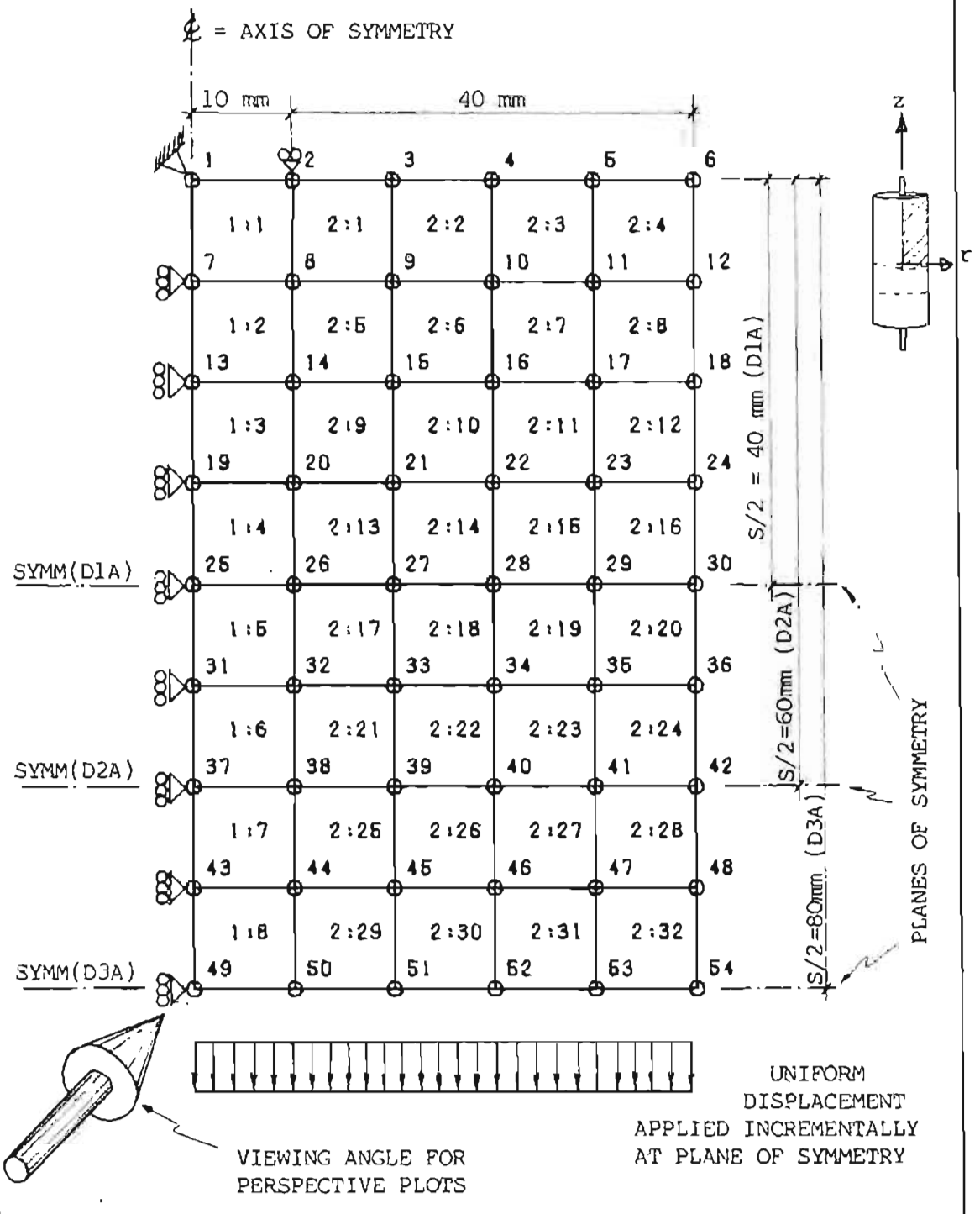

Notes on r-z-variable plots:

(i) Only theconcrete is shown.

(ii) The divisions on the perspective plots represent interpolation grids used by the contouring programme.

(iii) The reinforcing bar is always on the LHS. with the plane of symmetry at the bottom - as shown above.

Figure 5.9: Geometry and discretization of NOSTRUM models (D1A, D2A, D3A).

however, the analysis would not progress beyond a few increments of strain before coming to a halt because of lack of equilibrium convergence. When the convergence criterion was removed totally the analysis proceeded reasonably well up to an average steel strain of about 275 microstrain, at which point the convergence ratios increased rapidly and numerical instability caused the analysis to stop.

Examination of the stresses in the concrete showed that the point at which the analysis stopped corresponded to the point at which there was a complete breakdown of "bond" between the concrete and the steel. In other words the stresses in all of the elements adjacent to the bar had passed the peak value allowed and were on the descending part of the stress-strain curve.

Although it was acknowledged that the results obtained thus far were probably rather rough it was felt that there was little point in proceeding with further analyses unless this first one showed some promise of producing results. A considerable amount of time was therefore spent on examining the output of the analysis of model D1A.

Subsequent attempts to refine the models are discussed in section 5.3.

5.2.1.1 Analysis and presentation of results

The extraction and interpretation of relevant data beyond a simple displacement at one or two points becomes quite a problem with this type of analysis where the state of the entire model changes (and is of interest) with each new increment of load. The writer was anticipating certain occurrences at certain positions in the model and it was therefore possible to scan the output for these. To monitor what was happening to all the variables in the whole model throughout the whole loading range seemed to be a mammoth, if not impossible, task. The NOSTRUM post processor had the facility to plot vectors of principal stresses and displacement increments at the gauss points at any particular increment. Likewise "time-history" plots could be plotted for the value of a particular variable at a particular point over the full loading range. Even with the simple mesh used here there are 64 gauss points (in the concrete only) and since there are approximately seven variables that might be of interest at each point

that would mean plotting up to 448 different graphs! Clearly this would be a ridiculous task and a pile of 448 graphs would be just as indecipherable as a pile of digitized printout.

The writer therefore considered ways of presenting the results of the analysis in a more meaningful and readily interpretable way. To plot the results properly, one really needed to be able to portray a four-dimensional plot where the four axes would be: r and z directions, the value of the variable being considered, and the level of corresponding applied load.

Since it is only possible to satisfactorily represent a 3-dimensional plot, one of the four axes would have to be omitted, the problem being to decide which one. Obviously the variable under study could not be left out, thus the choice was between leaving out either the loading state or one of the coordinate directions.

In the event, the writer has produced some plots using both the above alternatives. The actual plotting was done by writing a FORTRAN routine to extract the relevant data from the NOSTRUM output file and rewrite it into a form suitable for use by the general "SACLANT GRAPHICS PACKAGE" which is available on the U.C.T. computer. This package has been specifically designed for producing contour and three dimensional perspective plots of any variable over an x-y grid.

As it was anticipated that the writer would be doing extensive finite element modelling using NOSTRUM the data extraction routine was written in a fairly general way, allowing any of seven variables to be plotted for the whole section at each increment of time (= load) for the whole range of times.

The results for model D1A are presented in figures 5.11 to 5.18. Except for figures 5.15 and 5.16 which are both representations of the maximum principal tensile stresses, each figure represents a different variable plotted over the area of the concrete portion of the model for each of five different loading stages.

The explanation of the layout of all of the figures 5.11 to 5.18 is given in figure 5.9. The plots are given both as contour plots and as

perspective plots because the latter tend to be easier to interpret whilst the former give the actual values of the variable under consideration. In the case of principal stresses, neither of these types of plots gives any idea of direction. Therefore the maximum principal stress plots have been included as well.

The most significant observation that can be made as a result of this analysis is of the way in which the concrete progressively fails in the zone adjacent to the reinforcing bar. This is shown very clearly in the perspective plots in figure 5.16, where as the loading increases, the stresses are reduced to almost zero in this zone. Alternatively the zone of maximum stress may be visualized as a wave travelling along the bar as the strain increases. The principal stress vector plots show clearly how the principal stress directions may be expected to change as the loading increases.

Figure 5.14, showing the t-t (or hoop) stress distribution shows how the model was starting to exhibit a zone of hoop tension adjacent to the primary crack. This tension all but disappears in the last step before breakdown of the analysis (time = 22), but it is unclear why this should happen. The peak value of hoop tension of 0,62 MPa actually occurs at t = 10, and then tails off. Why this happens is unclear as this stress does not appear great enough to cause failure in this direction. The writer thinks that the problem is related to the fact that the damage parameter in this material model is a scalar value. Later discussion on the analyses carried out with ABAQUS will show that it is reasonable to believe that, after the concrete surrounding the bar has cracked in tension, load continues to be transferred to the concrete by a truss action, where the outer reaction is provided by hoop tension. Thus after the row of elements adjacent to the bar have cracked in tension, they might be expected to go into compression. Figure 5.10 explains this theory.

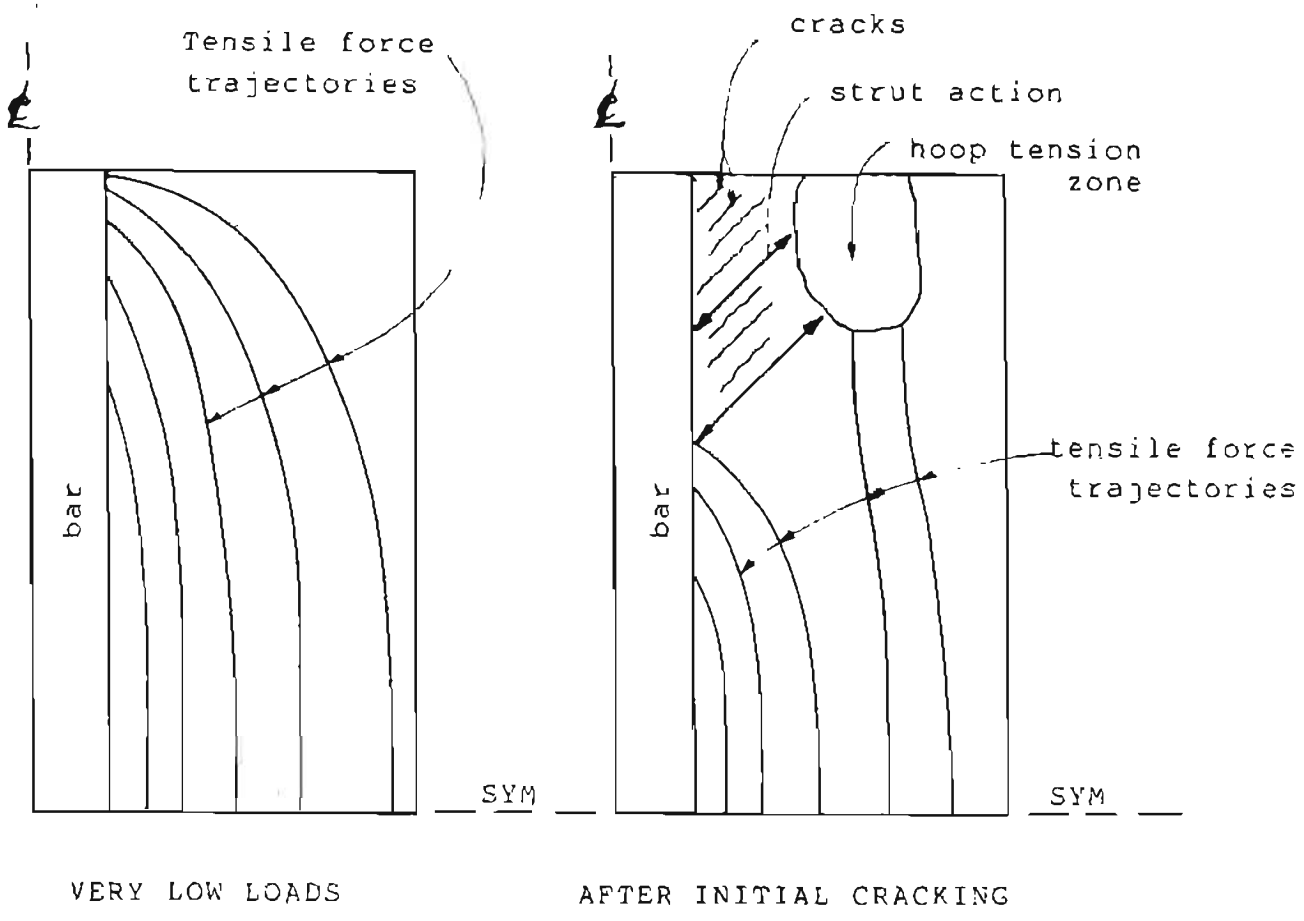

Figure 5.10: Strut and hoop tension theory for bond after initial tensile cracking.

Examination of the plots of various stresses does not show any such reversal of stress in the elements adjacent to the bar. The principal stress vector plots show that compressive forces do exist, and in the right directions to satisfy the truss hypothesis. These stresses however, are associated with the curvature of the trajectories of the primary tensile stresses and disappear with the primary tensile stresses as the concrete becomes progressively more damaged.

Thus, although Resende (1985)(a)) indicates that reversals of stress are possible with his damage mechanics model this has not occurred in this case. Resende's examples are limited to hydrostatic and uniaxial stress loadings and perhaps the more complex interplay of stresses in this case is the cause of the problem.

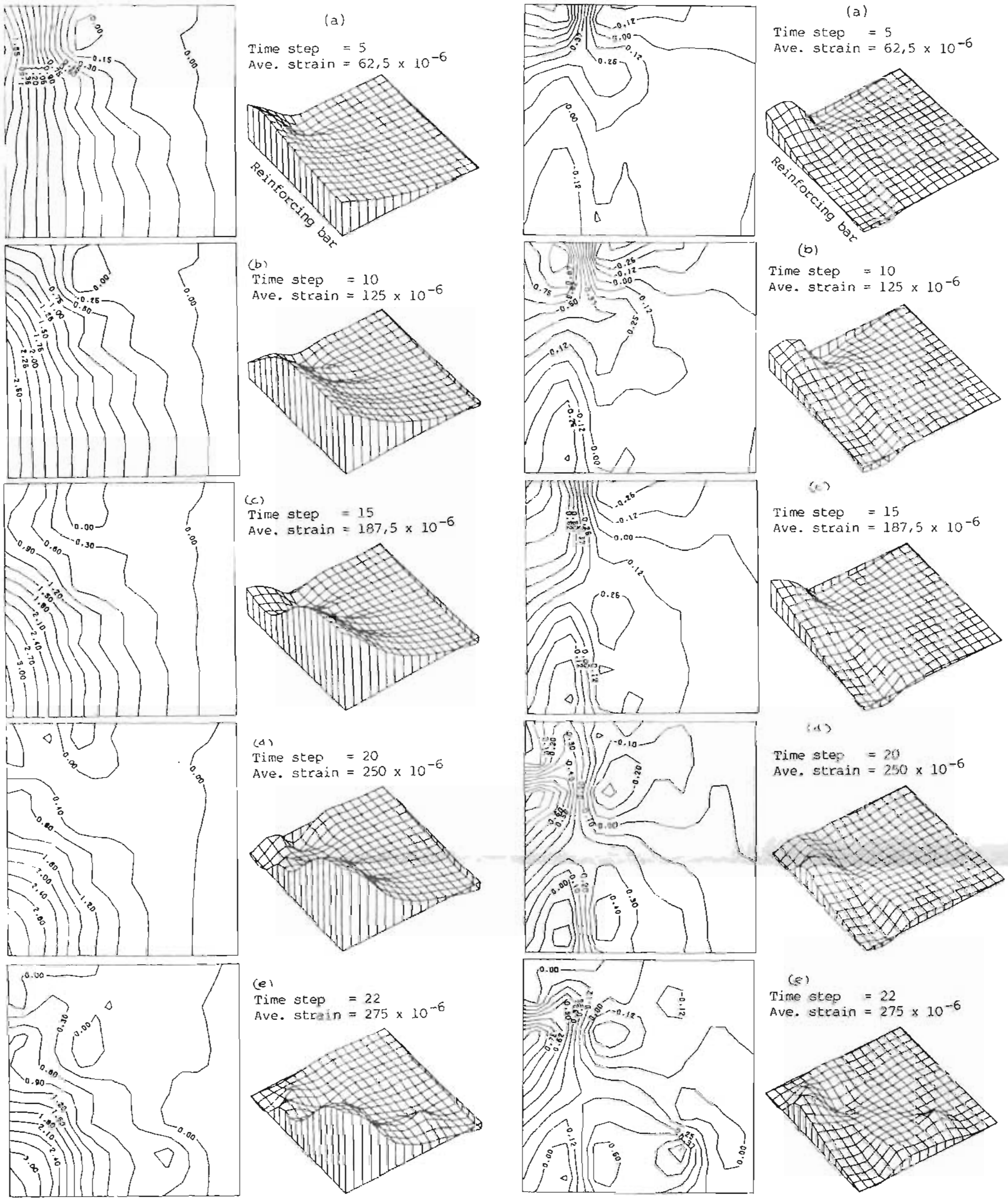

Figure 5.11

Model D1A : Plots of longitudinal stress at varying load increments

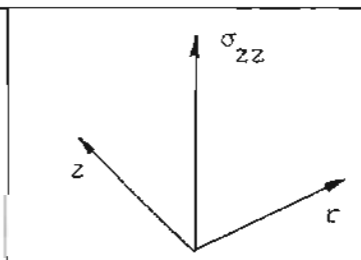

Figure 5.12

Model D1A : Plots of radial stress at varying load increments

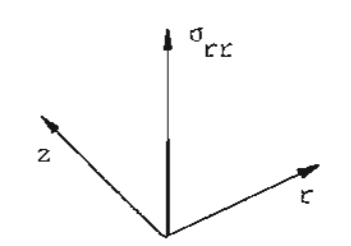

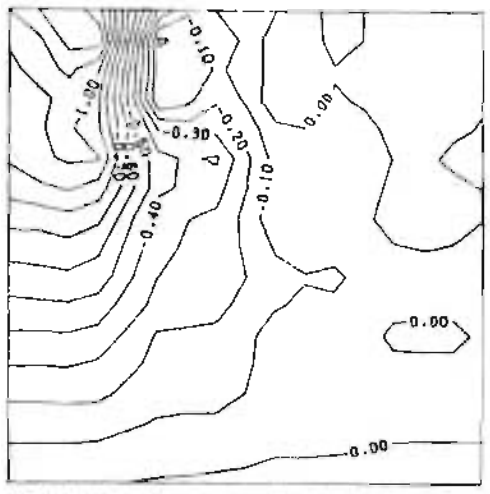

(a)
Time step = 5
Ave. strain = 62,5 x 10^{-6}

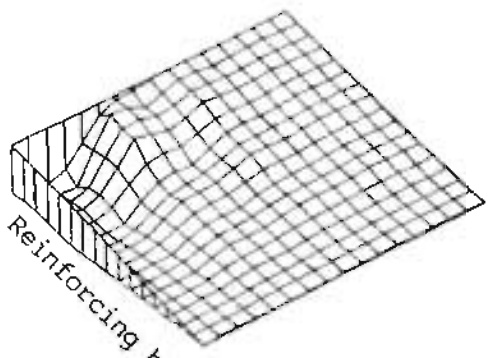

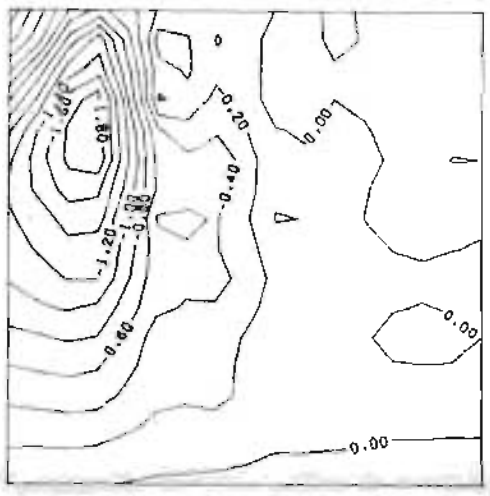

(b)
Time step = 10
Ave. strain = 125 x 10^{-6}

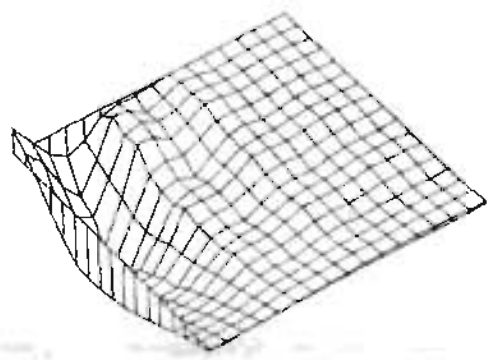

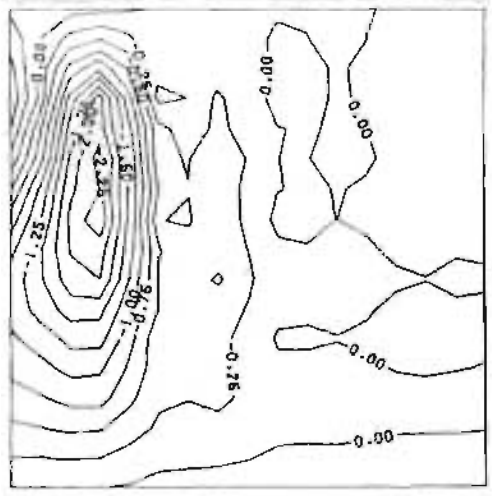

(c)
Time step = 15
Ave. strain = 187,5 x 10^{-6}

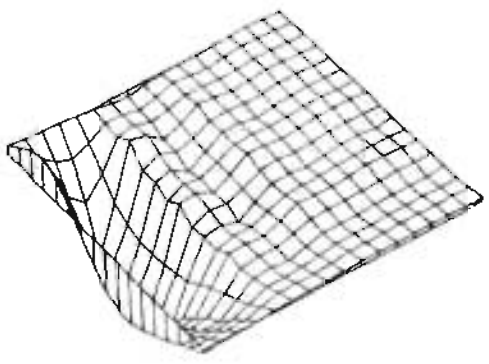

(d)
Time step = 20
Ave. strain = 250 x 10^{-6}

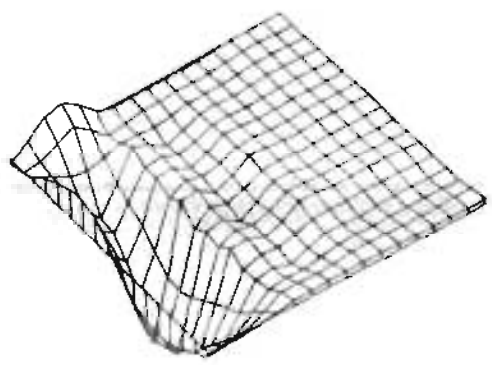

(e)
Time step = 22
Ave. strain = 275 x 10^{-6}

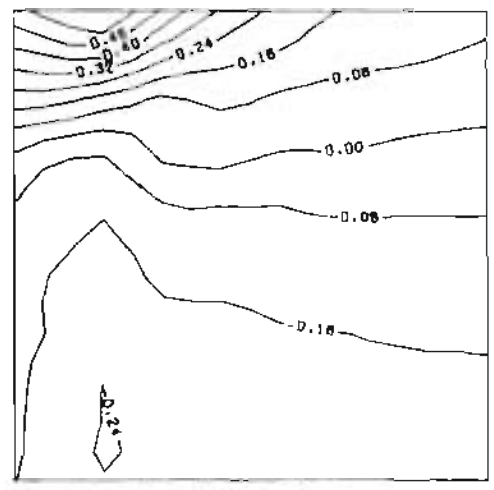

(a)
Time step = 5
Ave. strain = 62,5 x 10^{-6}

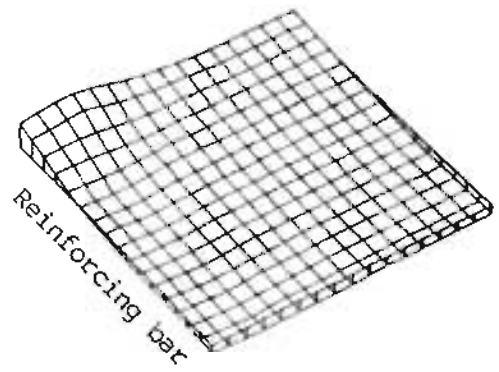

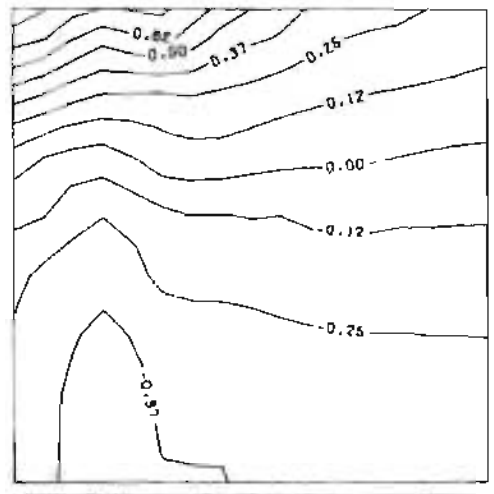

(b)
Time step = 10
Ave. strain = 125 x 10^{-6}

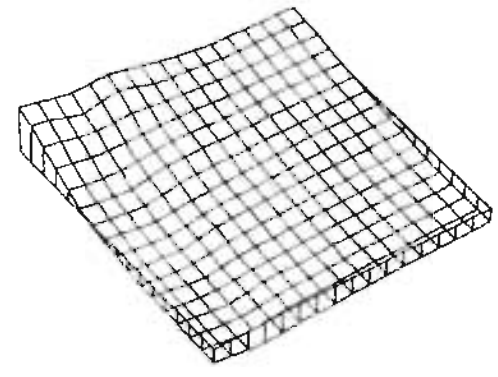

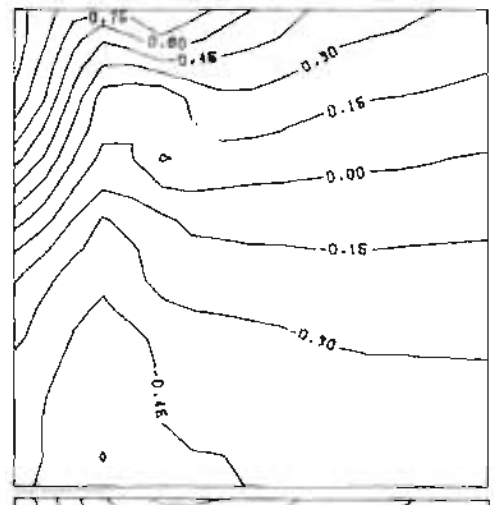

(c)
Time step = 15
Ave. strain = 187,5 x 10^{-6}

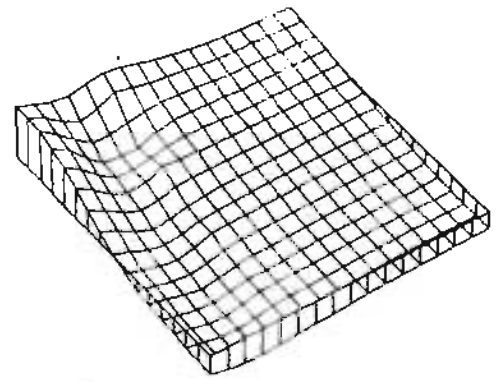

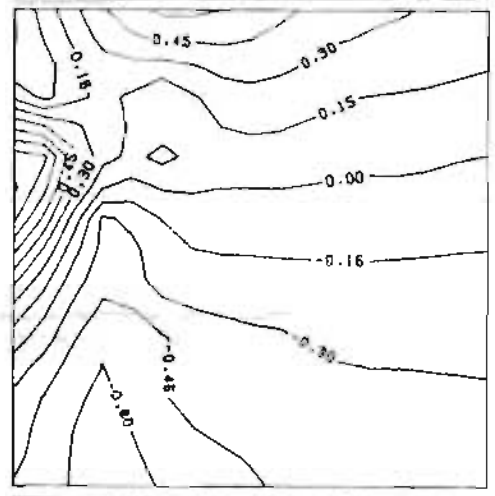

(d)
Time step = 20
Ave. strain = 250 x 10^{-6}

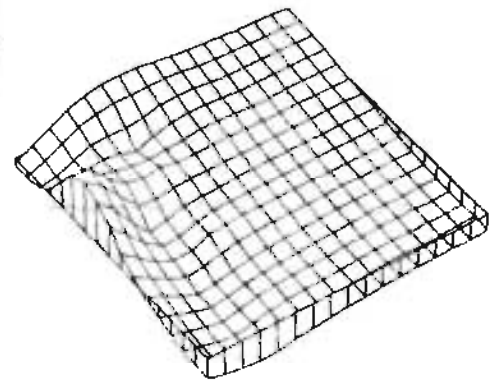

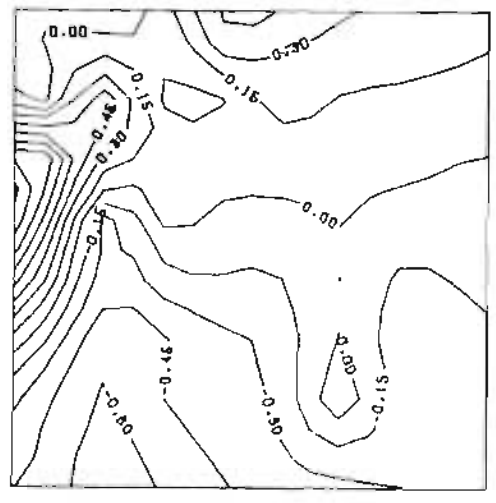

(e)
Time step = 22
Ave. strain = 275 x 10^{-6}

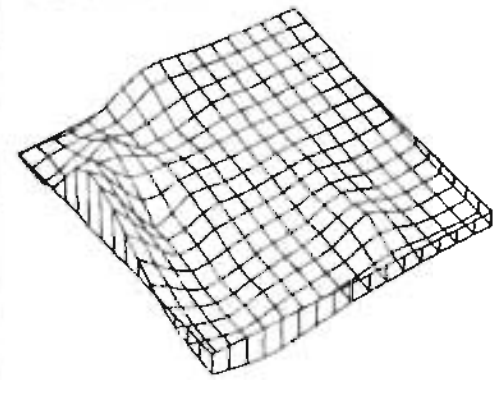

Figure 5.13

Model D1A : Plots of shear stress at varying load increments

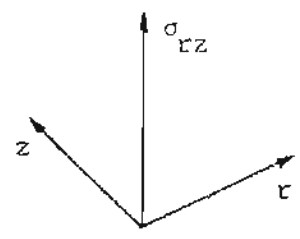

Figure 5.14

Model D1A : Plots of hoop stress at varying load increments

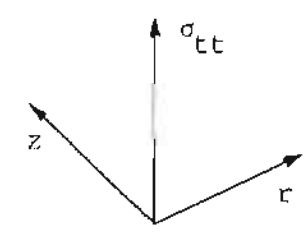

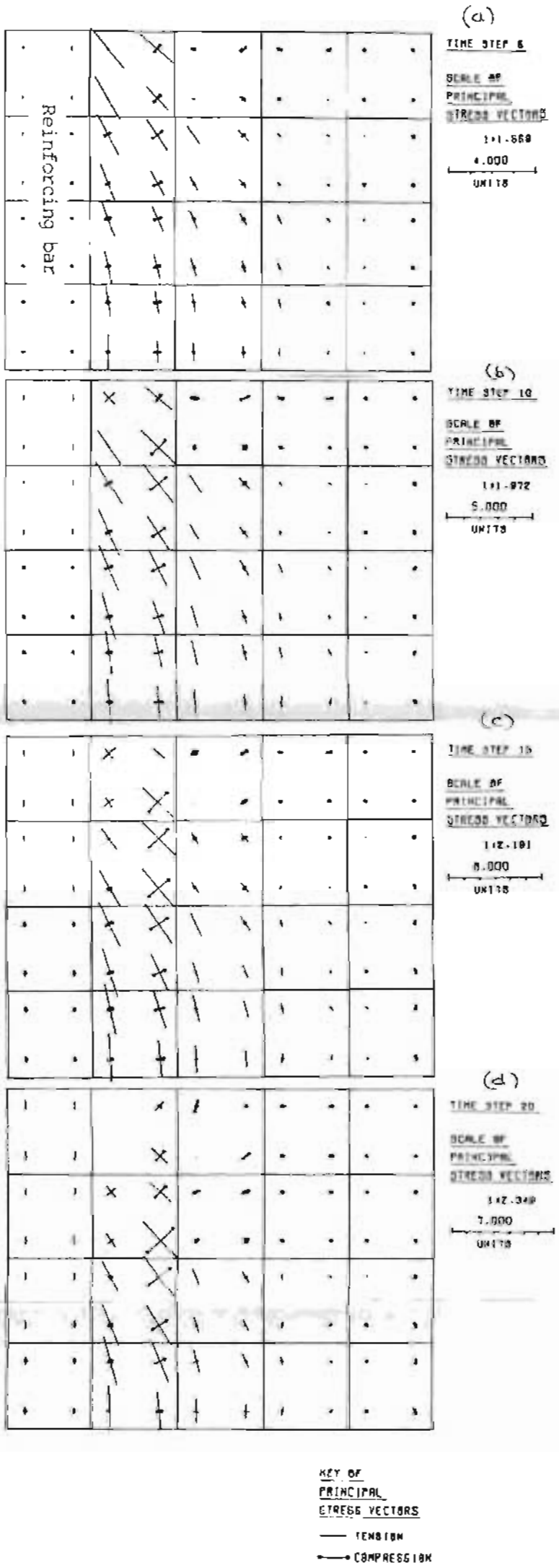

Note: Stress vectors in reinforcing bars have been scaled down to 1/100 of scale used for stress vectors in concrete.

Figure 5.15

Model D1A : Principal stress vector plots for varying load increments

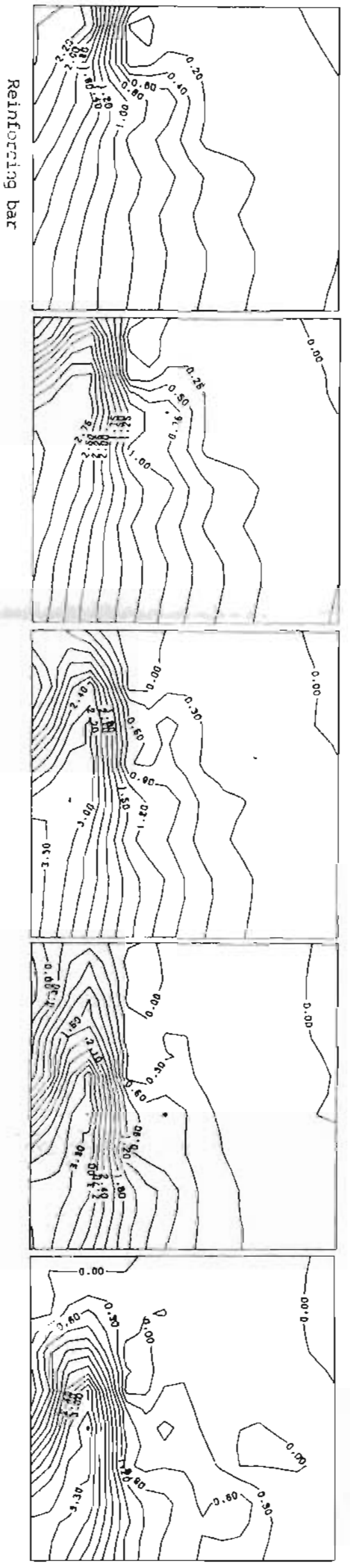

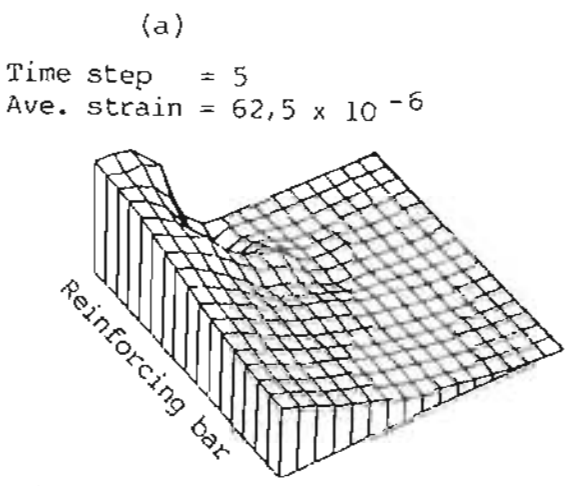

Figure 5.16

Model D1A : Plots of maximum principal tensile stress at varying load increments

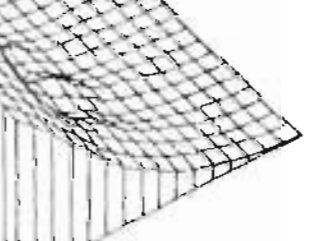

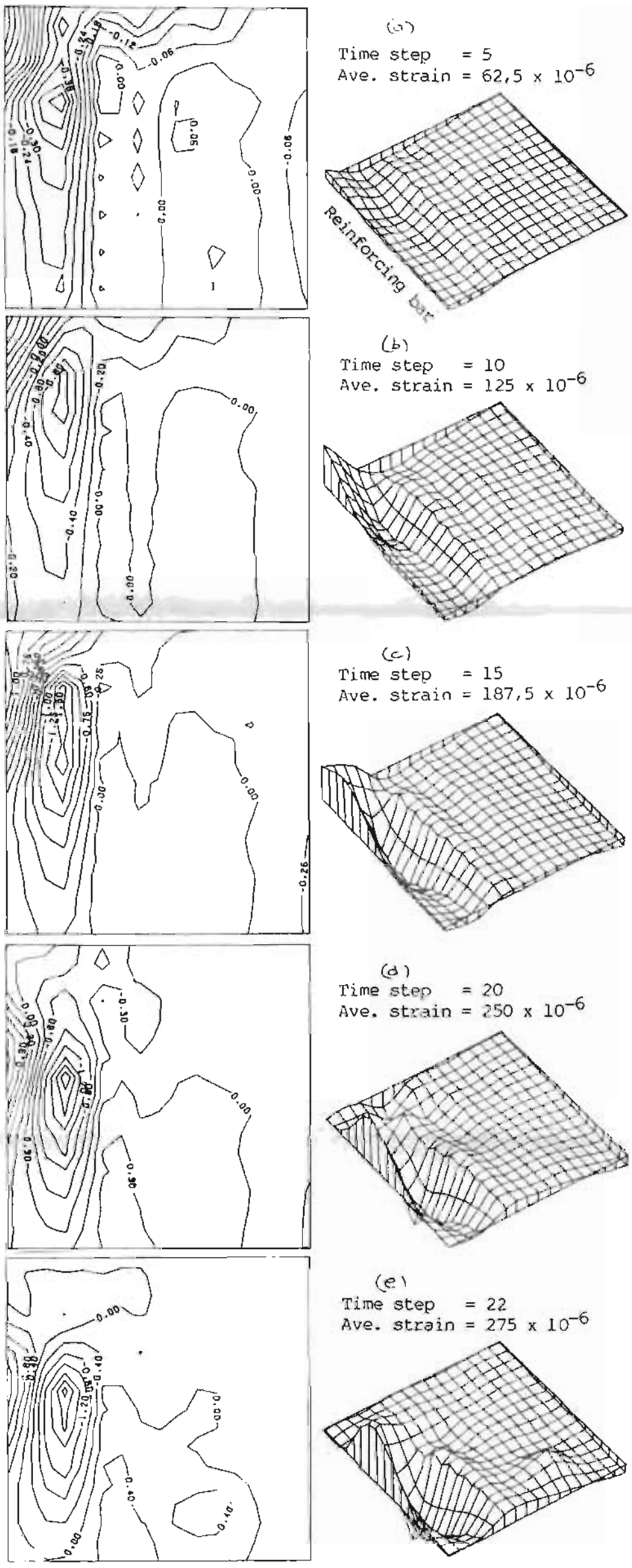

Figure 5.17

Model D1A : Plots of minimum principal stress at varying load increments

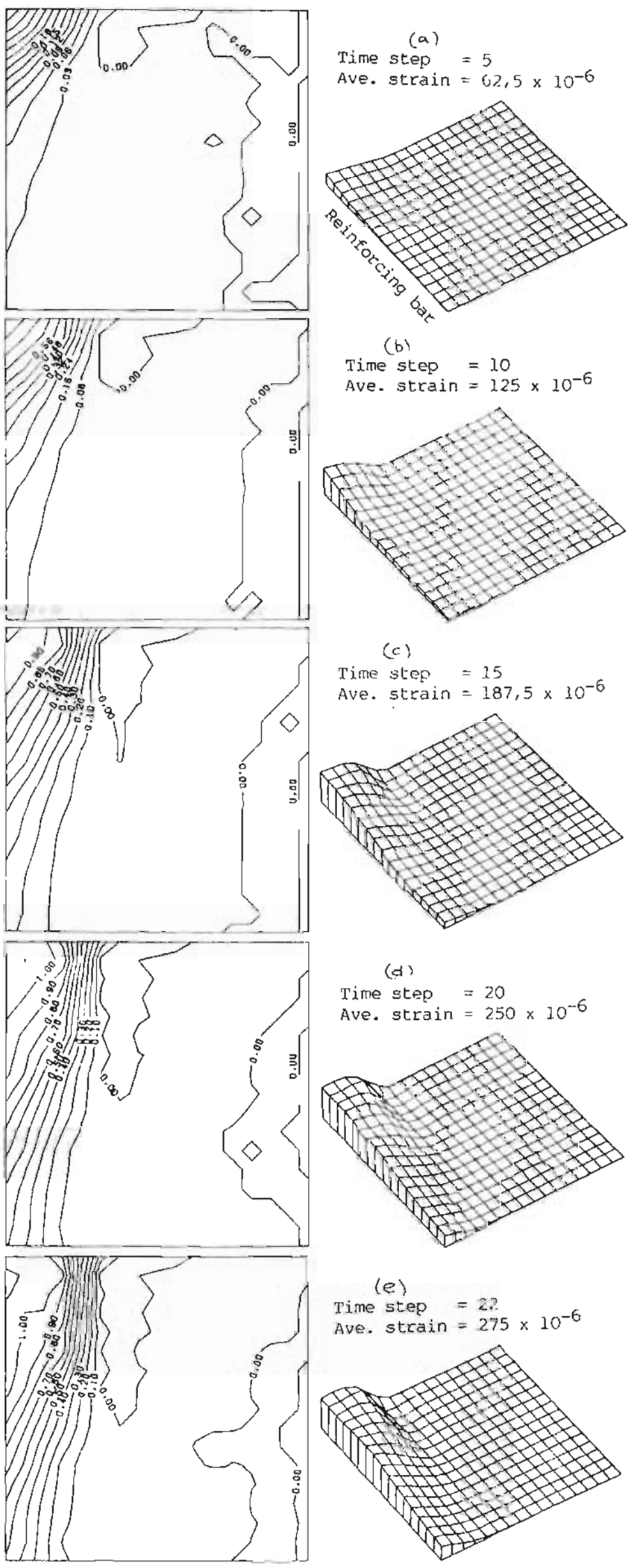

Figure 5.18

Model D1A : Plots of concrete damage parameter at varying load increments

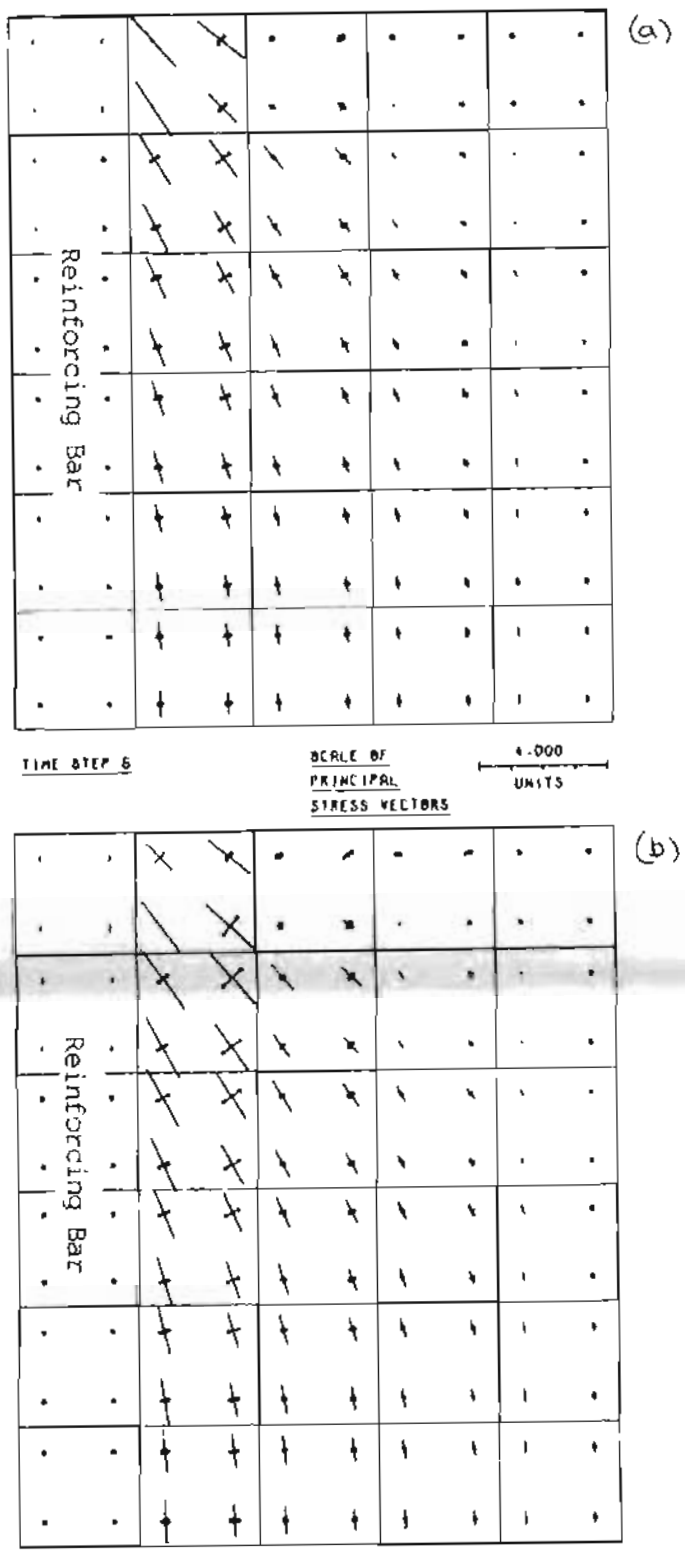

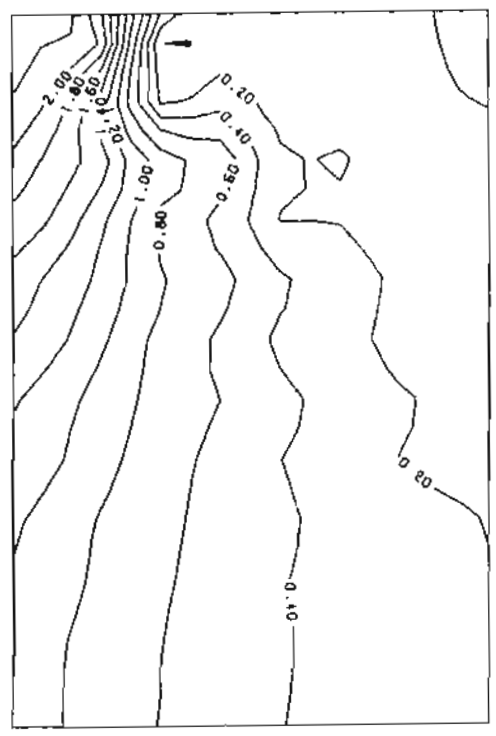

(a)
Time step = 5
Ave. strain = 41.7 microstrain

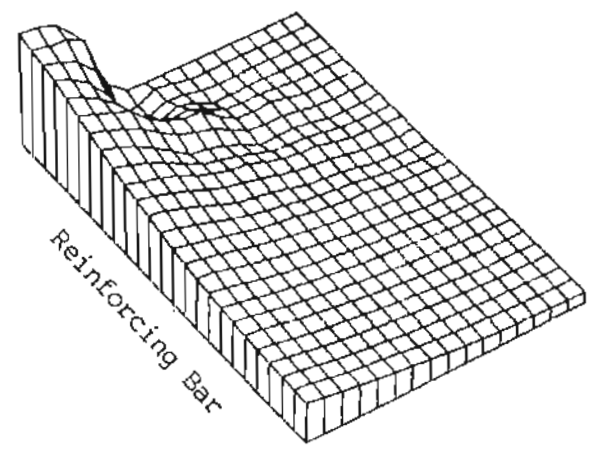

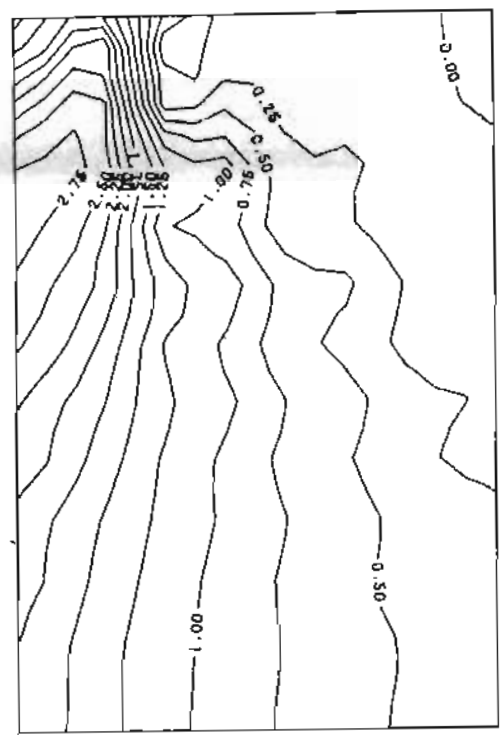

(b)
Time step = 10
Ave. strain = 83.3 microstrain

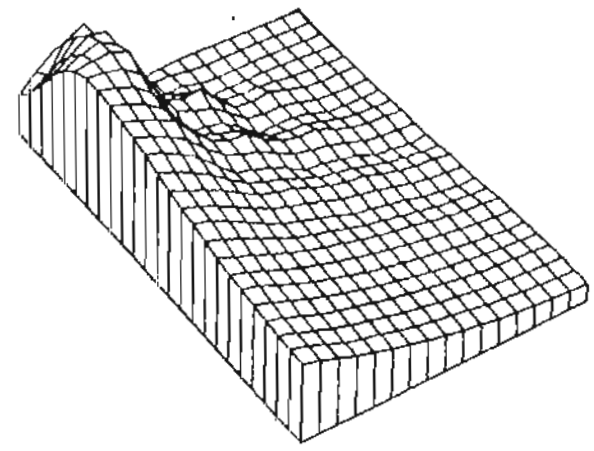

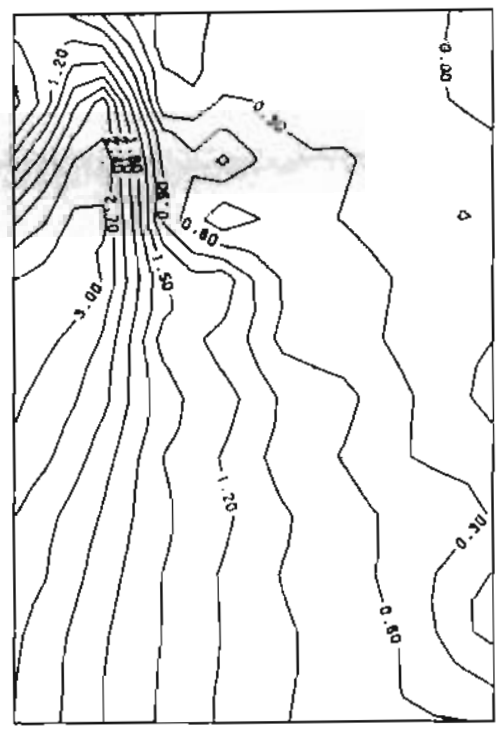

(c)
Time step = 15
Ave. strain = 125 microstrain

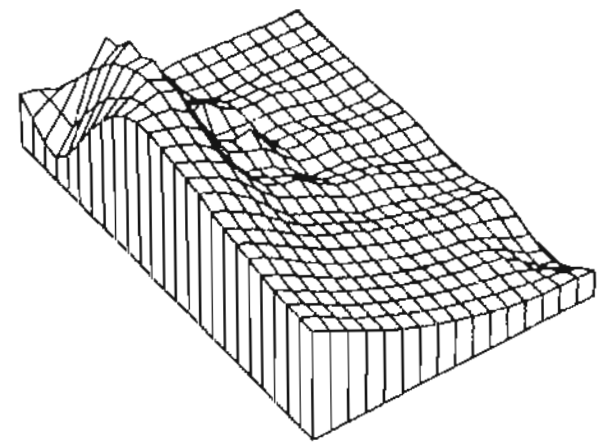

Figure 5.19

Model D2A : Principal stress vector plots at varying load increments

KEY OF PRINCIPAL STRESS VECTORS
TENSION
COMPRESSION

SCALE OF MESH
10.0E-3 UNITS

Figure 5.20

Model D2A : Plots of maximum principal tensile stress at varying load increments

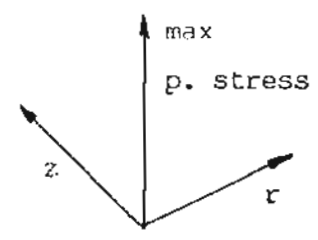

(a)

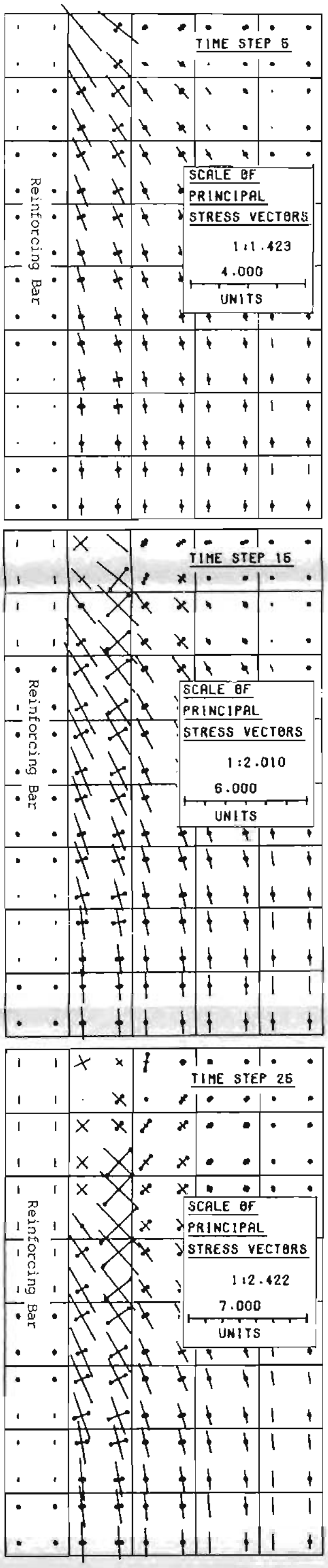

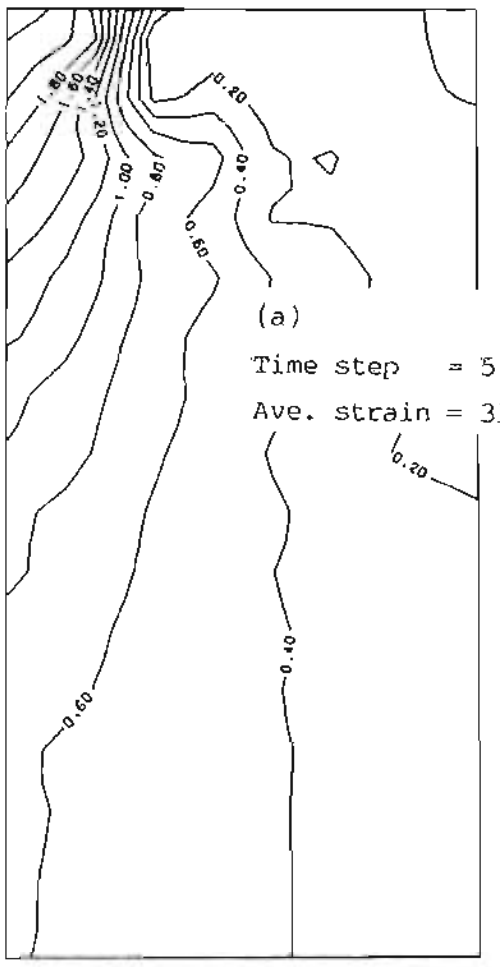

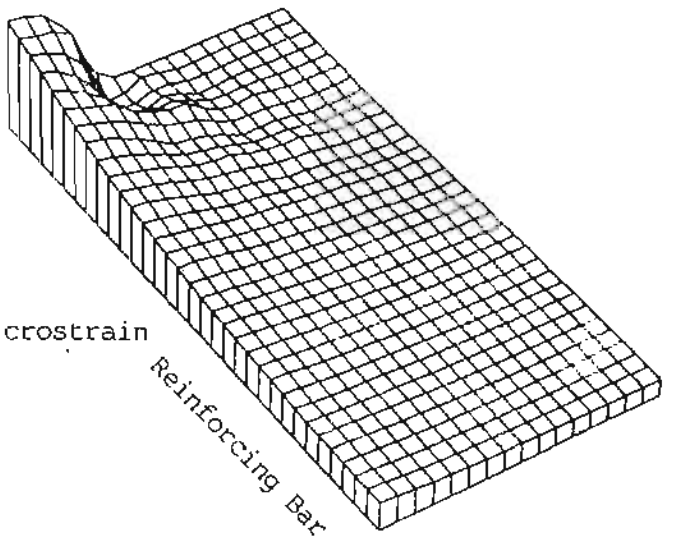

(b)

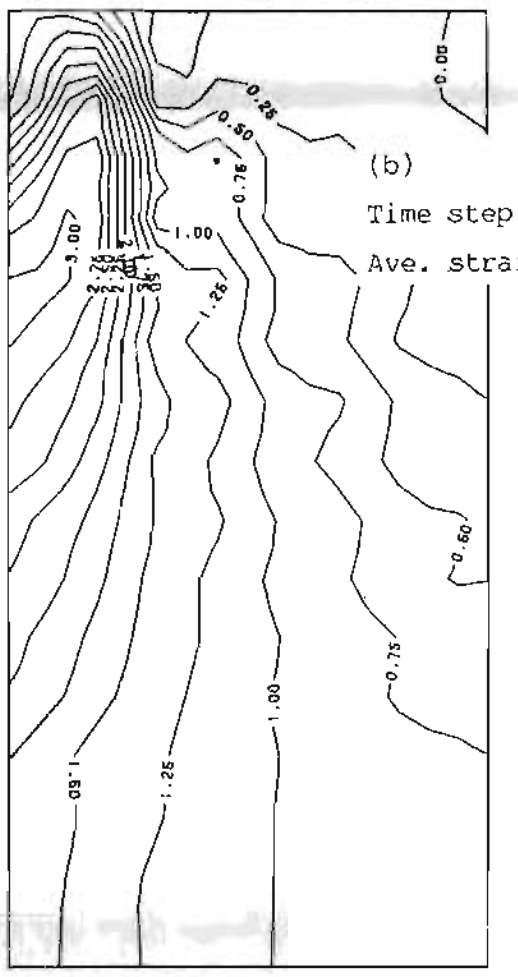

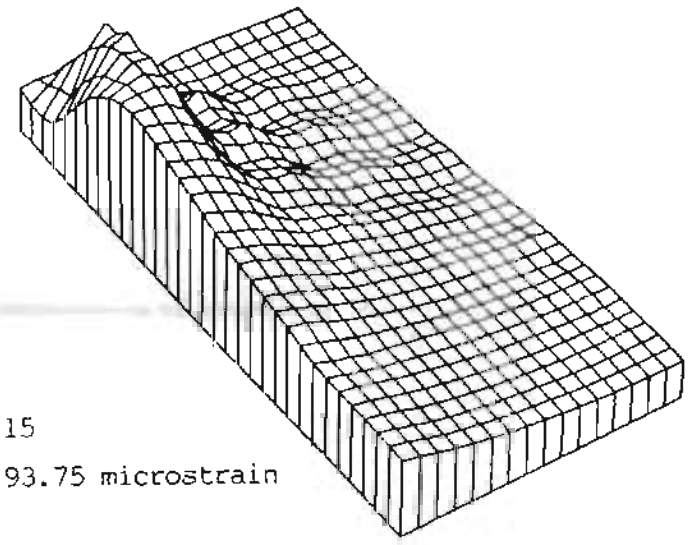

(c)

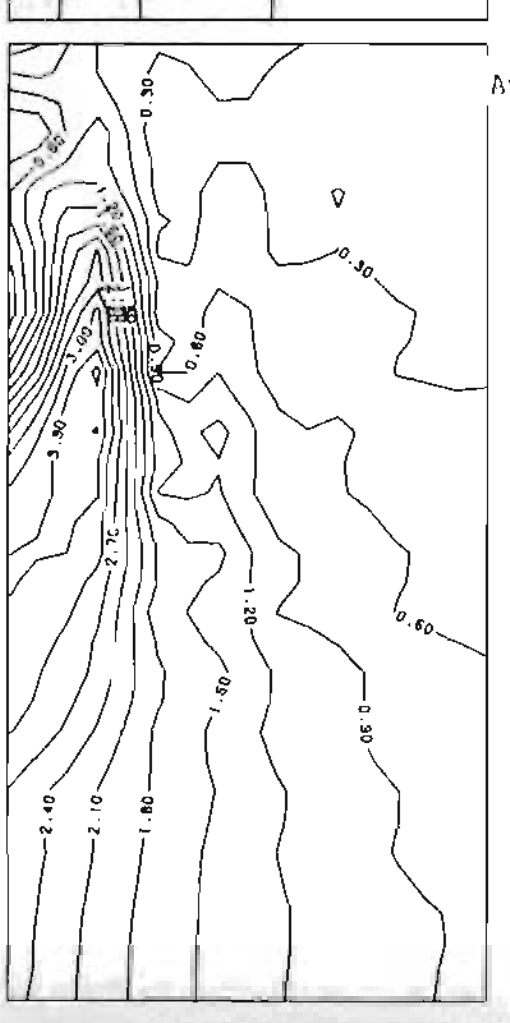

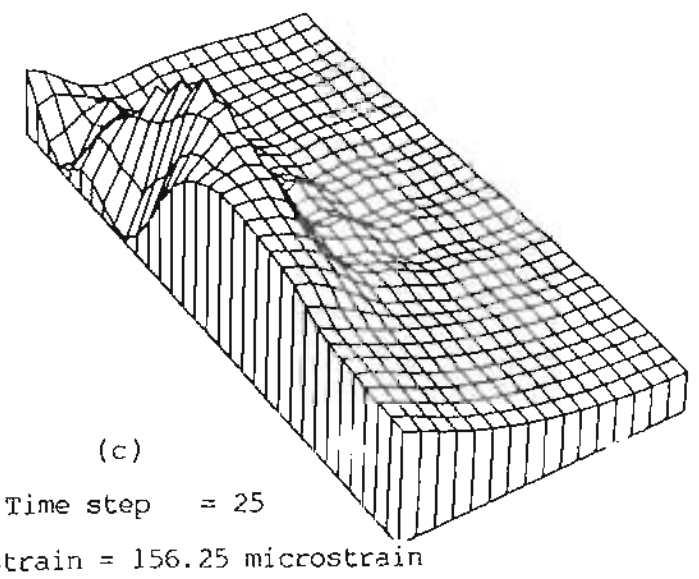

Figure 5.22 (left & above)

Model D3A : Plots of maximum principal tensile stress at varying load increments

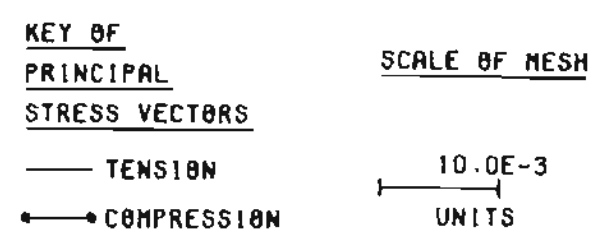

Figure 5.21 (far left)

Model D3A : Principal stress vector plots for varying load increments

5.2.2 D2A and D3A

As shown in figure 5.9, models D2A and D3A were derived by extending the distance between primary cracks to 120 mm and 160 mm respectively. Figures 5.19 to 5.22 show their behaviour in terms of the distributions of principal tensile stresses at various loading stages.

In these models the time steps represent identical displacement increments to those which were applied to model D1A. Since the models are longer these represent respectively smaller increments of average strain applied to the models which, it was hoped, would lead to the analyses going further before becoming numerically unstable. This was not the case. Model D2A progressed a total of 17 steps representing an average strain of 142 microstrain, compared to the 275 microstrain achieved by model D1A. Model D3A progressed some 28 time steps, or 175 microstrain, before it became numerically unstable. The analysis paths (strain vs time increment) are shown in figure 5.23.

These two models were behaving in a manner very similar to that observed in model D1A. The only results presented therefore are plots of the principal stresses at various time increments. These are presented vectorially, as well as by contour and 3-dimensional representations for the same reasons described earlier.

5.2.3 Comparison of the three analyses

Interesting points to note when comparing the analyses are:

(i) While the strains in the concrete are all still elastic (average strain less than 30 microstrain for model D3A) the stress distribution at the plane of symmetry midway, between the primary cracks, tends towards uniformity with increasing distance between cracks. This, it will be remembered, was one of the assumptions on which the empirical theories are based.

(ii) As the strains increase, however, the stress distribution at the plane of symmetry becomes less and less uniform, although in the examples with the wider

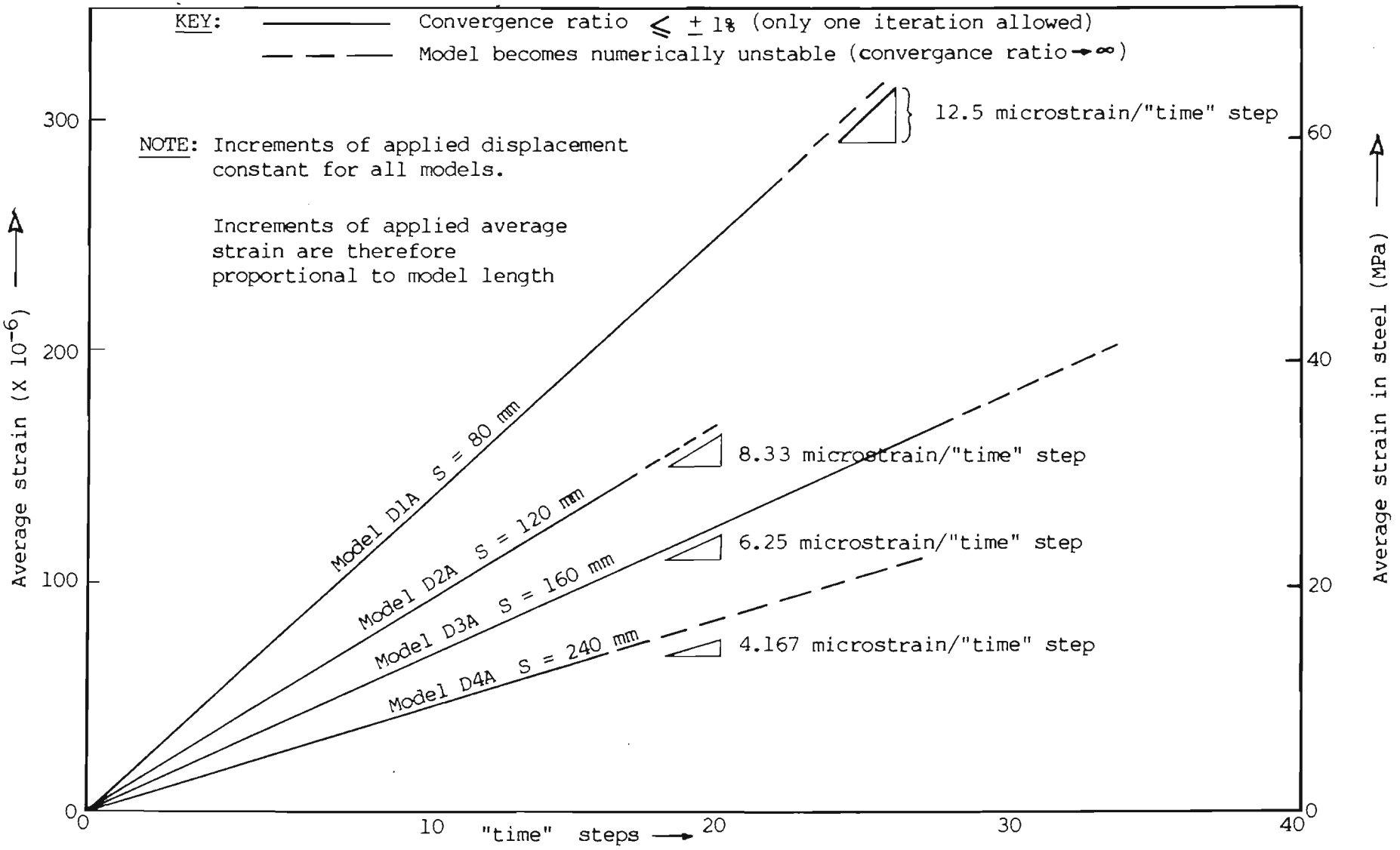

Figure 5.23: Incrementation of applied strain in models D1A to D4A

crack spacing the distribution remains more uniform than in the other.

(iii) In model D1A no tension at all is built up on the surface of the concrete between the cracks. In fact, examination of figure 5.11 will show that the longitudinal stress becomes negative.

(iv) Although the increments in average strain get progressively smaller from models D1A through to D3A (since the same displacement increments are applied at each "time" step) the size of stresses in the "corner" of concrete bounded by the primary crack and the bar do not reduce in proportion. (The "corner" consists of elements 2:1, 2:2, 2:5 and 2:6 for all of the NOSTRUM models - see figure 5.9). This may be seen quite clearly by comparing figures 5.16(a) and 5.22(a). The variable in both cases is principal stress, plotted to the same scale. Instead of being half of the size of those in model D1A, those in D3A are only in the ratio of 2,2/2,4 times as small. The explanation for this phenomenon appears to lie in the tremendous concentration of stress that occurs towards the "corners" of concrete at the primary cracks.

(v) Comparison of figures 5.16, 5.20 and 5.22 shows that, in line with the observation on stresses made in (iv) above, the progression of internal, or secondary, cracking is more closely related to the total extension between primary cracks than to the average strain.

(vi) Although it seemed with model D1A that the analysis had become numerically unstable because the concrete had effectively sheared off the bar, this was not the case with models D2A or D3A. Examination of the crest of the principal stress "wave" shows that at the time that the analyses ended the "wave" had not yet reached the plane of symmetry midway between the cracks. In other words there was still potential for an increased amount

of total force to be transferred to the concrete.

(vii) From (vi) above we may conclude that there is another reason for the numerical instability which caused premature termination of the analyses.

5.2.4. Model D4A (S = 240 mm, otherwise as for D1A etc.)

The case where the distance between cracks equals 240 mm was also analysed in an attempt to investigate the formation of new intermediate primary cracks. As with models D2A & D3A, the displacement increment applied to the plane of symmetry was kept constant, and thus the increments of average strain were reduced compared to the previous models. The analysis path of this model (strain vs time step) is shown in figure 5.23. As may be seen, despite the lower rate of application of strain to the member, the analysis proceeded less far than any of the others. No plots were made of the results as it was felt that the analysis had not proceeded for enough to make this worthwhile. An examination of the printout indicates that, up to when it became numerically unstable, the analysis was proceeding in a very similar manner to that shown by the earlier analyses.

5.3 ATTEMPTS TO REFINE NOSTRUM MODELS

As has been observed in the previous section, the analyses that were carried out using NOSTRUM were a little rough and ready in that

(i) the mesh was rather coarse,

and (ii) the equilibrium convergence criterion was removed.

It was also pointed out that the models became numerically unstable at fairly low load levels. In the best case the average strain of 275 microstrain for model D1A corresponds to an average steel stress of only 56,7 MPa (taking E_{steel} = 206 GPa). Since this level of stress is way below that which is usual in either conventional structural members, or even water retaining structures, the writer sought ways of enabling the analyses to proceed further. Amongst the ways investigated were:

(i) reducing the amount of displacement applied at the plane of symmetry at each load increment.

(ii) reducing the element size.

(iii) allowing a fairly large tolerance on the equilibrium convergence criterion.

Initially, the writer tried to improve the performance of model D4A by decreasing the amount of displacement increment applied at a time step. The resulting analysis paths are shown in figure 5.24. where it can be seen that this resulted in a slight improvement on how far the analysis proceeded, although at a considerable cost in the number of load steps analysed.

The NOSTRUM package has a facility for saving the state of the model as the analysis proceeds, and then, if the analysis runs into numerial trouble, using the last saved state for a restart analysis. In order to use this option the writer had to reintroduce the equilibrium convergence criterion so as to have a way of stopping the analysis from proceeding too far and ending up with the last saved state of the model consisting of rubbish. This was exactly what occurred with model D4A, where as a result, the runs with altered analysis paths had to be started from the beginning each time.

The convergence criterion flag was accordingly replaced in the input deck with a value of 1% for a re-analysis of model D1A. (1% was the typical value of the convergence ratios achieved without equilibrium iterations.) In addition the initial displacement increments were halved in size. Figure 5.24. shows that this was to no avail, and the analysis terminated due to lack of convergence at a lower strain than before. Upon restarting at the last saved state of the model with a displacement increment that had again been reduced, the same result was found. The restart analysis did not even pass the strain level achieved with the previous incrementation rate.

Accordingly, it was decided to stop trying to improve the situation by decreasing the increment step and to investigate whether reducing the element size would have any beneficial effect. Model D1B was analysed

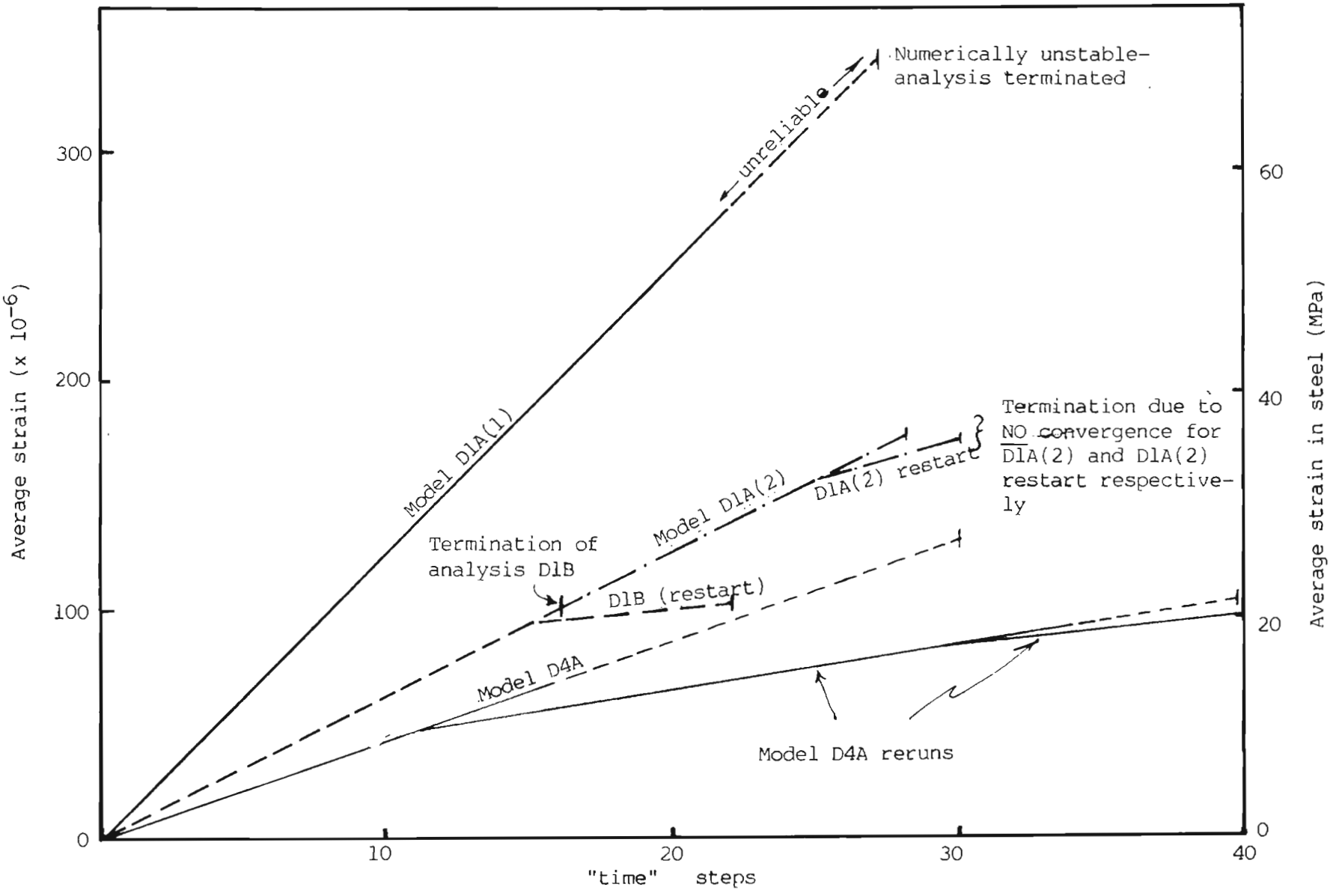

Figure 5.24: Analysis paths of "refined" NOSTRUM Models

with the element dimensions half of those for D1A. In other words, the model had four times as many elements as before. As shown in figure 5.24, this too was of no help and in fact, the contrary was found. Subsequently reducing the applied displacement increment after restarting again had no beneficial effect.

The third method proposed initially - increasing the equilibrium tolerance - was not tried since the model generally reached the 1% tolerance requirement in the first iteration right up to the point at which it became unstable. Here, when further iterations were tried the solution actually became worse. Thus the writer concluded that the problem was a convergence one, and not a tolerance one. Since, there was no immediately apparent reason for this convergence problem and since the ABAQUS concrete model was available for use by that stage, the writer decided to abandon further modelling with NOSTRUM in favour of using ABAQUS.

CHAPTER 6

FINITE ELEMENT MODELLING CARRIED OUT USING "ABAQUS" AND THE "ABAQUS" CONCRETE MODEL.

6.1 SALIENT FEATURES OF THE ABAQUS "CONCRETE" MODEL

The ABAQUS concrete model uses the stress surface developed by Chen and Chen (1975) to define the initial yield and failure values for concrete. Until the failure surface is reached, the theory of this model is a hardening plasticity theory, but the yield surface is specifically defined to simulate some of the salient features of concrete, particularly the difference in response under compressive and tensile stresses.

The ductility of the material is completely defined in terms of this theory by giving the stress-strain curve in a uniaxial compression test. The theory is then extended to the tensile region and multiaxial stress space by defining yield and failure surfaces in stress space, where each surface consists of two parts, namely a parabolic surface that is primarily located in the triaxial compression region and a hyperbolic surface in the remaining region (see figure 6.1).

The ABAQUS model is thus calibrated in several parts, namely uniaxial compression, biaxial (and by extension, triaxial) compression, uniaxial tension, and lastly biaxial (and triaxial) tension.

Each of the uniaxial curves may be defined in considerable detail as will be described in section 6.2.

6.1.1 Crack modelling by ABAQUS.

If the hyperbolic portion of the failure surface is reached (i.e. for stress combinations other than triaxial compression), the material is assumed to crack in a plane that is orthogonal to the largest principal strain. In the Chen and Chen model the concrete would immediately lose all of its strength in the direction of the crack.

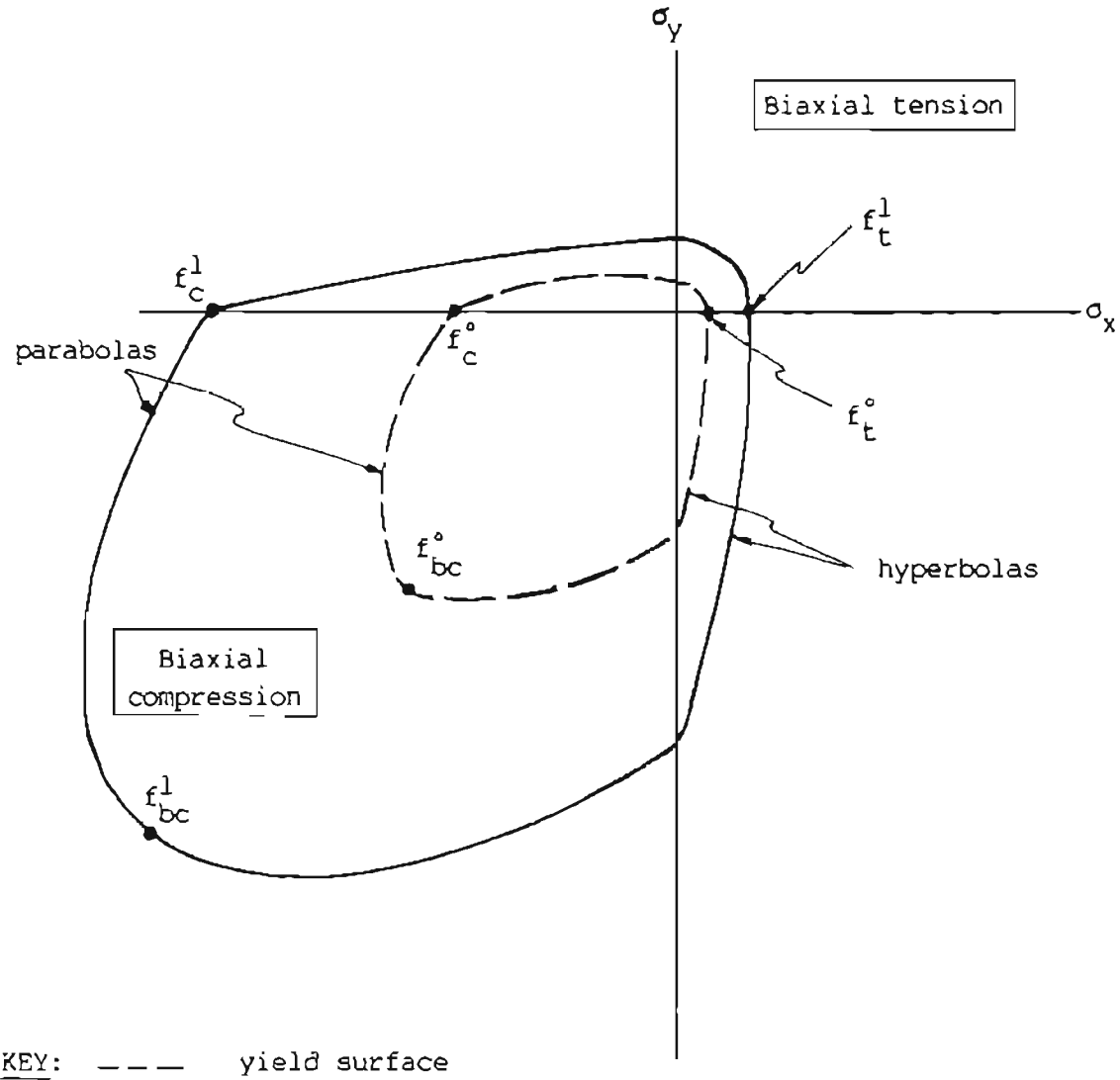

KEY: — — — yield surface

——— failure surface

f_c° = uniaxial yield stress in compression

f_{bc}° = biaxial yield stress in compression

f_c^1 = uniaxial failure stress in compression

f_{bc}^1 = biaxial failure stress in compression

f_t° = uniaxial yield stress in tension

f_t^1 = uniaxial failure stress in tension

Figure 6.1: Yield and failure surfaces in 2-dimensional stress space - ABAQUS Concrete Model.

This has been modified in the ABAQUS model and the user is given the option of specifying the downwards portion of the tensile stress-strain curve, as well as the amount of shear that may still be carried across a tension crack. Should a crack close during subsequent loading the material will recover its stiffness, although the original direction of the crack is recorded so that it can reopen. This cognizance taken by the model of the direction of cracking is a notable difference from the behaviour of the NOSTRUM damage model, which became damaged in all directions simultaneously by virtue of the scalar damage parameter used by the model.

The directions of "cracks" that have formed, are given by the ABAQUS programme as part of its output. These are smeared cracks rather than discrete cracks. In some smeared crack models for concrete, whole elements are allowed to crack at a time. An example is the model developed by Bazant and Cedolin (1979, 1980). This type of model however, has the problem that results obtained using it can be influenced by the size of finite elements used, unless fracturing is controlled by a suitable, non-linear, energy based formulation. A "crack" recorded by ABAQUS, reflects only the fact that the stress at a particular gauss integration point has reached the failure surface of the concrete model.

Because there is no "crack front", as there is in the discrete crack or crack band types of model, which would be sensitive to changes in element size, the ABAQUS model appears as if it should be independent of this variable.

As will be seen later in the discussion of results obtained with the model, the writer did find some problems which appear to be linked to the post-fracture behaviour of the model. The ability of the model to correctly model size effect in the member being analysed is also questioned. Otherwise, being the best available, apart from the NOSTRUM damage model to which it will be compared, it was hoped that the model would incorporate sufficient parameters that would ensure that, even if exactly correct numerical values were not obtained from its use, at least it should be able to give a fairly realistic indication of the mechanisms by which bond failure and cracking occur in reinforced concrete.

6.2 MATCHING THE CALIBRATION OF THE ABAQUS CONCRETE MODEL TO THE NOSTRUM DAMAGE MODEL (CALIBRATED FOR 30 MPa "KUPFER" CONCRETE)

6.2.1 General

In order to compare results obtained from different programs, these must obviously be fed with the same information to be used in the calculations. This is especially so in cases such as the present one where it was hoped that comparison of the response of the two models would provide some check of their numerical reliability.

The problem is not as simple as it may at first seem since the two programmes use rather different ways of inputting the base information about the concrete and then interpolate between the given points in different ways. In addition the two models use different algorithms to determine yield and failure surfaces and to calculate the values of inelastic stress. Nevertheless it was decided that the target calibration for the ABAQUS model would be to simulate the three test curves obtained with the damage model by analysing single element models in uniaxial tension and compression, and biaxial tension. The inelastic, biaxial compression response of the model is not important since, in the analyses to be carried out, the concrete is unlikely to ever reach stresses that go beyond the elastic limit in compression.

6.2.2 Uniaxial compressive stress response

This part of the model response is calibrated in two parts - the elastic region and the plastic region.

In the elastic region the stress is defined by giving the elastic properties of Young's modulus, E, and Poisson's ratio ν. Since, in the Damage model the parameters used to define the initial elastic concrete properties are the initial shear modulus, G_o, and the initial bulk modulus, K_o, we need to calculate the corresponding values of E_o and ν.

We use the following well established relationships:

$$G_o = \frac{E_o}{2(1 + \nu)} \qquad \ldots (6.1)$$

$$K_o = \frac{E_o}{3(1 - 2\nu)} \quad \ldots (6.2)$$

Rearranging, we get:

$$\frac{G_o}{K_o} = \frac{3}{2} \cdot \frac{1 - 2\nu}{1 + \nu} \quad \ldots (6.3)$$

But for our case we can substitute the values used in the damage model, G_o = 13 790 MPa

& K_o = 16 457 MPa

Solving, we get : ν = 0,1725

and, by back substitution : E_o = 32 338 MPa

Outside of the elastic region the stress-strain relationship is defined by giving the uniaxial compressive stress as a function of uniaxial compressive plastic strain. This is done by giving the stress and plastic strain values of (a) the point of first yield, (b) the point of maximum compressive stress, and (c) any other intermediate points to be defined or any points on the curve beyond the peak stress and into the strain softening range. For the analyses carried out as part of this thesis the points specified were those plotted in figure (6.2) and superimposed on the stress-strain curve obtained from the damage model. The curve may be continued into the strain softening region, but since the writer's analyses would not be reaching compressive stresses of this magnitude, no points on the stress-strain curve beyond the peak (or failure) point were specified. The calibration was tested by analysing a single element loaded under uniaxial compression. The resulting curve is plotted in figure 6.2.

6.2.3 Multiaxial compressive stress response

Having already defined the yield and maximum compressive stress points for uniaxial stress, these are extended to multiaxial stress space by defining ratios of biaxial stress/uniaxial stress and biaxial/uniaxial plastic strain at failure. The programme then fits a parabolic curve through the points defined in this way (See Figure 6.2). Extending this to three dimensions, we have a parabolic failure surface in three-dimensionalstress space. Although the ABAQUS user manual is not specific in this regard, the writer assumes that the ratios defined

above are also used to define the surface of initial yield in multiaxial stress space, with respect to the uniaxial yield points already given.

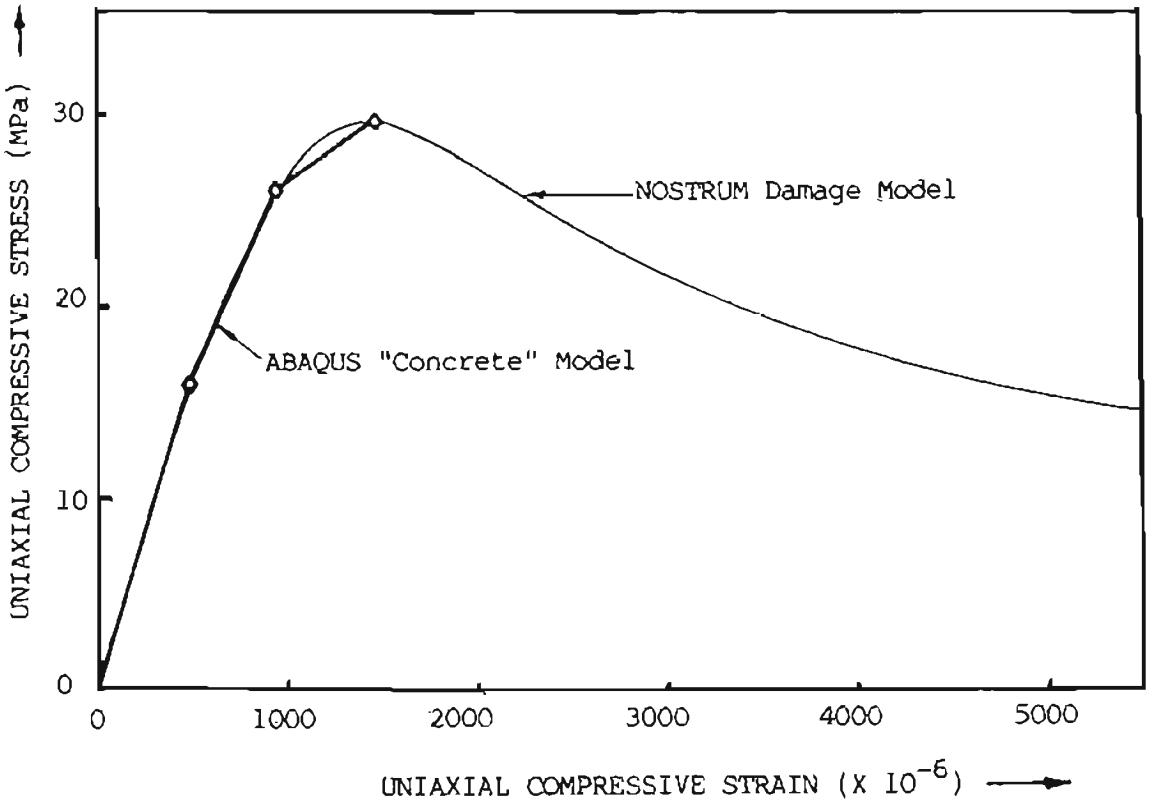

Figure 6.2: Uniaxial compressive stress response of the ABAQUS concrete model, compared to that of the NOSTRUM damage mechanics model.

6.2.4 Tensile stress response

The ABAQUS program requires, as input for the definition of the tensile response of the concrete model, the ultimate stress and strain under uniaxial tensile stress (see figure 6.1), defined as ratios of the corresponding ultimate stress and strain in uniaxial compression. The programme then assumes the same ratios apply for the determination of the tensile yield point with respect to the compression yield point. The values specified in this way are plotted on figure 6.3, superimposed on a plot of the damage model's uniaxial tensile response. A uniaxial tensile test done on a single element with ABAQUS gave the curve shown in the figure.

The model then allows completely independent specificatiion of what the authors call the "tension-stiffening" response. The writer, as

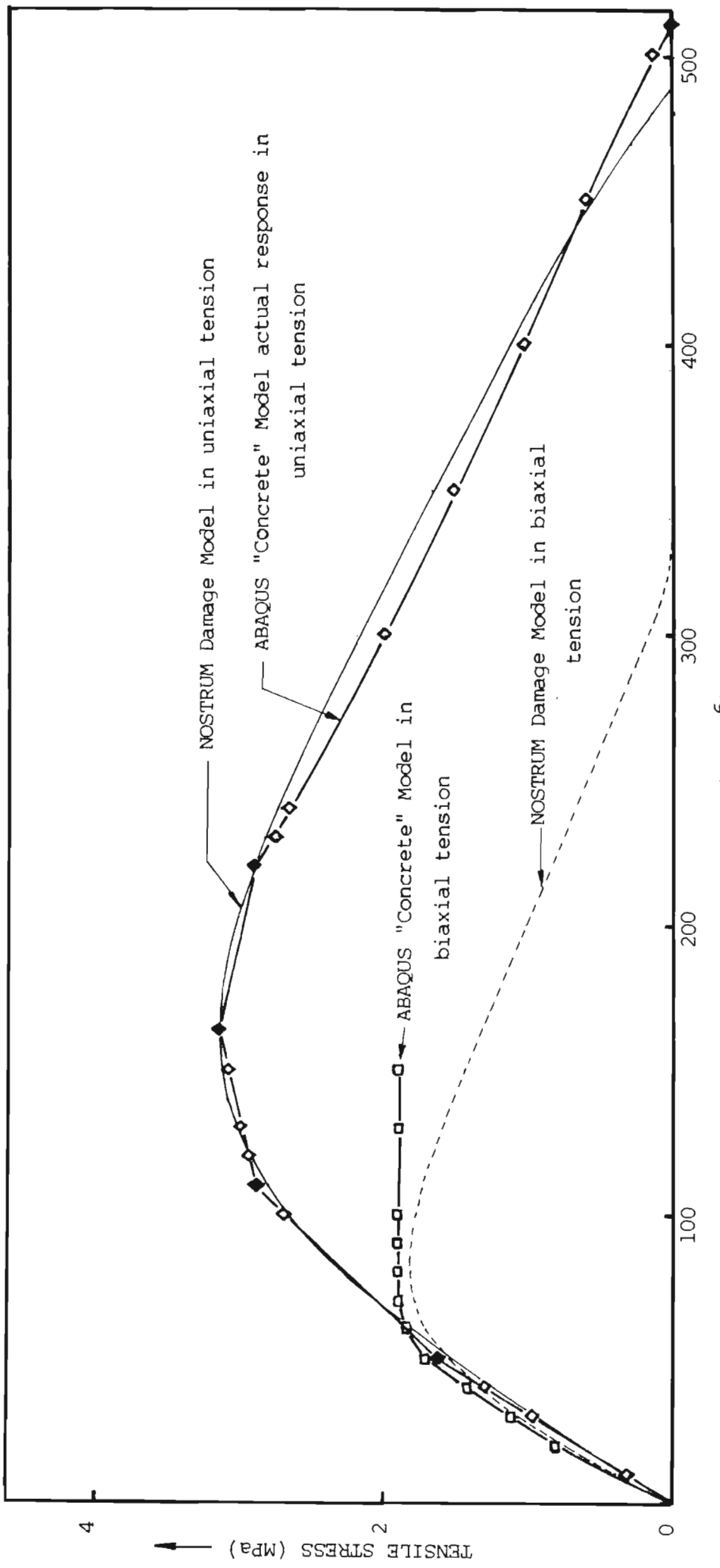

Figure 6.3: Comparison of uniaxial and biaxial tension responses of ABAQUS "Concrete" Model to NOSTRUM Damage Model.

already discussed for the calibration of the damage mechanics model, incorporated the decreasing portion of the stress-strain curve to allow for the known strain-softening property of concrete in tension. In the absence of any other data the model was calibrated to have the same strain softening curve as was used in the analyses using the damage model.

The response of the model to biaxial tensile or compression/tension stress states is defined by fitting a hyperbola through the uniaxial compression and tension failure points as shown in figure 6.1. This is extended to multiaxial stress space as a hyperbolic surface.

A problem noted by the writer with this method of determining the failure surface is that the user does not have direct control over the ratio between the uniaxial tensile failure stress and the biaxial tensile failure stress. A single element model was therefore analysed in biaxial tension to check the response of the model. The results of this analysis are presented in figure 6.3, superimposed on the biaxial response curve for the damage model. As may be seen the agreement is good until after the peak (failure) stress has been reached, when the ABAQUS model does not exhibit the expected strain softening, but rather, becomes perfectly plastic before the analysis breaks down. Close scrutiny of the analysis output indicated that there appeared to be a problem with the algorithm which determined the direction of cracking for the model. This however only appeared to be a problem when the concrete should crack simultaneously in two directions and, as this case was not expected to arise in the analyses to be carried out, the problem was accepted as being unimportant.

6.2.5 Shear retention

The ABAQUS concrete model has an option that enables the user to define how quickly the concrete will lose its ability to transfer shear across a crack. In the first analyses the writer was under the false impression that the default value of the shear retention was that it would reduce according to the same curve prescribed for "tension stiffening".

It was not expected that there would be cause for much shear transfer

across concrete that had already cracked in tension. This was as a result of the results already achieved using NOSTRUM where examination of the principal stress vector plots showed that the vectors did not change direction significantly after the concrete had passed its peak tensile stress (i.e. cracked).

When the writer did include the shear retention option in the concrete material model, the gradual decline in shear stiffness was specified to take place parallel to that of tensile stiffness. This was not an attempt to model shear retention due to aggregate interlock but rather, simply an added dimension to the tensile strain softening curve already included. It was felt by the writer that this would be a good starting point, and that the inclusion of a more realistic modelling of aggregate interlock would only be necessary if it were subsequently shown that a significant amount of shear took place parallel to existing cracks.

6.3 CONSIDERATION OF FEATURES OF THE PROGRAMME

6.3.1 Optimisation of the equilibrium tolerance criterion

As with NOSTRUM, ABAQUS requires the user to specify an equilibrium tolerance used by the programme to decide whether to continue iterating to a more accurate solution or continue to the next increment of load.

Obviously, the less demanding this tolerance is the quicker the solution will converge to within its limits, but, on the other hand, the solution will simultaneously become more unreliable. The first task then is to strike a happy medium between these two considerations.

In contrast with NOSTRUM which requires the force tolerance to be given as a percentage of the current levels of force in the model, ABAQUS requires the input of an absolute value of force, "PTOL", for use as the measure of tolerance. This clearly could be quite disadvantageous in the type of model to be studied here, where very great fluctuations in forces are expected (a) at different loading

stages and (b) at various positions through the model.

The user's manual suggests that the force tolerance be set at a small fraction ($\leqslant 1\%$) of the typical actual force values. The problem is to determine what force value may be considered typical.

Since the aspect of the results which is of most interest is the formation of cracks, the writer decided to use a typical cracking stress of 3 MPa as the value from which to calculate a corresponding typical actual force value.

Considering the first node away from the reinforcing bar in model A1B, the typical (longitudinal) cracking carried by this node is approximated by:

$$F_{node} = (r_2^2 - r_1^2)\,\pi \,.\, \sigma \qquad \ldots (6.4)$$

where r_1, r_2 = the radii of the midpoints of the inner and outer adjacent elements respectively.

σ = the stress in the elements

Substituting : $F = (0.0175^2 - 0,0125^2).\pi.3 = 1,41 \times 10^{-3}$ MN

The first analysis of model A1B was carried out using PTOL = 3.10^{-6} MN which corresponds to about 0,2% of the typical nodal cracking force calculated above. Figure 6.4 shows a plot of the analysis path of this model showing that, with this tolerance, the analysis proceeded slightly further than the best achieved using NOSTRUM. The maximum value of the average stress in the bar was still only approximately 70MPa however, and thus the writer decided to try using coarser equilibrium tolerances in an attempt to get the analysis to proceed further.

Since the programme's automatic incrementation scheme found that the initially chosen starting increment was too small, this was increased so as not to waste computing time stepping slowly through the fairly linear part of the analysis. It was also felt that minimising the number of steps in the early stages would help to minimise any possible cumulation of errors due to coarse tolerances.

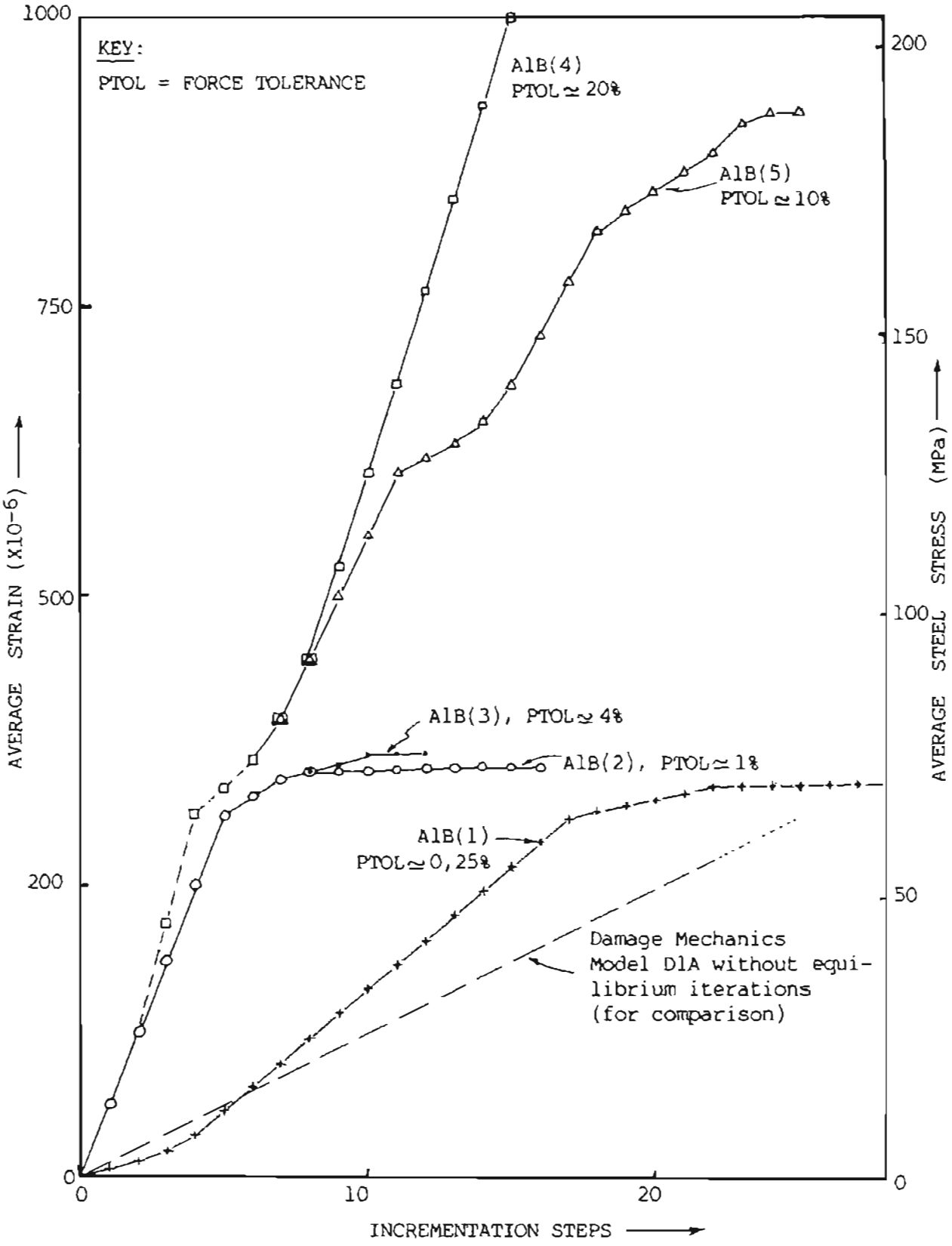

Figure 6.4: Comparison of analysis paths of model A1B using different force tolerances.

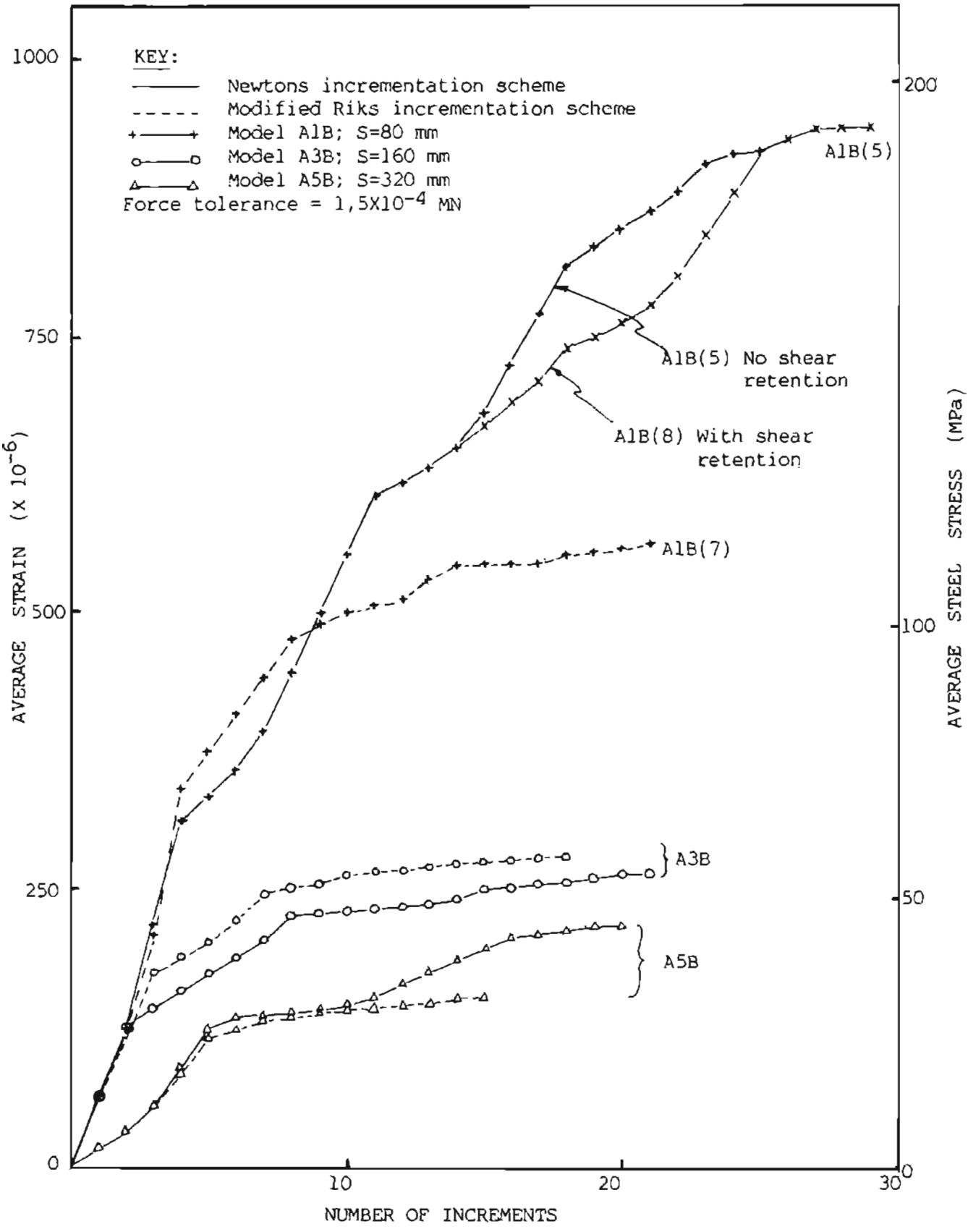

Figure 6.5: Comparison of analysis paths - Newton's automatic incrementation scheme vs tha modified Riks incrementation scheme.

A total of five analyses were done with various equilibrium tolerances. The various analysis paths are also plotted on figure 6.4 and show that it is only when the tolerance reaches approximately 10% of the value calculated above that the analysis proceeds to any reasonable level of average stress and strain in the steel. It is also immediately noticeable that the analyses consistently slow down (i.e. use smaller increments) at the same level of applied strain. This phenomenon is investigated later.

6.3.2 Consideratiion of incrementation schemes

The most important aspect of analysing for material non-linearity lies in the fact that the behaviour of most materials is history dependent i.e. the solution cannot be sought directly but must be obtained by following the actual sequence of loading on the structure.

Since we can do no better than follow the actual loading sequence in a stepwise manner, it follows that the choice of the size of the steps can become critical to the success or otherwise of the analysis.

NOSTRUM requires that the user define the size of step directly. Any subsequent change required in step size must be made by way of a restart analysis which is rather limiting in terms of analysis flexibility and efficiency as well as being laborious.

The programme ABAQUS offers the user three different ways of determining the size of the increment of load or imposed displacement to be applied to the model.

(i) Direct method:

With this alternative the user has full control over the size of the load or displacement increments to be applied. The major drawbacks of this method are that:
(a) the user needs to have considerable experience of the size of increment necessary for efficient running of the problem.
(b) the increment size may not easily be changed

halfway through an analysis should this become necessary.

(ii) Newton's method:

This method is used by the programme to decide automatically the size that the incrementation step should have. The size of increment is continually reviewed and altered, based on the number of iterations required to reach equilibrium at the current and preceding two increments.

(iii) The modified Riks method

This method is proposed for use when the maximum load magnitudes are considered to be a part of the solution. The method obtains equilibrium by controlling the path length along the load-displacement curve within each increment.

6.3.2.1 Comparison of the modified Riks and Newton methods of incrementation

In an attempt to get the analysis to proceed further, i.e. to higher steel stresses, it was decided to try using the modified Riks method of incrementaton.

The preliminary test using the Riks method was encouraging. Here the analysis proceeded marginally further than an equivalent analysis using the Newton method of incrementation.

It was hoped that, because of the nature of the incrementation scheme, i.e. limiting the increments along the load-displacement curve, the size of the imposed displacement increments might be reduced timeously in a curvilinear fashion, rather than in an abrupt manner after the model has already got into numerical trouble, as occurs with the Newton method.

Using force tolerance of $1,5 \times 10^{-4}$ MN (about 10% of typical cracking

force for an element) analyses were run using both incrementation schemes for a 20 mm bar, 40 mm cover, and distance between cracks of 90, 160, and 320 mm respectively. The analysis paths are plotted on figure 6.5 for comparison. It should be noted that the Riks analyses did not include the shear retention parameter which is included in two of the other three analyses. As has already been discussed in section 6.1.6, however, this parameter is not thought to have very much influence on how far the analysis proceeds.

Figure 6.5 shows that, for S = 80 mm there is a considerable gain to be had by using Newton's incrementation scheme, while for the S = 160mm and 320 mm respectively, the loss or gain in advantage to be had by using the Newton method over the modified Riks method is marginal.

6.4 DETAILS OF ABAQUS MODELS

6.4.1 Dimensions and discretization

The structural details of all of the models are as described in section 4.5 of chapter 4, and listed in table 4.1. The discretization is always into 4-noded elements with the dimension of each side being 0,005 m (5mm). The actual node and element numbering is not constant from model to model as was the case for the NOSTRUM analyses. This is because changes were made to parameters which precluded this; e.g. the diameter of the reinforcing bar. (The centre of an axisymmetric analysis must have its r-coordinate equal to zero.)

Accordingly in the description of the various areas of the model descriptive terms will be used and reference will be made to figure 6.6 which shows the typical layout of the various elements described.

6.4.2 Grouping of models into series

As may be noted in table 4.1, where the only parameter changed between models is the length between cracks, these models all have the same third character in their labels (see also Appendix A). In describing the behaviour of these models as a group, the writer finds it convenient to refer to these groups as "series X" where X is the third

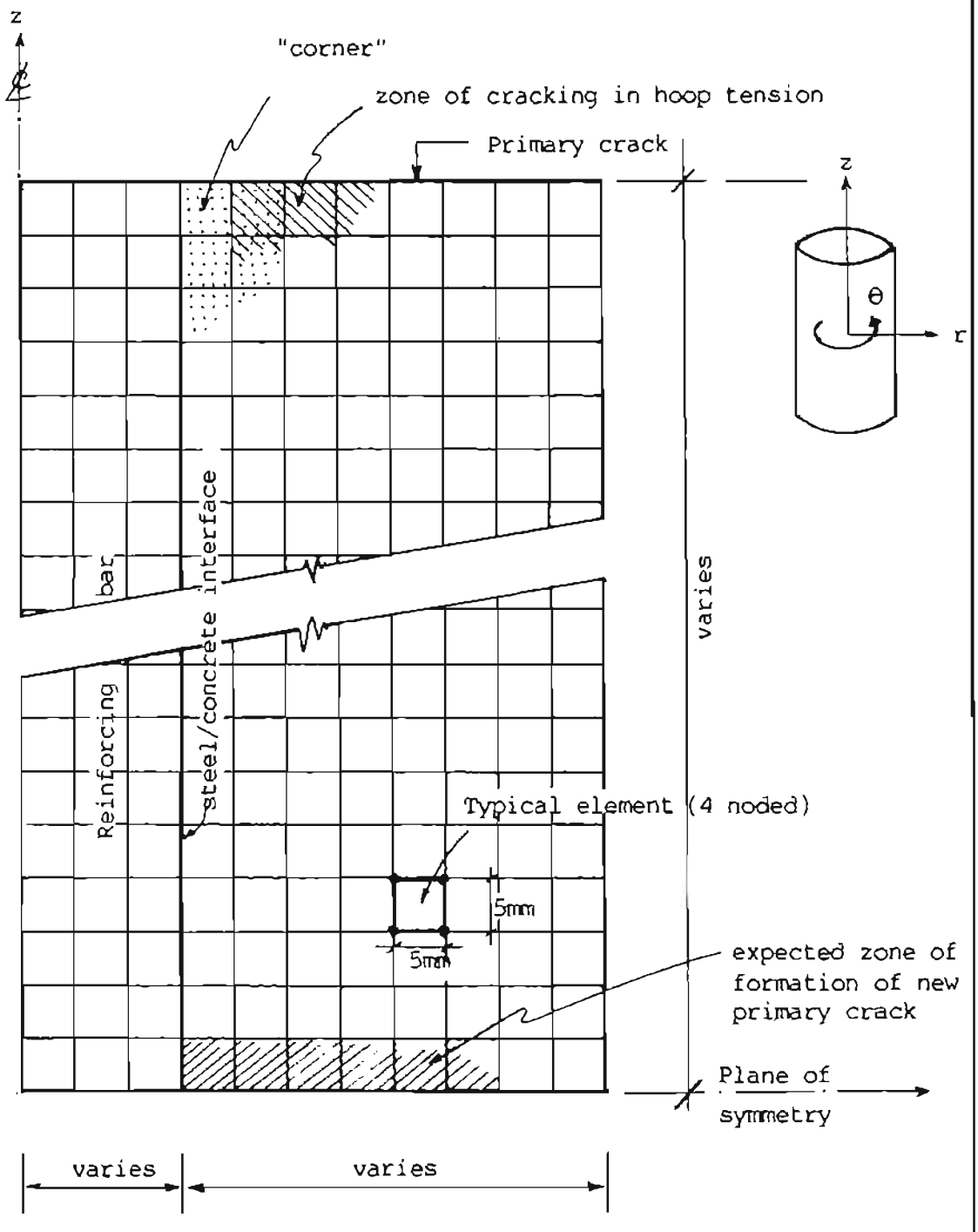

Figure 6.6: Typical layout and discretization of finite element models analysed using ABAQUS.

character in the name of each model. For example: "series B" consists of models A1B, A3B, and A5B.

6.4.3 Presentation of results from ABAQUS analyses

ABAQUS has the built in capacity to present results in the following ways:

(i) by printout

(ii) graphically as (a) contour plots of any stress or strain
(b) displaced shape plots
(c) variable vs time plots
(d) variable vs variable plots

(iii) to an output file for post-processing by the user

The same comment mentioned in the discussion of the presentaion of the NOSTRUM results applies to the presentation of the ABAQUS results. The printed out results for ABAQUS are even more voluminous than those of NOSTRUM and therefore it is quite impossible to print out all of the results.

e.g. printout for 1 element (4 noded) ⇒ 2/3 page/step

Model A1B has 80 elements ⇒ 53 pages/step
for a typical analysis ± 25 steps ⇒ 1325 pages!

For the larger models the potential printout volume would be up 4 times this amount (e.g. model A5B). This is clearly quite an unmanageable amount of paper, let alone a potentially very costly exercise. The practical solution obviously was that the writer had to limit the amount of printout produced by only printing results for selected areas of the models and also only at selected time intervals.

The first area concentrated on is the interface between the steel and the concrete, especially what the writer calls the "corner" of concrete, where (in the 2D presentation) the corner referred to is formed by the intersection of the reinforcing bar and the primary

crack. In some of the smaller models the results for the whole zone of the steel-concrete interface were printed out. This enabled the writer to trace the formation of secondary or internal cracks along this interface zone as the load increased.

The second area concentrated on was the row of elements adjacent to the plane of symmetry mmidway between primary cracks there, the writer was looking for indications of the possible formation of a new primary crack, although of course, one might have formed in some position away from this plane of symmetry due to numerical perturbations within the model itself due to the fairly coarse tolerances used.

Unfortunately, ABAQUS does not have a routine built in which plots stress vectors. These are an extremely useful way of representing the state of stress in a 2-D model as they show not only magnitude, but direction as well. The writer has written a routine which extracts data from the ABAQUS output file and rewrites it in a form suitable for input into the NOSTRUM post-processor which has an option for plotting principal stress vectors built into it. This routine was only written to handle results from elastic analyses and, although it would be a simple job to upgrade it to handle incremental analyses, the writer did not have time to do this.

Of the graphical presentation features that ABAQUS has built in, the most useful from the writer's point of view appeard to be the contouring facility. Unfortunately contour plots of principal stresses on their own do not mean too much without knowledge of the associated directions of the stresses. A full description of the state of stress in the whole model at any load step therefore requires the production of a contour plot of each of the component stresses at that load step, and this becomes almost uninterpretable. These plots are only included in the document in order to make particular points.

A disadvantage of ABAQUS's automatic incrementation schemes is that the user has no control of the amount or time of printout or graphs produced as these are produced at fixed load increment numbers and not at certain load levels. In the problems analysed by the writer, if the output interval was set too great, there would be a lack of data output for the early stages of the anlysis when the increments were

large, and too much as soon as the increments become very small.

With these problems in mind, the writer transferred all of the output from the analyses onto magnetic tape, which is the most economical way of storing it. The idea was that after running all of the analyses, selected areas and variables could be studied in more detail by suitable post processing, e.g. plotting principal stress vectors or series of perspective plots of stresses, such as those produced for the NOSTRUM analyses. In the end, there has been insufficient time to do this post processing. The writer will argue however, that not too much more information would have been gleaned from it than has been obtained by careful consideration of the limited printed results.

Because of their extreme bulk, those limited results which were printed out for the various models analysed cannot be included in this document. A sample of printout is given in Appendix C which shows the manner of presentation of stress results for each gauss integration point at each load increment. A sample data deck is given in Appendix D which lists the values used to define the model structurally, materially, and from the point of view of incrementation schemes, printout, graphical output, and file output requested. A detailed description of the meaning of the data deck may be obtained from the ABAQUS user's manual by Hibbett et al (1984).

For the rest the results of the analyses given in this document will be confined to that information which has been extracted from the printouts and is presented in the form of graphs which are discussed in the text.

The angles of cracks and strains at which they form, have been investigated and this data has been extracted. It is presented graphically in section 6.6 for model A1B and the calculations done as part of the extraction are presented in Appendix F.

6.5 DISCUSSION OF ANALYSES USING ABAQUS

6.5.1 General

The analyses carried out have been listed in table 4.1. The range of different analyses were selected in order to investigate the effect on crack widths of changing various parameters.

As was shown in chapters 2 and 3, the various parameters included in the formulae are only claimed to have an influence on crack width indirectly, by virtue of their apparent influence on crack spacing. This is because of the universally made assumptions that crack width is proportional to crack spacing and that a stabilized crack pattern exists.

Thus, besides being intended to test the proportionality between crack width and crack spacing, the length of the finite element models was altered to try to study the possible mechanisms involved in the formation of new primary cracks and the development of the "stabilized" crack pattern. The other two parameters varied, the bar size and the amount of cover to the bar have both been proposed in the literature as having an influence on the average crack spacing achieved in a stabilised pattern. Various theories have been postulated to explain these relationships, and the series of analyses are intended to test these theories as much as the relationships themselves.

Presentation of the results will not be by model but, rather, by series of models, with discussion of what it was hoped the series would check.

First of all however we will consider, in general terms, the validity of models and the mechanisms controlling the interactive behaviour of steel and concrete which they have brought to light.

6.5.2 Investigation of reasons for numerical problems in analytical models.

It has already been observed that the analyses do not proceed to a

very high average strain or stress before slowing down and, mostly, halting due to some type of numerical instablilty. (The actual halting is due to the programme requiring an increment step smaller than the minimum specified.) Investigation of what could have caused the numerical instability brought to light three phenomena which seem to be fairly closely related with sudden slow-downs in the analyses (i.e. reductions in increment sizes.) These are:-

(i) Tertiary cracking,

(ii) Secondary cracking is completed along the whole steel-concrete interface,

and (iii) a new primary crack tries to form at the midpoint of the model.

Phenomena (ii) and (iii) above are self explanatory whilst the third, tertiary cracking (usually called longitudinal cracking in the literature), is discussed later in section 6.6 on cracking modes of the finite element models.

Consideration of figures D.1 to D.6 in Appendix D which are plots of the analysis paths on to which the increment of first recording of these occurrences has been plotted, shows fairly clearly those occasions where the slowing down of the analysis appears to be linked with one or other of the above. It cannot, however, be stated categorically that any of those behavioural modes is the predominant controlling factor in determining the extent to which the analyses proceeded.

For all of the series "B" models the cause of the first numerical problems encountered by the programme appear almost definitely to be tertiary cracking. Series "L" models behave similarly. Two of the analyses of the series "C" models, on the other hand, seem almost without doubt to slow down and come to a halt as a direct result of the formation of new primary cracks. In the two shorter series "C" models, the effect of tertiary cracking is not obviously related to the first numerical problems whilst, in the third, tertiary cracking did not occur at all.

For the remaining models, the first numerical instabilities appear to

occur as a result of a combination of the effects of the occurrence of tertiary cracking and the fact that secondary cracking occurs over the entire steel-concrete interface zone.

Some of the models appear to recover numerically after going slowly through these portions of their loading histories and the analyses proceed to higher strain levels, where they slow down again and halt because the required increment steps become smaller than the mimimum set by the writer. (On two occasions, AIC & AIL, the analyses actually continued until the specified load step - up to 1000 microstrain - was completed.)

The only explanation which the writer can propose for this behaviour is that, since those models whose analyses terminated at very low average strains were all the longer models, this termination was related to some inability of the concrete model to form new primary cracks. This possibility is considered further in the next section.

6.5.3 Consideration of the load-displacement response of the models.

One of the things the writer has pointed out about the various models is that the greater their length, the lower the value of average strain at which the analysis became unstable.

It was thought that one way of investigating the possible reasons for this phenomenon was to consider the overall load-displacement response of the models.

Figure E.1 in Appendix E shows plots of load-displacement diagrams for the "series B" models. In order that the curves may be compared to each other, these have been "normalized" by dividing the displacement by the length of the member concerned. In other words, the load has been plotted against average strain in the members.

Immediately obvious in figure E.1 is the fact that the three curves have completely different slopes - even in the very low load stages when the behaviour is fully elastic. The explanation for this phenomenon becomes apparent when one considers the following:-

In general, the axial stiffness, K, of any member is given by:-

$$K = F/a$$

where F = force in the member due to displacement, a
a = axial displacement

In this case, as has been noted above, it is more expedient to consider the force required to cause unit strain. We will call this K'.

Thus $K' = F/\varepsilon = (\sigma.A)/\varepsilon = E.A.$

where the symbols have their usual meanings.

For a 20 mm reinforcing bar:

K' (steel) $= E.A = 206*10^{3}*(0,01^{2}.\pi)$ = 64 MN/unit strain.
= 64 kN/1000 microstrain

If the bar has 40 mm of cover all round it with a E value (as in the analyses) of 32 338 MPa

K' (whole prism) = 64 + [32 338.(0,05-0,01)] kN/1000 microstrain
= 307,8 kN/1000 microstrain.

Both of these lines are plotted on figure E.1. It is immediately apparent that they form the upper and lower bounds of the stiffness of the reinforced prism represented by the series B models.

An initial response might be to expect the load-strain curves of each of the series B models to have the same slope since they all theoretically have the same K' value (=EA) which is independent of length. One would then expect, as internal damage progresses, that the load-strain curves would be non-linear, as indeed they are. The reason for the initial difference in slope must be because, assuming perfect bond, the whole area of concrete is not immediately effective at the ends of the member (or adjacent to a discontinuity such as a primary crack). Thus the upper bound of the member stiffness only applies to

very long members where the subtraction due to this end effect is minimal.

The lower bound of member stiffness now takes on a new meaning. Where before it was simply the stiffness of a section of steel standing on its own, now it is also the lower bound of stiffness of a reinforced concrete member where the distance between primary cracks tends to zero. Thus, as new primary cracks form in tension members, we could expect to see an abrupt shift in load-strain behaviour in the direction of the lower bound of stiffness.

In the finite element models plotted here this does not occur, nor does there seem to be any intimation that it is about to occur, up until the time when the models become unstable. Model A3B does show a slight kink in the right direction, but then kinks back in the wrong direction, leading the writer to dismiss this as inconclusive and probably due to a numerical aberration.

Also plotted onto the load-strain curves are the points at which the models enter various phases of behaviour. These are:-

(i) The load point at which secondary cracking first occurs in this model (always right in the "corner"),

(ii) the load at which tertiary cracking first occurs,

(iii) the load at which the whole steel-concrete interface zone becomes cracked, if this occurs,

& (iv) the load, if any, at which a new primary crack occurs.

Considering the last three phases, it can be seen, for each of series B, C, E, F, & L, that these tend to begin at approximately the same load level for each of the different member lengths. This immediately invites comparison with the abrupt shift in stiffness, as postulated above, that would be expected as new primary cracks occur. It is possible that this shift can be achieved in more than one way, namely:-

(i) by formation of a new primary crack as suggested,

or (ii) by total loss of bond along a portion of the member caused by longitudinal splitting.

Since it is possible that a new primary crack could start at one of the secondary cracks which form near the plane of symmetry, complete cracking of the interface zone could herald the formation of a new primary crack.

Accordingly, the writer has shown dotted the general zones of the load-strain curves which are bounded by the occurrences listed above, as these are possible zones within which sudden shifts in stiffness might occur.

Obviously it would be nice if this theory could be confirmed by comparison with previous experimental data. Accordingly the writer sought experimentally obtained curves of the same nature, but to no avail. Several authors show typical curves such as the one presented by the writer in figure 5.7 but, with two exceptions found by the writer, these do not give any indications of scale. Of the two found, the first (figure 6.7) refers to lightweight concrete, so the numbers are inapplicable.

Here, Leonhardt has plotted the stress in the reinforcement at a crack against the average strain, in members with different steel contents which are being cracked under direct tension. Comparing this to the writer's figure E.1, it may be seen that the effect of dividing by the area of steel is to normalise the lower bound of member stiffness (i.e. make it independent of steel area) and the slope of this line now becomes equal to the Young's modulus of steel, E. On the other hand, dividing by the area of steel is somewhat meaningless when considering the upper bound of stiffnesses.

The second figure which gives any quantitative information on the shape of an experimentally obtained load strain diagram is that given by Rizkalla and Hwang (1984) which is reproduced in figure 6.8.

Unfortunately, the graph of these authors is not plotted to a scale which enables very much useful information to be read off it. For instance, it would be useful to know at what strain the first crack occurred. From the information given on the member to which this graph belongs we can calculate the upper bound of the stiffness, K', as follows:-

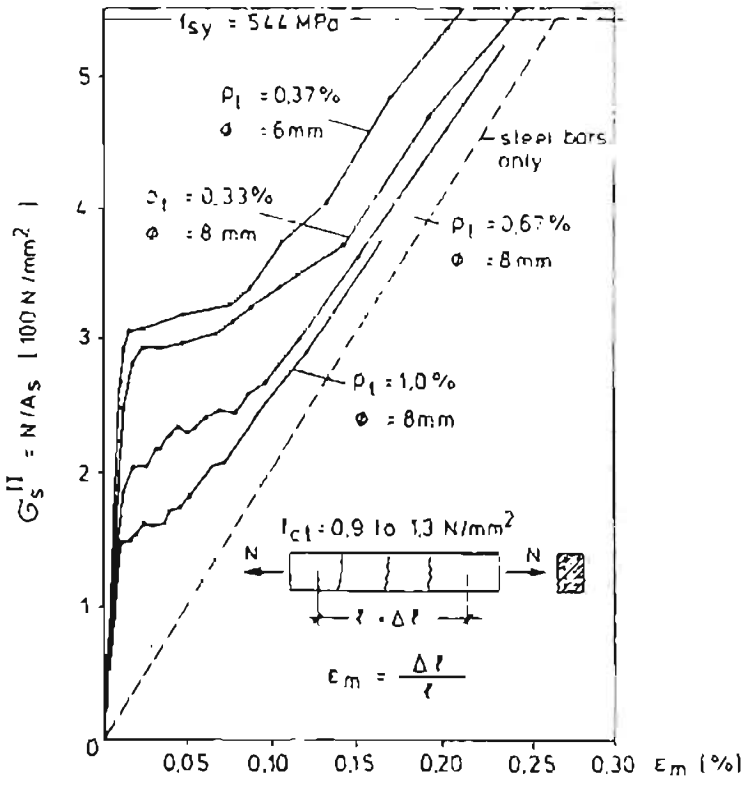

Figure 6.7: Test results of stress strain curves found by axially loaded light-weight aggregate concrete members - reported by Leonhardt (1977).

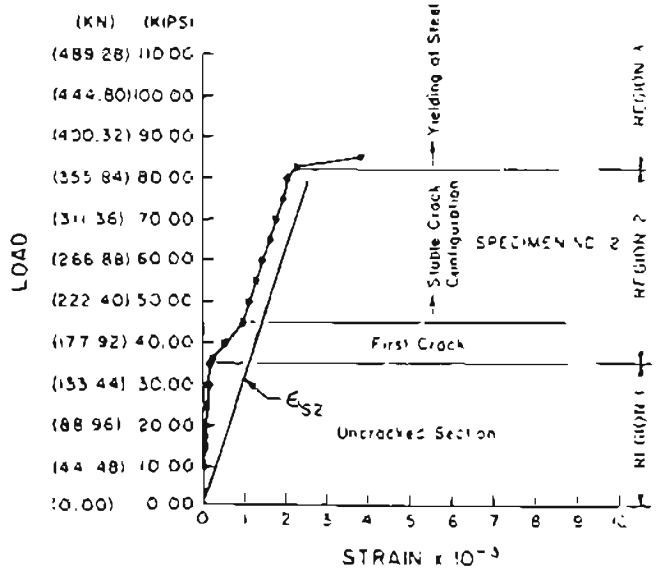

Figure 6.8: Typical load-strain relationship for a member in uniaxial tension - after Rizkalla & Hwang (1984).

Cross-sectional area = 84 in^2 = 54 193 mm^2

A_{st} = 0,0147 * 54 193 = 796,6 mm^2

$K' = E_c A_c + E_s A_s$

(assuming E_c = 30 GPa, E_s = 206 GPa)

K' = 1790 MN/unit strain

= 1,790 kN/microstrain

Assuming a long member and no internal damage in the member before the first primary crack occurs, this upper bound of stiffness may be used to determine the lowest value of strain at which the first crack could have occurred which corresponds to the cracking load of 156 kN (35 kips).

ε (1st crack) = 156/1,790

= 87 microstrain.

If this should be a typical value of the minimum strain at which a first crack could appear, we can investigate whether it ties in with the load-strain behaviour of the ABAQUS analyses. On figure E.1 (series B) it can be seen that the load corresponding to this minimum cracking strain is very much of the order of magnitude of the general zone where cracking would be expected. On figure E.2 (series C) however, it can be seen that the corresponding load is considerably less than the zone of formation of new primary cracks predicted by the analyses. Thus, it seems that the strain at which primary cracking commences is also a function of the shape of the member rather than being simply related to some particular strain or load level.

6.6 DISCUSSION OF CRACKING MODES EVIDENT IN THE FINITE ELEMENT MODELS

6.6.1 Modelling of the formation of new primary cracks.

Only in three cases (models A3C, A5C and A5E) did cracking occur right across the concrete at the plane of symmetry. In the three cases where this did occur, examination of the "load-displacement" curves of the models (see figures E.2 and E.4) shows that the cracks did not

open up markedly as would occur in the real situation. Indeed, in each of these cases, the model broke down numerically shortly after the strain reached the point at which these cracks occurred.

In the other models which did not exhibit cracking right through the concrete, the model got into similar numerical trouble at about the strain that the crack should have happened. It seems that the constitutive model used is inadequate for the purpose for which it was used here, in that it does not seem able to handle sudden large increases in strain when the stress condition of the concrete reaches the descending portion of the stress strain curve.

6.6.2 Modelling of secondary or internal cracking

The model does, however, appear to model the secondary, or internal cracking phenomenon quite well. At least it appears to remain numerically stable through the full range of permissible stresses and strains. It is thought by the writer that the significant difference between this cracking and the primary cracking is the restraint against sudden increases of strain offered by the adjacent bar.

6.6.3 Modelling of tertiary or longitudinal cracking

Shortly before most of the various models became numerically unstable a third phenomenon was observed in each case. Cracks occurred in a direction across the circumferential stresses in the concrete. (See sketch in figure 6.9). These cracks are commonly called longitudinal cracks in the literature as they are aligned parallel to the reinforcement. The writer prefers the term "tertiary crack" to indicate that they occur after the occurrence of the secondary or internal cracks.

These cracks are acknowledged in the literature as signalling the last stages of bond between the reinforcing and the concrete and it is at this stage that the concrete begins to spall away from the reinforcing.

Goto (1971) has observed that they first occur "near the bar at the faces of the primary cracks and then grow towards the outside of the specimen as the steel stress becomes fairly high".

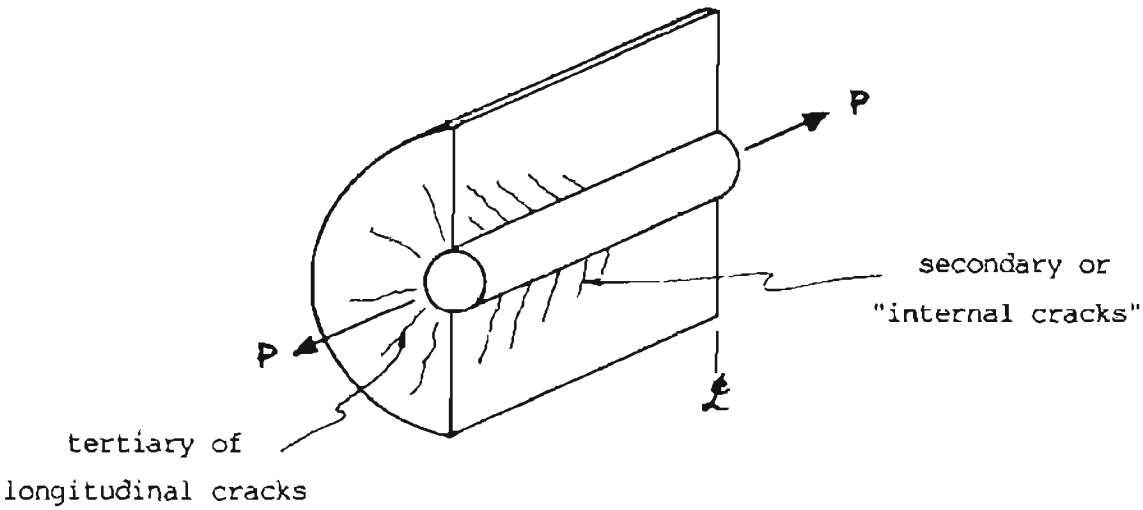

Figure 6.9: Cut-away section of an axisymmetric reinforced concrete prism stressed in tension, showing orientation of tertiary cracks.

This description parallels exactly the manner of occurrence of the tertiary cracking in the F.E. models where the tertiary cracking almost invariably first occurs in the element adjacent to the primary crack and one element away from the surface of the reinforcing bar, and also progresses towards the outside of the specimen. This may be seen in figure 6.10 which shows the orientation of cracks and order of their occurrence in ABAQUS model A1B.

It is thought by the writer that the model is again unable to handle the sudden large increases in strain which should occur when the longitudinal cracks occur as there is no controlling restraint such as there is for the secondary cracking phase.

6.6.4 Extraction and Interpretation of ABAQUS output on crack occurrences and crack directions.

As may be seen in Appendix C, the ABAQUS programme, in conjunction with the ABAQUS concrete model, gives as part of its output for each gauss integration point, both;

a) whether the concrete has cracked at that point

and b) the direction of the crack.

As was discussed in the beginning of this chapter, the cracking of the concrete means that the tensile stress has reached the failure surface defining the model, and applies to each gauss point merely as sample points in a continuum. In other words, one cannot link up a series of cracked gauss points to plot the course of propagation of a discrete crack.

One can however plot the directions of these samples of the smeared cracking of the continuum. This shows not only the directions of the maximum principal tensile stresses which caused the various areas to crack, but also the order in which the cracks occurred. Such a plot is given in figure 6.10, where the direction of crack is shown for each cracked gauss point in model A1B. Also shown is the increment number at which each point reached the failure envelope. In several cases the same point subsequently reached the failure envelope a second time to form a crack in a second direction. These cracks are shown too.

The ABAQUS output gives the rectangular components of the directions normal to the actual cracks, thus if the actual cracks are to be conveniently plotted as shown in figure 6.10, a certain amount of arithmetic manipulation is necessary to obtain the polar coordinates of the crack vectors. Although it would be quicker to automate the whole process, for the single example given here, the writer extracted the data manually and did the transformation using a micro-computer and a "spread-sheet" programme. The details of the data and formulae used for figure 6.10 are given in Appendix F.

In figure 6.11 the writer has plotted only the outlines of the zones cracked at any particular loading stage, in order to show these more clearly than in figure 6.10. These areas have been shaded in a dark to light pattern where the darker areas are those which cracked earlier. Definite trends appear, which, if the cracking were discrete, would possibly be replaced by the formation of single discrete cracks. Such a possible arrangement of cracks is marked up on figure 6.12.

What is apparent in the three figures is that the secondary cracks are aligned in a direction that is very favourable for the residual

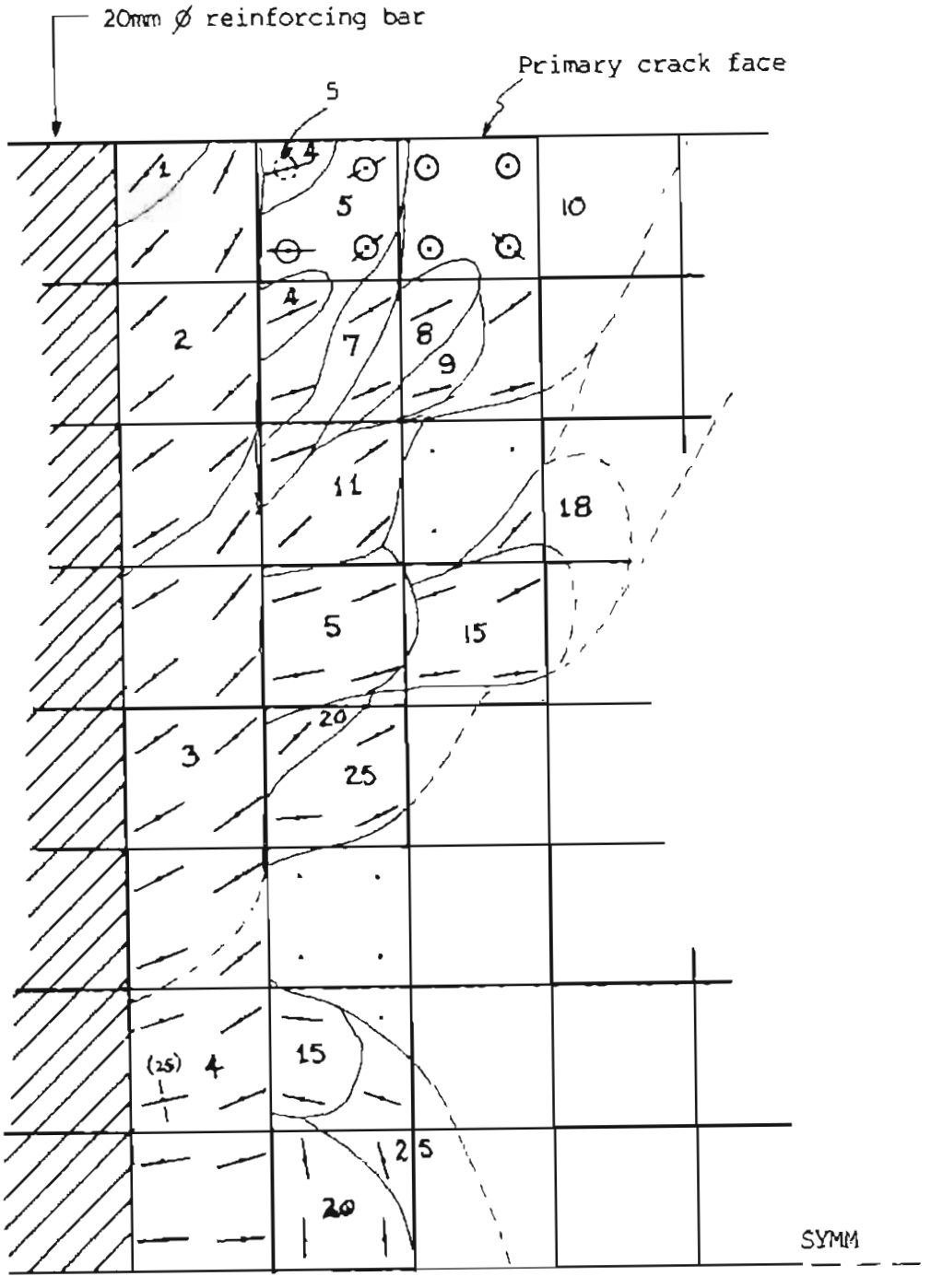

KEY: • gauss integration point

crack at gauss point orientated along line (secondary internal crack)

⊙ crack at gauss point orientated in plane of paper (i.e. tertiary or longitudinal crack)

Figure 6.10: Detail of ABAQUS Model A1B showing orientation and order of occurrence of crack with increasing load.

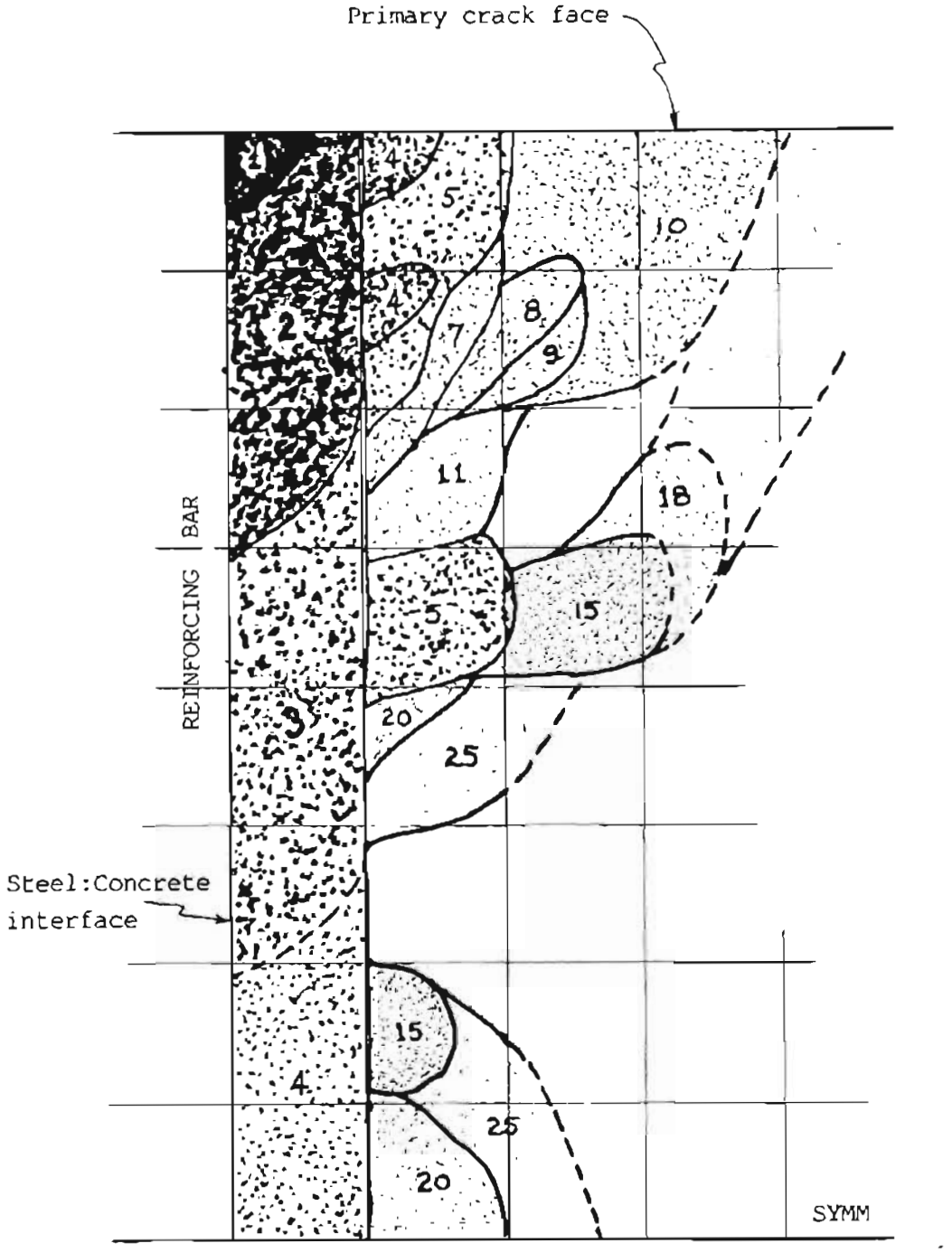

KEY: Cracking occurs first in the darker areas.

The numbers represent the increment at which the crack was first observed.

Figure 6.11: Model A1B: Progression of cracking through the model.

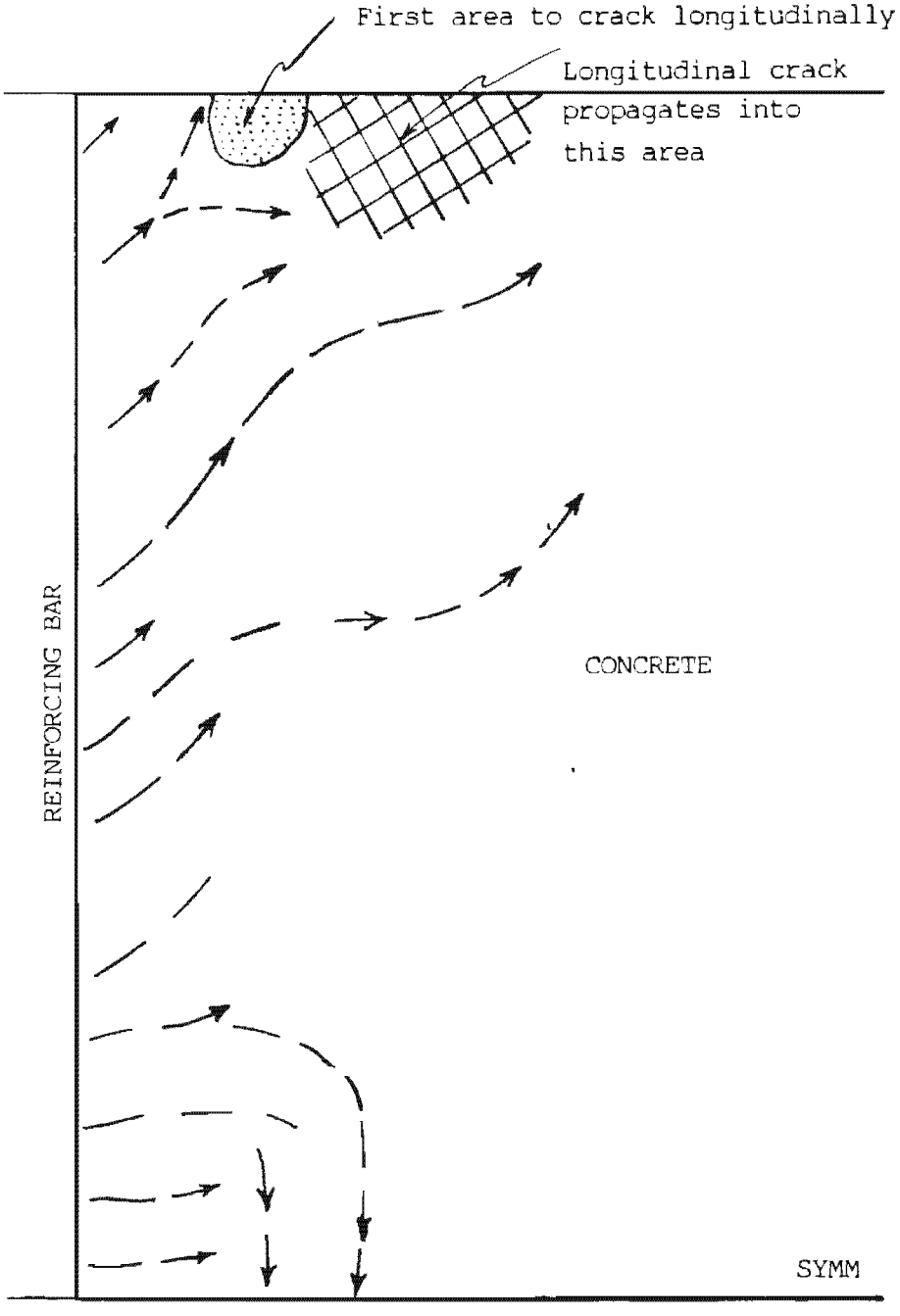

Figure 6.12: Possible pattern of propagation of discrete cracks - ABAQUS model A1B.

"teeth" of concrete to act as struts for the continued transference of stress from bar to concrete after the occurrence of secondary cracking. These struts would kick against the ribs on the bar at the one end and against a ring of hoop tension in the concrete at the other. (A sketch of this strut and ring tension effect was given in figure 5.1.)

It has already been noted that "tertiary" cracking occurs in nearly all of the models. The writer suggests that this cracking is as a result of the hoop tension developed by the action of the struts left between secondary cracks acting in compression.

6.7 EVALUATION OF THE VALIDITY OF THE FINITE ELEMENT MODELS BY COMPARISON WITH EXPERIMENTAL MODELS

In the consideration of the cracking behaviour of the analytical models an interesting point is the very low level of average steel strain at which both the secondary and tertiary cracking occur. In both of these cases, early cracking would seem to imply that there would be a complete loss of bond between bar and concrete at such low loads that half of the structures now in existence should have collapsed! In this section these analysis results are compared to the available experimental data on the topic.

Almost without fail the literature covering cracking in reinforced concrete members reports only on the widths of cracks found in sections with fully developed crack patterns, with the authors concentrating on relating this data to parameters such as cover, bar size, concrete area, etc.

Thus, besides the two load-strain curves already discussed, there is rather a dearth of information on the actual development of the crack patterns, the levels of stress and strain at which various types of cracks occur, and the mechanism of cracking in general, against which the predictions of the finite element analyses might be compared.

Information on cracking stresses has only been found in the papers by the following authors: Kaar and Mattock (1963), Hognestad (1962), Broms (1965c) and Goto (1971).

Kaar and Mattock give the graph shown in figure 6.13 which shows the crack spacing plotted against average steel stress for some of his specimens (all of which were flexural members).

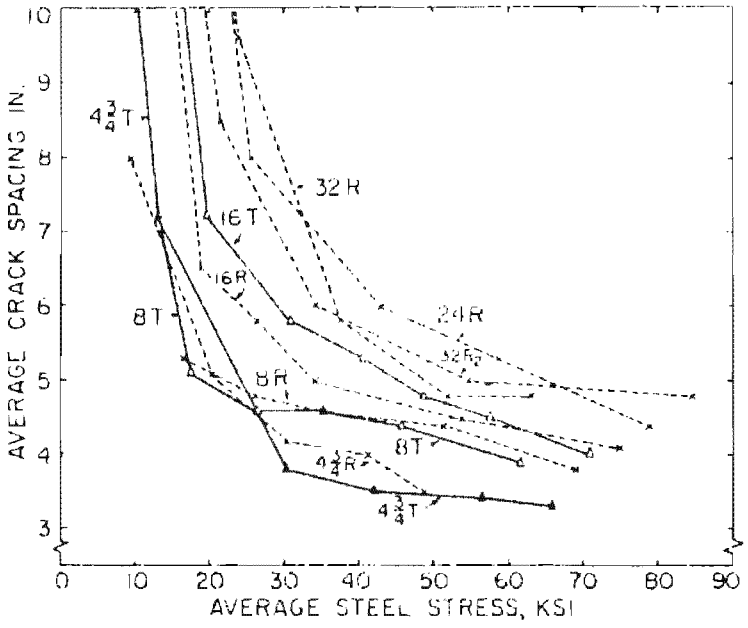

Figure 6.13: Relation of average crack spacing to average steel stress - after Kaar and Mattock (1963).

This figure shows that cracking starts at a steel stress of between 8 ksi and 28 ksi (55 to 150 N/mm^2). The corresponding range of average steel strains is 266 microstrain to 728 microstrain. Obviously this is a very wide range and does not therefore help us too much in making precise predictions.

Hognestad, during his tests on cracking of flexural members, monitored surface stress in the concrete on the underside and at the sides of his beams at the level of the reinforcement. He observed that "when initial cracking took place ... the concrete strains shifted abruptly into compression". Fortunately he gives plots of this information for four of his beams (see figure 6.14) and from these it may be seen that the average strains at which cracking occurred varied between 50 microstrain and 120 microstrain on the bottom face and 30 to 80 microstrain on the side face at the level of the steel.

Corresponding calculated steel stresses are 10 to 19 ksi (69 to 131 N/mm^2) which correspond to average strains in the steel of 334 microstrain to 636 microstrain. Why these figures do not correspond

to the measured strains in the concrete is unclear to the writer. It is to be expected that after cracking there will be a drop in surface strain in the concrete relative to the average steel strain. These figures however represent the level of initial cracking and thus indicate the situation before cracking has occurred. The only explanation that the writer can think of is that the author either had a calibration error in his equipment or that the cracking was not the first to occur in the concrete.

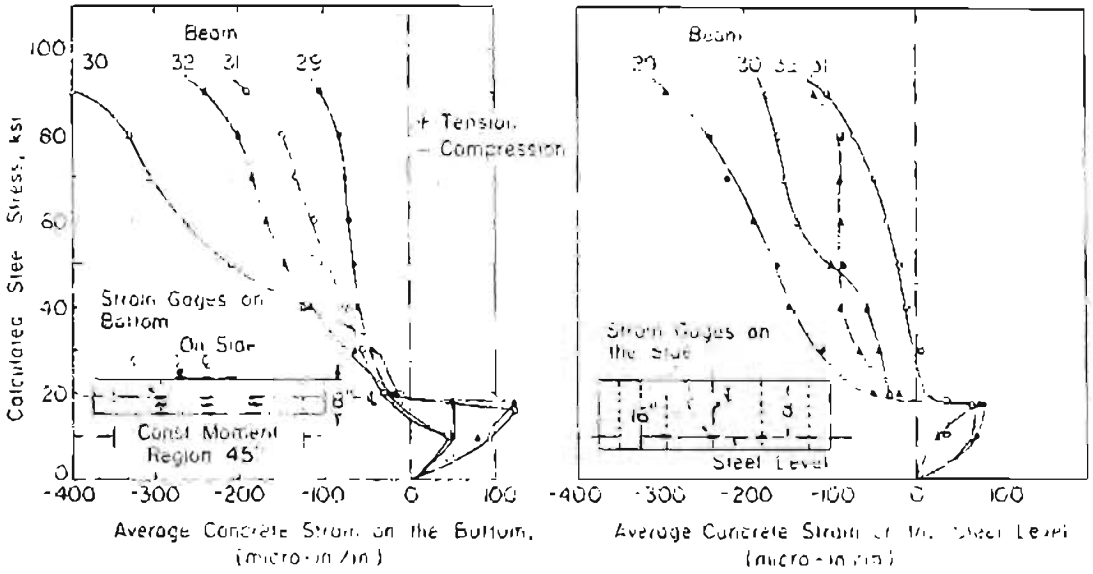

Figure 6.14: Concrete strains between two cracks – after Hognestad (1962)

Goto (1971) carried out a series of tests which consisted of examining cracking under conditions of pure tension in concrete prisms containing a concentrically placed single reinforcing bar. The tensile stress was induced by pulling on each end of the protruding reinforcement. The concrete prisms were notched at varying spacings between what Goto considered to be S_o and $2S_o$ (or S_{max}) at these spacings.

The concrete used in Goto's experiments had a (cylinder) crushing strength of 30 N/mm^2 and a tensile splitting strength of 2,8 N/mm^2. His reinforcing bars were 19 and 32 mm within square prisms of concrete with minimum cover to the reinforcement of 40 and 45 mm respectively.

Thus the conditions of his tests, although not identical, were similar

to those modelled by the writer's series of finite element tests. Although not all of Goto's results are reported in his paper those that are reported, indicate the following:

(i) Primary Cracks: Goto found that these occurred at steel stresses of between 57 N/mm^2 and 105 N/mm^2 for the notched positions and at stresses of 150 to 10 N/mm^2 for un-notched positions between the notched cracks when these were spread more than S_o apart.

This last range of stresses agree well with Broms's (1965c) observation that primary cracking stabilises at an average steel stress of between 140 and 210 N/mm^2.

Translating these figures into terms of average strain in the reinforcing we get the primary cracks forming at strains of between 275 and 500 microstrain (notched) and 725 to 920 microstrain (un-notched).

(ii) Secondary or Internal cracking: Goto is the only author found by the writer to have given any indication of the level of stress or strain at which internal cracking occurs. He reports this as occurring at a reinforcing stress of less than 100 N/mm^2 which, taking E_s = 206 GPa, corresponds to a steel strain of 485 microstrain.

In contrast with these figures, the F.E. models indicate that internal cracking starts at strains as low as 25 to 30 microstrain for the longer models, and about 80 microstrain for the shorter models. As has been shown, except for series C and E, there are no absolute indications as to when the F.E. models would have formed new primary cracks but the indications are that these would have formed at much lower loadings than those found experimentally. The tertiary cracking indicated by the F.E. models also seems to occur at loads that are far too low when it is considered that, in real life, the appearance of these cracks usually signals the final breakdown of bond between steel and concrete.

One of the problems of using the rather sketchy type of published data given above to try to calibrate the F.E. models is that one is never quite sure exactly how the data was derived. In this case a point of particular relevance is how the reinforcement stresses were measured. Hognestad is not specific but Kaar and Mattock refer to strain measurements in the reinforcement, thus implying direct measurement of the average stress and strain.

As has been seen in the examination of the load-strain curves of the F.E. models and the two similar experimental curves, we would expect cracking to occur over a range of average strains in the steel but at the same load, until the stabilized crack pattern has been achieved. The position of measurement of stress or strain of the reinforcement with respect to those cracks that have formed then becomes relevant. In the vicinity of a crack the strain would be higher than away from the nearest crack as the stiffness of the bar with its cracked surround will be lower than that of the bar and an uncracked surround. Thus, what appears to be a large scatter of results reported above could be representative of different positions in the horizontal portion of the load-strain curve. As such they would represent loads at which new primary cracks form of the order of 3 to 4 times those indicated by the F.E. models (series C and E). Even in this estimate, however, there is considerable scope for variation due to changes in member geometry.

The writer suggests that, if a proper calibration is to be made with experimental data, then a special series of tests will have to be carried out. Such a series could be extremely useful, not only from the point of view of calibrating the macro response of models such as the writer's but could be extremely useful in determining experimental data, via the calibration of this type of model, on the lower order concrete behavioural parameters such as fracture criteria, and strain softening curves in tension. This argument is pursued further in the next chapter.

6.8 CONCLUSIONS ON VALIDITY OF ANALYTICAL MODELS.

The present set of finite element models have been shown to have several serious shortcomings.

(i) They cannot adequately model the formation of new primary cracks or, apparently, any type of crack where resulting displacements could be very large.

(ii) They seem to indicate that cracking of various types will start at seemingly impossibly low loads.

(iii) As a result of (i) above, it has not been possible to model the full response of members with a length greater than the maximum crack spacing. No modelling has been done above the loading range where the pattern of primary cracks should stabilize.

(iv) Presentation and extraction of results is rather tedious (although this could be greatly improved by suitable automated post-processing).

(v) The models have not been adequately calibrated against experimental data. In fact suitable data probably do not exist that would be exactly right for calibrating the model.

In spite of these shortcomings, the models do seem to give a plausible representation of some of the mechanisms involved in bond and cracking. These will be investigated further in the next chapter. The writer will also discuss the consequences of the inability to model cracking behaviour at high load levels on the comparisons that were hoped to be made with the experimentally established crack width formulations. Finally, a proposal will be made for a series of experimental tests that could be extremely useful in determining modelling parameters of concrete at the "micro" level.

CHAPTER 7

FURTHER DISCUSSION ON MECHANISMS INVOLVED IN CRACKING WHICH IS CONTROLLED BY REINFORCEMENT.

7.1 GENERAL.

In all the papers that have been written about crack width formulae, much has been written about the relationships between various parameters and crack widths.

Some of the findings of different experimenters actually contradict each other. Many experimenters have identified certain peculiarities of behaviour but left them unexplained.

It was originally hoped that this chapter would consist of a comparison of the experimentally found effects of various parameters with the effects of these same parameters as found in the F.E. models. Since the analyses failed to model the full response of the singly reinforced tension members analysed this will not be possible. The reason for this is explained fully in the next section.

In this chapter then, the writer will concentrate on some of the issues raised by consideration of the F.E. analyses, in regard to possible explanations of mechanisms involved in the behaviour of cracking which is controlled by reinforcement.

7.2 CRACK WIDTH AND CRACK SPACING

All of the experimental work to date has shown that, as the average strain in a reinforced member increases, the crack spacing tends towards a stabilised value after which no more cracks will form. After this stabilised stage of cracking has been achieved, the research has also shown that the crack size is proportional to the average strain in the member. Thus the equation 2.2 was derived, equating crack width to the stabilized spacing and the strain in the member.

This equation is of overriding importance in all the observed

relationships as it is from this base that the theories concentrate on the development of relationships between crack spacing and other parameters and thus, only indirectly, of crack width to these parameters.

One of the severest limitations of the current set of analyses is that they are not able to indicate the formation of new primary cracks with any degree of accuracy. Thus, in the analyses, it is impossible to relate our independent variables directly to crack spacing as the dependent variable. Looking at the various formulae that relate crack width to various parameters, we saw in chapter 2 that they are all derived as formulae relating various parameters to the crack spacing, and then the derived value for spacing is substituted into equation 2.3 so that the spacing term disappears from the formulation.

It appears from the experimental data then, that direct relationships do exist between crack width and the various parameters, but the proviso still exists that this relationship only applies for a stabilized crack pattern. Thus, if we cannot model the formation of stabilized crack patterns properly we end up being unable to say anything definite about any of the relationships as a consequence of the results obtained by the various analyses.

What may be investigated however, is the effect of the parameters on the behaviour of the models at stresses up to those at which the stabilized patterns would occur. In this regard we have already examined the effect of crack spacing on the overall load-strain behaviour of the models. We observed that these curves started at slopes (stiffnesses) dependent on the crack spacing and then followed a non-linear path up to a point at which we would have expected sudden jumps in stiffness had new primary cracks formed.

In Appendix G, the surface widths of the primary cracks have been plotted against average strains in the members, in the same groupings as for the load-strain diagrams. Also plotted on the graphs are the lines that would be generated if the crack widths were exactly proportional to the crack spacing and strain.

i.e. if $w = S.\varepsilon_m$ ... (7.1)

which is the same as equation 2.3.

As may be seen the plots deviate increasingly from this relationship as the length, S, increases. Generally, for the longer models, the actual crack width achieved is considerably less than the theoretical value if equation 7.1 applied.

Examining figure G.1, which gives the crack width results for the series B models, a different situation may be seen to occur. Here, the actual width obtained with the analysis is marginally higher than the theoretical value according to equation 7.1. Examination of figure 7.1. which is a contour plot of the longitudinal stresses in model A1B (at increment 5) provides a possible explanation. Here it may be seen that the longitudinal stress on the surface of the model has actually become compressive, thus strain on the surface would be compressive too. As the average tensile strain in the reinforcing bar increases, so this compressive stress increases in the surface fibres of the concrete - see figure 7.2.

Examination of the other plots of surface crack width versus average steel strain show that in all cases the crack width for S = 80 mm is very close to and, mostly, slightly above the theoretical line. For the longer models, the crack widths are all considerably below the theoretical values except for model A3L (see figure G.3) where again the crack width plots above the theoretical line. In isolated comparison with model A1B one might notice that A3L and A1B both have the same cover to crack spacing ratio of 1/2. This could then be considered to be a critical ratio above which one gets compressive stresses occurring in the surface fibres of the concrete, leading to surface crack widths exceeding their theoretical value according to equation 7.1. If one postulated a possible link between these surface compressive stresses and whether or not new cracks can form, this would lead to the conclusion that in both cases the models were at the correct stabilized crack spacing for their respective cover sizes, and that the experimentally found dependence of crack spacing on cover width is correct.

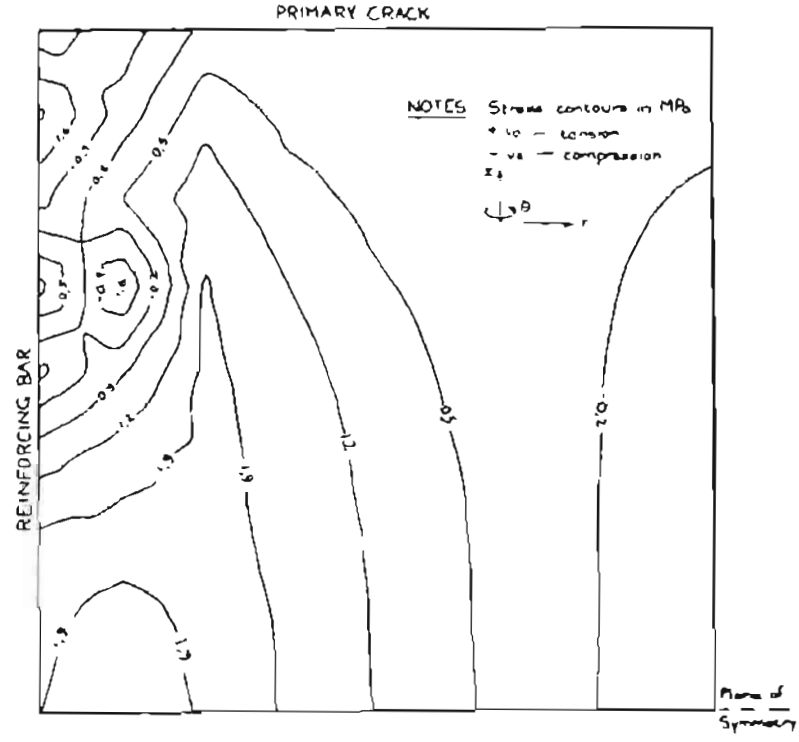

Figure 7.1: Contour plot of the longitudinal stresses in model A1B (at increment 5).

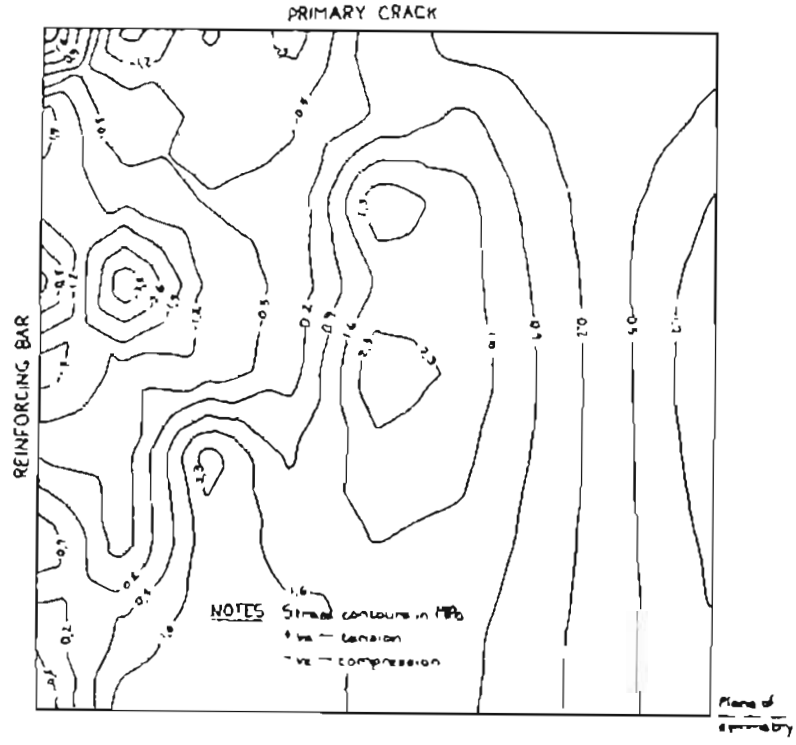

Figure 7.2: Contour plot of the longitudinal stresses in model A1B (at increment 25).

This theory however, is neatly destroyed by the fact that all of the models with S = 80 mm give plots of crack width against strain which are mostly above the theoretical lines governed by equation 7.1. Before we can consider theoretical reasons why this is so, it is first necessary to consider the mechanism by which the surface compression occurs.

7.2.1 A possible explanation for cracks occurring at early ages being wider than those at later ages.

The computer analyses have shown that, in members of varying spacing between primary cracks, the stress concentration adjacent to each primary crack is more nearly proportional to the tensile deflection of the member than the average tensile strain. This means that, for the longer members, one can expect a greater amount of internal cracking to occur in these zones for the same amount of strain. According to the analyses too, the tertiary cracking (ring tension) occurs at lower strains for the wider spaced primary cracks with the tertiary cracking strain increasing as the spacing decreases.

Thus, because of the tendency to concentrate bond stresses into the area nearest the crack it might be expected that greater bond damage will occur at the earliest forming cracks. Because most of the opening up of cracks has been shown to be due to inelastic strains (i.e. internal cracking) this cannot therefore be expected to be recoverable when another primary crack occurs.

As a result of these arguments, we might expect a bias of increasing crack widths towards those cracks which occur while the spacing is still relatively wide. Since those with wider spacings have to be the cracks that occur first, the resulting greater destruction of bond mechanisms adjacent to these cracks could be a reason for the occurrence of the occasional crack that is much wider than anticipated.

7.3 SURFACE STRESS OF CONCRETE

Almost all of the reasoning in the theory behind crack width formulae is based on assumptions regarding the stress in the concrete at the surface.

It is postulated that surface cracks will not form until the surface stress reaches its ultimate value. Generally, this stress is assumed to occur uniformly over the section at some distance, S_o, away from an existing crack. The various theories then concentrate on determining S_{min}.

Hognestad (1962), however, has shown that the latter assumption of uniform stress is incorrect. In fact, Hognestad found that, after the initial cracking had taken place the surface stresses between cracks, both on the side and bottom faces of beams, became compressive. (Plots of Hognestad's findings were given in figure 6.14).

Hognestad is unsure as to the cause of this phenomenon and states the following: "To reach a fundamental scientific understanding of the cracking phenomenon, the writer believes that the nature of these compressive strains on the concrete surface must be clarified."

Broms (1965b) also observed compressive longitudinal strains on the surface of his test members which occurred as soon as the first tensile crack occurred. He carried out elastic two dimensional analyses which are described in chapter 4. Although fairly primitive compared to the results achievable today with the finite element method, these analyses did show that the distribution of longitudinal stress is definitely not linear, at least within one cover dimension of the primary cracks. His results for the analysis of a member with primary crack faces spaced one cover dimension apart even showed the development of compressive stresses on the surface of the member. (The key features of these analyses and results are shown in figures 4.5 and 4.6).

Despite these earlier warnings that there was something seriously amiss with the assumption of uniform stress at a distance S_o away from a crack, subsequent researchers when deriving their formulae, have

almost without fail based their logic on just such an assumption.

Beeby (1970, 1971, 1972, 1979) built up a whole family of formulae based on this supposition. These formulae in turn form the basis of that given in the British Codes of Practice, so an error of logic could have fairly serious consequences. From the results of the analyses carried out, the writer cannot argue against the actual relationships given in these formulae but rather, in the light of these results will argue only that the "theoretical" reasoning, proposed to explain them, is flawed.

For instance, at distances away from a primary crack of the order of magnitude of one cover dimension, the longitudinal stress in the concrete gets nowhere near uniform, no matter how good the bond at the bar-concrete interface is. In fact, to get close to uniformity of stress in the concrete takes many times this distance from a primary crack. The writer's analyses extend to $S = 4c$ where uniformity is still not achieved, at least up to the maximum loading level analysed. Thus it appears that logic such as the "intuitive" 45° rule used by Beeby is completely wrong.

Thus, either the experimentally observed relationships are purely coincidental, or they may be explained by some other theory. If the former is the case it is little wonder that many deviations from the predicted results occur.

7.3.1 Consideration of the mechanism causing compressive stresses on the surface of concrete members.

An explanation for this behaviour may be had by considering figure 7.3 which is given by Stoffers (1978). The similarity between this figure and some of the principal stress vector plots obtained by the writer is immediately apparent. Stoffers's figure however, refers to shrinkage in a wall cast on a rigid base. Comparing this situation to that of stress transfer from a bar to surrounding concrete it may be seen that the most notable difference is that, in the latter case, the stresses have to spread radially, instead of merely in the plane as is the case for the wall. (Compare figure 4.8)

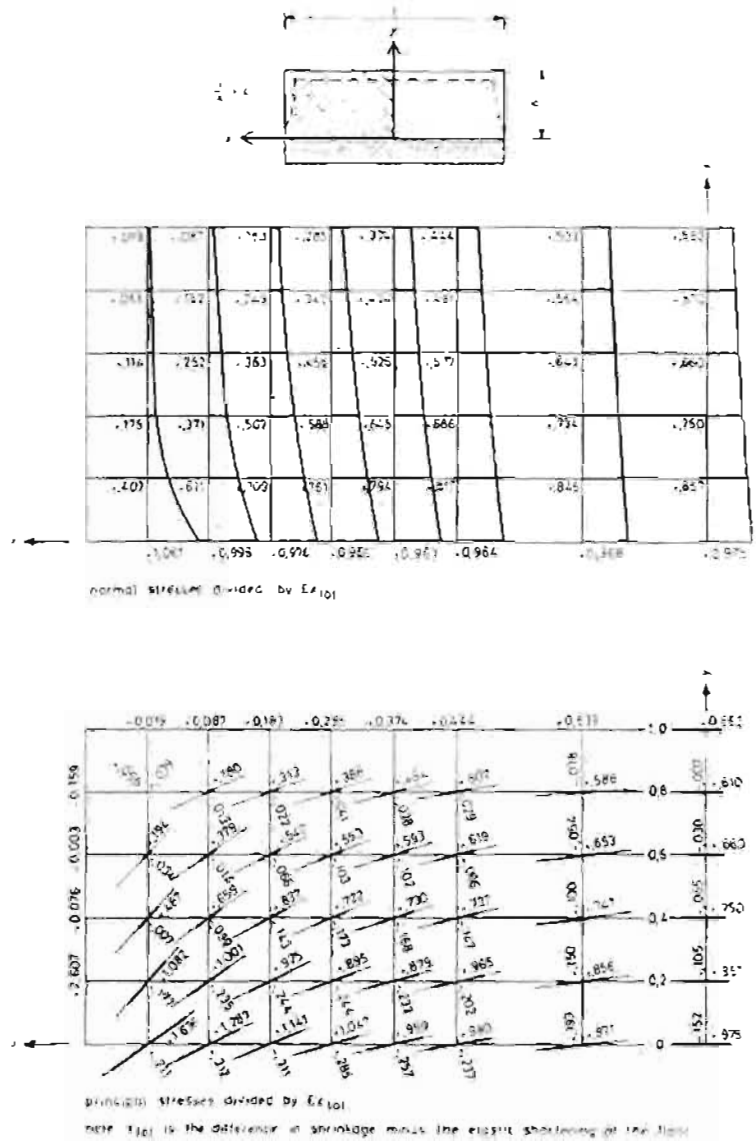

Figure 7.3: Stress distribution in a wall remaining straight (curvature = 0) - reported by Stoffers (1978)

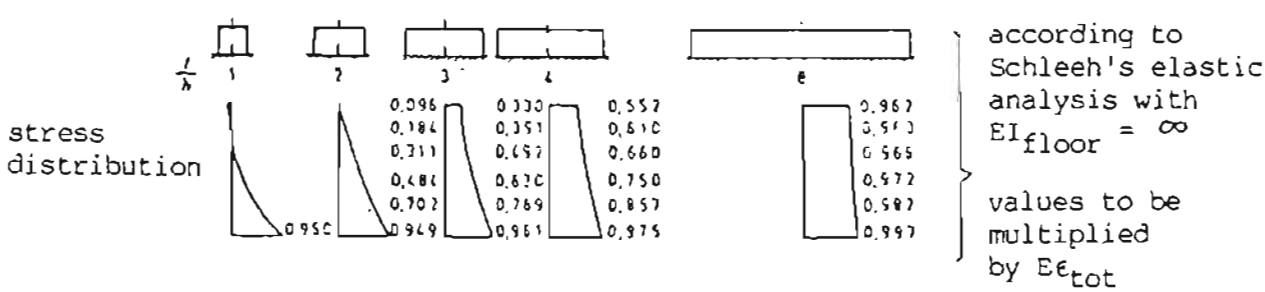

Figure 7.4: Stress distribution in the cross-section in the middle of a wall, in the elastic range, for various values of ℓ/h - reported by Stoffers (1978)

Stoffers reports that, depending on the length to height ratio of the wall, the distribution of stress at the midpoint alters as shown in figure 7.4. For short walls, (ℓ/h = 1) he reports that the tops of walls actually go into compression. Getting a stress distribution curve that crosses from tension to compression implies that there should be a neutral axis at the zero point and that there is rotation about the neutral axis. This is easy to accept for a case such as is shown in figure 7.5 where the base of the wall is rigid axially but not in bending. Thus resistance to shrinkage in the retaining wall by the base restraint causes curvature of the wall-base composite, with the resulting compressive stresses at the top of the wall. In the case of the wall where the base is so rigid that it cannot bend, curvature in the upper part of the wall may be explained by studying the directions of the principal stress vectors. At the ends of the wall, there is a significant stress component upwards, thus in these zones there must be an upwards strain relative to the midpoint. The top of the wall must therefore develop a slight curve. If the compressive stress induced in the concrete due to this curvature is greater than the axial tension component due to shrinkage in any part of the wall, then that part of the wall will be in compression.

The writer suggests that the behaviour of concrete around reinforcing is similar in nature to this. The results shown in figures 7.3 and 7.4 were derived from elastic analyses which are not unreasonable for steel concrete composites. On the other hand, the behaviour of the concrete surrounding a bar is definitely non-linear. Nevertheless it can be seen that at the outer fibre of concrete cover, a curvature could develop due to differential radial strains between the zones adjacent to primary cracks and the zone midway between cracks. This will occur whether the greater extension in the end zones is due to elastic straining, plastic straining or discrete cracking at diagonal angles. As the length between cracks becomes shorter, so the axial tension component in the outer fibre will reduce, and the transition will be made from tension to compression.

Stoffers reports that for walls, it has been found that the stress distribution is directly related to the ratio of length to height. Considering the experimental finding that crack spacing is proportional to cover leads one to wonder whether a similar situation

applies in the consideration of the concrete surrounding a bar. This aspect has already been discussed briefly in the previous section where it was discovered for the F.E. models that the relationship seems to hold for crack spacings above 80 mm, but not otherwise. Unfortunately only two analyses were done on a model with cover:spacing $\geq \frac{1}{2}$. Further investigation on some of the models with the smaller cover dimension might show more clearly the point at which the surface stress becomes compressive.

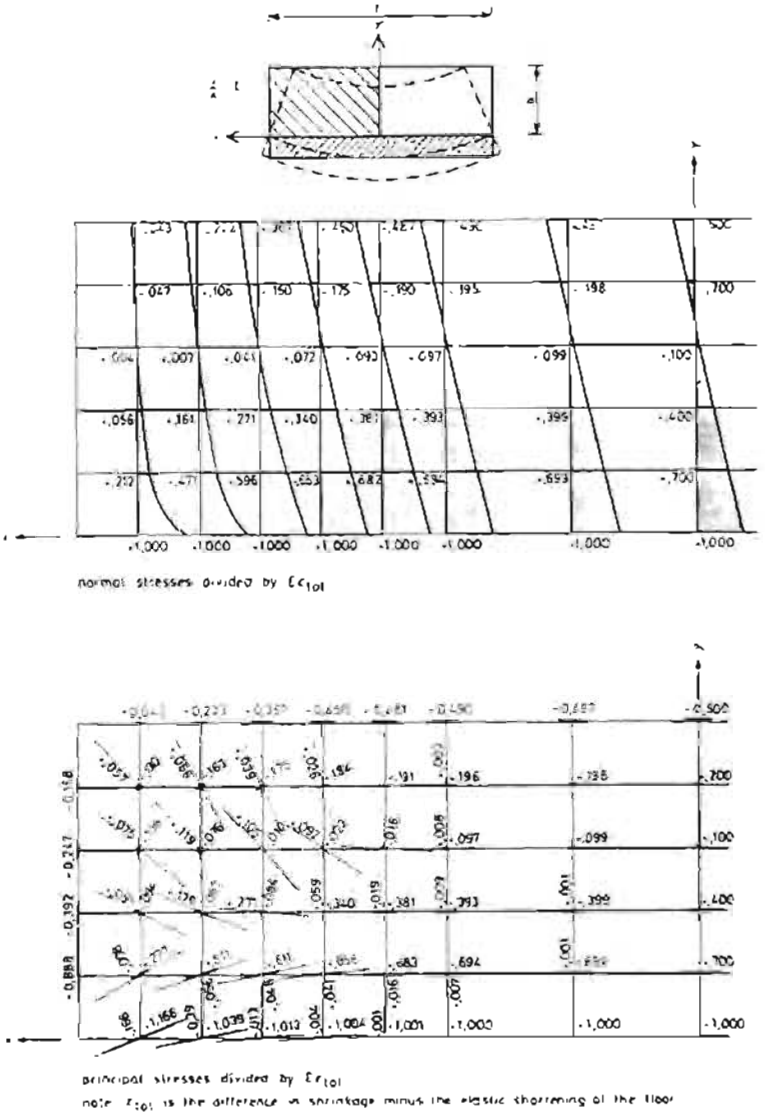

Figure 7.5: Stress distribution in a wall connected to a flexurally non-rigid floor - reported by Stoffers (1978).

In view of the difference between stress transfer in the wall example and in the bond situation, we could expect that the relationship between cover and spacing should not be one of strict proportionality. Some power law, to allow for the radial spread of stress and changing

moment of inertia of the concrete surrounding the bar, would not be unreasonable. The writer's analyses do not however provide sufficient data to make any predictions on this score and more tests, experimental and analytical, would need to be done.

7.4 EFFECT OF BAR TYPE AND CONSIDERATION OF THE MECHANISM OF BOND

From his series of tests, Hognestad (1962) found that American deformed bars were 1,6 times as effective at controlling cracking as were smooth bars.

Anticipating similar results with British steel, Base et al (1976) conducted tests where one of the major variables was the type of bar used. The results showed, somewhat surprisingly, that the crack widths for plain round bars were on average only 20% greater than those for deformed bars. The type of deformed bar was found to make little difference.

Most researchers have related their developments of cracking theory to the maximum amount of stress transferable from bar to concrete via bond stress, on the grounds that it was only after sufficient tension had built up in the concrete, that a new crack could form. With the advent of deformed bars and their greatly enhanced bond strengths, the bond strength theory began to lose credibility. Comparing the crack distributing abilities of various high bond bars and plain bars, Base et al (1976) found that the high bond bars were only about 20% more efficient than plain bars. Beeby (1970) comments that this difference is much smaller than that suggested by other workers and much less than the ratio of bond strengths of smooth and deformed bars.

As a result of the finite element analyses which have been performed, the writer believes some comment may be made on the nature of bond as it has been portrayed in the analysis results.

Almost immediately load was applied to each of the F.E. models, they started to exhibit non-linear behaviour in the "corners" at the primary cracks. At very low loads there appeared in these corners secondary cracks that exactly parallel those found experimentally, with the exception that the cracking load seems rather low. With

increasing load, this mode of cracking extends rapidly along the bar until, in most cases, it reaches the plane of symmetry between cracks. This, at first sight appears to indicate complete bond failure along this zone.

This occurs in the models at steel stresses that are so much lower than those attainable in practice that this discrepancy cannot be blamed on a poor calibration of the concrete model. (With the NOSTRUM damage model, it was possible to blame the concrete model for the halting of the analyses at this point because the scalar damage parameter used, caused the programme to consider a crack in one direction as destroying the concrete's properties in all other directions too. Thus no further mechanism could be found in these models of transferring load across this zone of damaged concrete.)

The question then arises as to exactly how there can be an increase in the load transferred to, and carried by the concrete after internal cracking has occurred all along the bar/concrete interface. Assuming that the secondary cracks have widened to a degree such that there is no longer a possibility of any tensile stress across them there appear to be two further mechanisms by which the concrete can continue to carry load:

(i) the remaining "teeth" between the secondary cracks, could carry load by bending (as proposed by Leonhardt 1977).

and (ii) they could act as struts, provided they have something to kick against.

The answer appears to lie in consideration of the cause of the tertiary cracks observed normal to the θ - axis. In other words, after the secondary cracking has occurred, some degree of ring tension occurs outside of the zone already cracked. The mechanism of this formation of ring tension is probably one of strut action. The orientation of the secondary cracks, observed by many authors, is extremely favourable for strut action being the predominant mechanism rather than bending but there is probably a small element of the latter too.

The strut and hoop tension theory has for some time been proposed as being the mechanism by which bond operates (e.g. Reynolds (1982)). The NOSTRUM models indicated that this type of bond was starting to form at the stage when those analyses terminated. Consideration of the hoop stresses (see figure 7.6) and cracking due to these stresses at slightly higher loads than those reached with the NOSTRUM models shows that it does indeed seem to form. Unfortunately no principal stress vector plots are available to prove, in a visual manner, the existence of the strut forces but their existence is the only reason the writer can put forward to explain the presence of the hoop stresses.

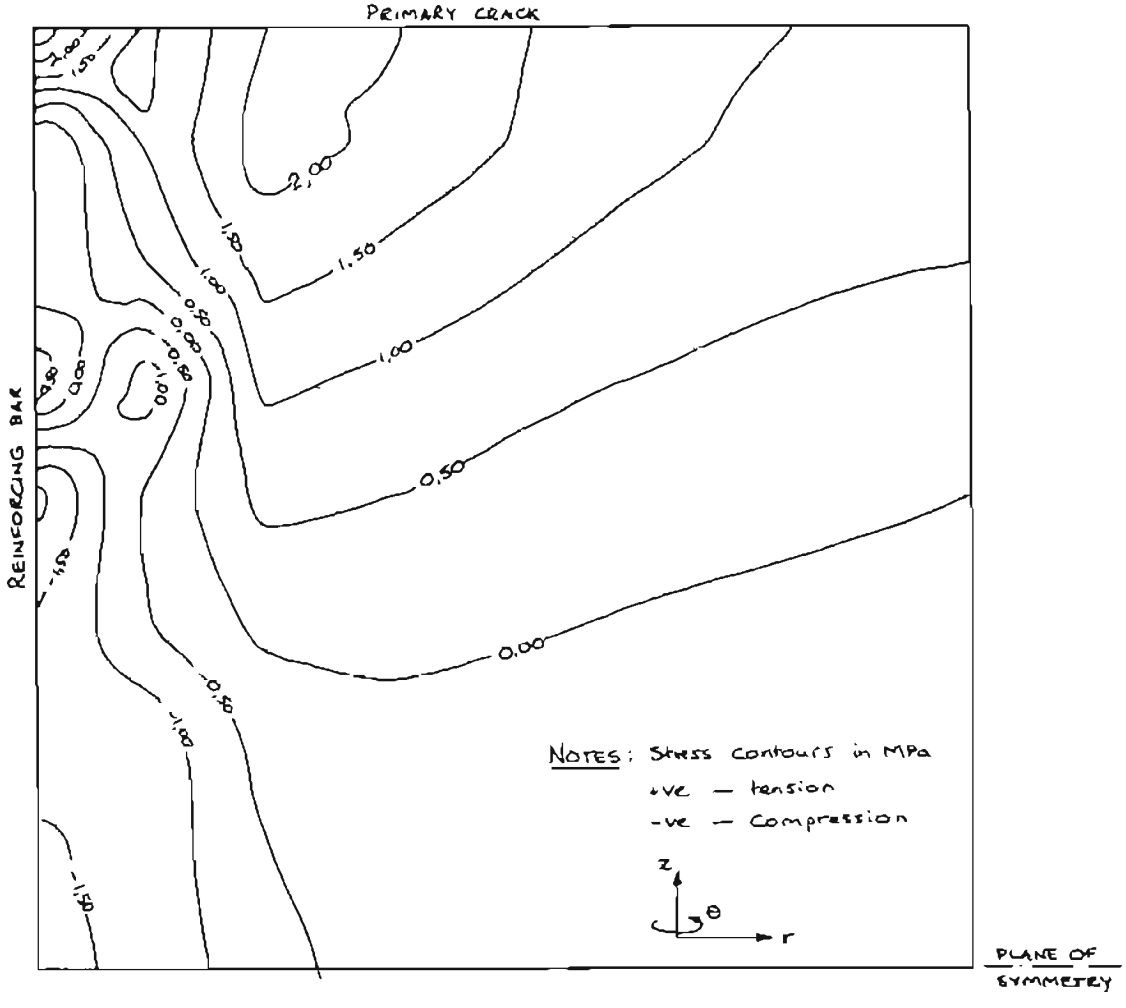

Figure 7.6: Hoop stresses in model A1B just after first longitudinal (hoop stress) cracking (Increment 5).

It may be postulated that the secondary cracks which the F.E. models have indicated start occurring at a very low load, do not constitute a significant loss of bond, and therefore composite stiffness, in a reinforced member. In this regard the writer is inclined to trust the

general trend shown by the analyses of gradual softening of the composite due to these internal cracks occurring.

Indeed, it may in fact be true that the commencement of internal cracking simply indicates the satisfaction of the compatibility requirements for a shift in bonding action from one of shearing to the strut and hoop tension mechanism.

Real loss of bond probably occurs through one of two mechanisms. In the first instance the concrete could crush where it bears on the reinforcing ribs, and thus alleviate the strut and ring tension stresses set up. Secondly, the concrete could start fracturing in a direction longitudinal to the bars, thus relieving the hoop tension.

Once one has accepted that a major factor in providing bond in reinforced concrete is by strut and ring tension action, one can perhaps explain the discrepancy between results obtained in pull out tests for bond, and the apparently disappointing results obtained for the crack distribution characteristics of deformed bars. In most pull out tests there has to be a reaction applied to the end of the member being pulled. Usually one would try to apply this via a platen with a large hole in the centre so as not to unduly influence the concrete immediately surrounding the bar. With the strut action, however, the zone developing useful compression would simply shift outwards to the position of the applied reaction. Through the action of friction this would take over much of the outwards thrust that would normally have to be taken by the ring tension, thus allowing more load to be carried by the bar before hoop splitting occurs. In addition the application of the reaction force might generally raise the level of hydrostatic compression in the concrete, thus raising the level at which shear failure might occur in the concrete which kicks against the ribs on the reinforcing bar. Making the concrete sample bigger and bigger so as to apply the reaction further and further out would indirectly have the same effect in that there would be more concrete to provide restraint against hoop splitting and any possible increase in volume due to shearing of the concrete.

7.5 REASONS FOR CRACKING AT LOWER STRESSES.

The reasons for the F.E. model's apparent cracking at loads far below those obtained in practice remain unresolved. The calibration of the concrete model appears to be approximately correct with regard to the stress at which tensile failure occurs. This has been tested with uniaxial and biaxial tensile models that performed as required.

The writer is inclined to believe the initial elastic behaviour of the models, and thus the very high concentration of stress that builds up in the "corner" formed between the bar and a primary crack. Thus it seems probable that the concrete does reach the anticipated failure stress in this area at the load that the F.E. analyses show it will. Admittedly, the tolerance used was fairly coarse, but the models all analysed this portion of the applied loading without any convergence problems, even with very tight tolerances. In addition, both the NOSTRUM and ABAQUS models are in approximate agreement on the very low level of load at which secondary cracking first occurs.

The writer, therefore can only propose some possibilities for future investigation:

(i) There may be some "size effect" in real life models which the F.E. analyses are failing to model. The fracture criterion of reaching a failure surface in stress space may in that respect be completely the wrong type of model for unreinforced concrete.

(ii) The use of a decreasing portion of the concrete's tensile stress-strain curve that was apparently too steep, might have the effect of shedding load from cracked areas too quickly and thus propagating cracks faster than in a real situation. This, however would not affect the load at which cracking started in the "corners" of the models.

Various researchers are working on obtaining more and better data on the fracturing of concrete under all conditions of stress, and on determining concrete's complete tensile stress strain curve. As has

been noted earlier in the text, this type of research requires some very expensive and sophisticated machinery. The writer will propose in the next section, a series of tests that could provide many of the answers to the above problems by "back-calculation" from a set of experimental tests that would be relatively simple and inexpensive to conduct.

7.6 PROPOSAL FOR A SERIES OF CALIBRATION TESTS

One of the most obvious needs in trying to calibrate and check the results of analytical models such as the F.E. models analysed by the writer, is to have an adequate base of experimental data.

What little data has been available to the writer has shown that the mechanisms brought to light by the F.E. models appear compatible with reality but the actual stresses, at which the various types of cracking happen, appear to be somewhat out.

The traditional type of experimental work that has been carried out on cracking of concrete has involved measurements of stress and strain that are really too coarse to give adequate definition to what is happening inside the models. Here, coarse is not meant in the sense of being inaccurate, but rather in the sense that the measurements tend to represent average values of stress and strain and do not give the detail that is necessary for a proper understanding of the problem.

To physically measure all of the detail required appears to be an impossible task with our present technology, and bearing in mind the random nature of the composition of concrete and the fact that its inelastic behaviour is, as a result, somewhat random too. This was the major reason why the writer decided to try finite element modelling of the problem. It was hoped that the models would afford the detailed information that the experimental results failed to do.

This has indeed been the case in that, although they failed to portray the full load-strain response of the models, the F.E. analyses did show the manner in which one could expect the stiffness of the models to vary as a result of the occurrence of cracks and the mechanisms which should control this.

Looking at possible ways to overcome the problem of getting greater definition in experimental data, the writer considered the fact that finite element modelling could give a fairly accurate indication of the overall response of the members modelled (at least from a mechanistic point of view). This led the writer to consider whether or not a similar series of experimental models might not be used to calibrate the F.E. models. This could have several advantages. The initial tests envisaged would be a series of tension tests of concrete prisms with a single reinforcing bar. The writer envisages testing a series of members with lengths ranging from less than the expected crack spacing to many times the expected spacing. The primary objective would be to measure the load-strain response of the members, thus instrumentation for this would be relatively simple. Detailed stress measurements would not be made, but rather, observations would be made on the time of occurrence of various phenomena such as internal cracking and tertiary cracking (including the microcracking stages). Some fairly sophisticated techniques, such as ultrasound for instance, might have to be used for non-destructive detection of the existence of cracks, but these have been well tried over the years. In addition the non-destructive tests should be checked against some models where the pattern of cracking has been "frozen in" by injecting ink or resin into the model. The writer envisages that the tests could be carried out in the following series:

(i) The internal damaging of concrete could be calibrated against the non-linear response of the members under low loads (i.e. loads that are insufficient to cause primary cracks to form). This calibration should be carried out for several different lengths of sample as done in the analytical models. A family of curves will now be built up such as those shown in the load-strain plots of the F.E. analyses in appendix E.

(ii) Loading the samples to the point at which new primary cracks occur should enable one to plot the shifts in stiffness across the family of curves built up from the tests in (i) above.

(iii) It would be interesting to plot the unloading and

reloading curves as well to observe the possible effects of "shakedown" on bond. Unloading should be investigated from various levels in the loading curve.

(iv) Different configurations of model (in cross-sectional area, shape, steel content, and steel layout) could be tested as described above to determine the differences in their behaviour which are determined by the changes of configuration.

The writer suggests that the series of curves obtained by series (i) above may be used for calibration, via the matching overall response of finite element models, of more realistic models of concrete than are presently obtainable with direct tension tests on concrete, even if these are carried out on very stiff machinery. Because of the concentration of stresses that occurs at the ends of the members it is only in this zone that the concrete need to be microscopically examined for the first signs of non-linear behaviour, microcracking, and discrete fracturing.

Because of the presence of the bar and the small size of the actual zone of concrete that will be fractured, the test should be very stable and sudden propagation of cracks due to release of stored energy in the testing rig should not occur.

Series (ii) should be of use in determining a more viable fracturing model for the concrete that can take account of the release of considerable strain energy within the model itself that will cause sudden (relatively) large displacements to occur. (Failure of the ABAQUS model to converge to equilibrium under this type of action seemed to be a possible cause of the early termination of the writer's analyses.)

Series (i) and (ii) would define the complete cracking behaviour of a particular configuration of bar and concrete cross-section in terms of its load-strain diagram. Should these curves prove to be repeatable and, outside of the inevitable experimental errors and random variations in material behaviour, the writer can see no reason why they should not be, knowing the position on the load-strain curve of

any particular sample should tell one exactly in what ways it is cracked. (One must also know the loading history of the sample for the above to apply).

If, by carrying out some tests on members with different configurations, we could find out what effect these changes in configuration had on the load-strain diagrams of the respective members, we would in turn have found out what effect these changes would have had on the cracking that might have occurred in any similar member.

This starts to have interesting possibilities for determination of the cracking behaviour of concrete members due to early age effects. By finding the position (at first application of external load) on the load-strain curve of a member which has been strained and cracked (perhaps only internally) due to early age effects, we could begin to quantify the extent of the early-age cracking. Some extra calibration by simulation of experimental results with finite element modelling would be necessary in this case to take account of the gradients of strain which occur due to both thermal and drying shrinkages.

Finally, the possibility exists, that with a fully calibrated set of load-strain curves, one could carry out full-scale load-deflection tests on real structures to determine the extent of cracking and built in stresses and strains that exist in the structure due to early-age effects. An example might be to measure the total extension of the walls of a circular reservoir as the load increases under the applied water pressure of first filling the reservoir. This would then be compared to the calibrated curves to see whether one could position the response of the reservoir on the calibrated curves.

CHAPTER 8

CONCLUSIONS AND RECOMMENDATIONS FOR FURTHER RESEARCH.

8.1 LITERATURE SURVEY OF CURRENT STATE OF KNOWLEDGE.

In the initial literature survey carried out for this thesis the single most important aspect that struck the writer was the lack of a cohesive and objective theory that could generally explain reinforcement controlled cracking in concrete.

A great deal of research has been done, resulting in a number of empirically observed relationships between cracking and various variables. Since reinforcement can only be as effective as the bond joining it to its surrounding concrete, the most obvious starting point for crack control theories was to base them on the bond between bar and concrete. These formulations have however been shown empirically to be inadequate and the search has been on ever since for theoretical reasons as to how to explain the deviations.

In the writer's opinion, this search has failed up to now because it has concentrated too much on trying to find relationships between cracking and a few "macro" parameters. In terms of the definitions given in the Addendum the writer felt that these parameters were often of too high an order for the level of modelling being attempted. The possibility exists that in some cases they are even "pseudo" parameters, with a purely fortuitous relationship to the spacing or size of cracks.

The writer has found that the problem of cracking due to restraint of early thermal and drying shrinkage movements has only really been addressed for the case of full externally applied restraint. In this regard the level of understanding of the mechanisms involved is on a par with the almost equivalent systems of externally applied loading.

The more complicated case of early age cracking due to various forms of internally applied restraints has not really been addressed at all in the literature in anything other than a very rough empirical way.

With regard to current codes of practice, the writer has found that these reflect the levels of knowledge and understanding of cracking as described above. The writer suggests that the formulae quoted in the codes are for the most part adequate "rules of thumb" but should not be considered to be much more than that.

In the case of the code of practice for liquid retaining structures BS 5337, the writer suggests that the theoretical derivation of the minimum steel requirement to prevent the occurrence of wide cracks due to yielding of the reinforcement may be flawed. This could result in an underestimate of the steel requirement.

The writer also found that BS 5337 fails to draw attention to the fact that in some instances both early thermal effects and effects of applied loading can assume significant proportions. The code does not specify that reinforcement required for early age effects and subsequent applied loading should be additive.

8.2 INVESTIGATION OF POSSIBILITIES FOR FURTHER RESEARCH.

It was found that to have any possibility of making any significant advance in understanding the mechanisms of cracking it would be necessary to find ways of examining the problem in far greater detail than has been the case up till now.

It was found purely from a point of view of physical and technological constraints, that it would be extremely difficult to obtain the necessary information by experiment. Experimental work with a variable substance such as concrete also necessarily involves a great deal of repetition to remove random effects.

In the Finite Element method the writer found a ready tool for analysing the problem. Recent developments in non-linear material modelling made the method particularly attractive.

8.3 CONCLUSIONS FROM FINITE ELEMENT ANALYSES CARRIED OUT.

8.3.1 NOSTRUM damage mechanics modelling.

In the series of models analysed using the NOSTRUM programme and the damage mechanics model of concrete, the analyses were found to terminate at rather low loads due to equilibrium convergence problems.

Before termination, the analyses showed that the zone of concrete immediately surrounding the bar would crack and become totally incapable of carrying load by shear at a much lower load than was expected. Examination of plots of the principal stress vectors showed that the cracking would be aligned diagonally in a manner that has been well established experimentally.

It seems probable that, equilibrium convergence problems aside, the current damage mechanics model would be incapable of analysing the problem to a reasonable level of load. This is because the damage parameter used was a scalar value, and after secondary cracking of the interface zone around the bar, no further mechanism could be found to carry load across this "totally" damaged zone.

8.3.2 ABAQUS modelling.

Because of its ability to crack vectorially and then carry load across a cracked zone either in compression or in another direction, the ABAQUS concrete model proved superior for the writer's purpose when compared to the NOSTRUM damage model. This model, however, still failed to perform 100 percent adequately. It appeared to have numerical/convergence problems as soon as any mode of cracking occurred where the resulting displacements were not controlled by the nearby proximity of a reinforcing bar. As a result it was not possible to model the full response of the longer models.

8.3.3 Mechanisms displayed by the models.

It was shown quite clearly that the only way in which a significant amount of bond can be achieved between bar and concrete is by a strut and ring tension mechanism.

The intuitive 45° rule was found not to apply with regard to the spread of longitudinal stresses.

It seems probable that for small spacing to cover ratios, new primary cracks form as a result of propagation of internal or secondary cracks from the surface of the reinforcement outwards. For larger spacing to cover ratios the direction of formation of cracks is probably random and dependent on weaknesses in the concrete.

In the shorter models surface compressive stresses were found to occur between cracks in confirmation of the experimental findings of some researchers. A mechanism has been proposed for the formation of these compressive stresses.

As a result of noting the effect of various modes of cracking on the overall load-strain response of reinforced concrete, the writer suggests that finding the position of the behaviour of any reinforced member on this curve might provide a better way of describing the cracking that has occurred in the member than by trying to quantify the size and number of externally evident cracks.

8.4 RECOMMENDATIONS FOR FURTHER RESEARCH.

One of the most noticeable results of the analyses was the extremely low level of loading at which the various modes of cracking occurred. Further research is needed in determining whether this was as a result of a size effect not allowed for in the analyses or whether it was as a result of poor calibration of the decreasing portion of the concrete stress-strain curve.

Finally, the writer has proposed a series of experimental tests designed to pursue almost any avenue of cracking in concrete by matching the overall load-strain response of simple reinforced tension specimens to that of models of the type analysed by the writer.

oooOOOooo

REFERENCES

ACI Committee 318, "Building code requirements for reinforced concrete (ACI 318-83) ", Amer. Concrete Institute, November 1983.

ADINA ENGINEERING AB, User's Manual, Report AE 84-1, December 1984.

APPLIED MECHANICS RESEARCH UNIT, "NOSTRUM USER'S MANUAL", Version 3.1, University of Cape Town, July 1984.

BASE, G.D., READ J.B., BEEBY, A.W. and TAYLOR, H.P.J., "An investigation of the crack control characteristics of various types of bar in reinforced concrete beams." Research Report 18, Part 1, Cement and Concrete Association, London, December 1966.

BAZANT, Z.P., & CEDOLIN, L., "Blunt crack band propagation in finite element analysis," J. Eng. Mech. Div., Proc. ASCE, Vol. 105, No. EM2, April 1979.

BAZANT, Z.P., & CEDOLIN, L., "Fracture mechanics of reinforced concrete", J. Eng. Mech. Div., Proc ASCE, Vol. 106, No EM6, Dec. 1980.

BAZANT, Z.P., & KIM J-K., "Size effect in shear failure of longitudinally reinforced beams", J. Amer. Conc. Inst., Sept - Oct. 1984.

BEEBY, A.W., "An investigation of cracking in slabs spanning one way", Technical Report TRA 433, Cement and Concrete Association, London, April 1970.

BEEBY, A.W., "An investigation of cracking on the side faces of beams", Technical Report 42.466, Cement and Concrete Association, London, December 1971.

BEEBY, A.W., "A study of cracking in reinforced concrete members subjected to pure tension." Technical Report 42.468, Cement and Concrete Association, London, June 1972.

BEEBY, A.W., "The prediction of crack widths in hardened concrete", The Structural Engineer. Vol. 57A, No. 1 pp 9-46, January 1979.

BOGUE, R.H., "The Chemistry of Portland Cement" Rheinhold Publishing Corporation, New York, 1947

BROMS, B.B. (1965(a)), "Technique for Investigation of Internal Cracks in Reinforced Concrete Members", J. Amer. Conc. Inst., Jan. 1965

BROMS, B.B. (1965(b)), "Stress Distribution in Reinforced Concrete Members with Tension Cracks", J. Amer. Conc. Inst., Sept. 1965.

BROMS, B. (1965(c)), "Crack width and crack spacing in reinforced concrete members", Part 1. J. Amer. Concr. Inst., Vol. 62 No. 10, pp 1237-1255 Oct. 1965.

BROMS, B.B., and LUTZ, L.A., "Effects of arrangement of reinforcement on crack width and spacing of reinforced concrete members", J. Amer. Conc. Inst., Nov. 1965.

BS 5337 : 1976, "Code of practice for the structural use of concrete for retaining aqueous liquids", (as amended 1977, 1982), British Standards Institution, London, 1976.

BS 8110: 1985, "Structural use of concrete" Part 2 : "Code of practice for special circumstances", British Standards Institution, 1985.

CEB-FIP, "Model Code for Concrete Structures", Third Edition, Comité Euro-International du Beton, 1978.

CHEN, A.C.T., & CHEN, W-F., "Constitutive relations for concrete", J. Eng. Mech. Div., ASCE, Vol. 101, No. EM4, Aug. 1975

CP 110 : 1972, "Code of practice for the structural use of concrete", Part 1, British Standards Institution, London, as amended, 1977.

CZERNIN, W., "Cement Chemistry and Physics for Civil Engineers",

Chemical Publishing Co. Inc., New York, 1962.

EVANS, E.P., and HUGHES, B.P., "Shrinkage and thermal cracking in a reinforced concrete retaining wall", Proc. Instn. Civil Engrs., No. 39, 1968. (Unseen - reprinted by Hughes and Miller (1970)).

EVANS, R.H., and MARATHE, M.S., "Microcracking and Stress-Strain Curves for Concrete in Tension", Materials and Structures, RILEM, Jan/Feb 1968, pp 61-64.

F.I.P., "Recommendations on practical design of reinforced and prestressed concrete structures based on the CEB/FIP Model Code (MC78)", Draft copy, June 1982.

FITZGIBBON, M.E., "Large pours - heat generation and control", Concrete, December 1976.

FULTON, F.S., "Concrete Technology, A South African Handbook", Portland Cement Institute, Johannesburg, 1977.

GERSTLE, W., INGRAFFEA, A.R., & GERGELY, P., "Tension stiffening: A fracture mechanics appproach", ex "Bond in Concrete" Edited by P. Bartons, Proc. Int. Conf. on Bond in Concrete, Paisley College of Technology, Scotland, June 1982. Applied Science Publishers, London.

GIURIANI, E., "On the effective axial stiffness of a bar in cracked concrete", ex "Bond in Concrete" Edited by P. Bartons, Proc. Int. Conf. on Bond in Concrete, Paisley College of Technology, Scotland, June 1982. Applied Science Publishers, London.

GOTO, Y., "Cracks formed in Concrete around deformed tension bars". Journal of the American Concrete Institute, April 1971.

HEGEMIER, G.A., MURAKAMI, H., & HAGEMAN, L.J., "On tension stiffening in reinforced concrete", Mechanics of Materials, No. 4, 1985.

HIBBETT, KARLSSON AND SORENSON, Inc., "ABAQUS user's manual", Version

4.5, May 1984, HKS Inc., Providence, Rhode Island, U.S.A.

HILLERBORG, A., MODEER, M., & PETERSSON, P.E., "Analysis of crack formation and crack growth in concrete by means of fracture mechanics and finite elements", Cement and Concrete Research Vol. 6, No. 6, 1976.

HOGNESTAD, E., "High Strength Bars as concrete reinforcement, Part 2, Control of flexural cracking", Journal of the Portland Cement Association Research and Development Laboratories, 4, No. 1, pp. 46-62, January 1962.

HUGHES, B.P., "Limit State Theory for Reinforced Concrete design", Third Edition, Pitman Books Ltd., London, 1980.

HUGHES., B.P., and CHAPMAN, G.P., "The complete stress - strain curve for concrete in direct tension", RILEM Bulletin No.30, March 1966, pp. 95-97.

HUGHES, B.P., and MILLER, M.M., "Thermal cracking and movement in reinforced concrete walls", Proc. Instn. Civil Engrs. (Supplement paper 7254 S), 1970.

INGRAFFEA, A.R., GERSTLE. W.H., GERGELY, P., & SAOUMA, V., "Fracture mechanics of bond in reinforced concrete", J. Struct. Eng., ASCE, Vol. 110, No. 4 April 1984.

JIANG, D.H., ANDONIAN, A.T., & SHAH, S.P., "A new type of bond test specimen" ex "Bond in Concrete" Edited by P. Bartons, Proc. Int. Conf. on Bond in Concrete, Paisley College of Technology, Scotland, June 1982. Applied Science Publishers, London.

KAAR, P.H., & MATTOCK, A.H., "High Strength Bars as Concrete Reinforcement, Part 4, Control of Cracking", Journal of the Portland Cement Assoc. Research and Development Laboratories, January 1963.

KAPLAN, M.F., "Crack Propagation and the Fracture of Concrete", J. Amer. Conc. Inst., Nov. 1961.

KAPLAN, M.F., "Stresses and Strains in Concrete at Initiation of Cracking and Near Failure", J. Amer. Conc. Inst., pp.853-857, July 1963.

KAPLAN, M.F., "Needed research into the behaviour and properties of concrete", UCT/CSIR Nonlinear Structural Mechanics Research Unit, Technical Report No 50, April 1984.

KNIGHT, R.B., "A method for the determination of the early strength of concrete", Concrete/Beton, Bulletin Conc. Soc. of S. Africa, No. 15, April 1973.

KOTSOVOS, M.D., & NEWMAN, J.B., "Fracture mechanics and concrete behaviour", Magazine of Concrete Research Vol. 33, No. 115, June 1981.

KUPFER, H.B., and GERSTLE, K.H., "Behaviour of Concrete Under Biaxial Stresses", J. Eng. Mech. Div., ASCE, 99, (EM 4), p.853, 1973. (unseen - reported by Resende (1985))

KUPFER, H.B., HILSDORF, H.K., and RUSCH, H., "Behaviour of Concrete Under Biaxial Stresses", Proc. ACI, 66, p.656, 1969. (unseen - reported by Resende (1985a)).

LABIB, F. & EDWARDS, A.D., "An analytical investigation of cracking in concentric and eccentric reinforced concrete tension members", Proc. Instn. Civ. Engrs., Part 2, No. 65, March 1978.

LEA, F.M., "The Chemistry of Cement and Concrete", Third Edition, Edward Arnold (Publishers) Ltd., Glasgow, 1970.

LEONHARDT, F., "Crack Control in Concrete Structures", IABSE Surveys S-4/77, 26 pp, Zurich, 1977.

LOEDOLFF, G.F., "Die Rol van Water in Beton", Nasou. Beperk, (in Afrikaans), Chapter 5, 1977.

LUTZ, L.A., "Analysis of Stresses in Concrete Near a Reinforcing Bar Due to Bond and Transverse Cracking", J. Amer. Conc. Inst.,

October 1970

MULLER, J.R., "Monitoring concrete temperature to determine formwork stripping time", The Civil Engineer in S. Africa, October, 1984

NALLATHAMBI, P., KARIHALOO, B.L., & HEATON, B.S., "Effect of specimen and crack sizes, water/cement ratio and coarse aggregate texture upon fracture toughness of concrete", Magazine of Concrete Research Vol. 36, No. 129, Dec. 1984

NGO, D. and SCORDELIS, A.C., "Finite element analysis of reinforced concrete beams", J. Amer. Conc. Inst., March 1976

RAPHAEL, J.M., "Tensile Strength of Concrete", J. Amer. Conc. Inst., March-April 1984, pp 158-165.

RESENDE, L., (1985a) "A damage mechanics constitutive theory for the inelastic behaviour of concrete", Technical Report No. 64, UCT/CSIR Applied Mechanics Research Unit, June 1985.

RESENDE, L., (1985b) Private Communication, 1985.

REYNOLDS, C.E., and STEEDMAN, J.C., "Reinforced Concrete Designers Handbook", Cement and Concrete Association, London, 1974

REYNOLDS, G.C., "Bond strength of deformed bars in tension", Technical Report No. 548, Cement & Concrete Assoc., May 1982.

RILEM, COMMISSION 42 - CEA, "Properties of set concrete at early ages, State of the art report", Materials and Structures, Vol. 14, No. 84, Nov-Dec 1981.

RIZKALLA, S.H., & HWANG, L.S., "Crack Prediction for Members in Uniaxial Tension", J. Amer. Conc. Inst., Nov-Dec. 1984.

SOMAYAJI, S., & SHAH, S.P., "Bond stress versus slip relationship and cracking response of tension members", J. Amer. Conc. Inst., May-June 1981

STOFFERS, H., "Cracking due to shrinkage and temperature variation in walls", Heron, Vol. 23, No. 3, 1978.

WEAVER, J., "Temperature development in hydrating concrete", Ph.D. Thesis, London University, 1971. (unseen - reported by Loedolff (1977))

YANKELEVSKI, D.Z., "A new finite element for bond-slip analysis", J. Struct. Eng., ASCE, Vol. 111, No. 7, July 1985

ADDENDUM

PHILOSOPHICAL CONSIDERATION OF SOUND MODELLING TECHNIQUES

AD.1 INTRODUCTION

AD.1.1 Modelling Levels

Kaplan 1984 reports the suggestion of F.H. Wittmann of the concept of three different structural levels, namely the microlevel, mesolevel, and macrolevel. This is called by Witmann the three-level or TL approach.

The writer would like to suggest that perhaps, for reinforced concrete structures, there are four levels which could be broadly defined as follows:

Level 4 : (macrolevel) The highest level - reinforced concrete components are considered to act as cohesive units

Level 3 : Cognisance is taken of the fact that reinforced concrete is made up of the concrete, which works in compression and reinforcing steel, which works in tension.

Level 2 : Cognisance is taken of the fact that the concrete component mentioned above, is made up of aggregate particles stuck together by a cement paste.

Level 1 : (microlevel) The sub-atomic, atomic, and molecular nature of the various components of concrete are recognised - this is the lowest level.

This concept of different structural levels is only readily apparent because the sub-division is made broadly in terms of the components whose properties are used to describe the physical and mathematical models associated with the various levels. Thus it is apparent that the different "structural levels" are somewhat artificial and exist only because there are different levels at which structures are

modelled. They might be better described, therefore as different "modelling levels".

AD.1.2 Prediction Levels

There is obviously a connection between results that are sought and the level of model that is commonly used in making predictions of those results.

One can quite easily see that those things which we might want to predict could well be classified on the macro to micro scale according to the level of model which makes the predictions with sufficient accuracy.

AD.1.3 Parameter Levels

In addition, the concept of different modelling levels leads naturally to the idea that the parameters used in the description of mathematical or physical models at the different levels should also be distinguishable according to some hierarchy of levels. The writer has chosen the term "dependance level" to describe this hierarchy, and to indicate that it is the degree of independence or dependance on other parameters that determines where a parameter fits in the hierarchy.

AD.1.4 Terminology

It is expedient at this stage to define some terms which are needed to describe the various levels of parameter dependance.

Absolute parameter: a parameter which does not depend for its value or any other parameter.

Low Level parameter: a parameter which is not absolutely independent but where the level of dependance on other parameters is minimal

e.g. inter-molecular forces, water/cement ratio.

High Level parameter: A parameter which is in fact a combination of a large number of absolute and low level parameters.

e.g. Concrete compressive strength, modulus of elasticity.

Pseudo parameter: Usually a high level parameter, a pseudo parameter would be one that is not directly dependant on certain lower level parameters but rather is only indicative of the behaviour of the lower level parameters. It is usually used because it is readily measured when the real parameters are not.

e.g. time, used as a parameter for judging how far a chemical reaction has proceeded.

Dependance Level: the relative position of a parameter in the absolute low to high range of parameters.

AD.2 A FUNDAMENTAL PRECEPT

A useful point of departure in attempting to create a model of any natural phenomenon is to assume that, no matter how complicated the phenomenon is, there are a number of totally independent parameters whose behaviour, when combined, exactly describe the behaviour of the whole. In other words, it is theoretically possible to describe any phenomenon exactly by a set of physical or mathematical laws.

A potential problem with this fundamental precept is how to model random occurrences. A first impulse is to say that provided the probability theory is applied to the correct variable the modelling is still exact.

For example, consider the tossing of a perfectly unbiased coin. One could say that the result is described exactly by saying that there is a 50% chance of each of the two possibilities of heads or tails

occurring. Alternatively, one could say that there are parameters such as the coin's initial vector of motion, air resistance, etc. which, for any one spin, uniquely predetermines the result.

Either view may be accepted as correct according to the observer's perception of the relative scale of importance of the occurrence. For the most part one is content to say that, for situations such as tossing a coin, the laws of probability exactly define the outcome of any one event. For reasons which are discussed in section AD.4 one can then build with confidence on this definition in examining other occurrences which are dependant on this first one.

AD.3 CHOICE OF MODELLING PARAMETERS

When analysing a structure, the effects that are to be analysed for predetermine the level of the structural model which is chosen. Obviously the model must be at a level which takes cognisance of the effects that are sought.

The primary object of this addendum is to point out that in order to satisfactorily model any naturally occurring phenomenon one must seek information about the phenomenon via the parameters that affect it at the lowest level.

Relationships do exist between certain high level parameters and various phenomena. However, the point being made here is that, because these high level parameters themselves depend on so many variables, any relationships based on them cannot be relied upon outside of the range of experimental values upon which the relationship is based. It is only when the behaviour of the high level parameters themselves are known in terms of their own variables that they may be used with confidence as parameters in their own right.

A useful analogy to real problems is to consider the way a digital computer operates. At the very lowest level we have a series of binary digits or bits which are governed by the simplest of functions - namely they are on or off.

Building from this starting point computer scientists have developed

the most complicated systems of interlinking of these bits to give us the computing power that we have at our fingertips today.

However, it would be tedious if every user had to think in terms of bits and bytes. Thus high level languages were written that are more accessible to the average human wanting to programme a computer. The analogy continues with the data input of sophisticated programmers becoming the ultra high level "parameters" of computer operation.

Consider for a moment the reverse situation of the complexity of breaking down a computer into its absolute components if one had no prior knowledge of the manner in which it worked.

If one were to make a study of cause and effect one might end up construing, after a superficial study, that certain keys on the keyboard were the absolute parameters that described the operation of the computer. One might find that the effects of certain keys were dependent on whether or not other keys had been used. This might lead one to the conclusion that these particular keys were not absolute parameters, but rather, were parameters at a higher level in that their actions were dependent on other keys.

Depending on what the computer was set up to do one might say after a certain amount of research work that one now knew the exact way in which it operated.

Imagine then one's consternation if while one's back was turned, someone loaded a different programme into the machine and suddenly all of one's previous knowledge was turned upside down.

Thus it seems to be with the real physical world. Our knowledge of many subjects is so superficial that we keep finding that the apparent parameters don't apply any more.

As an example of the physical world, consider the science of chemistry. Chemical reactions were not even remotely understood before chemists and physicists began to understand the actual nature of the structure of the atoms that were involved in the reactions. This understanding of the lower level parameters then enabled them to

construct the laws of chemistry with confidence at the higher level of parameter.

The point being made here is that if the analyst did not know that there was such a thing as a commputer programme, his analysis of the computer would be meaningless. In the same way, hidden parameters exist in real problems. The real task of the analyst is to find them.

Because many analysts, especially developers of empirical formulae, often take the easy route and simply try to relate sometimes totally arbitrary parameters to experimental results, the resulting mathematical models often leave much to be desired. The writer believes that there is a point in a particular problem where extending such empirical research at the macro level becomes more or less meaningless. Different methods must be tried if progress is to be made in understanding those problems which do not respond reasonably quickly to empirical investigation.

AD.3.1 Consistency of parameters

The writer proposes the theory that models and their parameters must be of a consistent level. This level must also be consistent with the level of accuracy required of the predictions of the model.

This may appear at first sight to be stating the obvious, but examples abound where macro-parameters are misused for micro-modelling.

To state the theory : A parameter must be of equal or lower relative dependence level than the model in which it is being used which in turn must be of equal or lower level than the results being sought.

It will be argued in this thesis that in the field of formulae for cracking of concrete many of the problems experienced with these formulae are due to just this kind of mis-application of parameters.

AD.4 STATISTICAL VERSUS MECHANISTIC APPROACH TO MODELLING

In any experimental study there is a physical limit to the amount of data that can be recorded. It is often not physically or

technologically possible to measure all of the parameters involved. Usually too, the measurable parameters of any experiment are high level ones or, quite likely, pseudo ones. The real parameters are often too many in number and too difficult to measure.

Thus there is always the temptation to look for oversimplified models of the phenomena being investigated. It is then all too easy to put all the lack of fit of the experimental data to the "theory" down to experimental scatter and introduce concepts of probability to explain this away.

Probability theories, however, are only as good as the models and parameters on which they are based. For example, given a pack of cards we can calculate exactly the probability of certain cards coming up under certain circumstances. We have all of the "absolute" parameters in this case. Say perhaps, the composition of the pack itself was changing. How good would our probability theories be then? The reason is obvious, the parameters on which the probability theory is based are no longer absolute.

Therefore, it seems there are two ways in which the probability theory may be used:

(i) The right way: all the parameters are known in their absolute form.

(ii) The wrong way: probability theories are introduced to explain away inadequacies in our knowledge of the real parameters of a problem.

APPENDIX A

METHOD OF LABELLING FINITE ELEMENT MODELS

The writer adopted the following system of labelling the finite element models which were analysed.

Each model name consisted of three or four digits as follows:

(i) The first digit represents the material model used in the analyses:

D Stands for damage mechanics.
and A for ABAQUS concrete model.

(ii) The second digit indicates the length between primary cracks where:

1 ..... 80 mm
2 ..... 120 mm
3 ..... 160 mm
4 ..... 240 mm
5 ..... 320 mm

(iii) The third digit represents changes in geometry other than the length between cracks or changes in discretization of the continua into elements.

(iv) Finally, some of the models were run more than once, using different incrementation sizes and schemes and different equilibrium tolerance. The various different runs were numbered sequentially from 1 to indicate some change in these criteria.

APPENDIX B

SAMPLE DATA DECK FOR ABAQUS MODEL
(Model A1F)

A B A Q U S I N P U T E C H O

```
     5   10   15   20   25   30   35   40   45   50   55   60   65   70   75   80
-----------------------------------------------------------------------------------
*HEADING
MODEL A1F(1) - BAR=10 C=40 S=80
*NODE
1,0.000,0.200
CARD  5  10,0.045,0.200
80,0.000,0.160
98,0.045,0.160
*NGEN
1,10,1
CARD 10  80,98,1
1,89,11
2,90,11
3,91,11
4,92,11
CARD 15  5,93,11
6,94,11
7,95,11
8,96,11
9,97,11
CARD 20  10,98,11
*NSET,NSET=CNTRE,GENERATE
1,89,11
*NSET,NSET=DISPD,GENERATE
80,98,1
CARD 25  *ELEMENT,TYPE=CAX4
1,12,13,2,1
*ELGEN
1,9,1,1,8,11,10
*ELSET,ELSET=BAR,GENERATE
CARD 30  1,71,10
*ELSET,ELSET=CONC,GENERATE
2,72,10
3,73,10
4,74,10
CARD 35  5,75,10
6,76,10
7,77,10
8,78,10
9,79,10
CARD 40  *ELSET,ELSET=CORNER
1,2,3,12,13,52
-----------------------------------------------------------------------------------
     5   10   15   20   25   30   35   40   45   50   55   60   65   70   75   80
```

```
     5   10   15   20   25   30   35   40   45   50   55   60   65   70   75   80
-----------------------------------------------------------------------------
*ELSET,ELSET=AXSYM,GENERATE
71,79,1
*MATERIAL,ELSET=BAR
CARD   45  *ELASTIC
206000.,0.3
*MATERIAL,ELSET=CONC
*ELASTIC
32338.,0.1725
CARD   50  *CONCRETE
16.,0.00
26.,.000140
29.6,.000560
*FAILURE RATIOS
CARD   55  1.16,0.106,1.28,0.106
*TENSION STIFFENING
0.923,56.0-006
0.0,356.0-006
*SHEAR RETENTION
CARD   60  1.0,356.0-006,1.0,356.0-006
0.923,56.0-006
*BOUNDARY
CNTRE,1
1,2
CARD   65  2,2
*PLOT
*DRAW,ELNUM,NODENUM
*STEP,INC=400,AMP=RAMP
*STATIC,PTOL=1.5-004
CARD   70  2.,160.,0.05
*BOUNDARY,OP=MOD
DISED,2, ,-0.00004
*EL PRINT,ELSET=CORNER
2,2
CARD   75  2,2,1,1,1,2
*EL PRINT,ELSET=AXSYM
2,2
2,2,1,1,1,2
2,2,2
CARD   80  *NODE PRINT
2,1,1,1,1,2,1
*PLOT,FREQUENCY=5
*DETAIL,ELSET=CONC
*CONTOUR
CARD   85  1
2
-----------------------------------------------------------------------------
     5   10   15   20   25   30   35   40   45   50   55   60   65   70   75   80
```

```
     5    10    15    20    25    30    35    40    45    50    55    60    65    70    75    80
----------------------------------------------------------------------------------------------
3
4
*EL FILE
CARD    9C   2,2
2,2,1,1,1,2
*NODE FILE
2,1,1,1,1,2,2,1
*END STEP
CARD    9S   EOF
----------------------------------------------------------------------------------------------
     5    10    15    20    25    30    35    40    45    50    55    60    65    70    75    80
----------------------------------------------------------------------------------------------
```

APPENDIX C

SAMPLE OF ABAQUS PRINTOUT
(Model A1F)

ITERATION 1 NO CONVERGENCE

MAXIMUM RESIDUALS ASSOCIATED WITH EACH D.O.F.

D.O.F.	MAXIMUM RESIDUAL	OCCURS AT NODE
1	1.997-004	14
2	-7.184-005	25

MAXIMUM DISPLACEMENT INCREMENT ASSOCIATED WIT

D.O.F.	MAXIMUM DISPLACEMENT INCREMENT	OCCURS AT NODE
1	1.885-007	3
2	-1.141-006	10

ITERATION 2 CONVERGENT SOLUTION

MAXIMUM RESIDUALS ASSOCIATED WITH EACH D.O.F.

D.O.F.	MAXIMUM RESIDUAL	OCCURS AT NODE
1	1.858-005	14
2	1.149-005	3

MAXIMUM DISPLACEMENT INCREMENT ASSOCIATED WIT

D.O.F.	MAXIMUM DISPLACEMENT INCREMENT	OCCURS AT NODE
1	3.065-007	3
2	-1.154-006	10

TIME COMPLETED DURING THIS STEP 1.150+001, TIME INCREMENT COMPLETED IS 4.500+000, FRACTION OF STEP IS 7.187
TOTAL ACCUMULATED TIME IS 1.150+001

E L E M E N T O U T P U T F O R E L S E T CORNER

ELEMENT 1 POINT 1					
STRESS COMPONENTS	1.848+000	2.386+001	2.916+000	-1.850+000	
STRESS INVARIANTS - MISES	2.174+001	TRESCA	2.233+001	EQU.PRESS	-9.543+000
PRINCIPAL STRESSES	1.694+000	2.916+000	2.402+001		
TOTAL STRAIN COMPONENTS	-3.003-005	1.089-004	-2.329-005	-2.335-005	
ELEMENT 1 POINT 2					
STRESS COMPONENTS	4.309+000	2.961+001	5.377+000	-7.824-001	
STRESS INVARIANTS - MISES	2.482+001	TRESCA	2.535+001	EQU.PRESS	-1.310+001
PRINCIPAL STRESSES	4.285+000	5.377+000	2.963+001		
TOTAL STRAIN COMPONENTS	-3.003-005	1.296-004	-2.329-005	-9.875-006	
ELEMENT 1 POINT 3					
STRESS COMPONENTS	5.586+000	2.547+001	4.518+000	-2.096-001	
STRESS INVARIANTS - MISES	2.044+001	TRESCA	2.095+001	EQU.PRESS	-1.186+001
PRINCIPAL STRESSES	4.518+000	5.584+000	2.547+001		

TOTAL STRAIN COMPONENTS	-1.65[illegible]-005	1.089-004	-2.329-005	-2.646-006
ELEMENT 1 POINT 4				
STRESS COMPONENTS	8.047+000	3.121+001	6.979+000	8.582-001
STRESS INVARIANTS - MISES	2.376+001	TRESCA	2.426+001	EQU.PRESS -1.541+001
PRINCIPAL STRESSES	6.979+000	8.015+000	3.124+001	
TOTAL STRAIN COMPONENTS	-1.655-005	1.296-004	-2.329-005	1.083-005
ELEMENT 2 POINT 1				
STRESS COMPONENTS	8.998-001	1.977+000	-7.347-002	-1.808+000
STRESS INVARIANTS - MISES	3.600+000	TRESCA	3.772+000	EQU.PRESS -9.344-001
PRINCIPAL STRESSES	-4.479-001	-7.347-002	3.325+000	
TOTAL STRAIN COMPONENTS	5.755-005	1.098-004	1.168-005	-1.724-004
PLASTIC STRAINS - MAGNITUDE	5.676-005	EQUIVALENT	4.234-005	ACTIVELY YIELDING
COMPONENTS	2.044-005	4.682-005	1.156-005	-5.827-005
CONCRETE CRACKED IN DIRECTION	5.957-001	-8.032-001	.000	
ELEMENT 2 POINT 2				
STRESS COMPONENTS	1.566+000	1.016+000	4.467-001	-1.511+000
STRESS INVARIANTS - MISES	2.791+000	TRESCA	3.072+000	EQU.PRESS -1.010+000
PRINCIPAL STRESSES	-2.448-001	4.467-001	2.827+000	
TOTAL STRAIN COMPONENTS	5.755-005	3.509-005	1.168-005	-1.243-004
PLASTIC STRAINS - MAGNITUDE	2.216-005	EQUIVALENT	1.773-005	ACTIVELY YIELDING
COMPONENTS	1.693-005	1.439-005	1.164-005	-1.467-005
ELEMENT 2 POINT 3				
STRESS COMPONENTS	1.320+000	1.351+000	-5.236-001	-2.372+000
STRESS INVARIANTS - MISES	4.509+000	TRESCA	4.743+000	EQU.PRESS -7.158-001
PRINCIPAL STRESSES	-1.036+000	-5.236-001	3.707+000	
TOTAL STRAIN COMPONENTS	1.057-004	1.098-004	1.168-005	-2.471-004
PLASTIC STRAINS - MAGNITUDE	9.103-005	EQUIVALENT	4.592-005	ACTIVELY YIELDING
COMPONENTS	5.923-005	6.258-005	2.234-005	-9.493-005
CONCRETE CRACKED IN DIRECTION	7.011-001	-7.130-001	.000	
ELEMENT 2 POINT 4				
STRESS COMPONENTS	1.908+000	3.821-001	-1.167-001	-2.110+000
STRESS INVARIANTS - MISES	4.086+000	TRESCA	4.488+000	EQU.PRESS -7.243-001
PRINCIPAL STRESSES	-1.099+000	-1.167-001	3.389+000	
TOTAL STRAIN COMPONENTS	1.057-004	3.509-005	1.168-005	-1.990-004
PLASTIC STRAINS - MAGNITUDE	5.340-005	EQUIVALENT	2.385-005	ACTIVELY YIELDING
COMPONENTS	4.209-005	2.076-005	9.424-006	-6.302-005

ITERATION 2 NO CONVERGENCE

MAXIMUM RESIDUALS ASSOCIATED WITH EACH D.O.F.

D.O.F.	MAXIMUM RESIDUAL	OCCURS AT NODE
1	-1.832-004	3
2	-1.278-004	4

MAXIMUM DISPLACEMENT INCREMENT ASSOCIATED WITH

D.O.F.	MAXIMUM DISPLACEMENT INCREMENT	OCCURS AT NODE
1	3.961-007	3
2	-1.483-006	10

ITERATION 3 CONVERGENT SOLUTION

MAXIMUM RESIDUALS ASSOCIATED WITH EACH D.O.F.

D.O.F.	MAXIMUM RESIDUAL	OCCURS AT NODE
1	-1.066-004	3
2	5.885-005	14

MAXIMUM DISPLACEMENT INCREMENT ASSOCIATED WITH

D.O.F.	MAXIMUM DISPLACEMENT INCREMENT	OCCURS AT NODE
1	3.612-007	4
2	-1.484-006	10

TIME COMPLETED DURING THIS STEP 4.926+001, TIME INCREMENT COMPLETED IS 5.695+000, FRACTION OF STEP IS 3.079
TOTAL ACCUMULATED TIME IS 4.926+001

E L E M E N T O U T P U T F O R E L S E T CORNER

ELEMENT 1 POINT 1

STRESS COMPONENTS	-4.096+000	8.666+001	-3.218+000	-2.727+000	
STRESS INVARIANTS - MISES	9.044+001	TRESCA	9.092+001	EQU.PRESS	-2.645+001
PRINCIPAL STRESSES	-4.178+000	-3.218+000	8.674+001		
TOTAL STRAIN COMPONENTS	-1.414-004	4.313-004	-1.359-004	-3.442-005	

ELEMENT 1 POINT 2

STRESS COMPONENTS	-7.483-001	9.447+001	1.297-001	-1.849+000	
STRESS INVARIANTS - MISES	9.484+001	TRESCA	9.529+001	EQU.PRESS	-3.128+001
PRINCIPAL STRESSES	-7.842-001	1.297-001	9.450+001		
TOTAL STRAIN COMPONENTS	-1.414-004	4.595-004	-1.359-004	-2.334-005	

ELEMENT 1 POINT 3

STRESS COMPONENTS	-1.023+000	8.798+001	-1.901+000	-4.955-001	
STRESS INVARIANTS - MISES	8.944+001	TRESCA	8.988+001	EQU.PRESS	-2.835+001
PRINCIPAL STRESSES	-1.901+000	-1.026+000	8.798+001		

TOTAL STRAIN COMPONENTS	-1.303-004	4.313-004	-1.359-004	-6.253-006	
ELEMENT 1 POINT 4					
STRESS COMPONENTS	2.325+000	9.579+001	1.447+000	3.825-001	
STRESS INVARIANTS - MISES	9.391+001	TRESCA	9.434+001	EQU.PRESS	-3.319+001
PRINCIPAL STRESSES	1.447+000	2.323+000	9.579+001		
TOTAL STRAIN COMPONENTS	-1.303-004	4.595-004	-1.359-004	4.828-006	
ELEMENT 2 POINT 1					
STRESS COMPONENTS	-2.406+000	-1.324+000	2.304+000	-1.785+000	
STRESS INVARIANTS - MISES	5.274+000	TRESCA	6.034+000	EQU.PRESS	4.755-001
PRINCIPAL STRESSES	-3.730+000	-1.735-018	2.304+000		
TOTAL STRAIN COMPONENTS	5.003-004	4.135-004	1.027-004	-1.233-003	
PLASTIC STRAINS - MAGNITUDE	8.821-004	EQUIVALENT	4.234-005		
COMPONENTS	5.826-004	4.588-004	1.156-005	-1.111-003	
CONCRETE CRACKED IN DIRECTION	5.957-001	-8.032-001	.000		
ELEMENT 2 POINT 2					
STRESS COMPONENTS	-2.036+000	-3.411+000	1.620+000	-2.635+000	
STRESS INVARIANTS - MISES	6.412+000	TRESCA	7.067+000	EQU.PRESS	1.276+000
PRINCIPAL STRESSES	-5.447+000	.000	1.620+000		
TOTAL STRAIN COMPONENTS	5.003-004	2.596-004	1.027-004	-1.074-003	
PLASTIC STRAINS - MAGNITUDE	7.599-004	EQUIVALENT	4.430-005		
COMPONENTS	5.665-004	3.705-004	2.355-005	-9.027-004	
CONCRETE CRACKED IN DIRECTION	7.913-001	-6.114-001	.000		
ELEMENT 2 POINT 3					
STRESS COMPONENTS	-2.618+000	-2.931+000	1.710+000	-2.574+000	
STRESS INVARIANTS - MISES	6.184+000	TRESCA	6.859+000	EQU.PRESS	1.146+000
PRINCIPAL STRESSES	-5.149+000	-3.469-018	1.710+000		
TOTAL STRAIN COMPONENTS	6.593-004	4.135-004	1.027-004	-1.387-003	
PLASTIC STRAINS - MAGNITUDE	1.015-003	EQUIVALENT	4.592-005		
COMPONENTS	7.449-004	4.962-004	2.234-005	-1.219-003	
CONCRETE CRACKED IN DIRECTION	7.011-001	-7.130-001	.000		
ELEMENT 2 POINT 4					
STRESS COMPONENTS	-1.864+000	-3.736+000	2.050+000	-2.639+000	
STRESS INVARIANTS - MISES	6.859+000	TRESCA	7.651+000	EQU.PRESS	1.183+000
PRINCIPAL STRESSES	-5.601+000	.000	2.050+000		
TOTAL STRAIN COMPONENTS	6.593-004	2.596-004	1.027-004	-1.228-003	
PLASTIC STRAINS - MAGNITUDE	9.024-004	EQUIVALENT	2.385-005		
COMPONENTS	7.206-004	3.825-004	9.424-006	-1.054-003	

CONCRETE CRACKED IN DIRECTION	8.168-001	-5.769-001	.000	
ELEMENT 3 POINT 1				
STRESS COMPONENTS	-2.138+000	2.426+000	1.978+000	-1.235-001
STRESS INVARIANTS - MISES	4.362+000	TRESCA	4.570+000	EQU.PRESS -7.552-001
PRINCIPAL STRESSES	-2.141+000	1.978+000	2.429+000	
TOTAL STRAIN COMPONENTS	-6.867-005	1.741-004	1.613-004	-5.294-022
PLASTIC STRAINS - MAGNITUDE	1.156-004	EQUIVALENT	6.485-005	ACTIVELY YIELDING
COMPONENTS	-2.564-006	9.823-005	1.017-004	8.956-006
CONCRETE CRACKED IN DIRECTION	.000	1.000+000	.000	
CONCRETE CRACKED IN DIRECTION	.000	.000	1.000+000	
ELEMENT 3 POINT 2				
STRESS COMPONENTS	-1.812+000	7.193-001	2.748+000	-1.469+000
STRESS INVARIANTS - MISES	4.705+000	TRESCA	5.234+000	EQU.PRESS -5.518-001
PRINCIPAL STRESSES	-2.486+000	1.393+000	2.748+000	
TOTAL STRAIN COMPONENTS	-5.960-005	6.041-005	1.613-004	-1.358-004
PLASTIC STRAINS - MAGNITUDE	6.432-005	EQUIVALENT	2.451-005	ACTIVELY YIELDING
COMPONENTS	2.719-007	2.850-005	7.047-005	-2.926-005
CONCRETE CRACKED IN DIRECTION	.000	.000	1.000+000	
ELEMENT 3 POINT 3				
STRESS COMPONENTS	-3.698+000	2.584+000	1.658+000	-1.508-001
STRESS INVARIANTS - MISES	5.880+000	TRESCA	6.290+000	EQU.PRESS -1.813-001
PRINCIPAL STRESSES	-3.702+000	1.658+000	2.588+000	
TOTAL STRAIN COMPONENTS	-1.355-004	1.972-004	1.613-004	-8.470-022
PLASTIC STRAINS - MAGNITUDE	1.229-004	EQUIVALENT	2.481-005	ACTIVELY YIELDING
COMPONENTS	-2.114-005	1.064-004	1.041-004	1.094-005
CONCRETE CRACKED IN DIRECTION	.000	1.000+000	.000	
CONCRETE CRACKED IN DIRECTION	.000	.000	1.000+000	
ELEMENT 3 POINT 4				
STRESS COMPONENTS	-3.194+000	1.112-001	2.126+000	-2.577+000
STRESS INVARIANTS - MISES	6.447+000	TRESCA	6.728+000	EQU.PRESS 3.190-001
PRINCIPAL STRESSES	-4.603+000	1.529+000	2.126+000	
TOTAL STRAIN COMPONENTS	-1.033-004	6.041-005	1.613-004	-2.404-004
PLASTIC STRAINS - MAGNITUDE	7.875-005	EQUIVALENT	8.072-006	ACTIVELY YIELDING
COMPONENTS	-3.972-006	3.993-005	7.911-005	-5.353-005
CONCRETE CRACKED IN DIRECTION	.000	.000	1.000+000	
ELEMENT 12 POINT 1				

APPENDIX D

ANALYSIS PATH PLOTS - ABAQUS MODELS

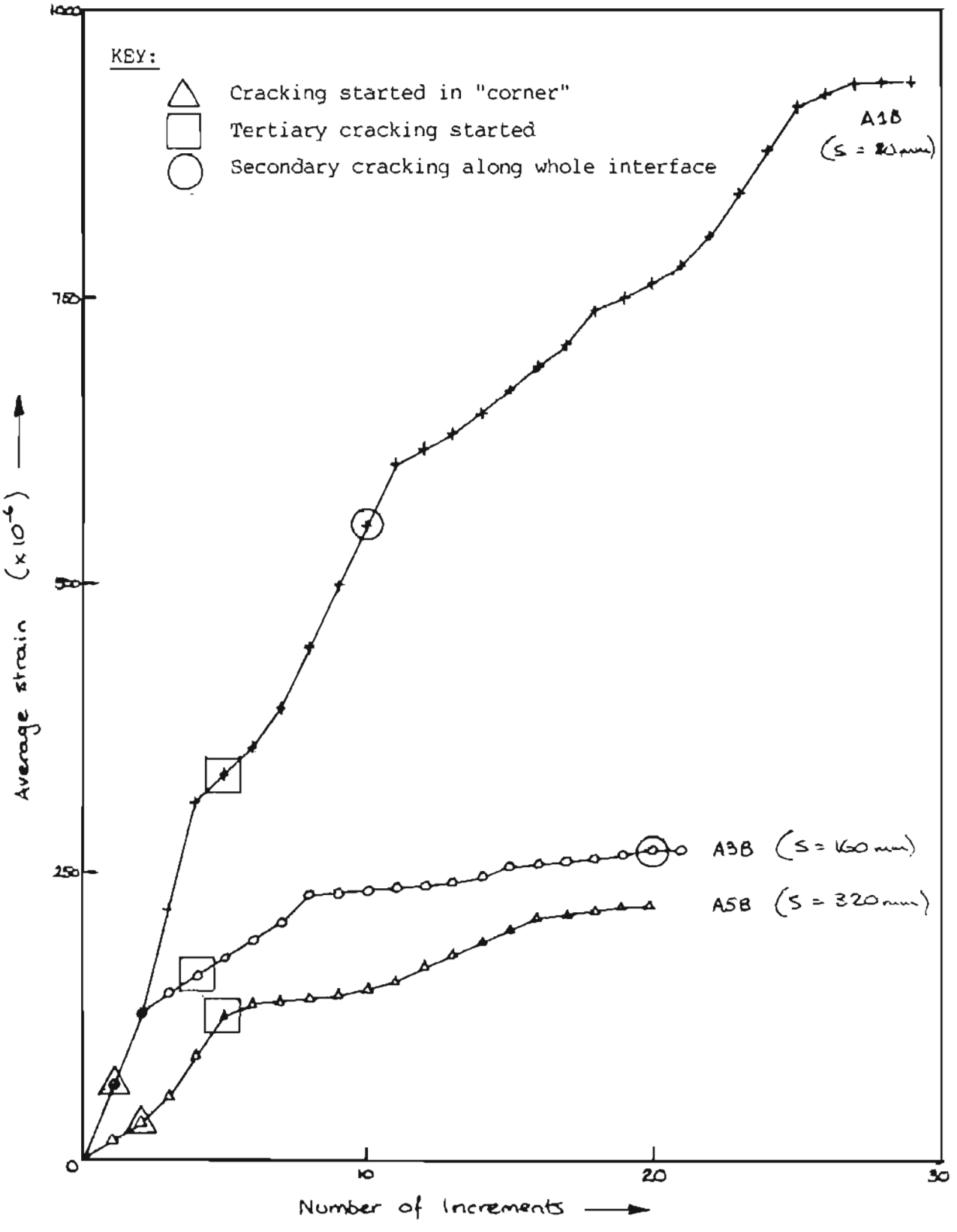

FIGURE D.1 : PLOTS OF PATHS OF ABAQUS ANALYSES

SERIES "B" : BAR ϕ = 20 mm

COVER = 40 mm.

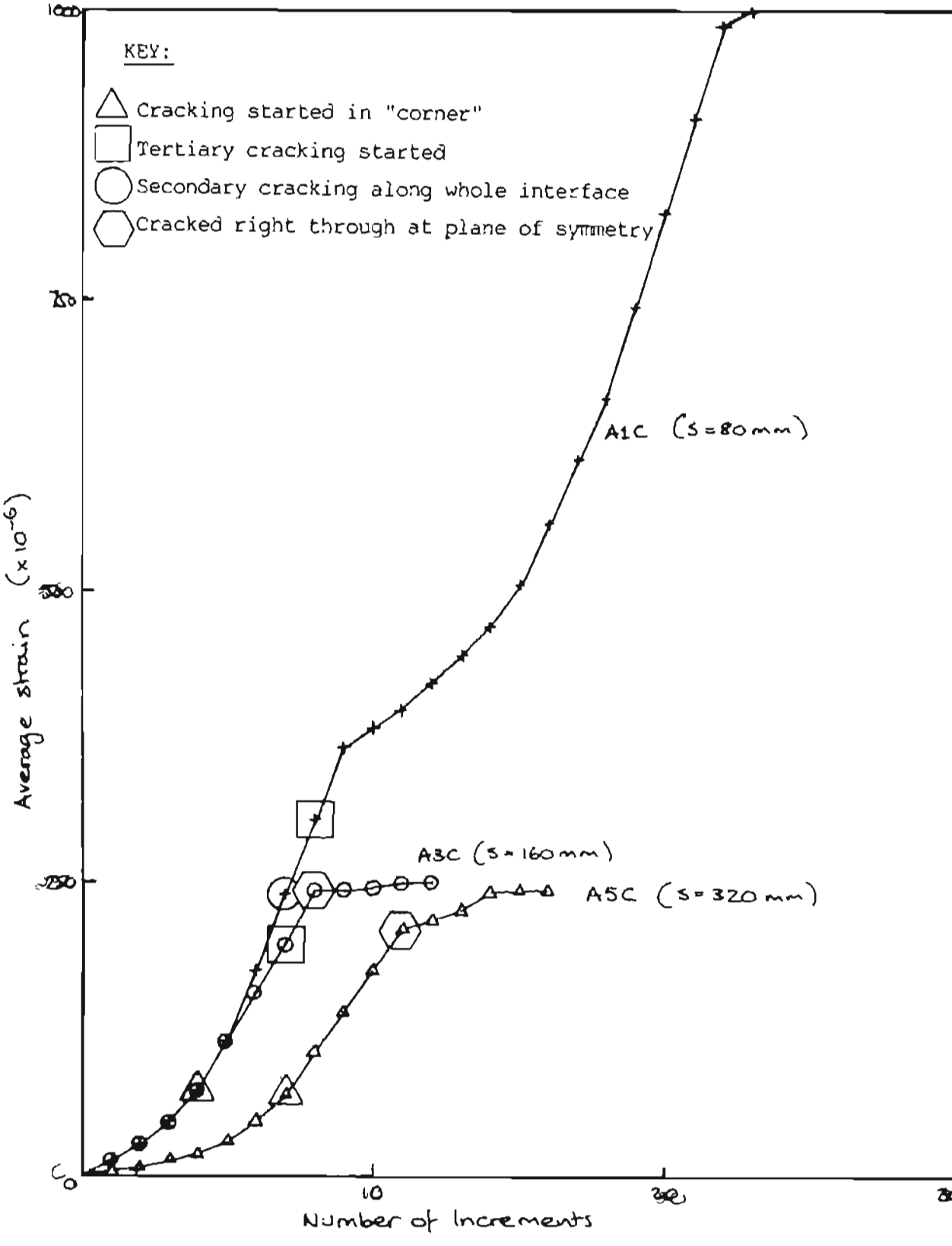

FIGURE D.2 : PLOTS OF PATHS OF ABAQUS ANALYSES
SERIES "C" : BAR ϕ = 20 mm
COVER = 20 mm

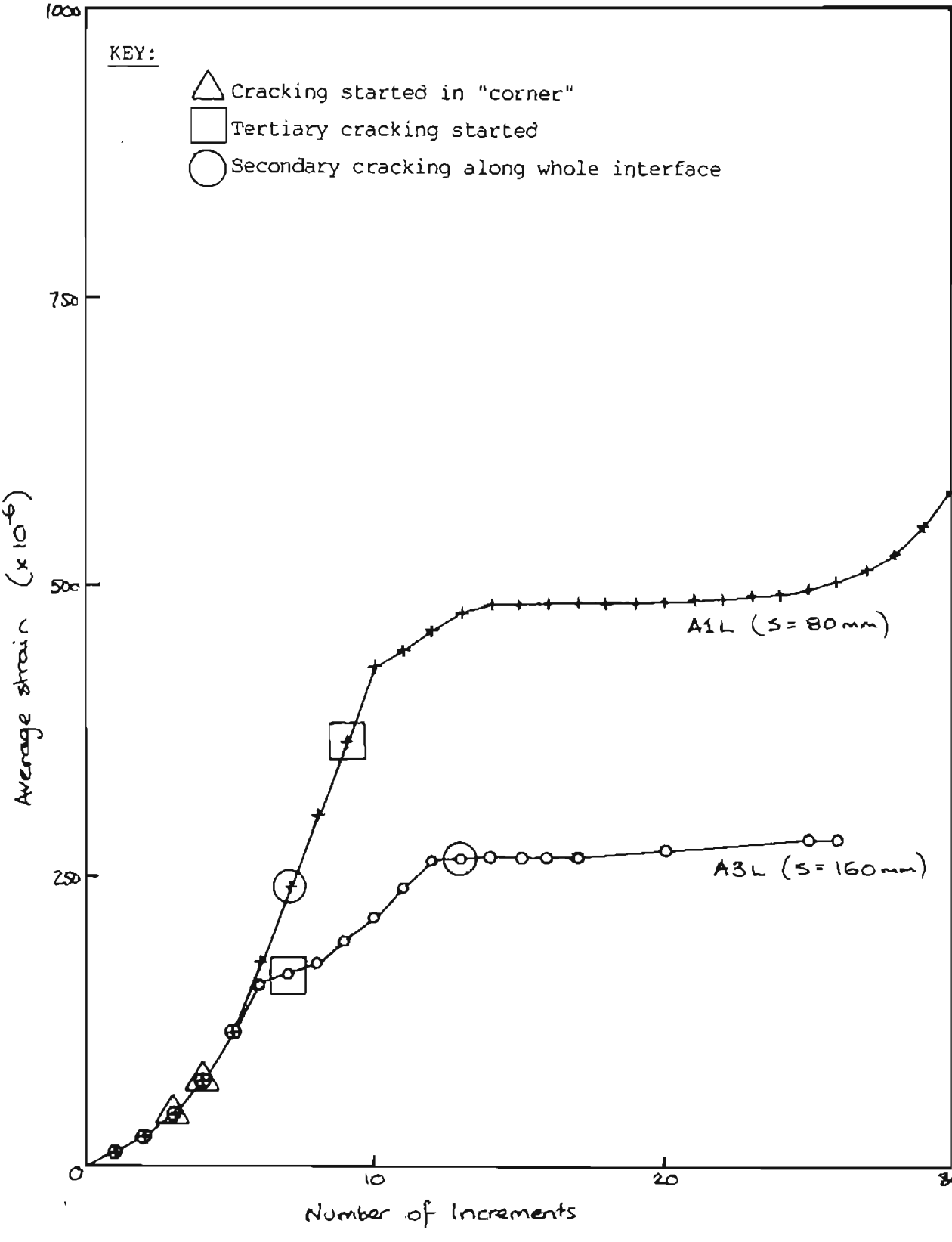

FIGURE D.3 : PLOTS OF PATHS OF ABAQUS ANALYSES

SERIES "L" : BAR ϕ = 20 mm

COVER = 80 mm

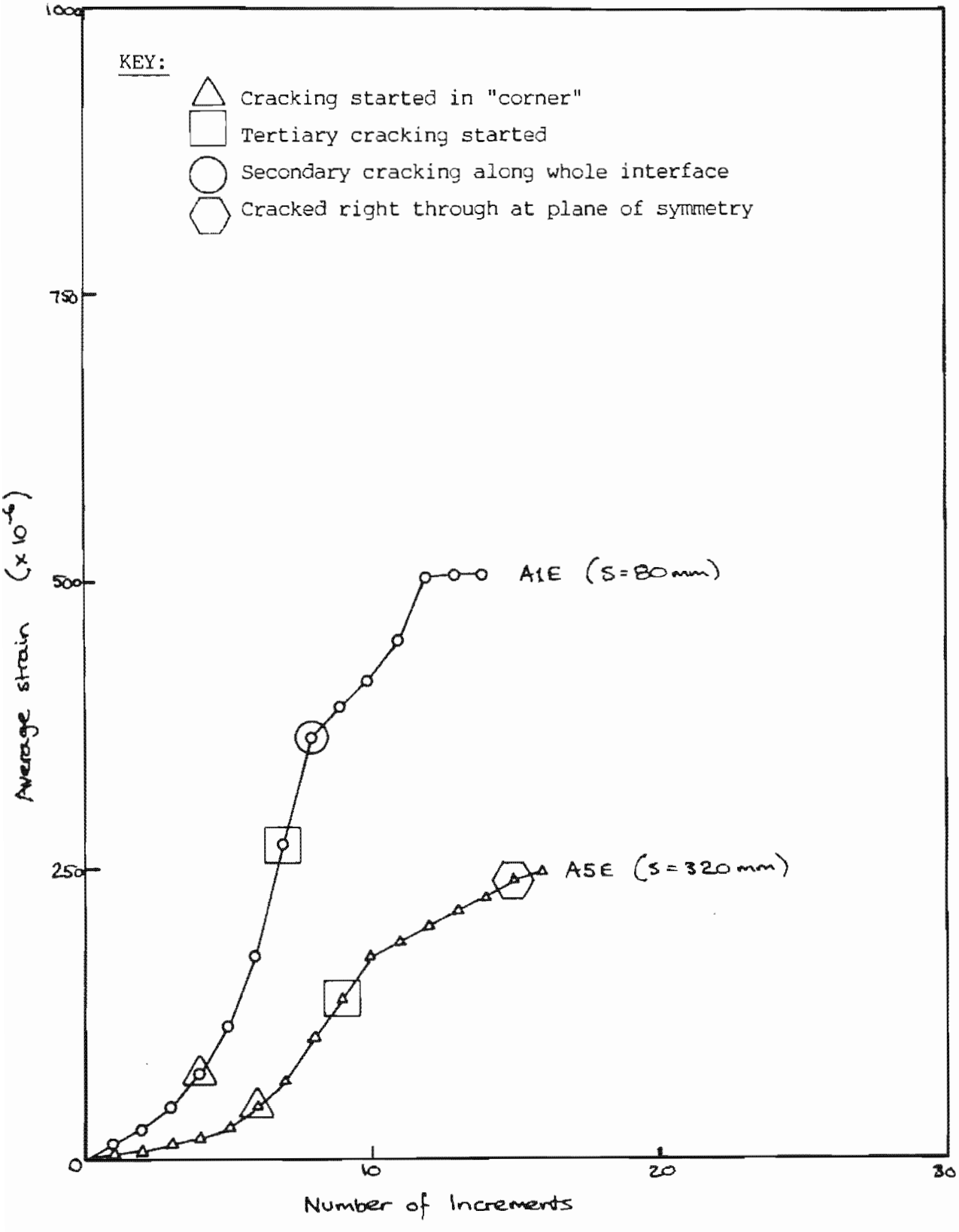

FIGURE D.4 : PLOTS OF PATHS OF ABAQUS ANALYSES

SERIES "E" : BAR ϕ = 10 mm

COVER = 20 mm

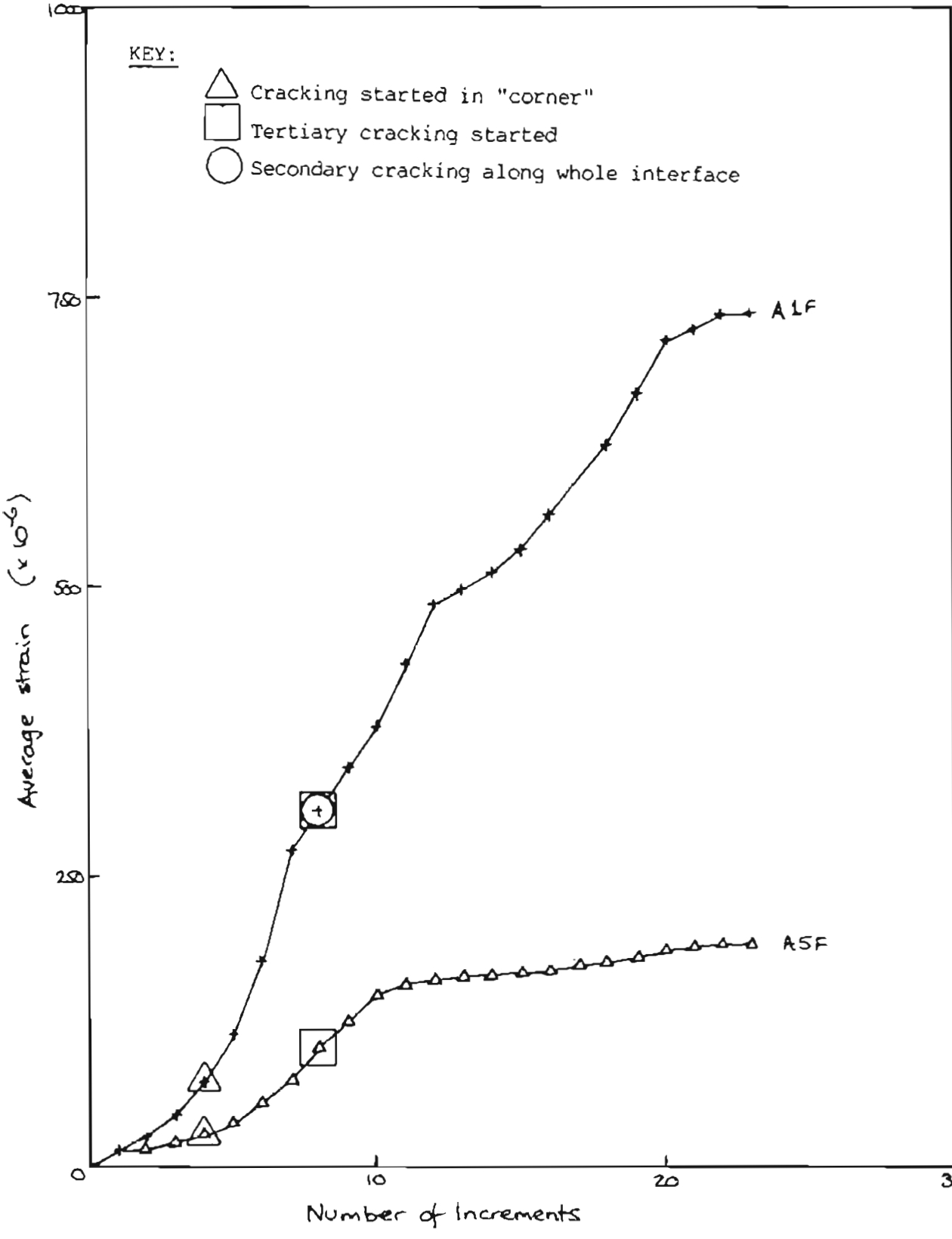

FIGURE D.5 : PLOTS OF PATHS OF ABAQUS ANALYSES
SERIES "F" : BAR ∅ = 10 mm
COVER = 40 mm

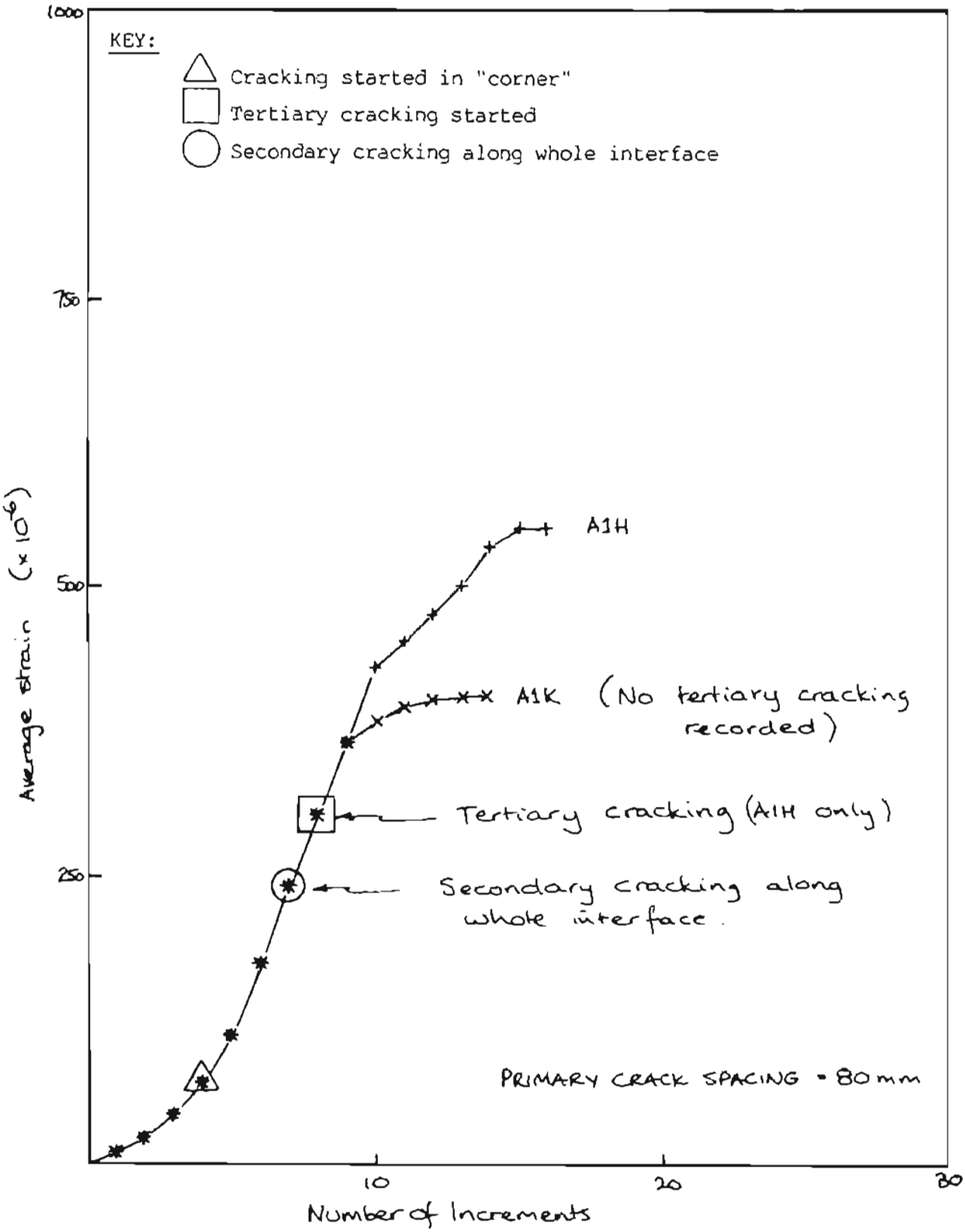

FIGURE D.6 : PLOTS OF PATHS OF ABAQUS ANALYSES

MODEL A1H : BAR ϕ = 30 mm
COVER = 20 mm

MODEL A1K : BAR ϕ = 30 mm
COVER = 80 mm

APPENDIX E

LOAD - STRAIN DIAGRAMS FOR ABAQUS MODELS

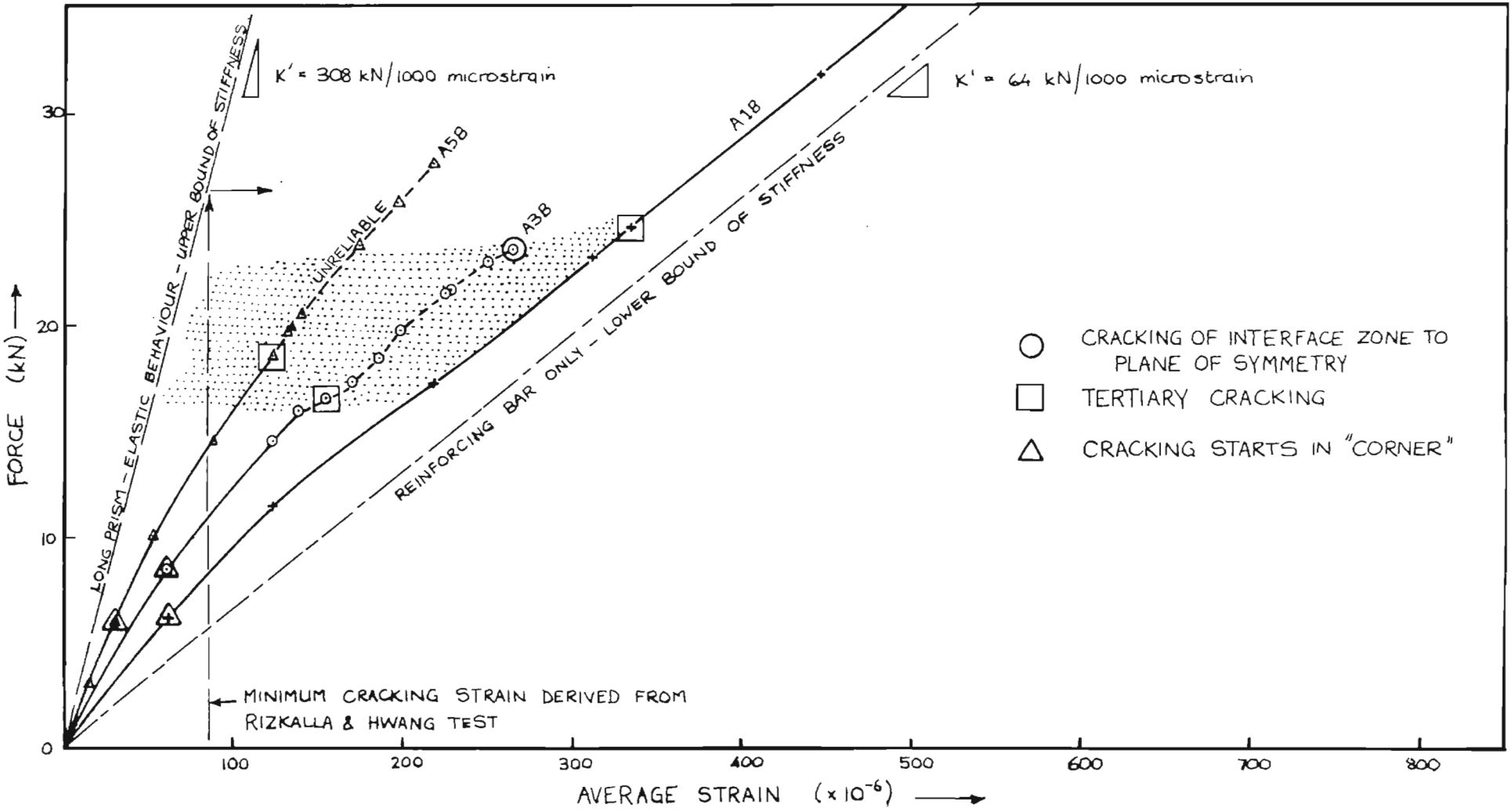

FIGURE E.1: LOAD-STRAIN DIAGRAM FOR SERIES B

(BAR ϕ = 20mm
COVER = 40 mm)

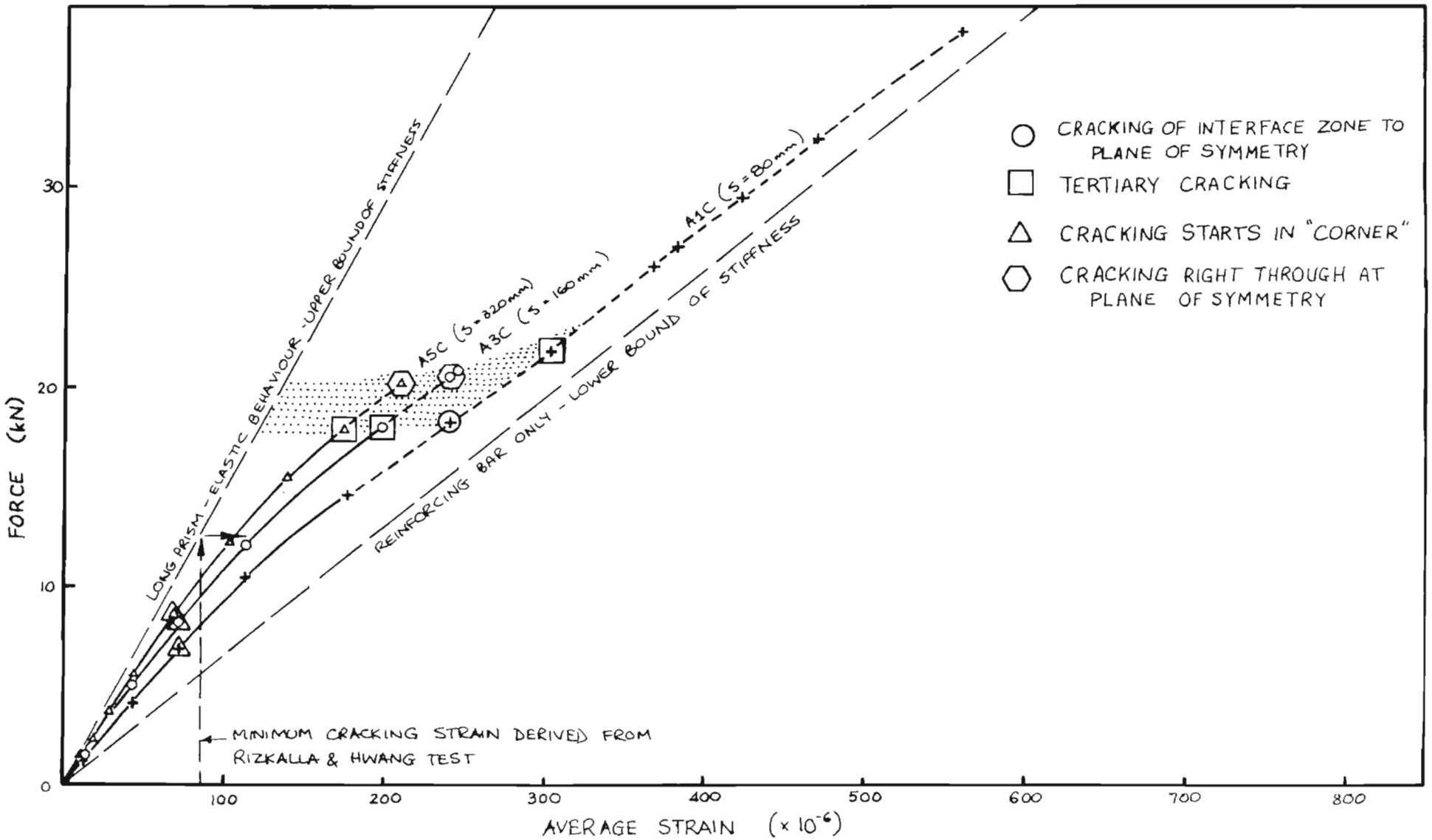

FIGURE E.2: LOAD-STRAIN DIAGRAM FOR SERIES C

(BAR ϕ = 20mm
COVER = 20 mm)

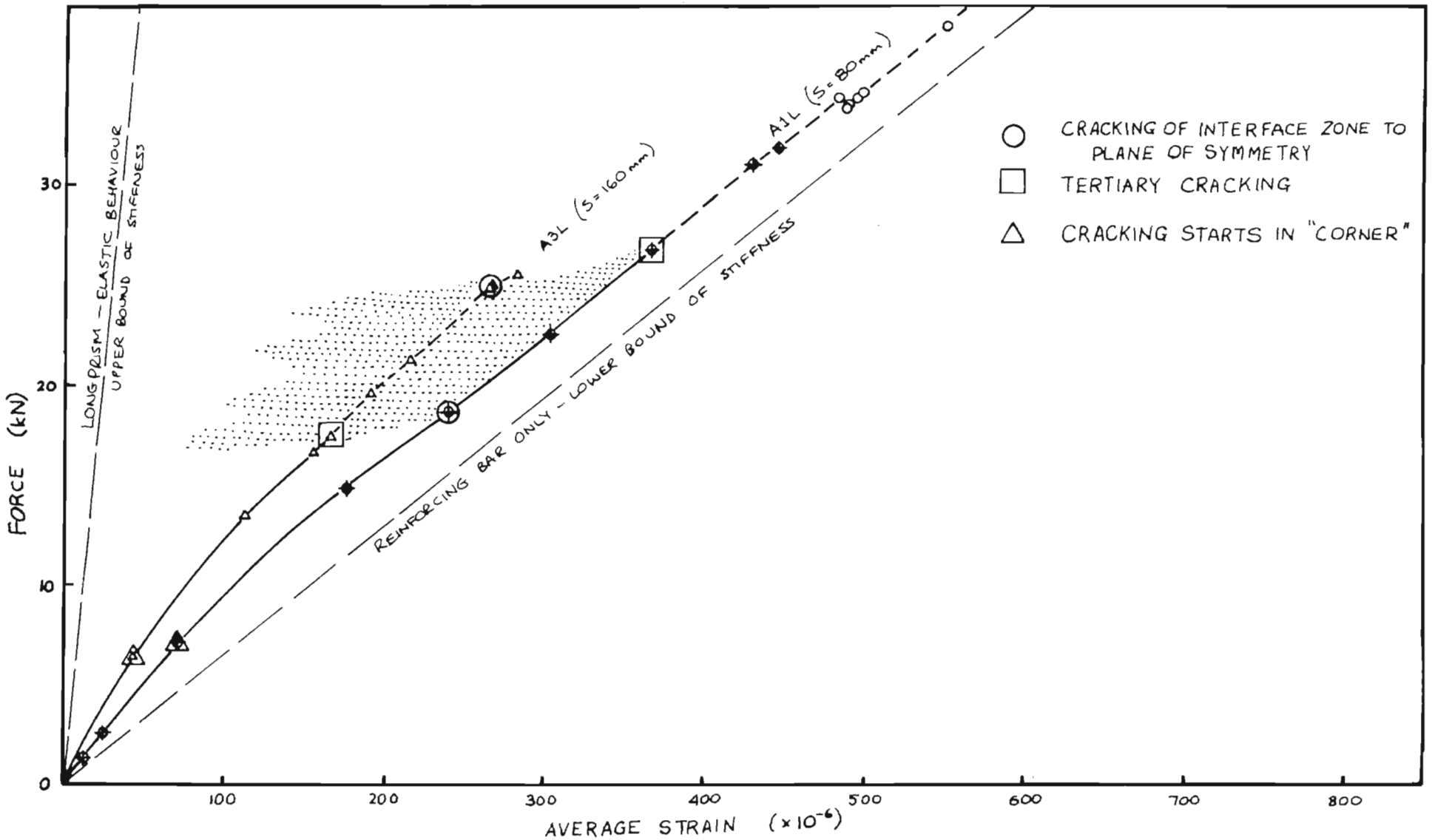

FIGURE E.3: LOAD-STRAIN DIAGRAM FOR SERIES L

(BAR ϕ = 20mm
COVER = 80mm)

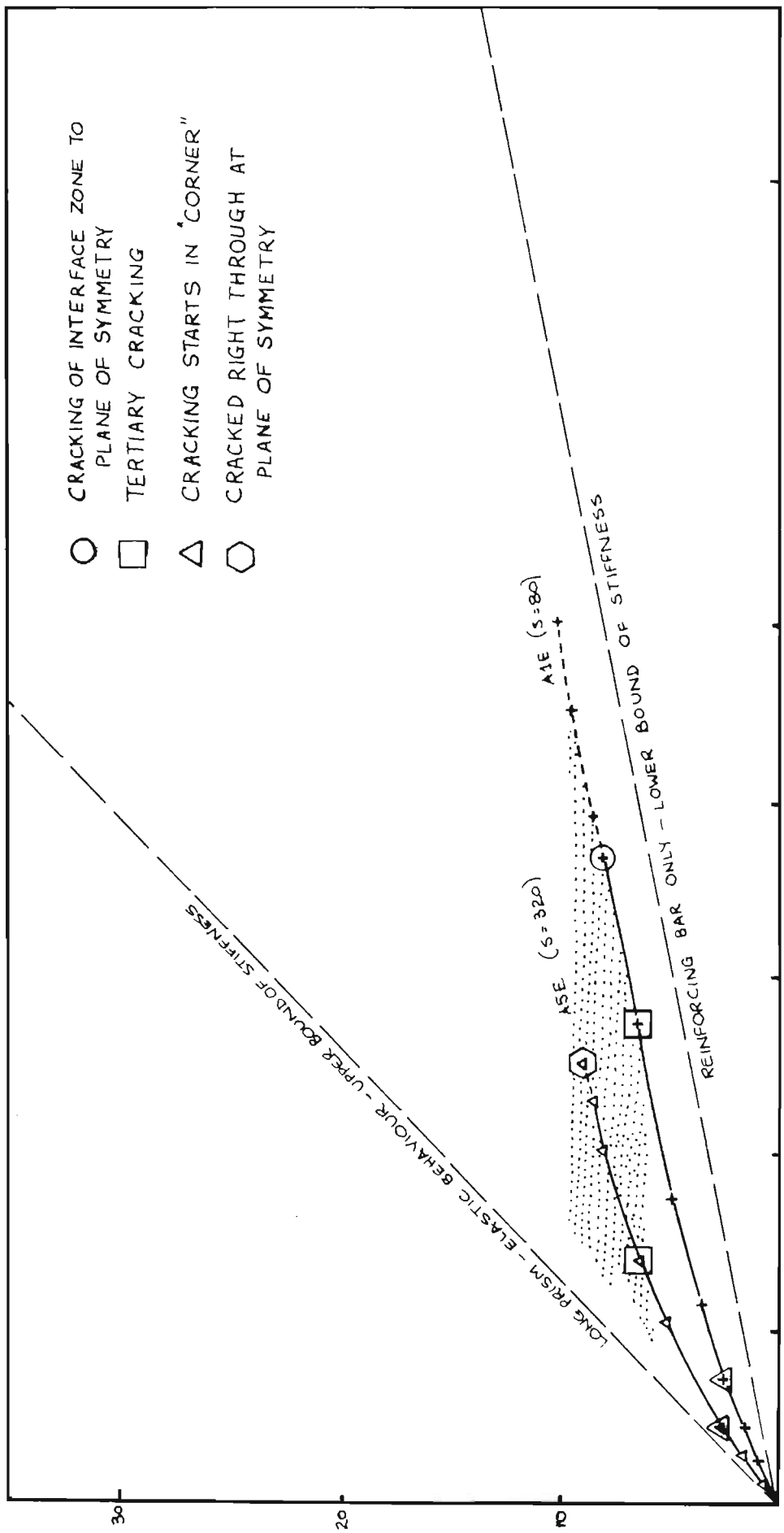

FIGURE E.4: LOAD-STRAIN DIAGRAM FOR SERIES E

(BAR ϕ = 10mm
COVER - 20 mm)

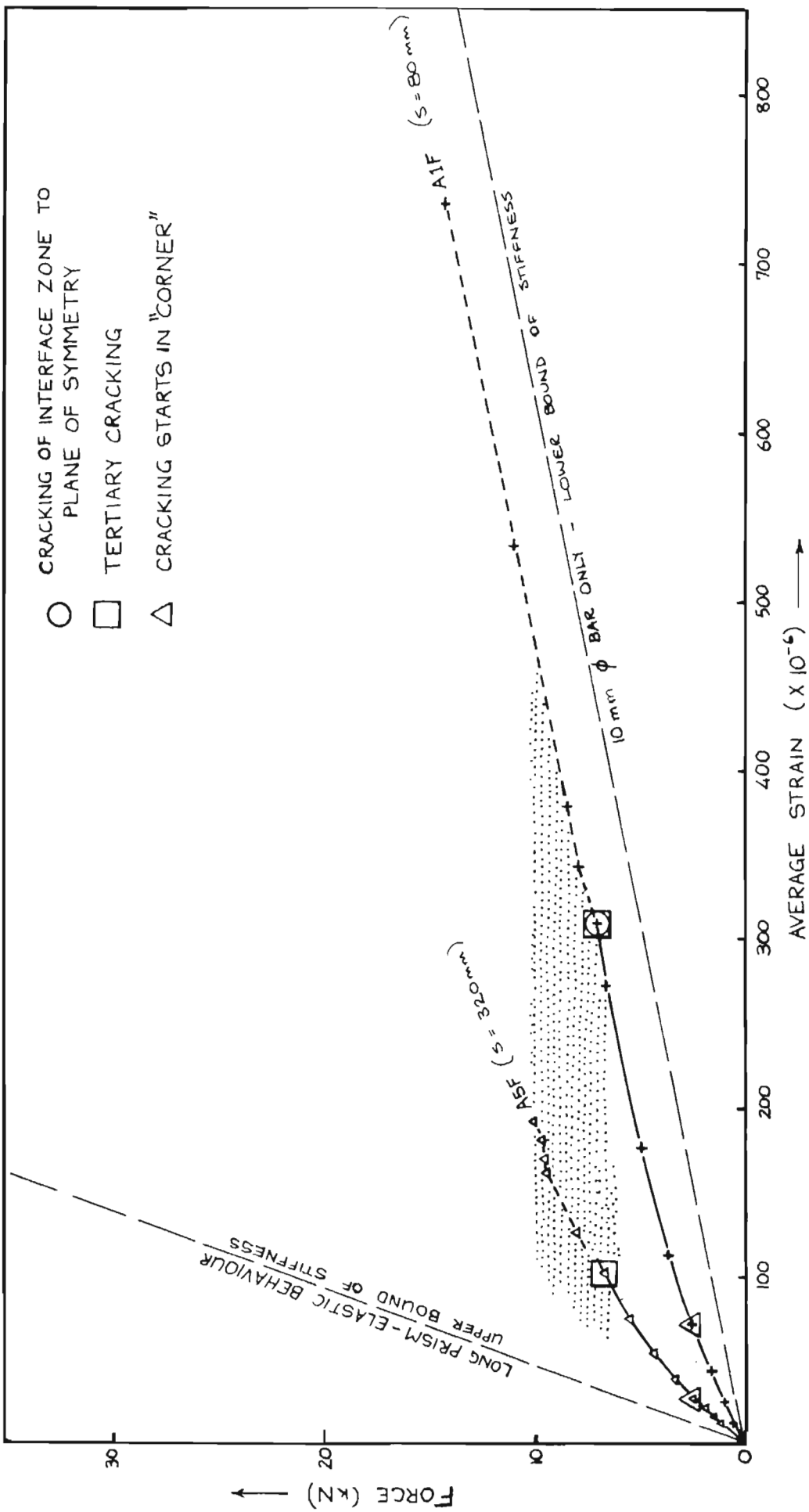

FIGURE E.5: LOAD-STRAIN DIAGRAM FOR SERIES F

(BAR ϕ = 10 mm
COVER = 40 mm)

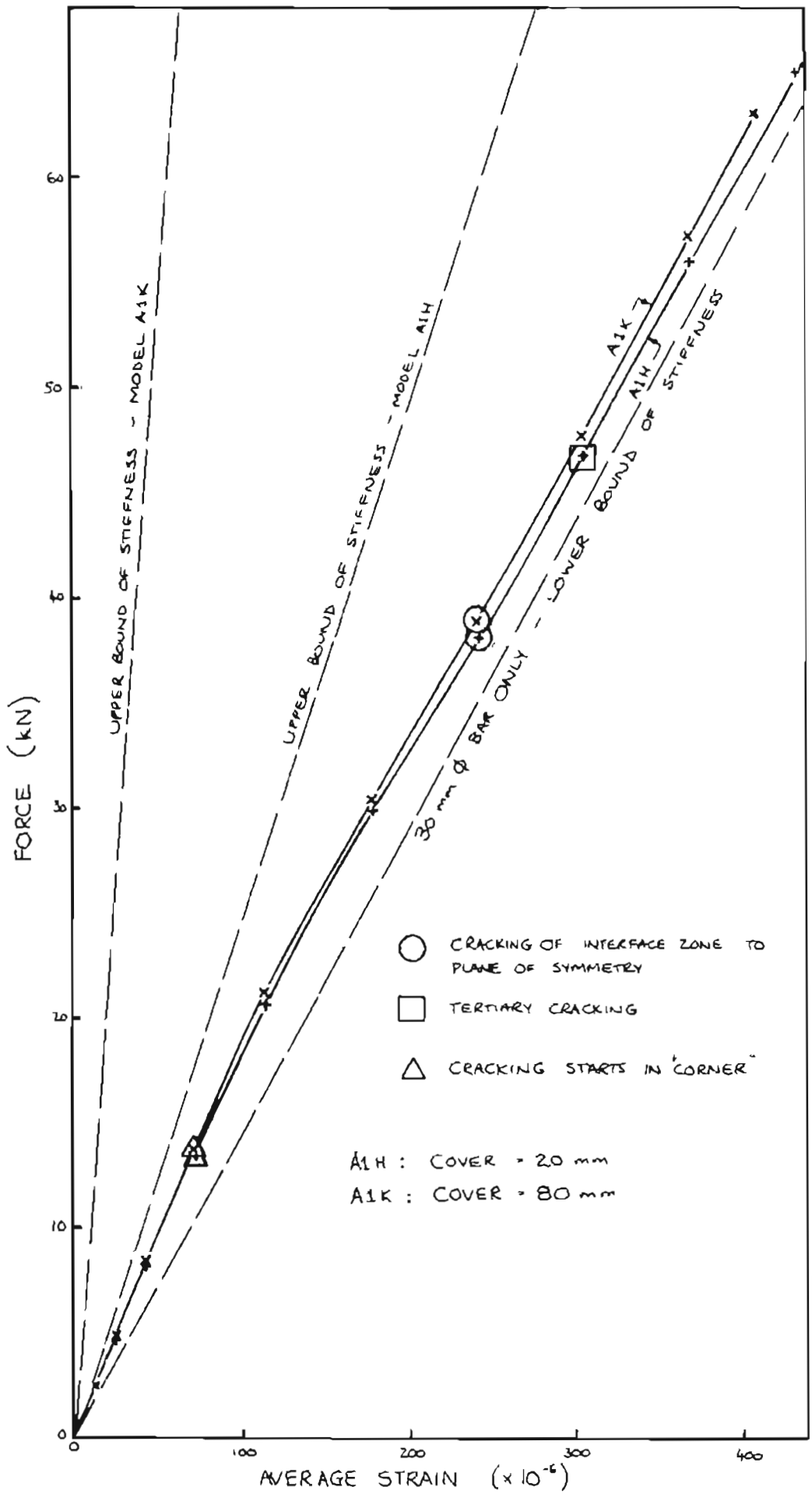

FIGURE E.6: LOAD-STRAIN DIAGRAMS – A1H & A1K

APPENDIX F

CRACK DIRECTIONS OF TYPICAL ABAQUS MODEL (MODEL A1B)

Explanation of calculation of angles from rectangular coordinates:-

Angle 1 = direction in which concrete fractures
(i.e. normal to the crack itself)
= arctan (y/x)

Angle 2 = direction of actual crack (for plotting)
= Angle 1 + 90°

Inc. of first cracking	Average strain (micro-strain)	Gauss point	DIRECTION VECTORS (rectangular) x	y	z	Angle 1	Angle 2
1	62.5	3.3	0.7363	-0.6767		-42.6	47.4
2	125.0	3.1	0.7108	-0.7034		-44.7	45.3
2	125.0	3.2	0.8432	-0.5376		-32.5	57.5
2	125.0	3.4	0.8818	-0.4717		-28.1	61.9
2	125.0	13.1	0.6074	-0.7944		-52.6	37.4
2	125.0	13.2	0.6868	-0.7268		-46.6	43.4
2	125.0	13.3	0.6693	-0.7430		-48.0	42.0
2	125.0	13.4	0.7375	-0.6754		-42.5	47.5
2	125.0	23.1	0.5319	-0.8468		-57.9	32.1
2	125.0	23.3	0.5864	-0.8100		-54.1	35.9
2	125.0	23.4	0.6408	-0.7677		-50.1	39.9
3	218.8	23.2	0.7929	-0.6093		-37.5	52.5
4	312.5	4.3	0.2457	-0.9693		-75.8	14.2
4	312.5	14.3	0.3884	-0.9215		-67.1	22.9
5	335.9	4.1	0.0000	1.0000		90.0	180.0
5	335.9	4.1			1.00		
5	335.9	4.2			1.00		
5	335.9	4.3			1.00		
5	335.9	4.4			1.00		
5	335.9	14.1	0.2843	-0.9587		-73.5	16.5
5	335.9	14.3	0.3884	-0.9215		-67.1	22.9
5	335.9	33.1	0.6009	-0.7993		-53.1	36.9
5	335.9	33.2	0.7083	-0.7059		-44.9	45.1
5	335.9	33.3	0.5083	-0.8612		-59.4	30.6
5	335.9	33.4	0.7555	-0.6551		-40.9	49.1
5	335.9	43.1	0.4860	-0.8740		-60.9	29.1
5	335.9	43.2	0.5687	-0.8226		-55.3	34.7
5	335.9	43.3	0.5609	-0.8279		-55.9	34.1
5	335.9	43.4	0.6362	-0.7715		-50.5	39.5
5	335.9	53.1	0.3588	-0.9334		-69.0	21.0
5	335.9	53.2	0.6251	-0.7806		-51.3	38.7
5	335.9	53.3	0.4442	-0.8959		-63.6	26.4
5	335.9	53.4	0.5078	-0.8615		-59.5	30.5

Inc. of first cracking	Average strain (micro-strain)	Gauss point	DIRECTION VECTORS (rectangular) x	y	z	Angle 1	Angle 2
5	335.9	63.1	0.2075	-0.9782		-78.0	12.0
5	335.9	63.2	0.3700	-0.9290		-68.3	21.7
5	335.9	63.3	0.3011	-0.9536		-72.5	17.5
5	335.9	63.4	0.5225	-0.8526		-58.5	31.5
5	335.9	73.1	0.0379	-0.9993		-87.8	2.2
5	335.9	73.2	0.0572	-0.9984		-86.7	3.3
5	335.9	73.3	0.1372	-0.9905		-82.1	7.9
5	335.9	73.4	0.2634	-0.9647		-74.7	15.3
7	394.5	14.4	0.4999	-0.8661		-60.0	30.0
7	394.5	24.3	0.3222	-0.9467		-71.2	18.8
8	447.3	4.2	-0.6511	0.7590		-49.4	40.6
8	447.3	4.4	-0.4542	0.8909		-63.0	27.0
8	447.3	14.2	0.3879	-0.9217		-67.2	22.8
8	447.3	15.3	0.4167	-0.9090		-65.4	24.6
9	500.0	15.1	0.2557	-0.9668		-75.2	14.8
10	552.7	5.1			1.00		
10	552.7	5.2			1.00		
10	552.7	5.3			1.00		
10	552.7	5.4			1.00		
10	552.7	15.2	0.2580	-0.9661		-75.0	15.0
10	552.7	15.4	0.5790	-0.8153		-54.6	35.4
10	552.7	34.1	0.1677	-0.9858		-80.3	9.7
10	552.7	34.2	0.2632	-0.9648		-74.7	15.3
10	552.7	34.3	0.2619	-0.9651		-74.8	15.2
10	552.7	34.4	0.3621	-0.9322		-68.8	21.2
11	605.5	5.2	-0.6446	-0.7646		49.9	139.9
11	605.5	24.1	0.6784	-0.7347		-47.3	42.7
11	605.5	24.2	0.6677	-0.7444		-48.1	41.9
11	605.5	24.4	0.5575	-0.8302		-56.1	33.9
15	671.4	35.1	0.1346	-0.9909		-82.3	7.7
15	671.4	35.2	0.1208	-0.9927		-83.1	6.9
15	671.4	35.3	0.3091	-0.9510		-72.0	18.0
15	671.4	35.4	0.4601	-0.8879		-62.6	27.4
15	671.4	64.1	0.2205	0.9754		77.3	167.3
15	671.4	64.3	0.0814	0.9967		85.3	175.3
18	740.6	25.2	0.7379	-0.6749		-42.4	47.6
20	762.8	44.3	0.1899	-0.9818		-79.1	10.9
20	762.8	73.1	-0.9993	-0.0379		2.2	92.2
20	762.8	73.2	-0.9984	-0.0572		3.3	93.3
20	762.8	73.3	-0.9905	-0.1372		7.9	97.9
25	917.2	44.1	0.0622	-0.9981		-86.4	3.6
25	917.2	44.2	0.4113	-0.9115		-65.7	24.3
25	917.2	44.4	0.4358	-0.9001		-64.2	25.8
25	917.2	63.1	-0.9782	-0.2075		12.0	102.0
25	917.2	64.2	0.3515	0.9362		69.4	159.4
25	917.2	73.4	-0.9647	-0.2634		15.3	105.3

APPENDIX G

CRACK WIDTH vs STRAIN DIAGRAMS FOR ABAQUS MODELS

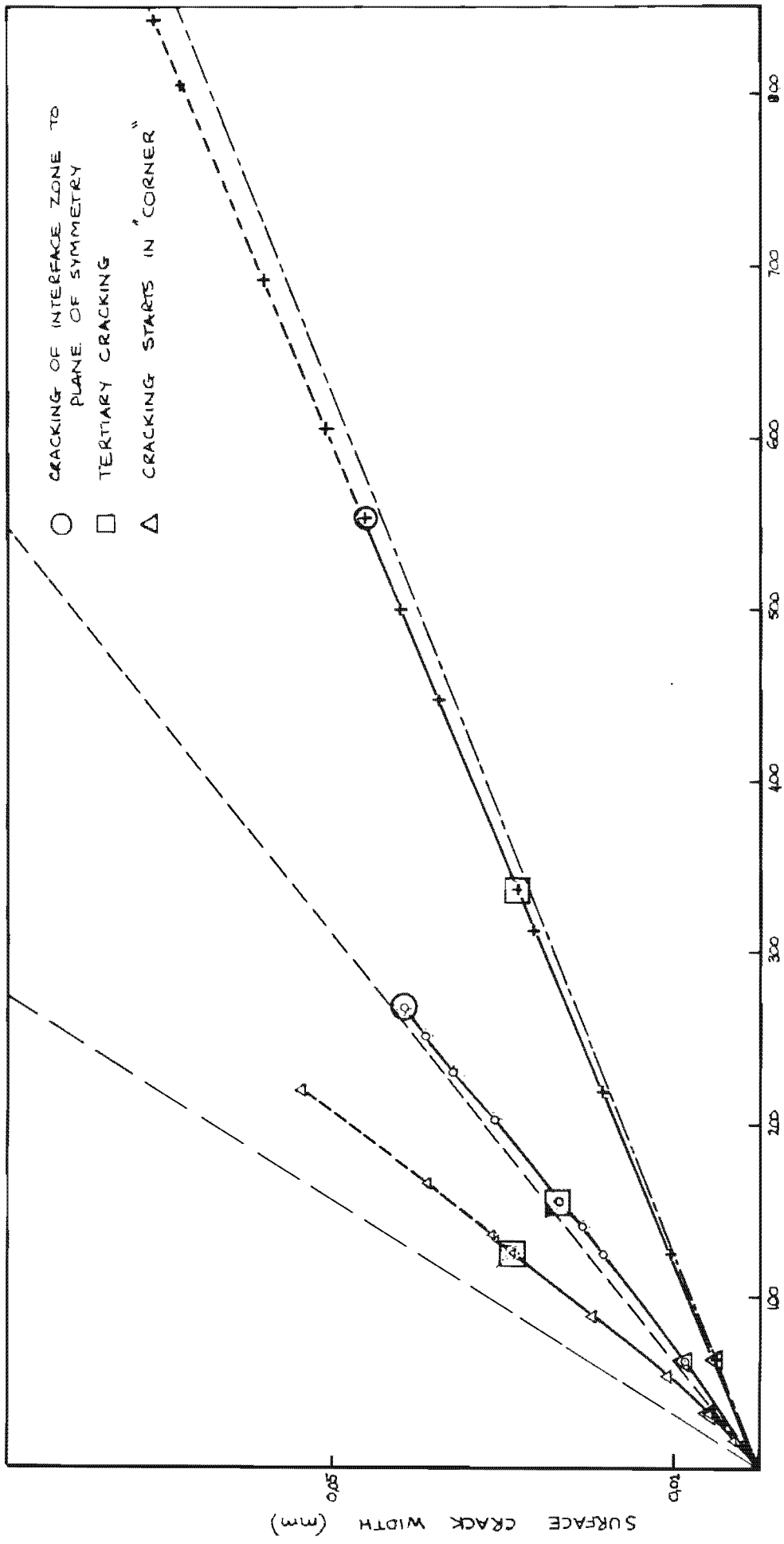

FIGURE G.1 : COMPARISON OF SURFACE CRACK WIDTHS - SERIES B (BAR ϕ = 20mm COVER = 40mm)

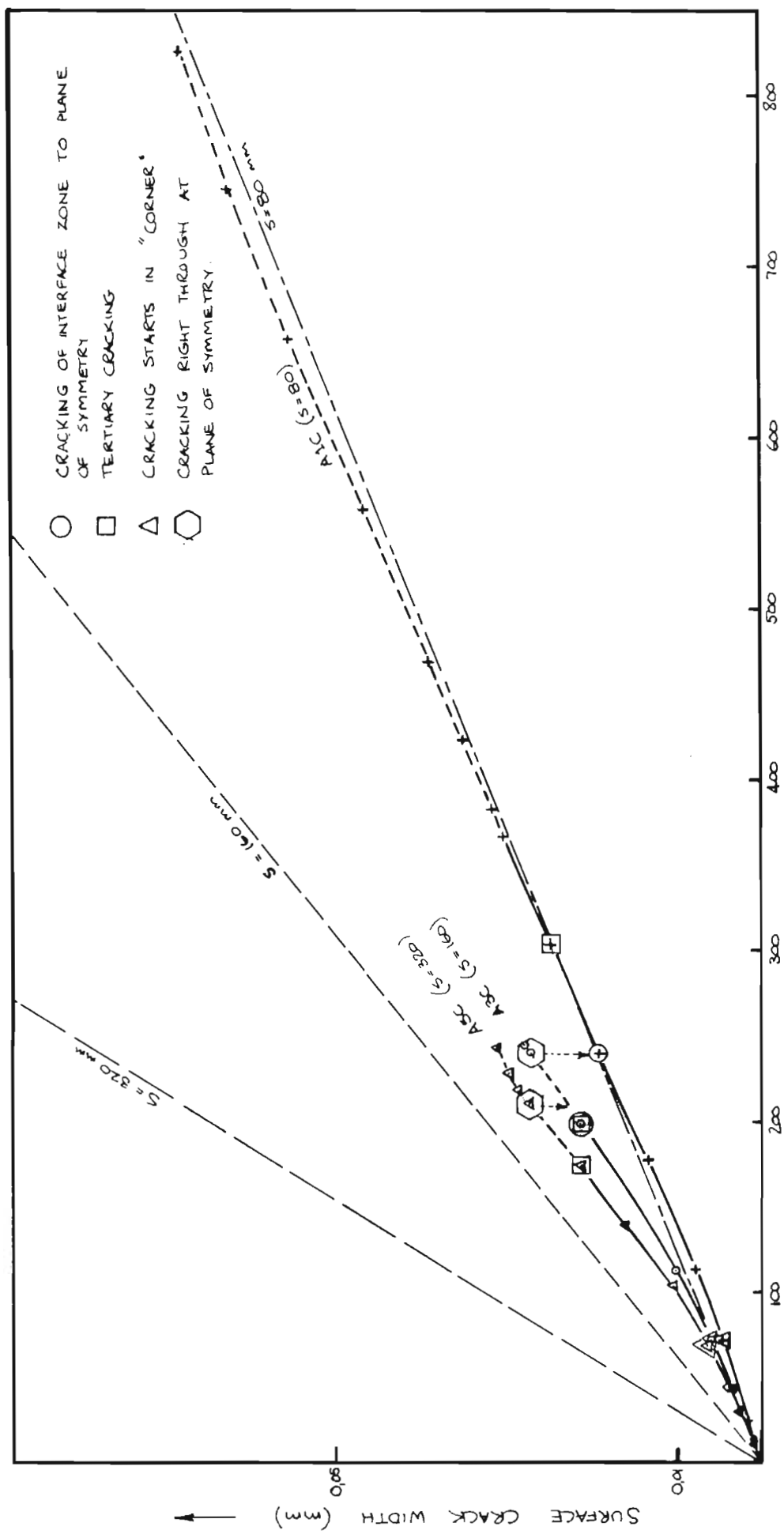

FIGURE G.2 : COMPARISON OF SURFACE CRACK WIDTHS - SERIES C (BAR ϕ = 20mm COVER = 20mm)

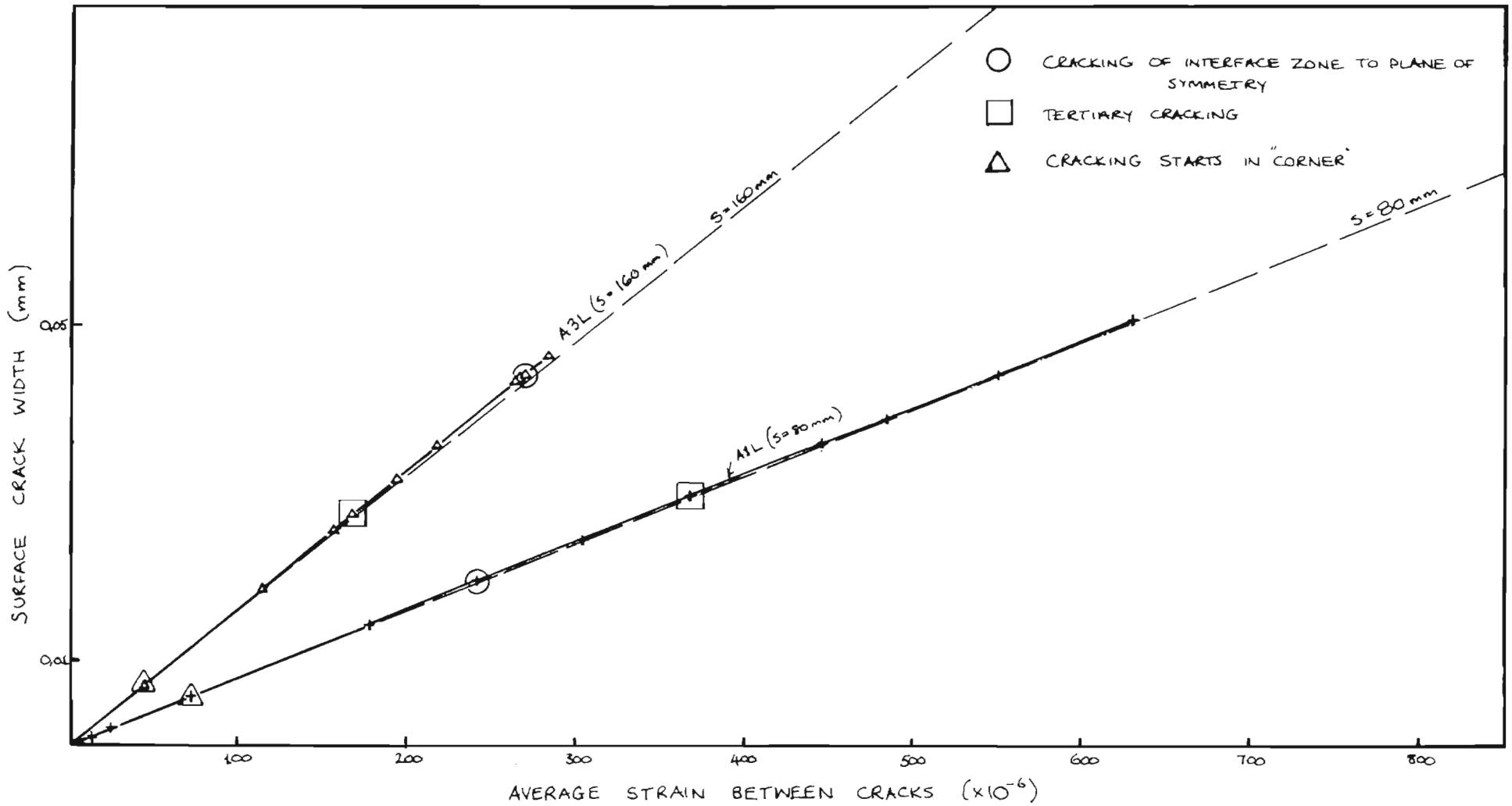

FIGURE G.3: COMPARISON OF SURFACE CRACK WIDTHS - SERIES L (BAR ϕ = 20mm COVER = 80mm)

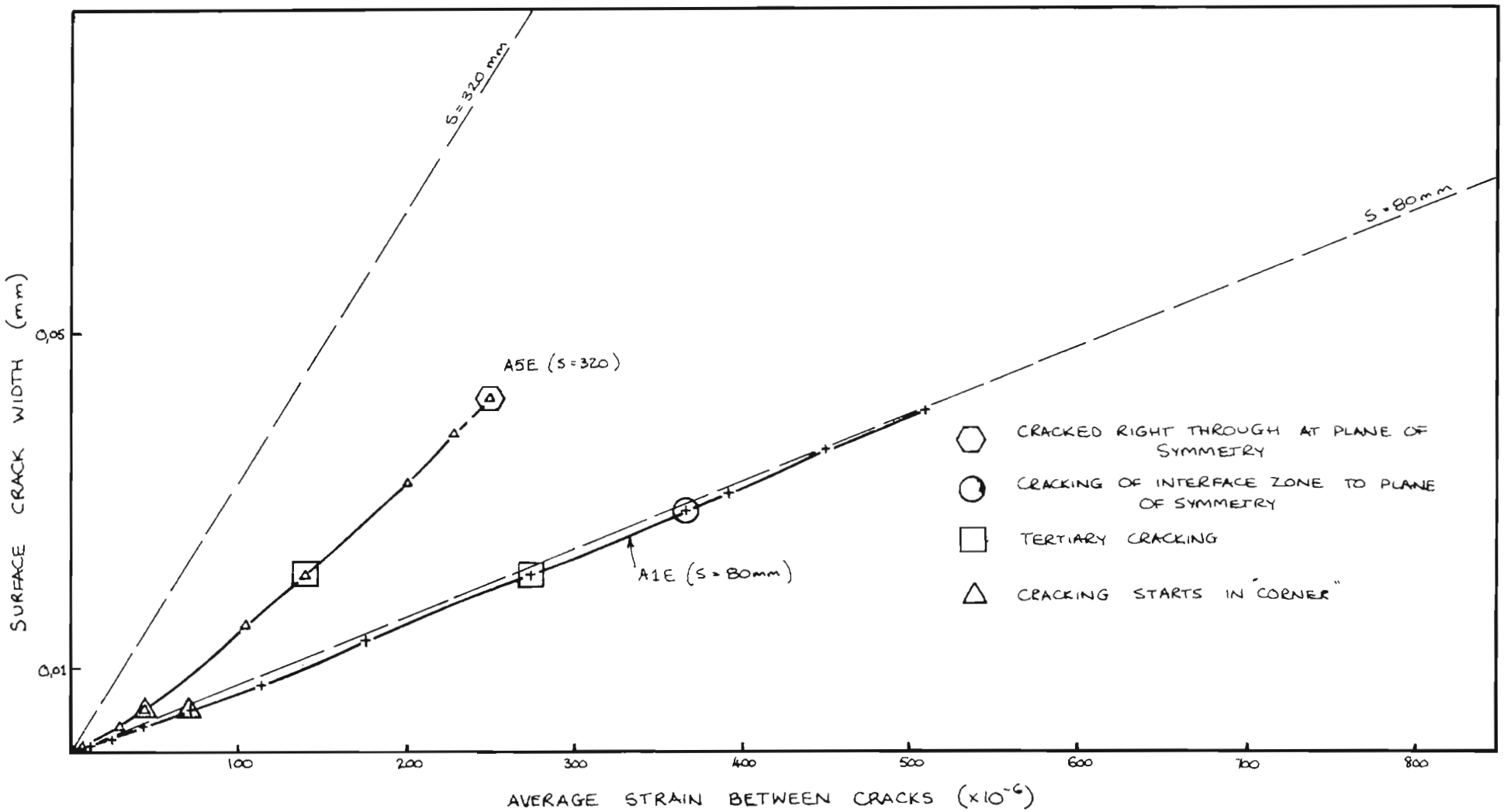

FIGURE G.4 : COMPARISON OF SURFACE CRACK WIDTHS – SERIES E (BAR ϕ = 10mm COVER = 20mm)

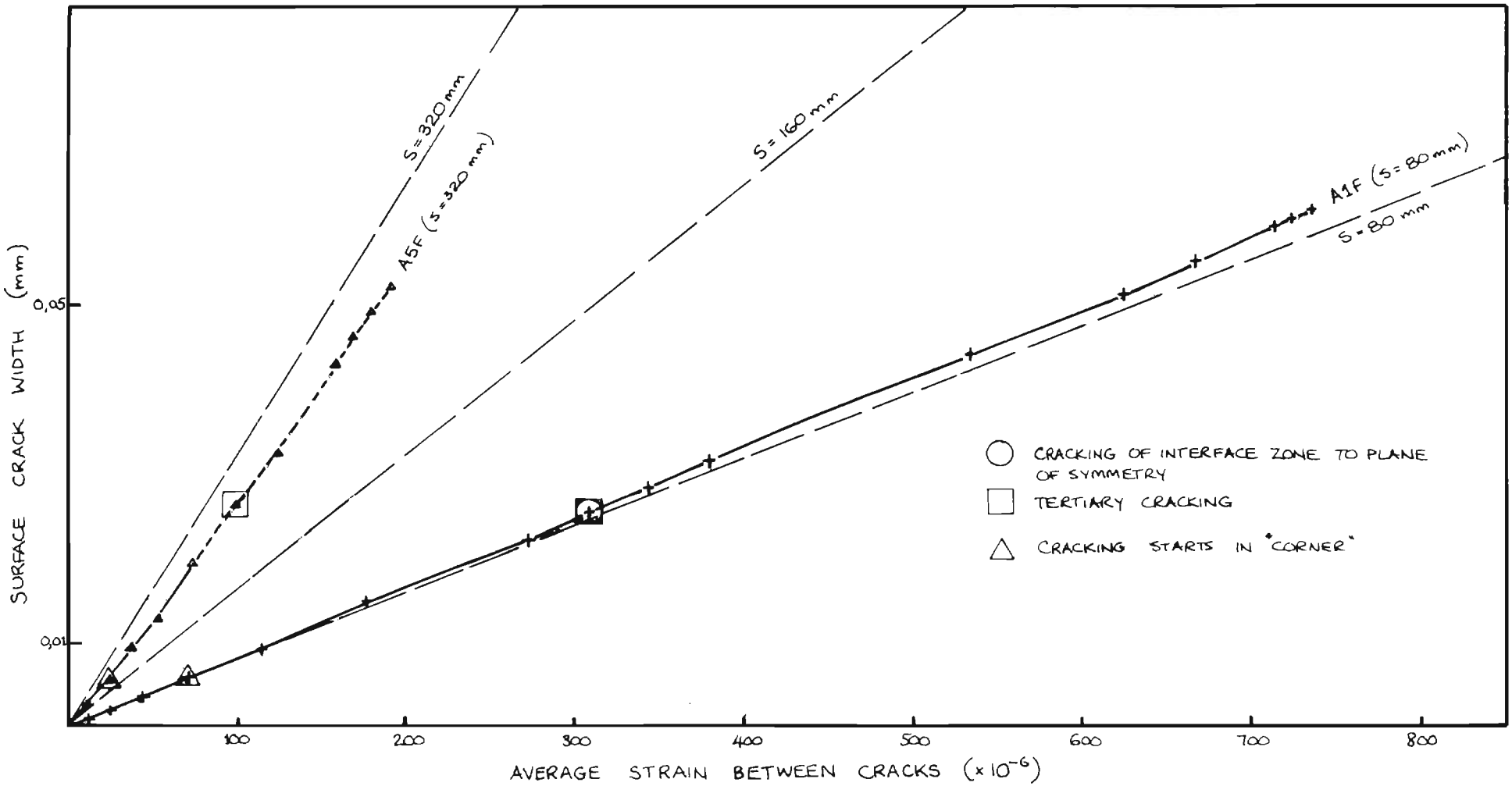

FIGURE G.5 : COMPARISON OF SURFACE CRACK WIDTHS – SERIES F (BAR ∅ = 10mm COVER = 40mm)

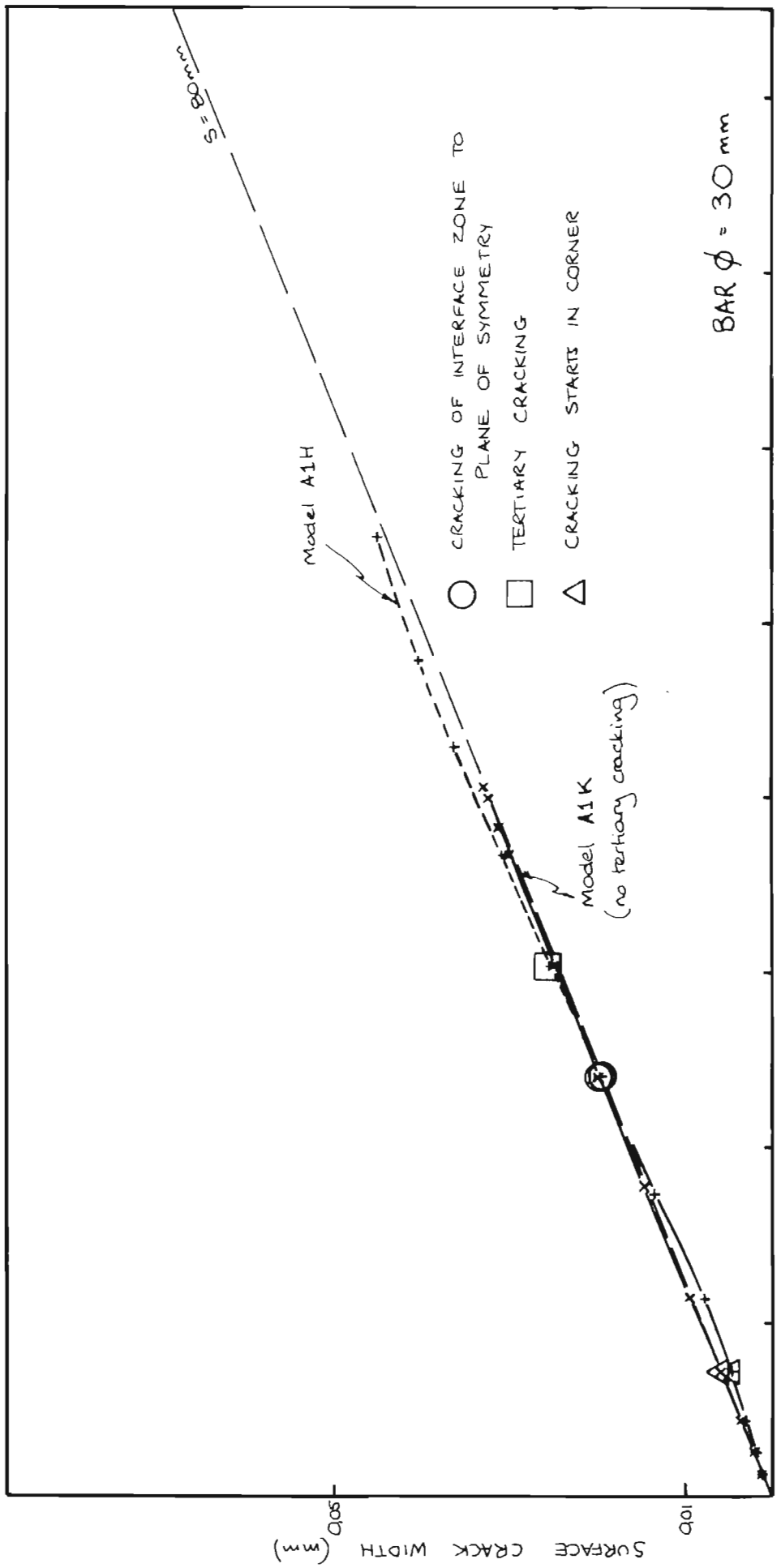

FIGURE G.6 : COMPARISON OF SURFACE CRACK WIDTHS — MODELS A1H (COVER = 20 mm) & A1K (COVER = 80 mm)

APPENDIX H

COURSES PASSED BY THE CANDIDATE

The candidate has previously passed the following postgraduate courses towards the degree of Master of Science in Engineering.

Course		Credit Rating
CE526	Coastal Engineering Practice (Exam and Project)	5
CE535	Engineering Economy (Exam)	3
CE532	Contracts and Contract Administration (Exam)	3
CE506	Properties of Concrete (Project)	4
CE551(a)	Frame Analysis (Exam)	2
CE552(a)	Introduction to Finite Element Analysis (Exam)	2
CE552(b)	Finite Element Analysis (Exam and Project)	3
CE5B4	Bridge Engineering (Exam and Project)	4
	TOTAL CREDITS	26

In terms of the requirements for the degree of Master of Science in Engineering, this thesis is therefore required to be of a value of not less than one-half of the value of a thesis submitted in complete fulfilment of the requirements for the degree. (Credit rating of a full thesis = 40 credits.)